

Synthetic and Mechanistic Studies of Coupling Reactions Involving C-H Bond Activation

Ki Hyeok Kwon
Marquette University

Recommended Citation

Kwon, Ki Hyeok, "Synthetic and Mechanistic Studies of Coupling Reactions Involving C-H Bond Activation" (2011). *Dissertations (2009 -)*. Paper 134.
http://epublications.marquette.edu/dissertations_mu/134

SYNTHETIC AND MECHANISTIC STUDIES OF COUPLING REACTIONS
INVOLVING C-H BOND ACTIVATION

by

Ki Hyeok Kwon, B.S., M.S.

A Dissertation submitted to the Faculty of the Graduate School,
Marquette University,
in Partial Fulfillment of the Requirements for
the Degree of Doctor of Philosophy

Milwaukee, Wisconsin

August 2011

ABSTRACT
SYNTHETIC AND MECHANISTIC STUDIES OF COUPLING REACTION
INVOLVING C-H BOND ACTIVATION

Ki Hyeok Kwon, B.S., M.S.

Marquette University, 2011

Transition metal-catalyzed C-C bond forming reactions involving C-H bond activation have been shown to be effective methods for functionalization of unreactive compounds. Since Murai's pioneering work on ruthenium-catalyzed regioselective arene-to-alkene coupling reactions, a number of well-defined, late transition metal catalysts have been shown to mediate regioselective C-C bond forming reaction involving C-H bond activation. Recently, late transition metal complexes have also been found to catalyze the regioselective coupling reaction of nitrogen containing compounds with alkenes as well as sp^3 bond insertions and oxidative coupling reaction of alkenes. The catalytic C-C bond forming reaction involving C-H bond activation would provide simple and atom economic pathways for making functionalized molecules. Although there are many examples of stoichiometric reaction of aromatic C-H bond activation with transition metal compounds, catalytic C-H bond activation reactions via catalytic system have been rarely employed in organic synthesis.

An efficient catalytic conjugate addition reaction protocol has been developed for the synthesis of tetrasubstituted olefin products. The cationic ruthenium-hydride complex was found to be an effective catalyst for coupling reaction with α,β -unsaturated carbonyl compounds and simple alkenes. The kinetic and spectroscopic data are consistent with three different mechanistic pathways depending on substrate employed. The reaction of an α,β -unsaturated carbonyl compounds with simple olefins predominantly gave the tetrasubstituted olefin products. The mechanistic studies suggest that the olefin insertion into an α,β -unsaturated carbonyl substrate is the rate-limiting step for conjugate addition reaction. On the other hand, the coupling reaction of α -methyl α,β -unsaturated cinnamide with aromatic alkenes gave oxidative coupling products. The kinetic and spectroscopic studies support the different mechanistic pathway, which involves the rate-limiting vinyl C-H activation step, in comparison with the conjugate addition reaction. This synthetic methodology promises to provide a straightforward route to the valuable organic compounds such as tetrasubstituted olefins which are difficult to synthesize by using traditional synthetic methods.

TABLE OF CONTENTS

LIST OF TABLES.....	iv
LIST OF FIGURES.....	vi
CHAPTER	
I. INTRODUCTION.....	1
1.1 C-H bond Activation of Alkanes	2
1.2 Arene C-H Bond Activation	8
1.2.1 Chelate-Assisted Arene C-H bond Activation Reactions	8
1.2.2 Nonchelate-Assisted Reactions.....	15
1.3 Chelate-Assisted C-H Bond Activation Reaction of Alkenes	18
1.4 C-H Bond Activation Reactions of Nitrogen Containing Compounds	22
1.4.1 C-H Bond Activation of Pyrrolidine Derivatives	22
1.4.2 C-H Bond Activation of Indole and Quinoline derivatives	25
1.4.3 C-H Bond Activation of Pyridine derivatives	30
1.4.4 C-H Bond Activation of Amide, Amine, and imine derivatives ..	33
II. Synthetic and Mechanistic Studies of Chelate-Assisted Oxidative Coupling Reaction of Arylamides and Unactivated Alkenes.....	41
2.1 Optimization Studies for Coupling of Arylamide with cyclopentene	45
2.1.1 Catalyst Survey	45
2.1.2 Solvent Effect	46
2.2 Reaction Scope	48

2.3 Mechanistic Study	51
2.3.1 Phosphine Inhibition	51
2.3.2 Isotope Effect Study	52
2.3.3 Deuterium Labeling Study	13
2.3.4 Isolation of Catalytically Relevant Species	59
2.3.5 VT NMR Study	62
2.4 Proposed Mechanism	63
III. Stereoselective Catalytic Conjugate Addition and Oxidative Coupling Reaction of Simple Alkenes to α,β -Unsaturated Carbonyl Compounds.....	67
3.1 Catalyst Survey	71
3.2 Reaction Scope	72
3.2.1 Coupling Reactions of α,β -Unsaturated Ester and Enones with Alkenes	73
3.2.2 Coupling Reactions of α,β -Unsaturated Amides with Alkenes...	75
3.2.3 Coupling Reactions of α -Substituted α,β -Unsaturated Carbonyl Compounds with Alkenes	78
3.2.4 Oxidative Coupling Reactions of α -Substituted α,β -Unsaturated Carbonyl Compounds with Aromatic Alkenes	81
3.4.5 Intramolecular Coupling Reaction of α,β -Unsaturated Esters with Simple Olefins	83
3.3 Mechanistic Studies	87
3.3.1 Reaction Profile	87
3.3.2 Hammett Study	89
3.3.3 Isotope Effect Studies	93
3.3.4 Deuterium Labeling Studies	100

3.3.5 Isolation of Catalytically Relevant Species	105
3.4 Empirical Rate Law Derivation	107
3.5 Thermodynamic Parameters	108
3.6 Proposed Mechanism	110
IV. Aqueous Phase C-H Bond Oxidation Reaction of Arylalkanes Catalyzed by a Water-Soluble Cationic Ru(III) Pymox Complex.....	118
4.1 Synthesis of Water-Soluble Ruthenium Pymox Complexes.....	131
4.2 Optimization Studies for C-H Oxidation Reaction of Arylalkanes ..	135
4.2.1 Catalyst Survey	135
4.2.2 Survey of Oxidizing Agents	137
4.2.3 Reusability of the Cationic Ruthenium Complex in Aqueous Solution	138
4.3 Reaction Scope	139
4.4 Mechanistic Studies	142
4.4.1 Isotope Effect Study	142
4.4.2 Hammett Study	143
4.4.3 Detection of Catalytically Relevant Species	144
4.5 Proposed Mechanism	146
V. Experimental Section.....	151
References.....	203
Appendix A (Molecular Structures of 90-99).....	213
Appendix B (Crystal Data and Structure Refinement for 90-99).....	218

LIST OF TABLES

Table 1. Catalyst Suvery on the Reaction of $C_6H_5CONMe_2$ with Cyclopentene.....	46
Table 2. Solvent Effect on the Coupling Reaction of $C_6H_5CONMe_2$ with Cyclopentene Catalyzed by 26	47
Table 3. Oxidative C-H Coupling Reaction of Arylamides with Alkenes.....	48
Table 4. Average ^{13}C Integration of the Recovered and Virgin Sample of $C_6H_5CONEt_2$	54
Table 5. Catalyst Survey for the Coupling Reaction of (<i>E</i>)- $C_6H_5CH=CHCO_2Et$ and Propylene.....	72
Table 6. Conjugate Addition Reaction of Simple Olefins to α,β -Unsaturated Ester and Enones.....	74
Table 7. Conjugate Addition Reaction of Simple Olefins to α,β -Unsaturated Amides	77
Table 8. Conjugate Addition Reaction of Simple Olefins to α -Substituted α,β -Unsaturated Compounds	80
Table 9. Oxidative Coupling Reaction of Aromatic Olefins to α -Substituted α,β -Unsaturated Amides.....	82
Table 10. Intramolecular Coupling Reaction of α,β -Unsaturated Esters with Simple Olefins Catalyzed by 26	84
Table 11. Average ^{13}C Integration of the Recovered and Virgin Samples of (<i>E</i>)- $C_6H_5CH=CHCONEt_2$	94
Table 12. Average ^{13}C Integration of the Recovered and Virgin Samples of (<i>E</i>)- $C_6H_5CH=C(CH_3)CONHCH_3$	97
Table 13. Average ^{13}C Integration of the Recovered and Virgin Samples of (<i>E</i>)- $C_6H_5CH=C(CH_3)CONHCH_3$	98
Table 14. Kinetics and Isotope Effects for the Coupling Reaction of α,β -Unsaturated Carbonyl Compounds with Alkene.....	111
Table 15. Kinetics, Intra- and Intermolecular Deuterium Isotope Effects for the Ruthenium Catalyzed Oxidation of Hydrocarbons with <i>t</i> -BuOOH.....	120

Table 16. Catalyst Survey for Oxidation Reaction of Ethylbenzene with <i>t</i> -BuOOH....	136
Table 17. Oxidizing Agent and Additive Effects on Oxidation of Ethylbenzene.....	137
Table 18. Aqueous Phase C-H Bond Oxidation of Arylalkanes.....	141
Table 19. Crystal Data and Structure Refinement for 30a	197
Table 20. Crystal Data and Structure Refinement for 56	198
Table 21. Crystal Data and Structure Refinement for 80	199
Table 22. Crystal Data and Structure Refinement for 81	200
Table 23. Crystal Data and Structure Refinement for 82	201

LIST OF FIGURES

Figure 1. Molecular Structure of Cationic Ruthenium-Hydride Complex 26	44
Figure 2. PCy ₃ Inhibition Study for the Coupling Reaction of C ₆ H ₅ CONEt ₂ with Cyclopentene Catalyzed by 26	52
Figure 3. First-Order Plots of $-\ln([C_6H_5CONEt_2]_t/[C_6H_5CONEt_2]_0)$ vs Time for Coupling Reaction.....	53
Figure 4. (a) ¹ H NMR Spectrum of Mixture of 23h-d_n and 24h-d_n , (b) ² H NMR Spectrum of Mixture of 23h-d_n and 24h-d_n , (c) ¹ H NMR Spectrum 24h , (d) ¹ H NMR Spectrum of 24h-d_n	57
Figure 5. (a) ¹ H NMR Spectrum of <i>N,N</i> -Diethyl Benzamide- <i>d</i> ₅ , (b) ¹ H NMR Spectrum of Recovered <i>N,N</i> -Diethyl Benzamide- <i>d_n</i> , (c) ² H NMR Spectrum of Recovered <i>N,N</i> -Diethyl Benzamide- <i>d_n</i> , (d) ² H NMR Spectrum of Recovered Cyclopentene- <i>d_n</i> and Cyclopentane- <i>d_n</i>	58
Figure 6. Molecular Structure of 30	61
Figure 7. van't Hoff Plot of $\ln K$ vs $1/T$	63
Figure 8. Structure of Tamoxifen 33 and Rofecoxib 34	67
Figure 9. Newman Projection of Compound 36t	76
Figure 10. Newman Projection of Compounds 37l and 37m	79
Figure 11. Kinetic Profile of the Conversion of 44 to 35g	88
Figure 12. Hammett Plot of the Coupling Reaction of <i>para</i> -Substituted (<i>E</i>)- <i>p</i> -X-C ₆ H ₄ CH=CHCO ₂ Et (X = OCH ₃ , CH ₃ , H, F, Cl, CO ₂ Me, CF ₃) with Propene.....	89
Figure 13. Hammett Plot of the Coupling Reaction of (<i>E</i>)-C ₆ H ₄ CH=CHCO ₂ Et with <i>para</i> -Substituted Styrene <i>p</i> -Y-C ₆ H ₄ CH=CH ₂ (Y = OCH ₃ , CH ₃ , H, Cl, CF ₃).....	90
Figure 14. Hammett Plot of the Coupling Reaction of (<i>E</i>)-C ₆ H ₄ CH=C(CH ₃)CONHCH ₃ with <i>para</i> -Substituted Styrene <i>p</i> -Y-C ₆ H ₄ CH=CH ₂ (Y = OCH ₃ , CH ₃ , H, F, Cl, CF ₃).....	92
Figure 15. First-Order Plots of $-\ln[\text{cinnamate}]_t/[\text{cinnamate}]_0$ vs Time for the Coupling Reaction of (<i>E</i>)-C ₆ H ₅ CH=CHCO ₂ Et with Ethylene or Ethylene- <i>d</i> ₄	95
Figure 16. First-Order Plots of $-\ln([\text{cinnamide}]_t/[\text{cinnamide}]_0)$ vs Time for the Coupling Reaction of (<i>E</i>)-C ₆ H ₅ CH=C(CH ₃)CONHCH ₃ with Styrene or Styrene- <i>d</i> ₈	99

Figure 17. First-Order Plots of $-\ln([\text{cinnamide}]_t/[\text{cinnamide}]_0)$ vs Time for the Coupling Reaction of (<i>E</i>)-C ₆ H ₅ CH=C(CH ₃)CONHMe or (<i>E</i>)-C ₆ H ₅ CD=C(CH ₃)CONHMe with Styrene.....	100
Figure 18. (a) ¹ H NMR Spectrum of 36c-d_n , (b) ² H NMR Spectrum of 36c-d_n , (c) ² H NMR Spectrum of Recovered Propene.....	102
Figure 19. (a) ² H NMR Spectrum of (<i>E</i>)-C ₆ H ₅ CD=C(CH ₃)CONHCH ₃ , (b) ² H NMR Spectrum of the Coupling Reaction Mixture of (<i>E</i>)-C ₆ H ₅ CD=C(CH ₃)CONHCH ₃ with Styrene.....	104
Figure 20. Molecular Structure of 56	106
Figure 21. Plot of Observed Reaction Rate vs Catalyst Concentration for the Coupling Reaction.....	107
Figure 22. Plot of Observed Reaction Rate vs Propene Concentration for the Coupling Reaction.....	108
Figure 23. Plot of Observed Reaction Rate vs (<i>E</i>)-C ₆ H ₅ CH=CHCO ₂ Et Concentration for the Coupling Reaction.....	108
Figure 24. Eyring Plot for the Coupling Reaction of (<i>E</i>)-C ₆ H ₅ CH=CHCO ₂ Et with Propene.....	109
Figure 25. Arrhenius Plot for the Coupling Reaction of (<i>E</i>)-C ₆ H ₅ CH=CHCO ₂ Et with Propene.....	110
Figure 26. Selectivity for catalyzed C-H bond oxidation by [Fe(<i>S,S</i> -PDP)(CH ₃ CN) ₂][SbF ₆] ₂ , 70	124
Figure 27. Molecular Structure of 80	134
Figure 28. Molecular Structure of 81	134
Figure 29. Molecular Structure of 82	135
Figure 30. First-Order Plots of $-\ln([\text{ethylbenzene}]_t/[\text{ethylbenzene}]_0)$ vs Time for C-H Bond Oxidation Reaction of Ethylbenzene or Ethylbenzene- <i>d</i> ₁₀ with <i>t</i> -BuOOH.....	143
Figure 31. Hammett plot of the C-H Bond Oxidation Reaction of <i>para</i> -Substituted Ethylbenzene Substrates <i>p</i> -X-C ₆ H ₄ CH ₂ CH ₃ (X = OMe, CH ₃ , H, F, Cl) with <i>t</i> -BuOOH.....	144
Figure 32. Cyclic Voltammogram of 80 in CH ₂ Cl ₂	145

Figure 33. UV-vis spectra of **82** (20 μM), **82** (20 μM)/*t*-BuOOH (30 equiv)/NaBF₄, and **80** (20 μM) in water..... 146

Chapter I

Introduction

Over the past few decades, one of the main goals in catalytic chemistry has been the quest for the most economic ways to form C-C bonds.¹ Transition metal-catalyzed cross-coupling reactions have been one of the most useful synthetic tools for the formation of C-C bonds since Heck firstly reported his pioneering work in 1968.² Even though a broad range of donors and acceptors are amenable for Heck type coupling reactions, these coupling reactions absolutely require an aryl halide (or triflate) with an alkene and a stoichiometric amount of base and palladium catalyst in forming a substituted alkene products. To overcome these drawbacks for Heck type coupling reaction, the formation of C-C bond involving C-H bond activation of unreactive C-H bonds has attracted considerable interest and remains a long term challenge for the chemical and pharmaceutical industries. The catalytic C-H bond activation would provide simple and atom economic pathways for making functionalized molecules. Although there are many examples of stoichiometric aromatic C-H bond activation reactions with transition metal compounds, catalytic C-H bond activation reactions via catalytic system have been rarely employed in organic synthesis.

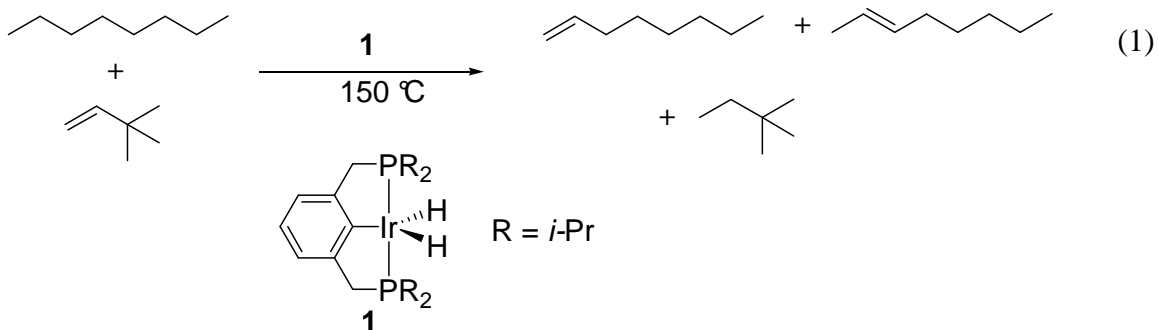
Generally, it is believed that the formation of C-C bond involving the cleavage of a C-H bond was a difficult process due to its bond strength. In 1993, Murai et al. reported a highly efficient, ruthenium-catalyzed addition of aromatic C-H bonds to olefins.³ Trost and Murai independently reported ruthenium-catalyzed C-H activation and alkylation of α,β -unsaturated carbonyl compounds with alkenes.⁴ Since then, numerous examples of catalyzed C-H bond activation have been extended to a wide variety of aromatic and

olefinic substrates by a number of research groups.⁴⁻¹⁴ However, examples of catalytic reactions involving the sp^3 C-H bond activation are still rare. Recently, Yu has reported a remarkably selective and direct olefination of sp^3 C-H bonds for amides by a Pd(II)-catalyzed reaction.¹⁵ Ellman and Bergman have also reported a rhodium mediated stereoselective alkylation of α,β -unsaturated imines via the direct C-H bond activation.¹⁶ Transition-metal-catalyzed regioselective and stereoselective C-H bond functionalizations have attracted much attention due to their synthetic utility in organic synthesis. This chapter provides a literature summary for the transition-metal-catalyzed formation of C-C bond via C-H activation and their applications.

1.1 C-H bond Activation of Alkanes

Alkanes are among the least reactive compounds. Because of their low reactivity particularly at the terminal position, the direct conversion of alkane into industrially important and valuable chemicals, such as linear alcohols, α -olefine, and amines, has been a long-term challenge in catalytic chemistry. Controlling selectivity for desired products containing a single functional group at the end of an alkyl chain is especially difficult because reactions of alkanes typically form a mixture of products. Certain transition metals were found to selectively react at the terminal carbon of the alkane to produce *n*-alkyl complexes,¹⁷ but these transformations involve stoichiometric amounts of expensive metal reagents. Jensen and Goldman discovered efficient and selective dehydrogenation of linear alkanes to give α -olefins in the presence of iridium “pincer” complexes $(^{i\text{-Pr}}\text{PCP})\text{IrH}_2$ ($^{i\text{-Pr}}\text{PCP} = 2,6\text{-bis}[\text{di}(\text{isopropyl})\text{phosphinomethyl}]\text{phenyl}$) (**1**) (eq 1).¹⁸ Isomerization limits the yield of the α -olefin products generated under these reaction

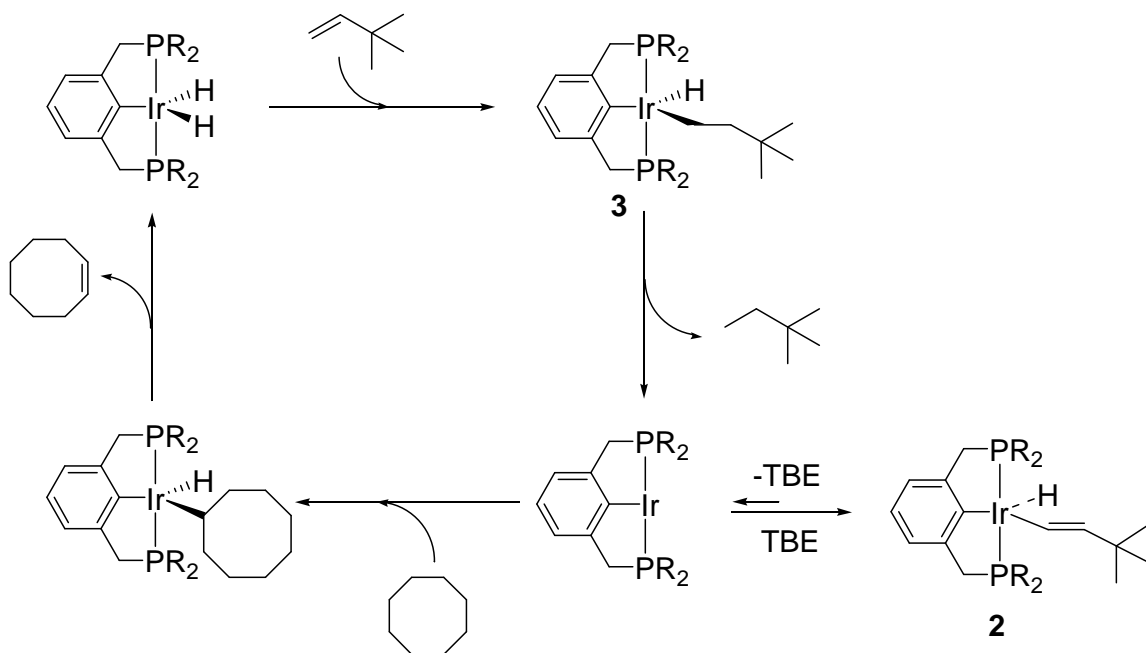
conditions. They suggested that preventing isomerization by modifying catalyst/acceptor combination or efficient separation of the α -olefin would improve the yields of dehydrogenation products.



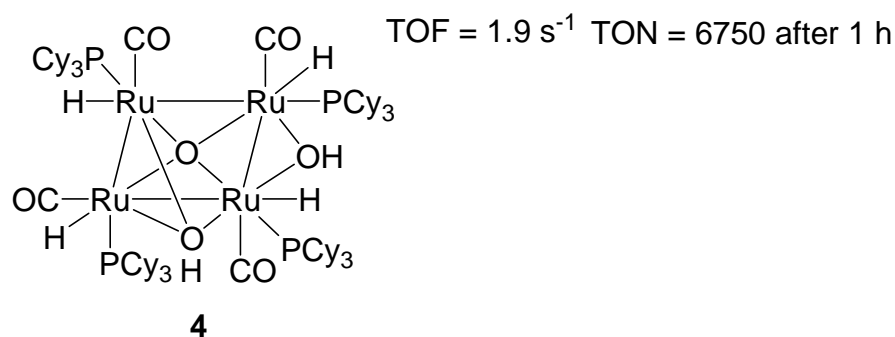
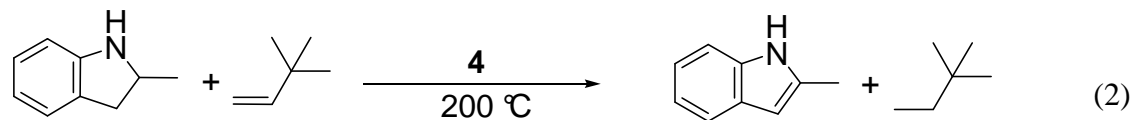
The mechanism of (PCP)IrH₂ catalyzed transfer-dehydrogenation has been disclosed for the prototypical substrate/acceptor combination, COA/TBE (cyclooctane/*t*-butylethylene) at 55 °C (Scheme 1). The catalytic cycle may be viewed as the sum of two reaction: (1) hydrogenation of TBE by (PCP)IrH₂ and C-H addition of a second mole of TBE to give (PCP)IrH(*t*-butylvinyl) (**2**), and (2) dehydrogenation of COA by (PCP)IrH(*t*-butylvinyl) have been observed as resting states during catalysis and the ratio of these two complexes is found to be proportional to [TBE].¹⁹ Based on the proportionality constant obtained and the catalytic rate as a function of [TBE] (which reaches a maximum at ca. 0.3 M), the respective rate constants for the hydrogenation and dehydrogenation segments can be obtained. A good agreement is found between reaction rates independently obtained from stoichiometric and catalytic runs. For the overall TBE-hydrogenation reaction, labeling experiments indicate that the rate-limiting step is reductive elimination of TBA (2,2-dimethylbutane) from (PCP)IrH(*t*-butylethyl) (**3**). Based on the considerations of microscopic reversibility, it can be further inferred that the

rate-limiting step for alkane dehydrogenations is the oxidative C-H addition to iridium center rather than the β -hydride elimination.

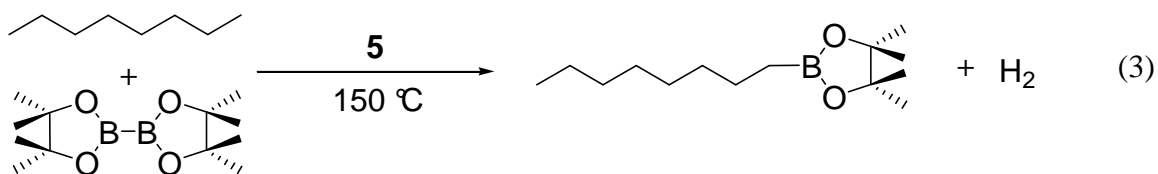
Scheme 1



Recently, our research group has reported that the tetranuclear ruthenium- μ -oxo-hydroxo-hydride complex $\{[(PCy_3)(CO)RuH]_4(\mu_4-O)(\mu_3-OH)(\mu_2-OH)\}$ (**4**) is a highly effective catalyst for the transfer dehydrogenation of amines and carbonyl compounds.²⁰ For example, the initial turnover rate of the dehydrogenation of 2-methylindoline was measured to be 1.9 s^{-1} with TON of 7950 after 1 h at $200 \text{ }^\circ\text{C}$ (eq 2). From a synthetic point of view, the ruthenium catalyst **4** has a number of salient features compared to other dehydrogenation catalysts, in that it is air- and water-stable in solid state and is compatible with a variety of heteroatom functional groups.



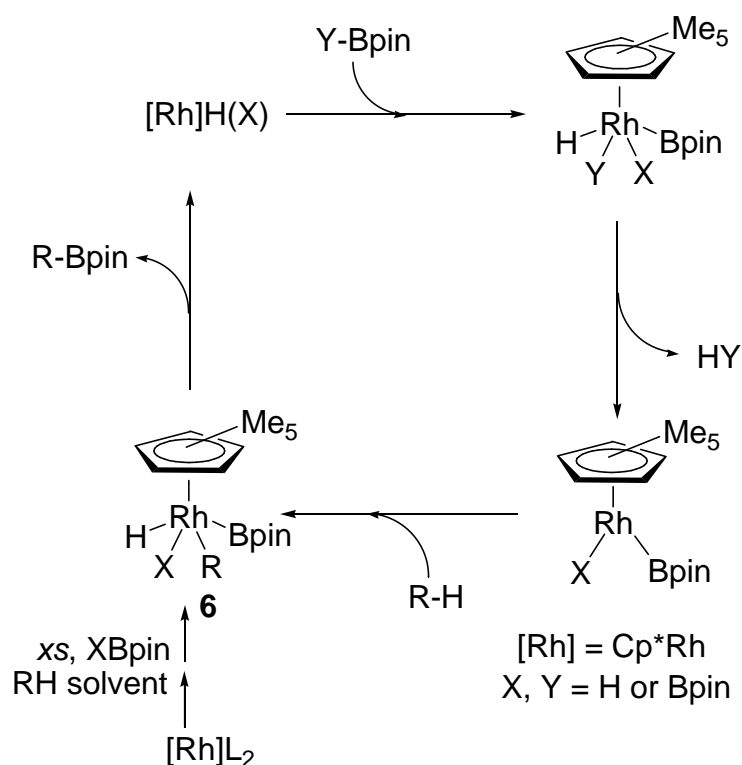
Hartwig reported regiospecific functionalization of linear alkanes catalyzed by the rhodium complex Cp*Rh(η^4 -Cp*) (**5**) under thermal conditions, specifically the coupling of linear alkanes with borane reagents of form primary alkylboranes (eq 3).¹⁴ These borane products are valuable synthetic precursor in organic chemistry. They can be easily converted to amines, alcohols, alkenes, and other classes of functionalized molecules.



A detailed mechanism for the overall catalytic reaction has not been deduced, but an outline of possible mechanism is provided in Scheme 2. Oxidative addition of borane or diboron compound, depending on the boron reagent present, could form a hydridorhodium boryl complex or a rhodium bis(boryl) complex. After H₂ or borane elimination, such complex could then react with alkane to produce an alkyrhodium boryl

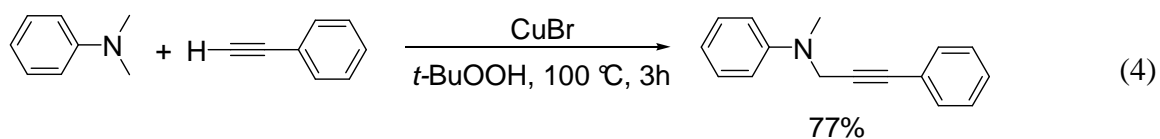
complex (**6**). Rapid B-C bond formation would then lead to product. To probe for the presence of metal-boryl intermediates, they obtained ^{11}B NMR spectra of reactions of the diboron compound with *n*-octane at high catalyst loads. They observed a signal at δ 40 ppm during the reaction, and this chemical shift, which is located downfield of the organoboronate esters and pinacolborane, is characteristic of a metal-boryl species.

Scheme 2

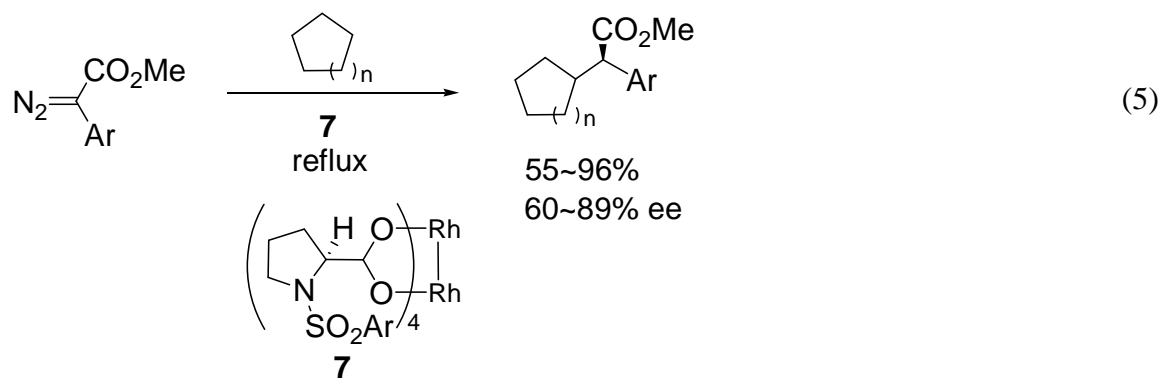


Direct oxidative functionalization of tertiary amines is of considerable importance in organic synthesis. Propargylic amines are of considerable pharmaceutical interest and are synthetic intermediates for the synthesis of various nitrogen containing compounds as well as carbohydrates. Li reported an oxidative cross-coupling of amines and alkynes via

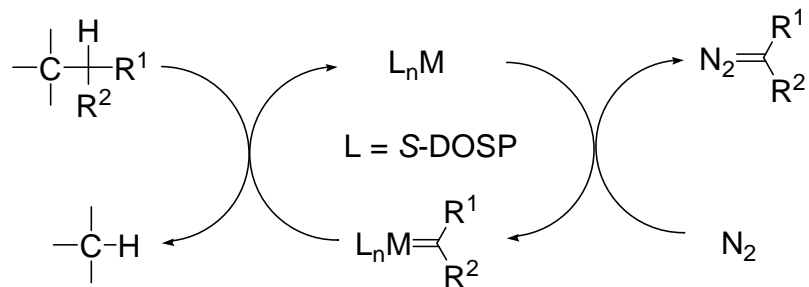
a direct sp^3 C-H bond alkylation in presence of CuBr as a catalyst. The reaction of *N,N*-dimethylaniline with phenylacetylene catalyzed by CuBr with *t*-BOOH at 100 °C for 3 h was produced to *N*-methyl-*N*-(3-phenylprop-2-ynyl)benzenamine in 77% isolated yield (eq 4).²¹



Rhodium carbenoids derived from methyl aryldiazoacetates are efficient catalyst for asymmetric C-H activation of a range of alkanes and tetrahydrofuran through a C-H insertion mechanism. The decomposition of methyl aryldiazoacetates catalyzed by dirhodium tetrakis(*S*-(*N*-dodecylbenzenesulfonyl)prolinate) ($\text{Rh}_2(\text{S-DOSP})_4$) (**7**) in the presence of alkenes gave an intermolecular C-H insertion having a good control of regioselectivity, diastereoselectivity, and enantioselectivity (eq 5).²² The carbenoids derived from methyl aryldiazoacetates are greatly more chemoselective than those derived from diazoacetates. They favor C-H insertions into secondary and tertiary sites and the formation of side products which is caused by carbene dimerization is not a major problem with rhodium carbenoids derived from aryldiazoacetates.



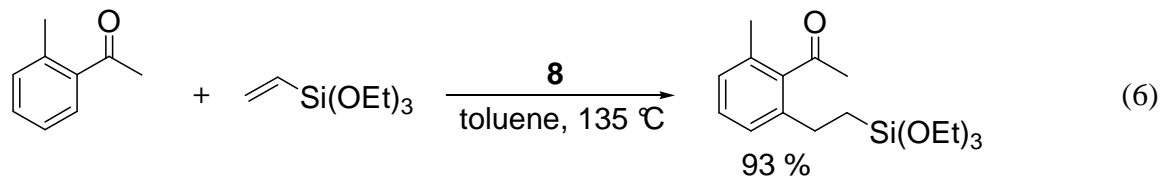
Scheme 3



1.2 Arene C-H Bond Activation

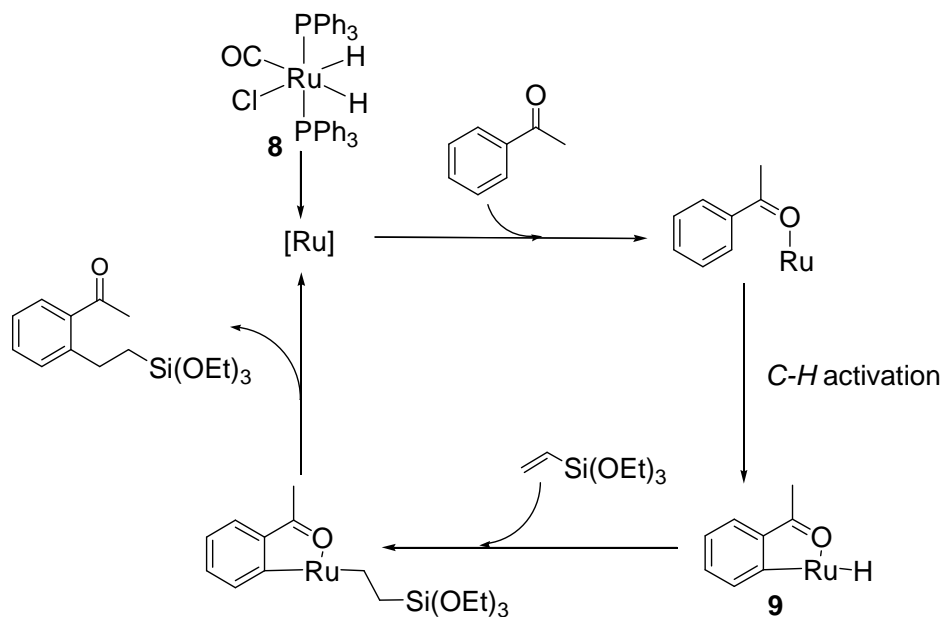
1.2.1 Chelate-Assisted Arene C-H bond Activation Reactions

Murai pioneered chelate-assisted, regioselective, catalytic C-H bond activation of arene and olefin coupling reaction.³ For example, acetophenone is added to vinyl silane to yield regioselectively alkylated product at the *ortho* position (eq 6). The ruthenium complex $\text{RuH}_2(\text{CO})(\text{PPh}_3)_3$ (**8**) was found to be an efficient catalyst for this coupling reaction. This reaction is a quite effective synthetic method, and, in many cases, gave nearly quantitative yields.



As shown Scheme 4, Murai proposed that the reaction involves the coordination of the carbonyl group of arylketones to the ruthenium center and is placed in a favorable position for the cleavage of the C-H bond. The ruthenium hydride complex **9** has been suggested as a key intermediate species. The rate-limiting step of the coupling reaction is the C-C bond forming step instead of C-H activation step.

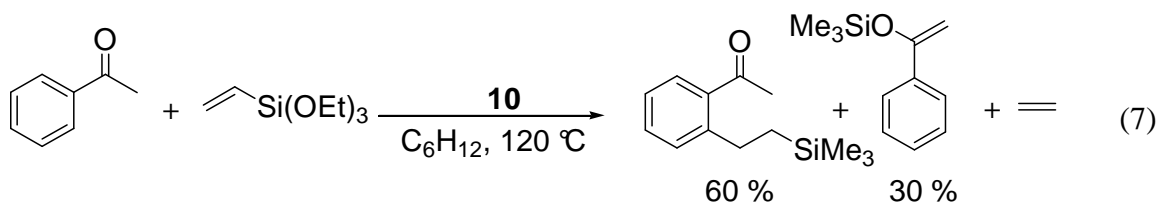
Scheme 4



The reaction was extended to various arene and olefin coupling reactions. One of the most important findings in elucidation of the mechanism of coupling reaction is that

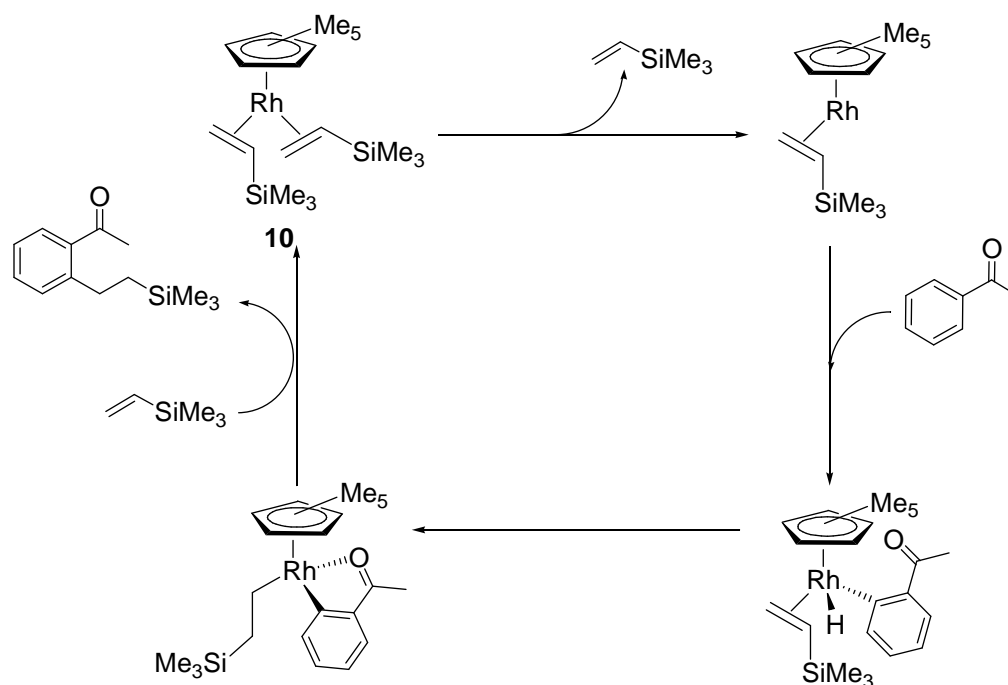
the C-H bond cleavage step is not the rate-limiting step. Instead a rapid equilibrium exists prior to the reductive elimination step that leads to the C-C bond formation. Murai has established that the reductive elimination of alkylated products is the rate-determining step.

The rhodium bis-olefin complex $[\text{Cp}^*\text{Rh}(\text{CH}_2=\text{CHSiMe}_3)_2]$ (**10**) has also been shown to be an effective catalyst for selective addition of olefins to the *ortho* position of arylketones (eq 7).⁸ A main difference between eq 1 and eq 3 is that in the ruthenium-catalyzed process, a carbonyl coordination is presumed to be the first step, which directs the C-H bond activation to the *ortho* position of the aromatic substrate.

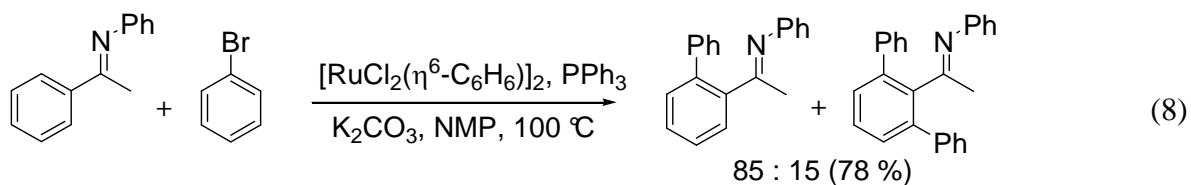


H/D exchange experiments establish that *para* and *meta* C-H bonds are not activated in the ruthenium system. The rhodium catalytic processes, on the other hand, are not discriminating in the C-H bond activation step and activation of all sites (*ortho*, *meta*, and *para*) of the substrate is observed. Murai has established that the C-H bond activation is fast and reversible in the ruthenium case and reductive elimination of the alkylated product is the rate-limiting step. It is believed that the similar features are applied to the rhodium system as well, but no conclusive evidence is available concerning this point. In the both systems, the energy barrier for reductive elimination which then forms the product is decreased by chelation of the carbonyl group to the metal center.

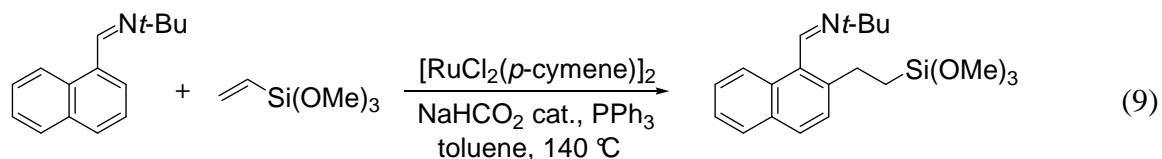
Scheme 5



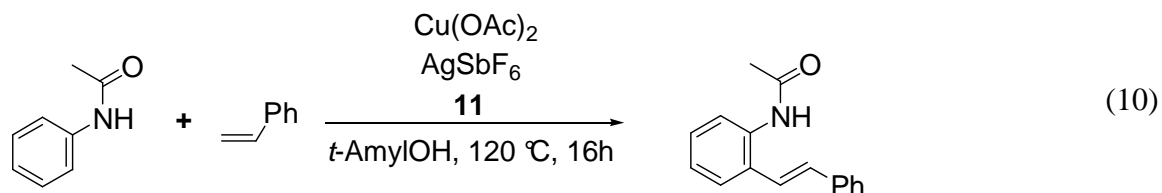
The *ortho* position of imine substituted aromatic compounds is directly arylated and alkenylated with organic halides in the presence of catalytic amount of a ruthenium-phosphine complex. In this reaction, the imine group acts as a directing group for *ortho*-metallation step (eq 8).²³



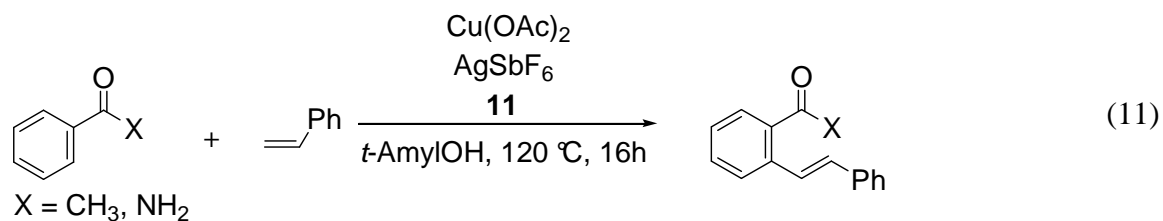
Aromatic aldimines have been found to be a suitable substrate for coupling reaction with either vinylsilanes or styrenes in the presence of ruthenium(II) complex and phosphine ligand via C-H bond activation at the *ortho* position (eq 9).²⁴



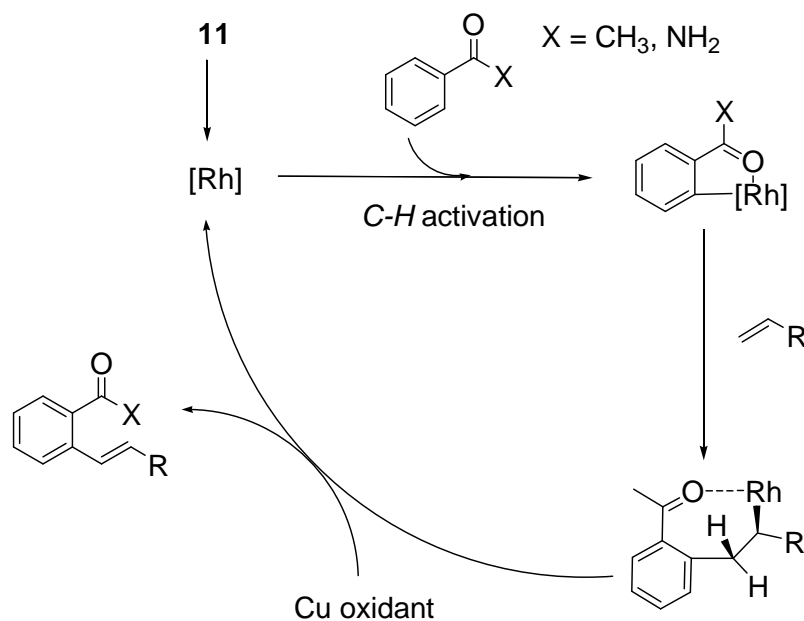
Recently, Glorius has reported the selective rhodium catalyzed oxidative olefination of aromatic carbonyl compounds such as acetanilide, acetophenone and benzamide derivatives with olefins involving *ortho* C-H activation.²⁵ The C-H bond activation of acetanilide and subsequent coupling to styrene was found to proceed smoothly at 0.2 M in tert-amyl alcohol as solvent employing only 0.5 mol% of $[\text{RhCp}^*\text{Cl}_2]_2$ (**11**) catalyst precursor (eq 10).



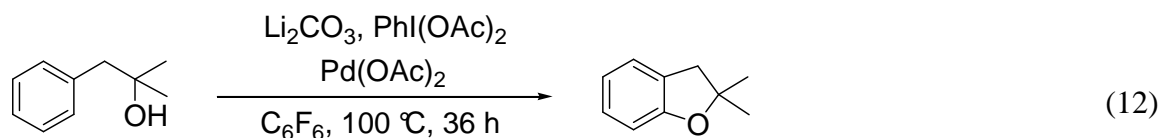
Glorius has also published the oxidative olefination of acetophenones and electronically related benzamides with various olefins. Acetophenone and benzamide coupled with styrene selectively to give a single product each in good yield (eq 11).²⁶ He also proposed that the oxidative olefination reaction proceeds through chelate-assisted *ortho* C-H activation, followed by olefin insertion to rhodium center and subsequent β -hydride elimination to selectively yield the *E* selective coupling product. (Scheme 6).



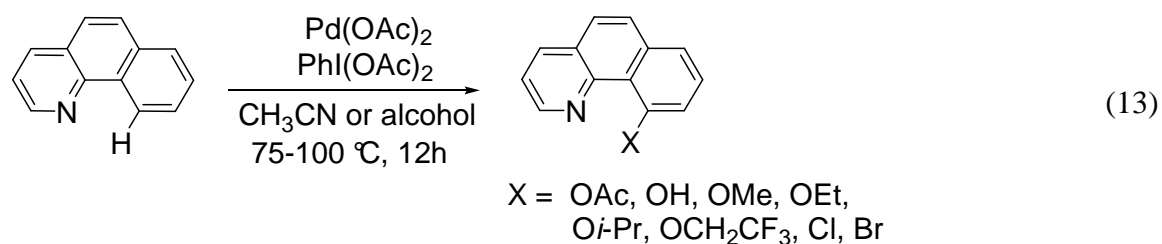
Scheme 6



Yu has developed a new dihydrobenzofuran ring-forming process via hydroxy-directed C-H activation/C-O bond formation (eq 12).²⁷ Tertiary alcohols were cyclized to give the corresponding dihydrobenzofurans in good yield in the presence of Pd(OAc)₂ with PhI(OAc)₂ as an oxidant. This reaction provides a new method for constructing dihydrobenzofurans, including spirocyclic analogues, a process that is potentially applicable to natural product synthesis.



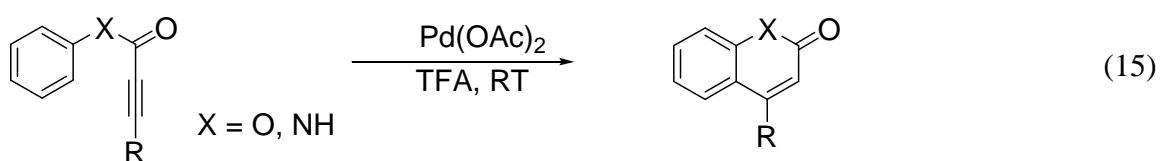
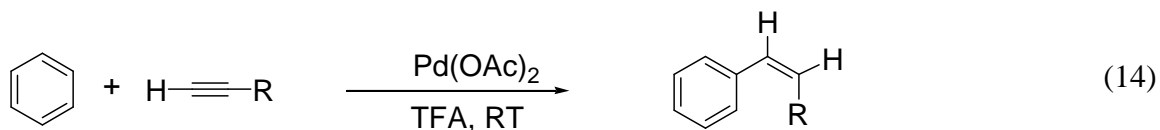
Sanford has developed a selective catalytic coupling method for the oxidative functionalization of C-H bonds.²⁸ The combination of 1 equiv of benzo[*h*]quinolone with PhI(OAc)₂ (2 equiv) and 2 mol% Pd(OAc)₂ in CH₃CN at 75 °C for 12 h produces an 1:1 ratio of the monoacetoxyated product (X = OAc) and the analogous phenol (X = OH) in 86% isolated yield (eq 13). They has also found that simple modification of the reaction condition allows the selective installation of a variety of different functional groups at C₁₀. For example, reaction of benzo[*h*]quinolone with PhI(OAc)₂/catalytic Pd(II) in alcohol solvents produces a range of sterically and electronically diverse alkyl-aryl ethers (X = OMe, OEt, *Oi*-Pr, OCH₂CF₃) in good yield. Alternatively, when oxidation is carried out in the presence of excess LiX (X = Cl, Br) in CH₃CN, traces of mono-halogenated products are formed.



1.2.2 Nonchela-Assisted Reactions

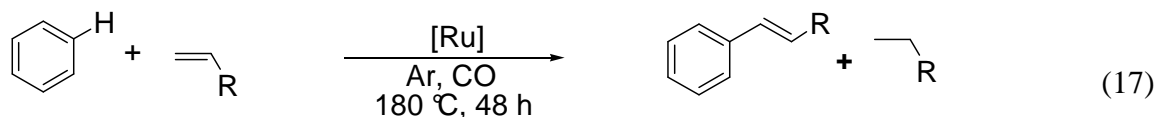
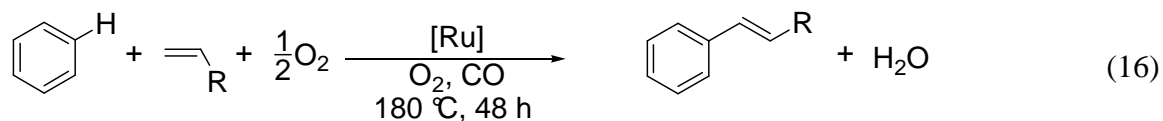
Fujiwara reported the effective metalation of aromatic C-H bonds at room temperature using highly-electrophilic, *in situ* generated, Pd(II) and Pt(II) cationic species

in trifluoroacetic acid (TFA), leading to the regioselective inter- and intramolecular addition of simple arenes to C-C multiple bonds (eqs 14 and 15).²⁹



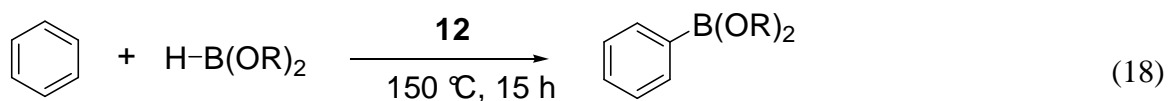
In most cases, the addition of alkynes exclusively affords the thermodynamically less stable *cis*-aryl alkene. The intramolecular hydroarylation of C≡C bonds is facile and regioselective because of the electrophilic metalation of aromatic C-H bonds by the Pd(II) cationic species which is assisted by ethynyl coordination. In fact, this intramolecular reaction combines both chelation assistance and electrophilic metalation.

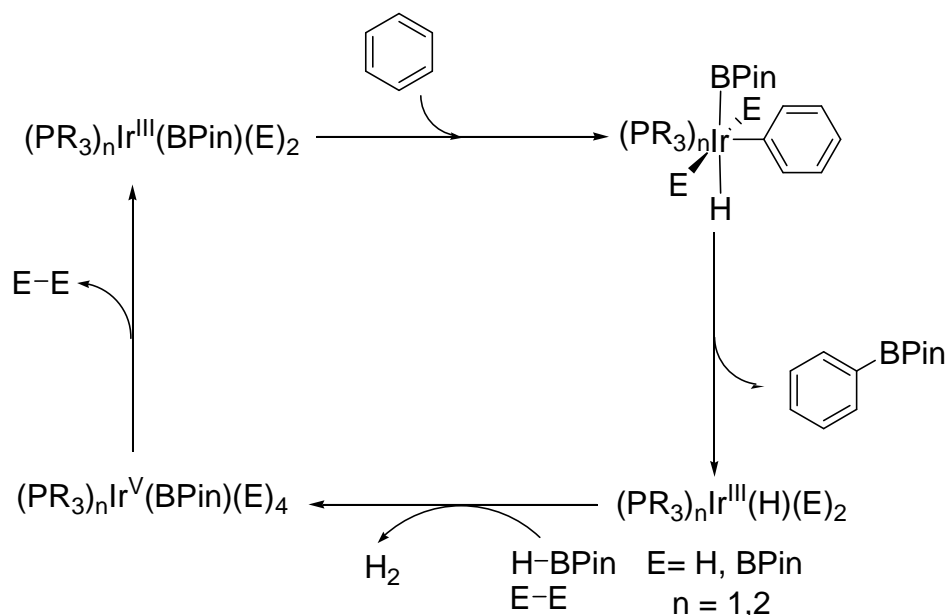
Milstein's Heck-type oxidative coupling reaction, which was found to be promoted by molecular oxygen, is among the most remarkable examples of ruthenium-catalyzed arene C-H bond insertion reactions (eqs 16 and 17).³⁰ The catalytic oxidative coupling of arenes with alkenes to generate aryl alkenes, in which the double bond is preserved, is a highly desirable goal. Since the reaction does not require the utilization of reactive substituent and does not form any byproducts, it has a unique advantage over other methods for the preparation of aromatic alkenes, especially when compare to the well-known Heck reaction for the vinylation of aryl halides.



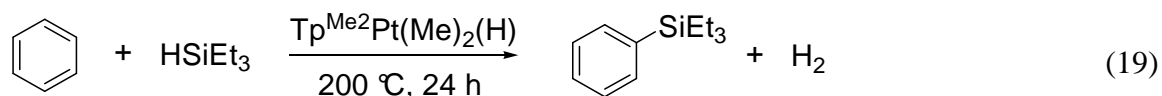
In Milstein's Heck type coupling, dioxygen can be directly used as the oxidant, while still retaining good catalytic activity. The reaction is catalyzed by ruthenium complexes under a CO atmosphere condition. Readily available ruthenium complexes such as $\text{RuCl}_3 \cdot 3\text{H}_2\text{O}$, $[\text{Ru}(\text{CO})_3\text{Cl}_2]_2$, $[(\eta^6\text{-C}_6\text{H}_6)\text{RuCl}_2]_2$, $\text{Ru}(\text{NO})\text{Cl}_3 \cdot 5\text{H}_2\text{O}$, and $\text{Ru}(\text{F}_3\text{CCOCHCOCF}_3)_3$ show essentially the same catalytic activity.

Smith has described that iridium catalysts $(\text{MesH})\text{Ir}(\text{BPin})_3$ ($\text{MesH} = \eta^6\text{-mesitylene}$, $\text{BPin} = \text{oxaborolane}$) (**12**) are efficient for direct synthesis of arylboron compounds from aromatic hydrocarbons and boranes under "solventless" conditions (eq 18).³¹ The Ir catalysts are highly selective for C-H bond activation and do not interfere with subsequent transformations, including Pd-mediated cross-coupling with aryl halides. By virtue of their favorable activities and exceptional selectivities, these Ir catalysts impart the synthetic versatility of arylboron reagents to C-H bonds both aromatic and heteroaromatic hydrocarbons.



Scheme 7

Smith proposed a reaction mechanism involving Ir(III) and Ir(V) intermediates as shown in Scheme 7. The following evidence supports the mechanism proposed in Scheme 7: (a) Borylation products of iodobenzene are not obtained when Ir(I) sources are used under stoichiometric or catalytic conditions, whereas Ir(III) complexes effect both stoichiometric and catalytic borylations. (b) Improved catalytic activity is observed with chelating phosphines and inhibition is observed when [phosphine]:[iridium] ratios equal or exceed 3:1, strongly supporting the viability of bisphosphine intermediates (Scheme 4, $n = 2$), which could be generated via E-E reductive elimination ($\text{E} = \text{H, BPin}$) from an 18-electron bisphosphine Ir(V) resting state. (c) The 18 electron bisphosphine compound, $\text{IrH}_5(\text{PMe}_3)_2$, is an efficient precatalyst for the borylation.

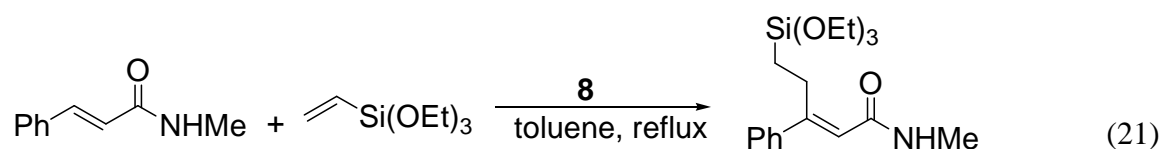
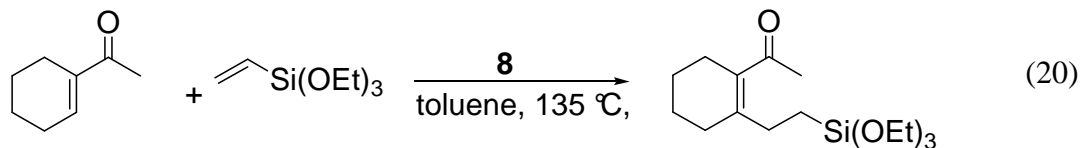


Hartwig discovered a highly selective, acceptorless dehydrogenative coupling of silanes with arene C-H bonds in good yields in the presence of $\text{Tp}^{\text{Me}_2}\text{PtMe}_2\text{H}$ (Tp^{Me_2} = hydridotris(3,5-dimethylpyrazolyl)borate) and related platinum(IV) complexes (eq 19).³² The reaction of the arenes occurred selectively at the least sterically hindered C-H bonds and preferentially with more electron-poor arenes. If the dehydrogenative coupling of simple silanes with aromatic and aliphatic C-H bonds could be developed, then useful reactions could result. Because of the higher stability of silanes toward disproportionation than boranes, they could undergo tandem or sequential reactions that would be impossible using borane or even disilane reagents.

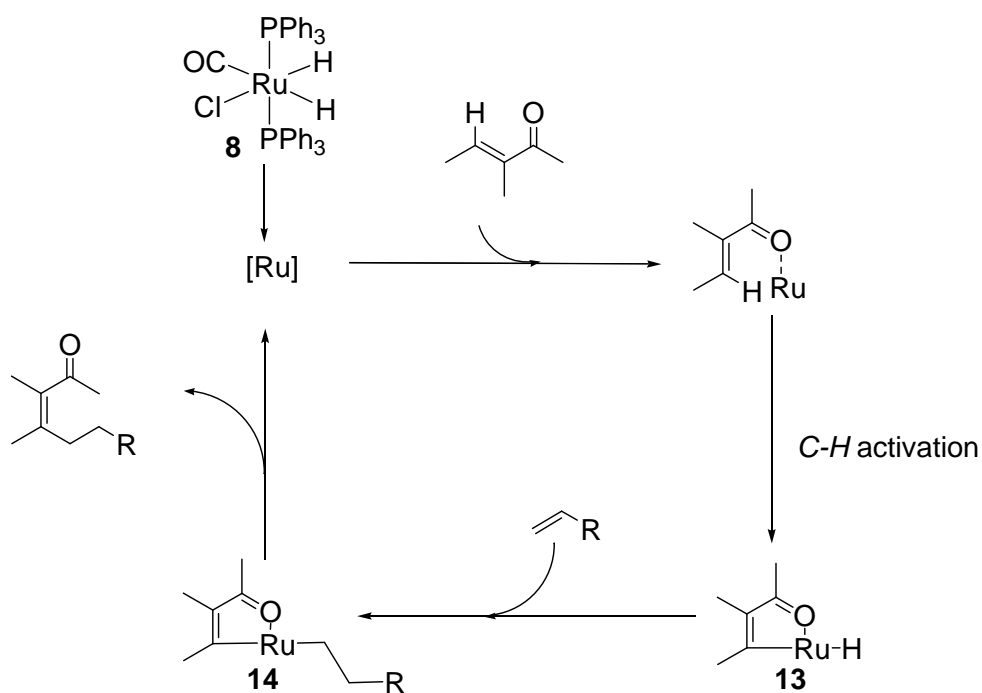
1.3 Chelate-Assisted C-H Bond Activation Reaction of Alkenes

Trost and Murai independently reported the ruthenium catalyzed C-H activation and alkylation of 1-acetylcyclohexene and α,β -unsaturated esters with alkenes such as silylethylenes and styrene.^{4(b),(e)} The reaction of 1-acetylcyclohexene and *N*-methylcinnamide with triethoxyvinylsilane in presence of $\text{Ru}(\text{H})_2(\text{CO})(\text{PPh}_3)_3$ (**8**) gave the coupling product involving vinyl C-H activation (eqs 20 and 21). They proposed the plausible reaction mechanism for olefin-olefin coupling reaction as shown in Scheme 8. The chelation-assisted insertion of ruthenium into the C-H bond by vinyl C-H activation gives **13**. Hydrometallation of alkene would result in the formation of **14**. Reductive

elimination from **14** provides coupling product, regenerating the catalytically active species.



Scheme 8

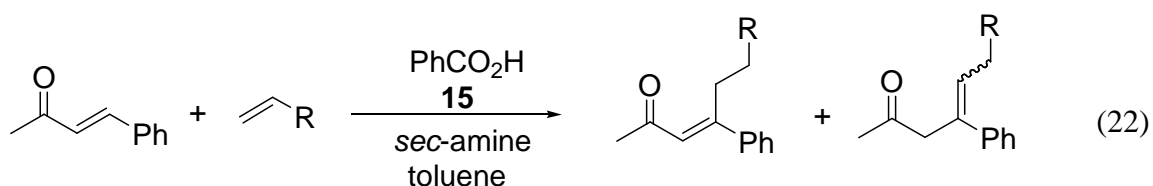


Jun has developed a rhodium(I) catalyzed β -alkylation of the α,β -unsaturated ketone with 1-alkenes employing diethylamine as a efficient chelation-assistant tool.³³

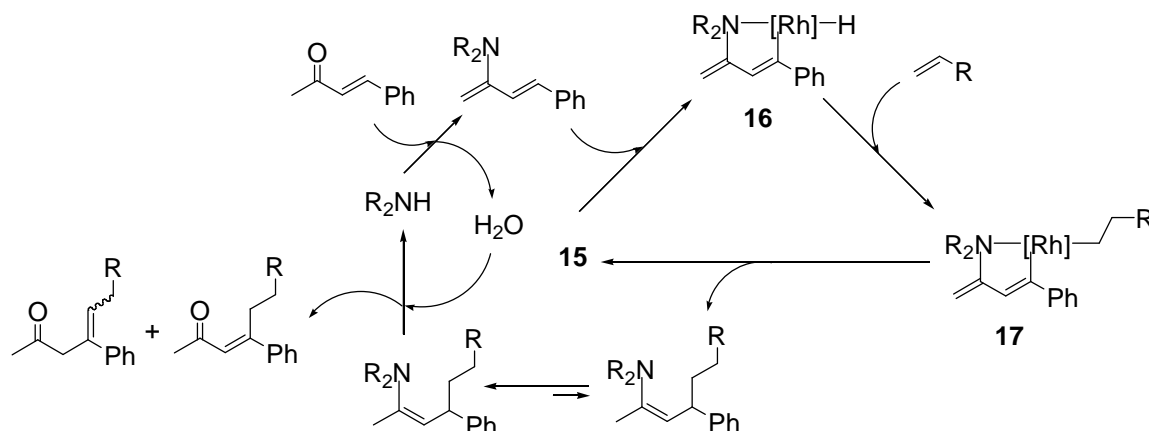
The β -alkylation of 4-phenyl-3-butene-2-one with 1-hexene in presence of $\text{RhCl}(\text{PPh}_3)_3$

(**15**), benzoic acid and diethylamine was found to proceed smoothly at 130 °C for 24 h in good yield (eq 22).

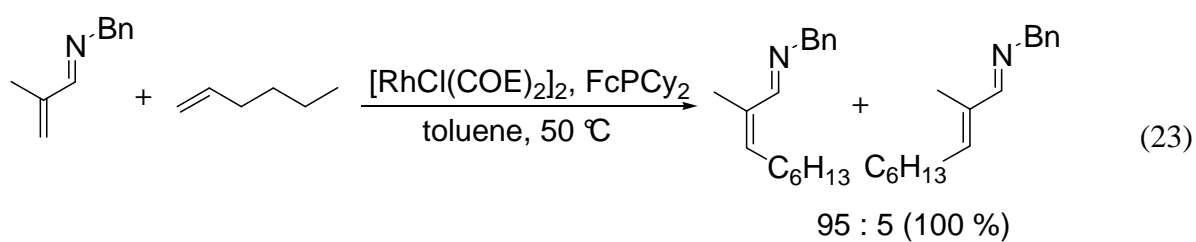
He also proposed the plausible mechanism of this reaction which is illustrated in Scheme 9. Precoordination of a rhodium species to the nitrogen functionality of the dienamide, derived from condensation of the enone with dialkylamine, can facilitate the cleavage of the vinyl C-H bond to generate the stable 5-membered metallacyclic rhodium hydride **16**. Coordination of an olefin followed by migratory insertion of an olefin into the Rh-H bond gives alkylrhodium species **17**. Reductive elimination in **17** furnishes the β -alkylated dienamine compound that equilibrates with regioisomer and regenerates a rhodium catalyst to complete the catalytic cycle. Following acidic hydrolysis of both dienamine regioisomers leads to the β -alkylated products.



Scheme 9



Ellman and Bergman have reported the stereoselective alkylation of α,β -unsaturated imines via the directed activation of a C-H bond by rhodium catalyst.³⁴ The rhodium complex which is $[\text{RhCl}(\text{COE})_2]_2$ has been found to be effective catalyst with phosphine ligands for coupling reaction with α,β -unsaturated imines and a variety of alkenes (eq 23).



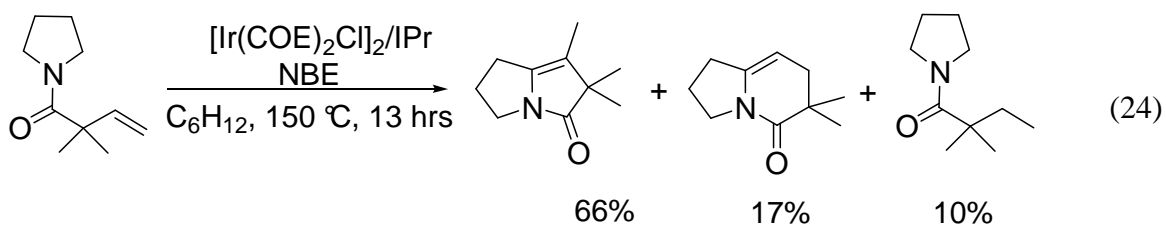
Imine groups are synthetically useful because they can be easily converted to many other functional groups such as ketones, alcohols, carboxylic acids, and amines and the imine is sometimes utilized as a directing group in transition metal catalyzed direct functionalization of aryl or aliphatic compounds using alkenes and alkynes.

1.4 C-H Bond Activation Reactions of Nitrogen Containing Compounds

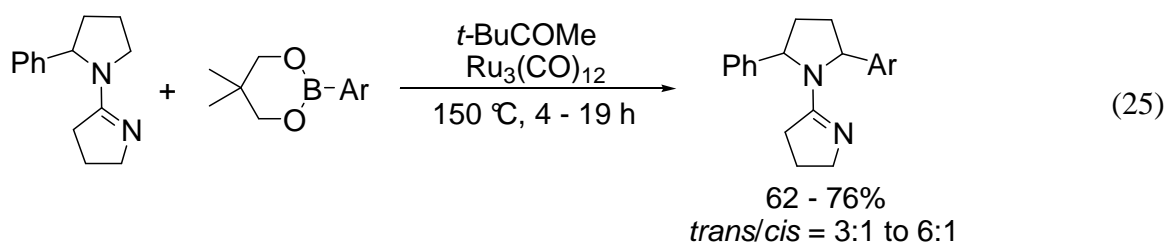
The catalytic reactions and functionalizations which involve cleavage of sp^2 or sp^3 C-H bonds within nitrogen containing compounds, such as amines and amides have attracted considerable attention, in part due to their prominent role in the synthetic utilities of natural products and pharmaceutical agents. Highly regioselective catalytic reactions via C-H activation of nitrogen-containing compounds, especially heterocyclic compounds have been reported by several research groups.³⁵⁻⁴⁷ However, coupling reactions of amide substrates by regioselective C-H activation with alkenes are still very rare.^{16, 48-51, 53}

1.4.1 C-H Bond Activation of Pyrrolidine Derivatives

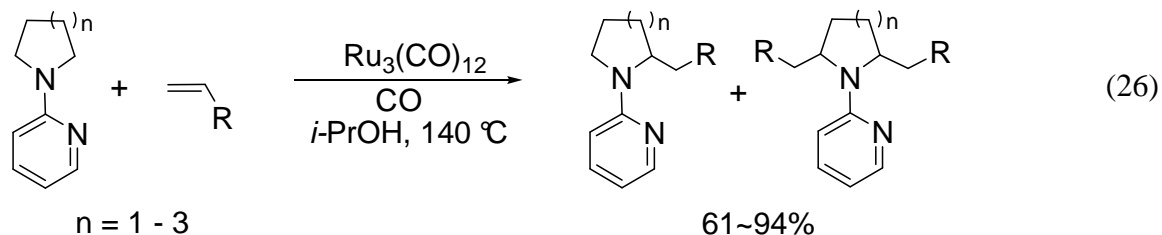
Sames and co-workers have reported the oxidative intramolecular cyclization reaction of alkene-amide substrates under neutral and catalytic conditions. This overall transformation requires tandem sp^3 C-H bond activation at the position adjacent to the amide nitrogen and C-C bond formation. For example, pyrrolidine substrate was converted to pyrrolizidinone and indolizidinone products in 66% and 17% yield, respectively, in presence of $[\text{Ir}(\text{COE})_2\text{Cl}]_2$ with carbene ligand IPr (*N,N'*-bis(2,6-diisopropylphenyl)imidazolyl carbene), and the hydrogen acceptor NBE or TBE (NBE = norbornene) (eq 24).³⁵



with an arylboronate ester.³⁶ Importantly, $\text{Ru}_3(\text{CO})_{12}$ as the catalyst gave the desired product in good yield. The amidine substrates and phenylboronate ester in the presence of ruthenium catalyst and ketone produced a 3:1 ratio of *trans* and *cis* diastereomers (eq 25). The trinuclear ruthenium cluster is required for α -arylation of amidine derivatives because mononuclear and dinuclear ruthenium complexes were found to be much less effective (<10%).

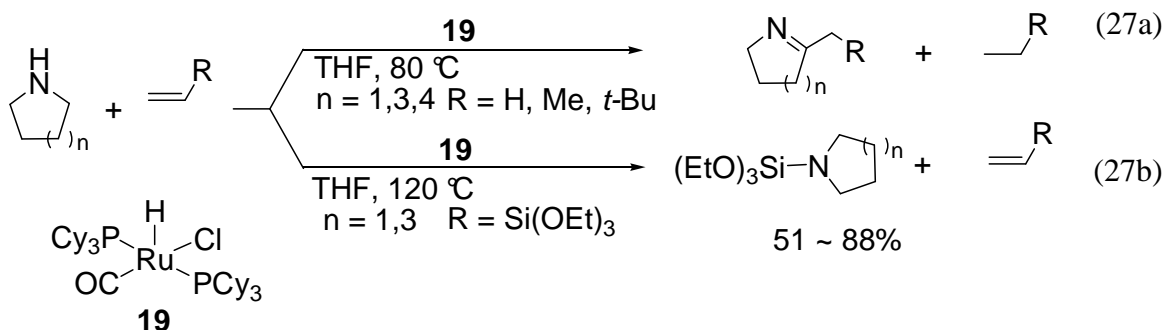


Murai reported catalytic reactions that involve the cleavage of the sp^3 C-H bond adjacent to the nitrogen atom in *N*-2-pyridinyl alkylamines. The use of $\text{Ru}_3(\text{CO})_{12}$ as the catalyst resulted in the insertion of alkenes into sp^3 C-H bonds of the pyrrolidine to give the coupling products (eq 26).³⁷



A variety of terminal, internal, and cyclic alkenes were found to be suitable substrates for the coupling reaction. The presence of a pyridine ring as a directing group on the nitrogen in cyclic amines is necessary for the reaction to proceed, suggesting the importance of the coordination of the pyridine nitrogen to ruthenium.

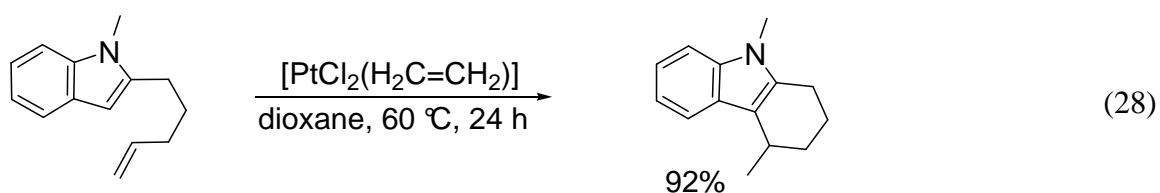
Yi has reported that the complex $(\text{PCy}_3)_2(\text{CO})\text{RuHCl}$ (**19**) is an effective catalyst for dehydrogenative coupling reactions of cyclic amines and alkenes. The coupling reaction of secondary cyclic amine with unactivated alkenes, especially terminal alkenes such as ethylene, propylene, and TBE, preferentially afforded C-H bond insertion products which were selectively activated by sp^3 C-H bond adjacent nitrogen in cyclic amines (eq 27a). In contrast, the reaction of amines with vinylsilane gave the *N*-silylation products (eq 27b).³⁸



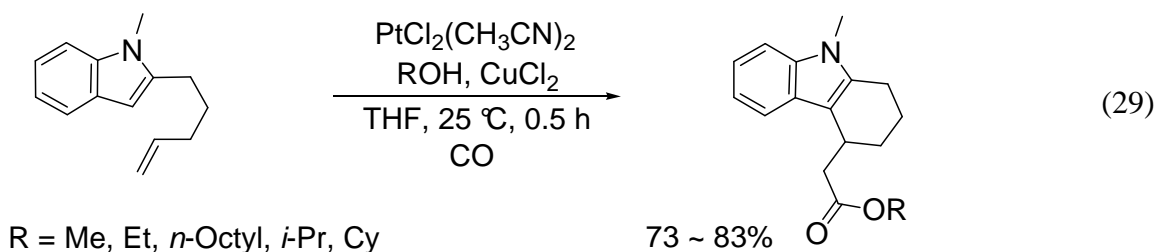
1.4.2 C-H Bond Activation of Indole and Quinoline derivatives

Widenhoefer has reported that the intramolecular alkylation of 2-alkenyl indoles with a catalytic amount of $\text{PtCl}_2(\text{CH}_2=\text{CH}_2)$ in dioxane that contained a trace of HCl at 60 °C for 24 h led to tetrahydrocarbazoles as cyclization products (eq 28).³⁹ Platinum-catalyzed cyclization of 2-(4-pentenyl)indoles showed good generality and tolerated

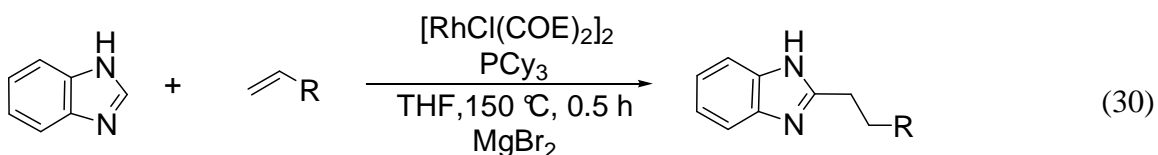
substitution at each position of the 4-pentenyl chain including the internal and *cis*- and *trans*-terminal position. Also, this synthetic method was applicable to the synthesis of tetrahydro- β -carbolinones and was effective for cyclization of unprotected indoles. 2-(3-Butenyl)indoles were carried out platinum-catalyzed cyclization with 6-*endo*-trig regioselectivity. Mechanistic studies established a mechanism for the platinum-catalyzed cyclization of 2-alkenyl indoles involving a nucleophilic attack of the indole on a platinum-complexed olefin.



In contrast, the reaction of 1-methyl-2-(4-pentenyl)indole with a catalytic amount of $\text{PdCl}_2(\text{CH}_3\text{CN})_2$, and a stoichiometric amount of CuCl_2 in methanol under CO atmosphere at room temperature for 0.5 h, led to the cyclization and carboalkoxylation to form the corresponding tetrahydrocarbazole as a single regioisomer in 83% yield (eq 29).⁴⁰ Palladium-catalyzed cyclization/carboalkoxylation of 2-(4-pentenyl)indoles tolerated substitution along the alkenyl chain and at the internal and *cis*-terminal positions. A variety of alcohols were also tolerated for palladium-catalyzed cyclization/carboalkoxylation. This cyclization/carboxylation catalyzed by palladium complex was also effective for cyclization of 2-(3-butenyl)indoles, 3-(3-butenyl)indoles, 3-(4-pentenyl)indoles, and 2-(5-hexenyl)indoles.

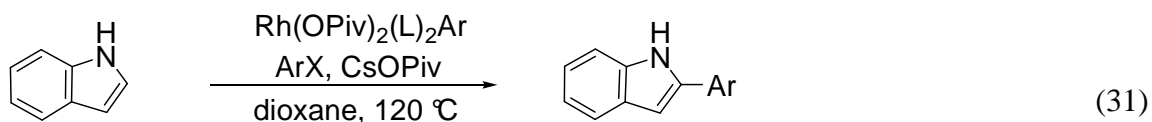


Bergman and Ellman have reported the first intermolecular coupling of unactivated alkenes to heterocycles by using Rh(I) catalyst (eq 30).^{16(b)} A wide range of heterocycles were employed in the reaction, and a variety of functional groups could be incorporated, including esters, nitriles, and acetals. The intermolecular coupling were found to be promoted by weak Lewis acids such as MgBr_2 , which dramatically increased the reaction rate of both the inter- and intramolecular reactions. Different functional groups can be introduced from readily available starting materials, leading to the potential use of this reaction in drug discovery and process chemistry.



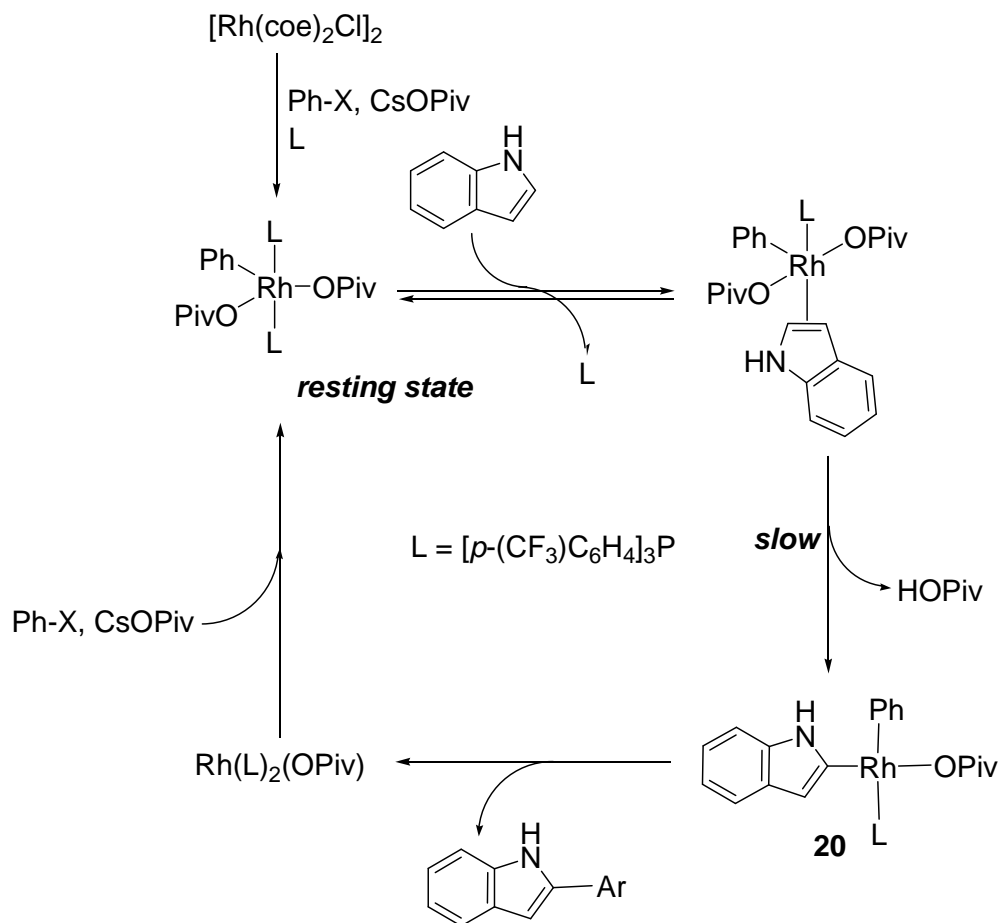
Aryl-rhodium(III) complexes generated *in situ* from the reaction of $[\text{RhCl}(\text{COE})_2]_2$ (COE = *cis*-cyclooctene), $[p\text{-(CF}_3\text{)C}_6\text{H}_4]_3\text{P}$, and CsOPiv efficiently catalyzed the direct C-arylation of free (NH)-indoles and (NH)-pyrroles in presence of mild base in good yields and with high regioselectivity (eq 31).⁴¹ The reaction displayed excellent functional group compatibility and low moisture sensitivity. Kinetics studies

support a mechanism involving phosphine displacement by an indole in Ar-Rh(III) pivalate complexes (resting state of catalyst), followed by a rate-limiting C-H bond metalation.

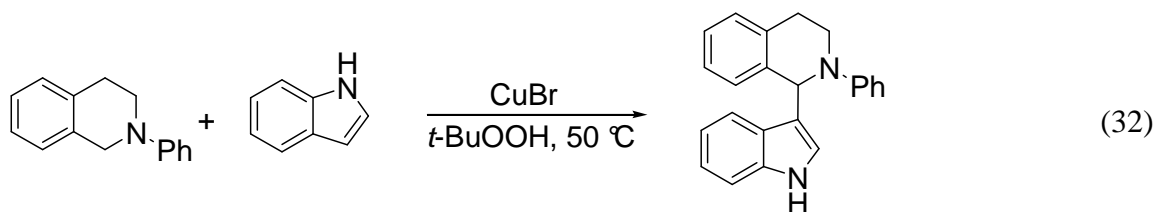


An Ar-Rh(III) pivalate complex is assembled in situ and represents the resting state of the catalyst. Subsequently, displacement of the phosphine ligand by indole takes place in a pre-equilibrium step to form indole-Rh(III) complex, which is followed by the slow C-H bond metalation step as shown Scheme 11. The resulting intermediate **20** then undergoes reductive elimination, furnishing the desired coupling product. The rhodium(I) complex formed in this step is rapidly converted back to the resting state via an oxidative addition of iodobenzene and a halide-pivalate exchange. Thus, the oxidative addition of haloarene precedes the slow C-H transformation step. The model is further supported by the large kinetic isotope effect ($k_{\text{H}}/k_{\text{D}} = 3.0$) at the 2-position of indole. Although the intimate mechanistic details of the C-H metalation step are unclear, they propose that the pivalate ligand assists the C-H bond dissociation as an internal base. This is consistent with the fact that the initial rates of the reaction between indole and Ar-Rh(III) pivalate complex were not affected by the addition of CsOPiv.

Scheme 11

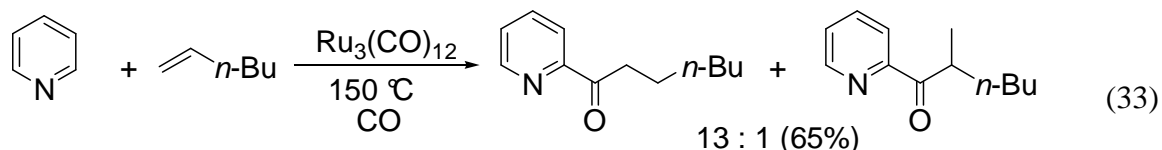


As shown in eq 32, Li has developed a new type efficient C-C bond formation method via a cross-dehydrogenative coupling (CDC) reaction of indoles and tetrahydroquinolines catalyzed by copper bromide in the presence of an oxidizing reagent, like *t*-BuOOH (eq 32).⁴² The CDC reaction provides a simple and efficient catalytic pathway to construct indolyl tetrahydroisoquinolines via combination of sp^3 C-H and aryl sp^2 C-H bond activation followed by C-C bond formation.



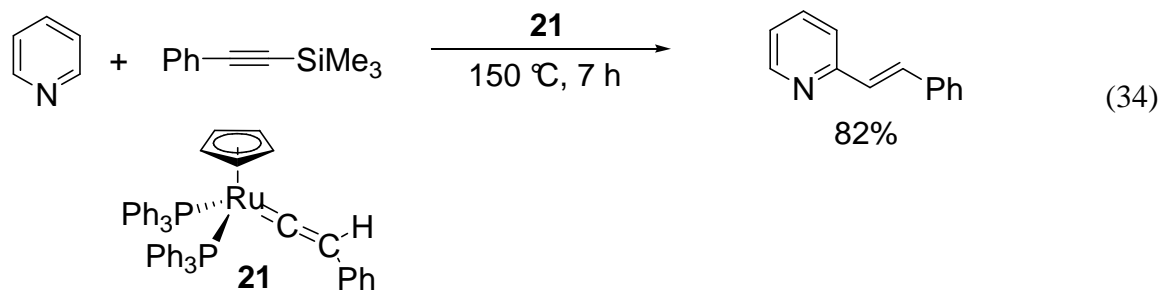
1.4.3 C-H Bond Activation of Pyridine derivatives

Moore reported that $\text{Ru}_3(\text{CO})_{12}$ was found to be a selectively active catalyst for the *ortho* positions in pyridine (eq 33).⁴³ For instance, pyridine is used as solvent and the reaction is conducted at $150\text{ }^\circ\text{C}$ under 10 atm of carbon monoxide. Conversion of 1-hexene to pyridinyl ketone mixture results in the high regioselectivity of the reaction. In addition, no other pyridine containing products are observed.

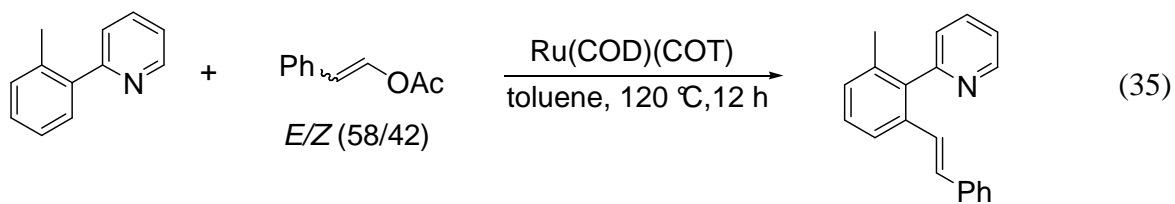


The cationic ruthenium vinylidene complex $[\text{CpRu}(\text{=C}=\text{CHR})(\text{PPh}_3)_2]\text{PF}_6$ (**21**) has been reported to be an effective catalyst for the direct alkenylation reaction of pyridines (eq 34).⁴⁴ Heating the cationic ruthenium vinylidene complex in pyridine at $100\text{--}125\text{ }^\circ\text{C}$ for 24 h gives (*E*)-2-alkenylpyridine. Initially, pyridine coordinates to ruthenium center by displacement of one of the phosphine ligands. Then [2+2] heterocycloaddition occurs to form a 4-membered ruthenacyclic complex. Deprotonation of the β -hydrogen affords a neutral π -azaallyl complex. Protonolysis produces the product. As a result, a vinylidene group is inserted into the α -C-H bond of pyridine. The

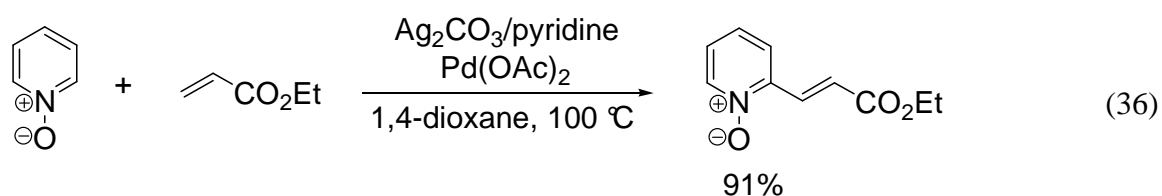
alkenylation reaction is made catalytic in ruthenium by the use of (alkyn-1-yl)silane as the vinylidene source. Treatment of (alkyn-1-yl)trimethylsilane with pyridine in the presence of cationic ruthenium complex affords the corresponding (*E*)-2-alkenylpyridine not only in a good yield but also in a regio- and stereoselective manner.



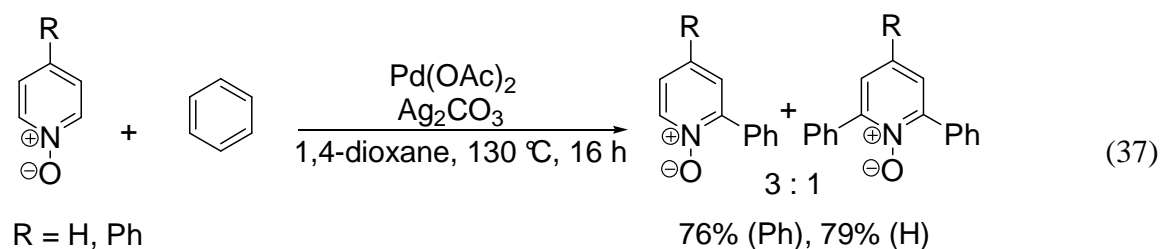
Recently, Kakiuchi has reported a new method for producing π -conjugated aromatic compounds by the ruthenium catalyzed alkenylation of an aromatic C-H bond in arylpyridines and related compounds with alkenyl esters (eq 35).⁴⁵ This reaction provides a new halogen-free reaction condition that can be used in the synthesis of π -conjugated aromatic compounds. For example, the reaction of 2-(2-tolyl)pyridine with styryl acetate in presence of Ru(COD)(COT) (COD = 1,5-cyclooctadiene, COT = 1,3,5-cyclooctatriene) as a catalyst, provides the *E*-isomer as the sole product in 98% yield.



Chang has reported two new types for the oxidative C-C bond formation of pyridine *N*-oxides; selective alkenylation and direct cross coupling reaction with unactivated arenes (eq 36).⁴⁶ For selective alkenylation, reaction proceeds highly efficiently when Pd(OAc)₂ was used in combination with Ag₂CO₃ (1.5 equiv.) and pyridine (1.0 equiv.) with pyridine *N*-oxides and ethyl acrylate affords highly site selective coupling product in good yield.

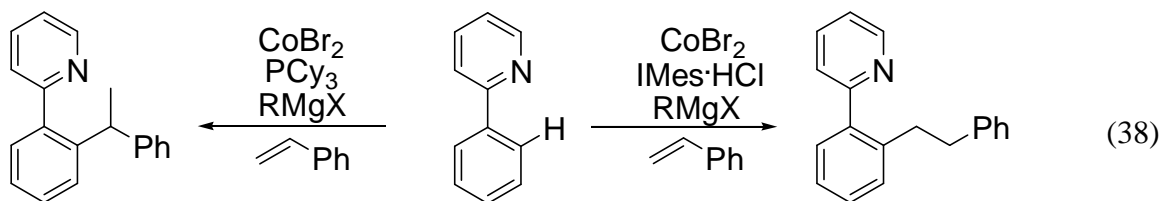


Chang also discovered the direct arylation of pyridine *N*-oxides with unactivated arenes catalyzed by palladium complex. For instance, reaction of pyridine *N*-oxide or its *para* derivative with benzene as unactivated arene afforded the corresponding *ortho* phenylated products with 3:1 ratio in high yields (eq 37).



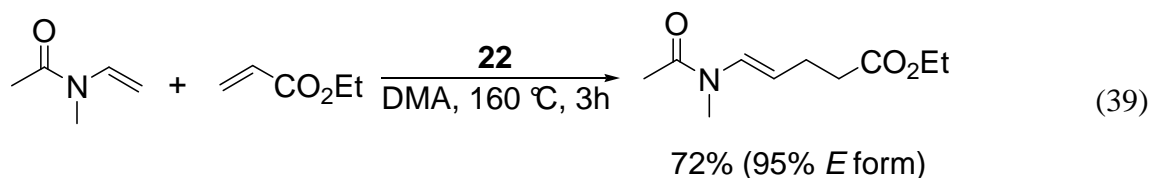
A cobalt-catalyzed, chelate-assisted hydroarylation reactions of styrenes, described by Yoshikai demonstrated that the chelate-assisted C-H bond activation at

ortho position of phenylpyridine derivatives allowed for tuning of the branched/linear regioselectivity by ligand control (eq 38).⁴⁷ The reaction of 2-phenylpyridine with styrene in presence of CoBr_2 , PCy_3 , and $\text{Me}_3\text{SiCH}_2\text{MgCl}$ at 60 °C in THF for 12 h gave a branched product in 88% yield, with high regioselectivity (*b/l* = 96:4). In contrast, when the reaction of 2-phenylpyridine with styrene was performed using $\text{IMes}\cdot\text{HCl}$ (1,3-dimesitylimidazolium chloride), a precursor of an *N*-heterocyclic carbene (NHC) ligand, instead of PCy_3 a near complete switch of the regioselectivity was observed. Thus the reaction afforded the linear product in 84% yield with a regioselectivity of 97:3.

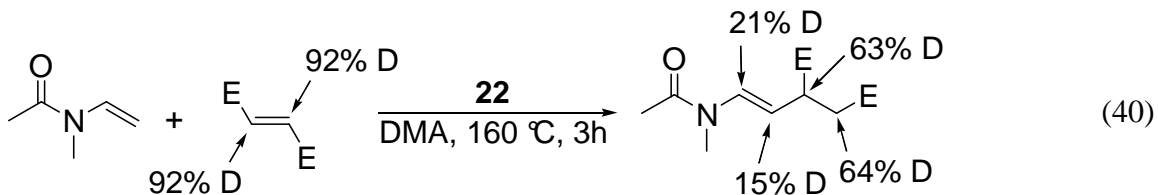


1.4.4 C-H Bond Activation of Amide, Amine, and Imine Derivatives

Recently, Kondo has reported the novel ruthenium-catalyzed regio- and stereoselective codimerization of *N*-vinylamides with alkenes or alkynes. Treatment of *N*-methyl-*N*-vinylacetamide with ethyl acrylate in the presence of a catalytic amount of $[\text{Ru}(\eta^6\text{-COT})(\eta^2\text{-DMFM})_2]$ (COT = 1,3,5-cyclooctatriene, DMFM = dimethyl fumarate) (**22**) in *N,N*-dimethylacetamide (DMA) at 160 °C for 3 h gave the linear codimer, ethyl-5-(*N*-methylacetylamino)-pent-4-enoate, in 90% yield with 95% *E* selectivity (eq 39).⁴⁸



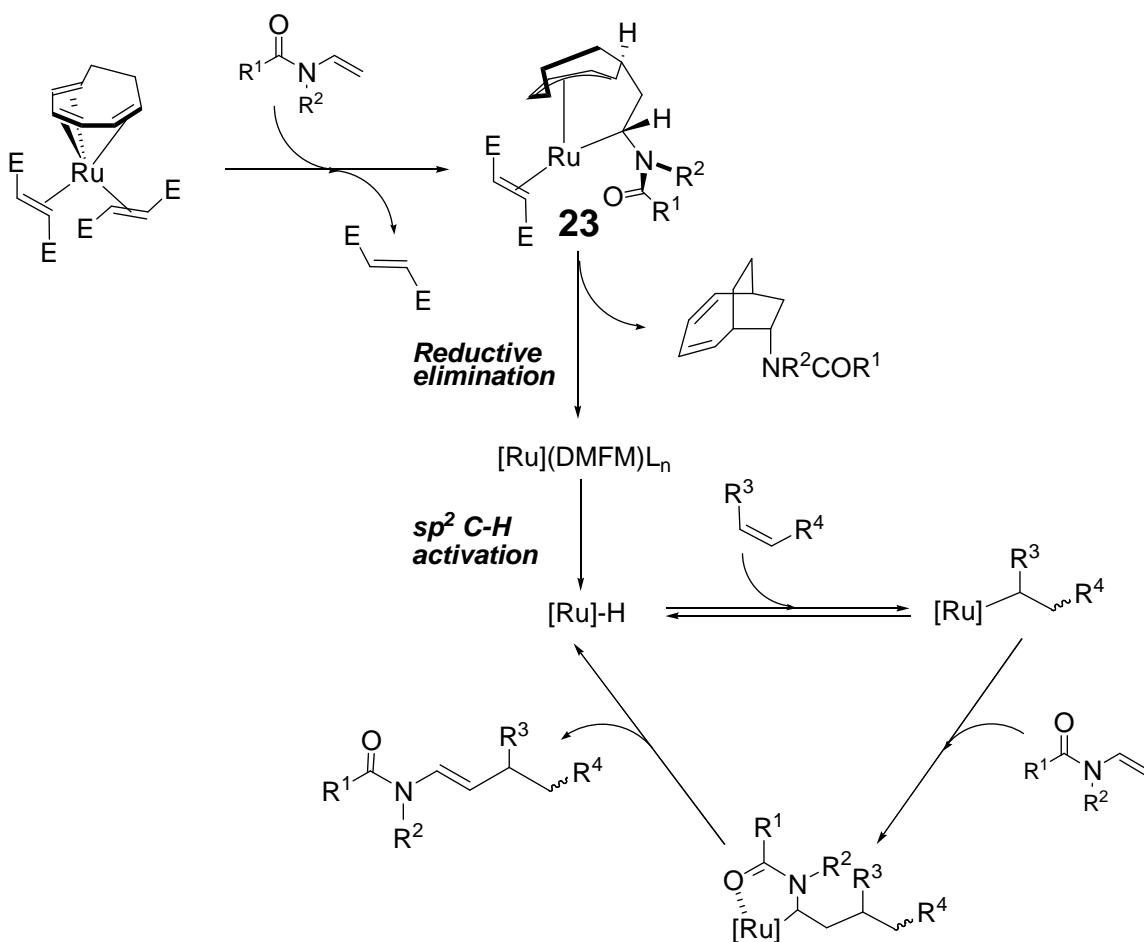
To learn more about this reaction mechanism, they performed a deuterium labeling study. The reaction of *N*-methyl-*N*-vinylacetamide with dimethyl fumarate-*d*₂ was carried out in the presence of [Ru(η^6 -COT)(η^2 -DMFM)₂] catalyst in DMA at 160 °C for 3 h to give the deuterium incorporated product (eq 40). The results of deuterium labeling studies could be explained by the formation of a ruthenium hydride species at an early stage in the catalytic cycle.



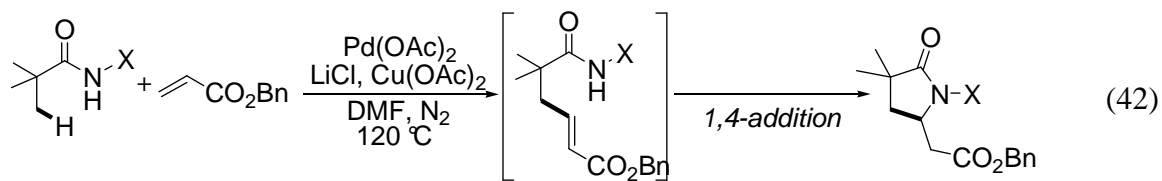
They proposed a reaction mechanism for the codimerization of *N*-vinylamides with alkene (Scheme 12). The reaction starts with the removal of a COT ligand in [Ru(η^6 -COT)(η^2 -DMFM)₂] by *N*-vinylamide through metallacycle formation of **23** and reductive elimination to generate coordinatively unsaturated zero-valent ruthenium hydride species through activation of sp² C-H bonds in alkenes or a DMFM ligand. Alkenes are inserted into a Ru-H bond, followed by the successive chelate-assisted insertion of *N*-vinylamides

into a Ru-C bond. Subsequent β -hydride elimination gives the products with regeneration of an active ruthenium hydride species.

Scheme 12

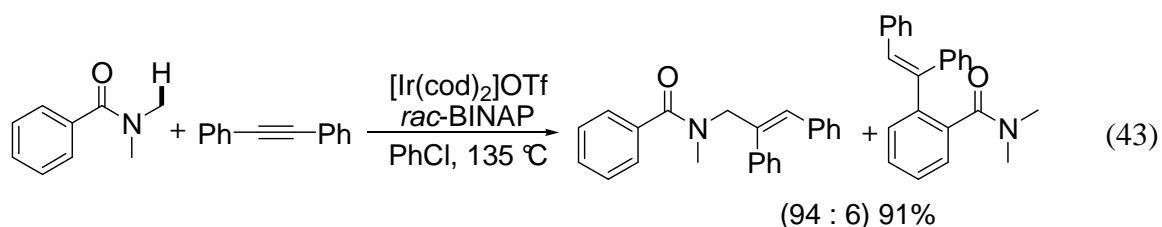


Chatani has discovered the ruthenium-catalyzed cyclocarbonylation of aromatic amides leading to phthalimides through C-H bond activation. The reaction of *N*-(2-pyridinylmethyl)benzamide with CO and ethylene as a H₂ acceptor and H₂O in presence of Ru₃(CO)₁₂ in toluene at 160 °C did not give carbonylation product; instead, the



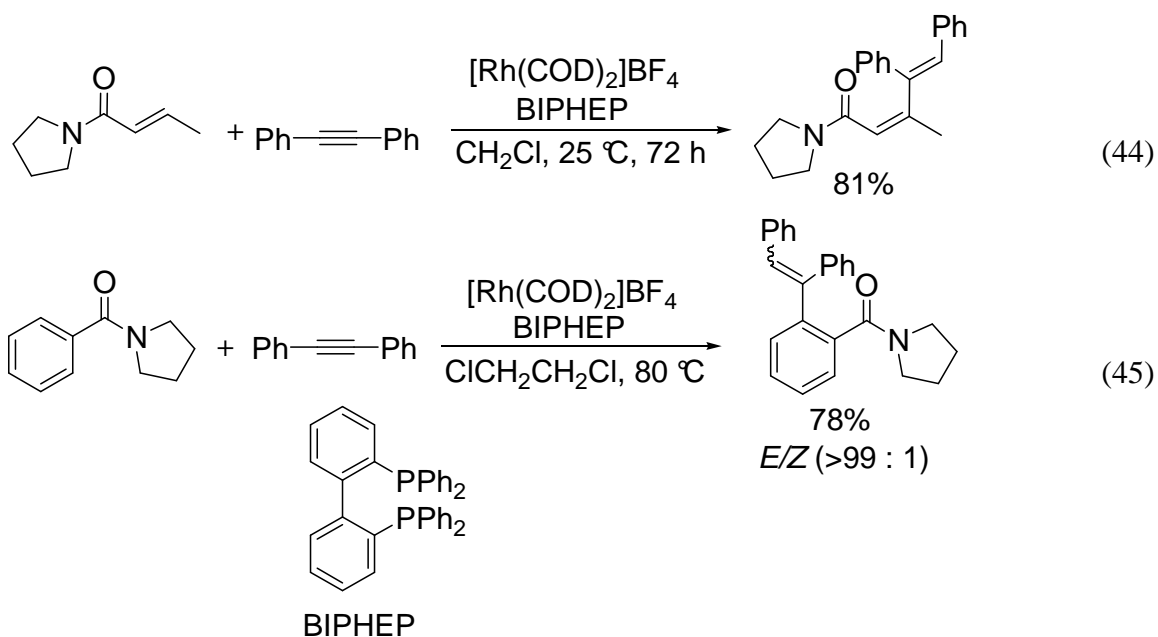
X =	OMe	Ph			
	0%	1%	47%	Ar¹ 71%	Ar² 88%

Shibata has also found that a cationic Ir(I)-BINAP complex showed high catalytic activity in sp^3 C-H bond alkenylation of amide with alkynes through carbonyl-directed C-H bond activation, which prevailed over aromatic sp^2 C-H bond activation. Alkenylation of amides with alkynes via carbonyl directed sp^3 C-H bond activation was proceeded with Ir(I)-BINAP.⁵⁰ For example, the reaction of *N,N*-dimethylbenzamide with diphenylacetylene in the presence of in situ formed cationic Ir(I)-BINAP complex gave the allylamide product as an E-isomer in good yield (eq 43).



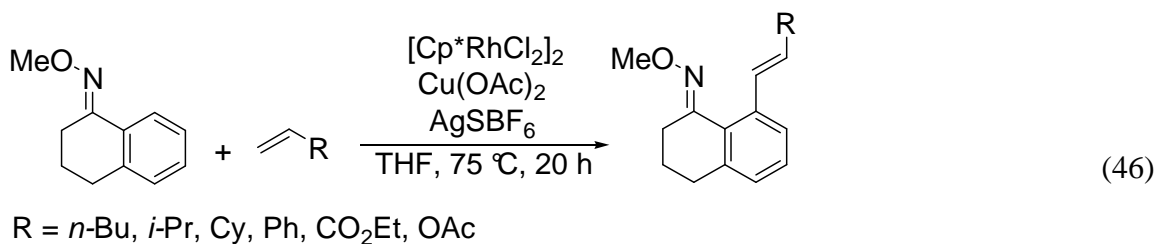
Tanaka reported that cationic rhodium(I)/BIPHEP complex catalyzes 1-pyrrolidinecarbonyl-directed regioselective alkenylations of olefinic or aromatic sp^2 C-H bonds in good yields under mild reaction conditions.⁵¹ The reaction of crotonamide with

diphenylacetylene catalyzed by $[\text{Rh}(\text{COD})_2]\text{BF}_4/\text{BIPHEP}$ afforded stereoselective coupling products in good yield (eq 44). A 1-pyrrolidinecarbonyl group as a directing group is essential for this transformation. Dimethylcarbamoyl and 1-piperidinecarbonyl groups significantly decreased the reaction rate, and ester and ketone carbonyl groups completely shut down the reaction. The reaction between benzamide and alkynes also proceeded in presence of the same rhodium catalyst (eq 45). Indeed, the desired alkenylation proceeded at ambient temperature, and the 1-pyrrolidinecarbonyl group is also the best directing group.

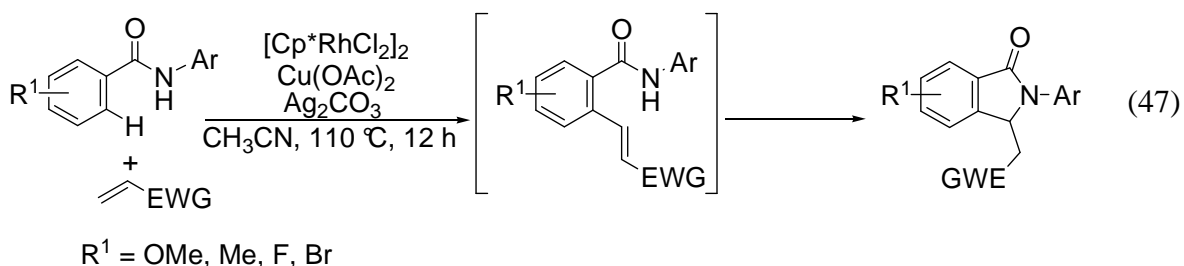


Recently, Ellman and Bergman have reported the oxidative coupling of aryl *O*-methyl oximes with unactivated alkenes via C-H bond functionalization catalyzed by Rh(III) complex (eq 46).⁵² A wide range of unactivated alkenes were employed in the reaction, and a variety of functional groups could be incorporated, including phenyl, ester, and halogen groups. The oxidative coupling of aryl *O*-methyl oximes with alkenes

using $[\text{Cp}^*\text{RhCl}_2]_2$ as the catalyst in the presence of $\text{Cu}(\text{OAc})_2$ as an oxidant and with THF as the solvent gave their corresponding oxidative products.

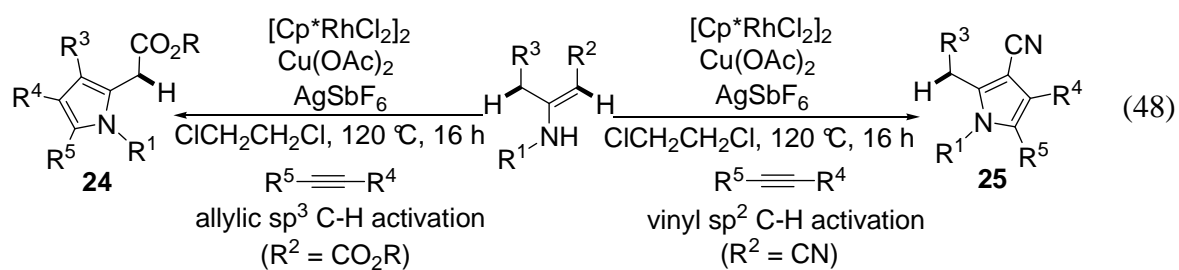


Li and coworkers has developed the C-H olefination of such bezamides at the C-aryl ring. When electron-poor olefins are utilized, the coupled products may further undergo in situ Michael addition to give γ -lactams (eq 47).⁵³ This reaction would proceed by the oxidative olefination of the *ortho* C-H bond in the C-aryl ring, followed by intramolecular hydroamination. Benzamides with electron-donating or -withdrawing groups affords lactams in high isolated yield when electron-poor olefins are employed.



Recently, Glorius has reported that the challenging allylic sp^3 C-H activation and also an alternative vinylic sp^2 C-H activation of enamines and the subsequent coupling with unreactivated alkynes yielding pyrroles.⁵⁴ The reaction of *N*-acetyl enamine

derivatives with internal alkyens in precence of $[\text{Cp}^*\text{RuCl}_2]_2$ and AgSbF_6 as the catalyst together with $\text{Cu}(\text{OAc})_2$ as the oxidant in 1,2-dichloroethane resulted in the formation of pyrroles (**24**) as a single regioisomer (eq 48). On the other hand, the change from ester to a nitrile resulted in the α -functionalization of the enamine and, consequently, the formation of a regioisomeric pyrrole (**25**). This important results indicate the crucial role of the ester group to activate the allylic sp^3 C-H bond.



Chapter II

Synthetic and Mechanistic Studies of Chelate-Assisted Oxidative

Coupling Reaction of Arylamides and Unactivated Alkenes

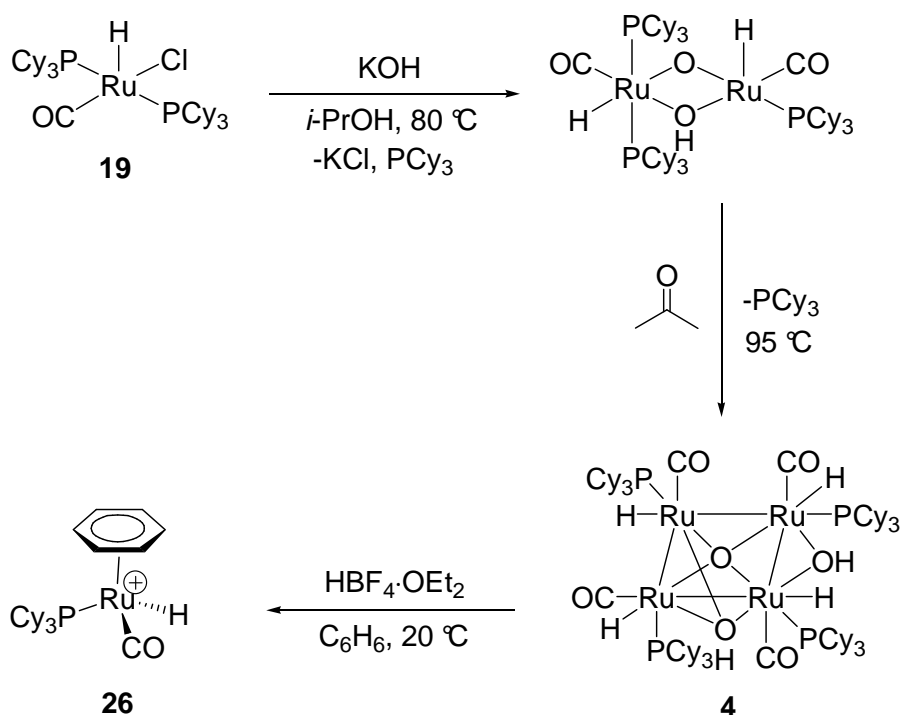
Chelate-assisted catalytic coupling reactions involving C–H activation have emerged as one of the most powerful C–C bond formation methods for arene compounds.¹ Among the chelate-directed catalytic C–H activation and functionalization reactions, oxidative coupling methods have been found to be particularly effective in forming new C–C and carbon-to-heteroatom bonds to sp² arene C–H bonds.^{1d,e} Since Fujiwara's seminal reports on the oxidative coupling reactions of arene compounds,⁵⁵ oxidative C–N, C–O and C–halogen bond-forming reactions of arene compounds have been achieved by using chelate directing groups.⁵⁶ Fagnou reported regioselective cross coupling reactions of unactivated arene compounds by using amino and amide directing groups.⁵⁷ Late transition metal catalysts have been found to be most versatile in mediating Heck-type C–H oxidative alkenylation of heteroarene compounds, where the regioselectivity has often been found to be dictated by both steric and electronic nature of the arene substituents and chelate directing groups.⁵⁸ By screening amino acid ligands, Yu recently developed a remarkably selective Pd-catalyzed C–H olefination of carboxy-substituted arene compounds.⁵⁹ Still, most of these oxidative coupling methods either require stoichiometric amounts of metal oxidants or reactive reagents. Thus development of direct oxidative C–H coupling methods which do not require strong oxidizing agents or reactive substrates with increased the efficiency of the coupling reaction would be beneficial from both synthetic and, environmental points of view.

Results and Discussion

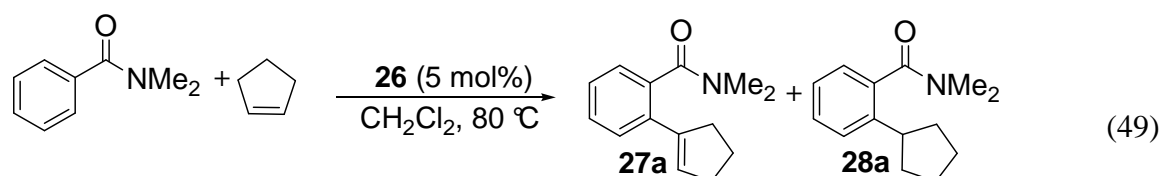
The regioselective coupling reactions of nitrogen containing compounds catalyzed by late transition metal catalysts have been developed by several research groups, as well as sp^2 and sp^3 C-H bond activation of nitrogen heterocycles and amide derivatives.^{15, 48-51, 53} The selective C-H bond activation of amide compounds is a highly attractive synthetic tool because organic compounds which contain amide functional groups are very useful materials in natural products and pharmaceutical agents. Our research group has reported that the *in-situ* formed cationic ruthenium-hydride complex is a highly effective catalyst for the coupling reaction of arylketones and linear alkenes involving C-H bond activation.^{60(a)} Recently, our research group also developed a convenient and efficient method to synthesize a cationic ruthenium-hydride complex $[(\eta^6\text{-C}_6\text{H}_6)(\text{PCy}_3)(\text{CO})\text{RuH}]^+\text{BF}_4^-$ (**26**) from the protonation reaction of tetrameric ruthenium complex $\{[(\text{PCy}_3)(\text{CO})\text{RuH}]_4(\mu\text{-O})(\mu\text{-OH})_2\}$ (**4**) which was synthesized in two steps from ruthenium-hydride complex $(\text{PCy}_3)_2(\text{CO})\text{RuHCl}$ (**19**) (Scheme 13).^{60(b), 60(c)} Thus, the treatment of tetrameric ruthenium complex **4** (200 mg, 0.12 mmol) with $\text{HBF}_4\cdot\text{OEt}_2$ (64 μL) in C_6H_6 at room temperature cleanly afforded the cationic ruthenium-hydride complex **26**, which was isolated as an ivory-colored solid in 95% yield (Scheme 13). The ruthenium-hydride signal was observed at δ -10.39 (d, $J_{\text{PH}} = 25.9$ Hz) by ^1H NMR spectroscopy of **26** in CD_2Cl_2 , and a single phosphine signal was detected at δ 72.9 ppm by $^{31}\text{P}\{^1\text{H}\}$ NMR spectroscopy. The molecular structure of cationic ruthenium-hydride **26**, characterized by X-ray crystallography, showed a three-legged piano-stool geometry, which is capped by an η^6 -benzene moiety (Figure 1).⁴⁸ The $\text{Ru}_1\text{-P}_1$ distance for complex

26 is 2.32 Å and the average bond length of Ru₁-C₁₋₆ is 2.32 Å. The C₇-Ru₁-H_{1M} angles is 88° and P₁-Ru₁-H_{1M} angles is 83°.

Scheme 13



In an effort to extend the synthetic utility, we have begun to explore the coupling reactions of arylamides and alkenes. For example, the treatment of C₆H₅CONMe₂ (0.5 mmol) with cyclopentene (10 mmol) in the presence of cationic ruthenium-hydride complex **26** in CH₂Cl₂ at 80 °C for 5 h gave an 89 : 11 ratio of the olefination product **27a** and the C-H insertion product **28a** in 52% conversion (eq 49).



The reaction of arylamide substrates with cyclic alkenes in the presence of cationic ruthenium-hydride complex **26** proceeds via a different reaction pathway compared to the reaction of arylketone with alkenes. This result means that C-H activation proceeded selectively at the *ortho*-position of the aromatic ring of arylamide. Furthermore, the major product is olefination product, which is more synthetically useful, compared to the C-H insertion product. To confirm the structure of the coupling products, the hydrogenation reaction was performed on the product mixture using the same catalyst. Thus, the treatment of a crude reaction solution with H₂ (1 atm) at 80 °C in the presence of cationic ruthenium-hydride complex **26** in CH₂Cl₂ led to **28a** which was isolated by column chromatography on silica gel, and its structure was completely established by spectroscopic methods. Intrigued by this initial discovery, we surveyed a number of different coupling reaction of arylamides and alkenes.

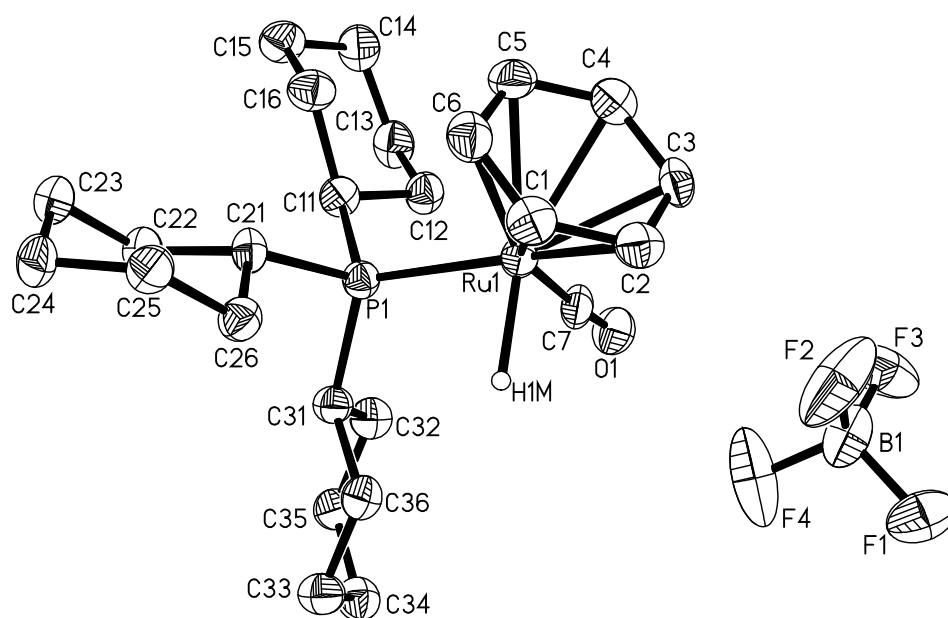
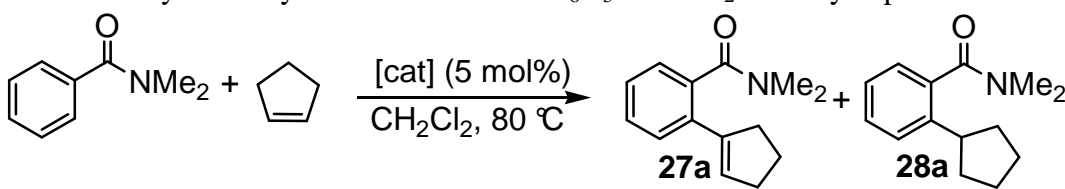


Figure 1. Molecular Structure of Cationic Ruthenium-Hydride Complex **26**.

2.1 Optimization Studies for Coupling of Arylamide with cyclopentene

2.1.1 Catalyst Survey

Initially, the coupling reaction of a benzamide and cyclopentene was used to screen for catalyst activity (Table 1). Thus, the treatment of $C_6H_5CONMe_2$ (0.5 mmol) with an excess amount of cyclopentene (2.5 mmol) in the presence of a metal catalyst (5 mol%) in CH_2Cl_2 at 80 °C was analyzed by GC after 5 h of reaction time. Among the surveyed ruthenium catalysts, complex **26** exhibited uniquely high activity and selectivity for the oxidative coupling product **27a** over the simple *ortho*-C–H insertion product **28a** (entries 2 and 3). The addition of $HBf_4 \cdot OEt_2$ to complex **26** was found to slightly decrease the activity compared to no additive (entry 4). $RuHCl(CO)(PCy_3)_2$, which is known to be an effective catalyst for both hydrovinylation and silylation reaction of alkenes and alkynes, showed no activity for the coupling reaction (entries 5 and 6).⁶¹ It is noteworthy that the reaction catalyzed by $RuH_2(CO)(PPh_3)_3$, which is well known to be highly efficient in a similar coupling reaction of arylketones with alkenes, did not proceed even when it was carried out in the presence of $HBf_4 \cdot OEt_2$ (entries 9 and 10). Also, commonly available ruthenium complexes such as $RuCl_2(PPh_3)_3$, $RuCl_3 \cdot 3H_2O$, $Ru_3(CO)_{12}$ and $[Ru(p\text{-cymene})Cl_2]_2$, which are representative ruthenium catalysts for C–H bond activation, showed no activity for the coupling reaction under the standard reaction conditions.

Table 1. Catalyst Suvery on the Reaction of C₆H₅CONMe₂ with Cyclopentene.^a


entry	catalyst	ratio (27a : 28a)	conversion(%) ^b
1	{[(PCy ₃)(CO)RuH] ₄ (μ-O)(μ-OH) ₂ } (4)		0
2	4 /HBF ₄ ·OEt ₂	86 : 14	52
3	[(η ⁶ -C ₆ H ₆)(PCy ₃)(CO)RuH] ⁺ BF ₄ ⁻ (26)	88 : 12	52
4	26 /HBF ₄ ·OEt ₂	80 : 20	48
5	RuHCl(CO)(PCy ₃) ₂		0
6	RuHCl(CO)(PCy ₃) ₂ /HBF ₄ ·OEt ₂		0
7	RuCl ₂ (PPh ₃) ₃		0
8	RuCl ₂ (PPh ₃) ₃ /HBF ₄ ·OEt ₂		0
9	RuH ₂ (CO)(PPh ₃) ₃		0
10	RuH ₂ (CO)(PPh ₃) ₃ /HBF ₄ ·OEt ₂		0
11	[RuH(CO)(PCy ₃) ₂ (CH ₃ CN) ₂] ⁺ BF ₄ ⁻		0
12	RuCl ₃ ·3H ₂ O/HBF ₄ ·OEt ₂		0
13	Ru ₃ (CO) ₁₂ /NH ₄ PF ₆		0
14	[Ru(<i>p</i> -cymene)Cl ₂] ₂ /PPh ₃		0
15	Re(CO) ₃ (THF) ₂ Br/HBF ₄ ·OEt ₂		0
16	AuCl(PPh ₃) ₃		0
17	AuCl(PPh ₃) ₃ /HBF ₄ ·OEt ₂		0
18	HBF ₄ ·OEt ₂		0
19	Cy ₃ PH ⁺ BF ₄ ⁻		0

^a Reaction conditions: C₆H₅CONMe₂ (0.5 mmol), cyclopentene (2.5 mmol), catalyst (5 mol%), CH₂Cl₂ (2 mL), 5 h. ^b The conversion of C₆H₅CONMe₂ as determined by GC analysis using C₆Me₆ as an internal standard.

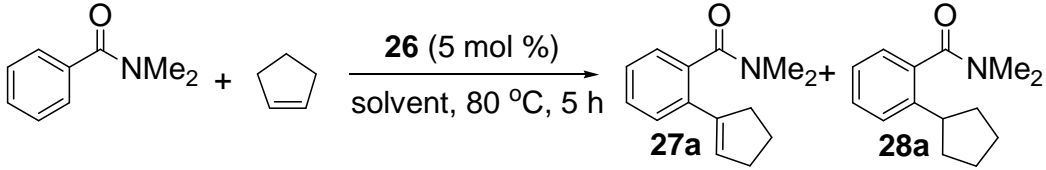
2.1.2 Solvent Effect

In order to find optimal solvent, the solvent effect on the activity and selectivity was examined for the coupling reaction of arylamides and alkenes. The reaction of C₆H₅CONMe₂ (0.5 mmol) with cyclopentene (2.5 mmol) in the presence of cationic ruthenium-hydride complex **26** was performed in a variety of solvents and the yield of

coupling products was determined by GC (Table 2). It was found that the nature of the solvents considerably affects the activity of the coupling reaction.

Both CH_2Cl_2 and PhCl were found to be most suitable for the coupling reaction among the screened organic solvents (entries 1 and 2). A stable 18-electron complex was formed in CH_3CN because of the solvent's strong coordinating ability, which ultimately leads to no catalytic activity (entry 4). Weakly coordinating solvents such as THF showed lower activity compared to non-coordinating solvents (entry 5). Other solvents such as C_6H_6 , PhCH_3 and Et_2O also were found to show moderate activity for the coupling reaction. The formation of an equivalent amount of cyclopentane was detected in the crude reaction mixture.

Table 2. Solvent Effect on the Coupling Reaction of $\text{C}_6\text{H}_5\text{CONMe}_2$ with Cyclopentene Catalyzed by **26**.^a



entry	solvent	ratio (27a : 28a)	conversion(%) ^b
1	CH_2Cl_2	88 : 12	52
2	PhCl	89 : 11	51
3	$\text{ClCH}_2\text{CH}_2\text{Cl}$	90 : 11	50
4	CH_3CN		0
5	THF	93 : 7	28
6	Et_2O	93 : 7	33
7	C_6H_6	92 : 8	39
8	PhCH_3	88 : 12	33

^a Reaction conditions: $\text{C}_6\text{H}_5\text{CONMe}_2$ (0.5 mmol), cyclopentene (2.5 mmol), **26** (15 mg, 5 mol%), 5 h. ^b The conversion of $\text{C}_6\text{H}_5\text{CONMe}_2$ as determined by GC analysis using C_6Me_6 as an internal standard.

2.2 Reaction Scope

The scope of the coupling reaction was explored by using the catalyst **26** (Table 3). Both secondary and tertiary arylamides were found to react smoothly with cyclic olefins to give the oxidative coupling products predominantly, but the primary arylamide benzamide was less reactive for coupling reaction with cyclopentene (entry 6). The secondary amides with *N*-electron withdrawing group were found to promote the oxidative coupling product **27** over the insertion product **28** (entries 10-12). Cyclic alkenes generally give the oxidative coupling products **27** preferentially, but cyclohexene resulted in a low yield of the coupling products (entry 13). Steric and electronic environments on the amide group were found to be less important with 1,1-disubstituted and terminal olefins in yielding a mixture of **27** and **28** for these cases (entries 17-24). In contrast, the reaction with 1-hexene yielded a complex mixture of **27** and **28** that resulted from the coupling with both terminal and internal olefins. 3-Acetyl-*N*-methylpyrrole is also a suitable substrate for the oxidative coupling reaction (entry 26).

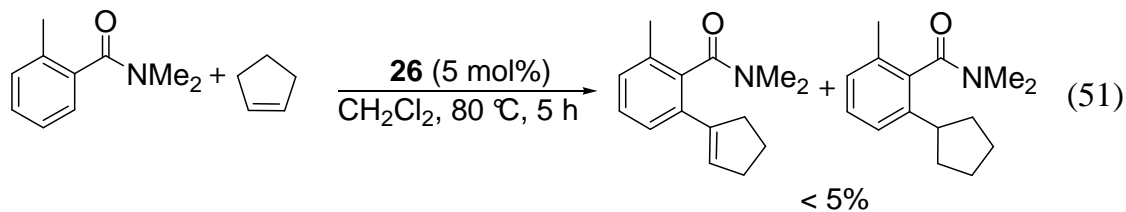
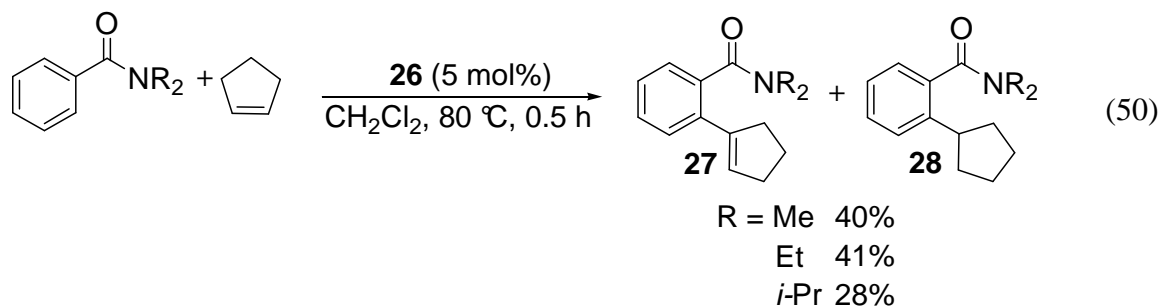
Table 3. Oxidative C-H Coupling Reaction of Arylamides with Alkenes.^a

entry	substrate	alkene	products	temp (°C)	yield (%) ^b
1	X = H		27a 28a (88 : 12)	80	52
2	X = Me		27b 28b (82 : 18)	80	54
3	X = Cl		27c 28c (80 : 20)	80	62
4	Y = OMe		27d 28d (91 : 9)	80	76
5	Y = Cl		27e 28e (88 : 12)	80	73

6	R = H, H	n = 1	27f 28f	(75 : 25)	150	36
7	R = H, Me	n = 1	27g 28g	(95 : 5)	80	55
8	R = Et, Et	n = 1	27h 28h	(87 : 13)	80	80
9	R = H, Bz	n = 1	27i 28i	(92 : 8)	80	65
10	R = H, Ph	n = 1	27j 28j	(100 : 0)	80	56
11	R = H, <i>p</i> -MeO-C ₆ H ₄	n = 1	27k 28k	(100 : 0)	80	57
12	R = H, <i>p</i> -Cl-C ₆ H ₄	n = 1	27l 28l	(100 : 0)	80	55
13	R = Me, Me	n = 2	27m 28m	(90 : 10)	150	15
14	R = Me, Me	n = 3	27n 28n	(92 : 8)	150	25
15	R = H, Bz	n = 3	27o 28o	(87 : 13)	150	53
16	R = Me, Me	n = 4	27p 28p	(95 : 5)	150	72
17	R = R' = Me		27q 28q	(40 : 60)	130	84
18	R = Me, R' = Ph		27r 28r	(30 : 70)	150	82
19	R = H, R' = <i>t</i> -Bu		27s 28s	(30 : 70)	150	83
20	R = R' = Me		27t 28t	(40 : 60)	130	84
21	R = H, R' = <i>t</i> -Bu		27u 28u	(30 : 70)	150	81
22	cyclopentene		27v 28v	(80 : 20)	80	61
23	R = R' = Me		27w 28w	(40 : 60)	130	82
24	R = H, R' = <i>t</i> -Bu		27x 28x	(35 : 65)	150	46
			27y 28y	(85 : 15)	80	63
			27z 28z	(70 : 30)	150	40

^a Reaction conditions: carbonyl compound (0.5 mmol), cyclopentene (2.5 mmol), **26** (15 mg, 5 mol%), 5 h. ^b Isolated yield.

To examine the steric effect for the coupling reaction, substrates with different size alkyl group at nitrogen site have been explored. A change from methyl to isopropyl led to a decrease in the initial reaction rate, but the isolated yield of each substrate was comparable over long reaction time (eq 50). Also we attempted the coupling reaction with more sterically demanding substrate such as *N,N*,2-trimethylbenzamide, but exceedingly low amounts of product were formed (eq 51). Methyl group at the 2-position in aromatic ring inhibited the coupling reaction with alkenes due to steric repulsion. This suggests that chelation of carbonyl group to ruthenium center is important step to proceed the coupling reaction.



2.3 Mechanistic Studies

2.3.1 Phosphine Inhibition

The coupling reaction was strongly inhibited by the addition of phosphines. The amount of coupling products was determined for the coupling reaction of $C_6H_5CONEt_2$ with cyclopentene in presence of cationic ruthenium-hydride complex **26** (5 mol %) and various amounts of PCy_3 . The conversion dramatically decreased with increasing amount of added PCy_3 (0 ~ 6.3 mol %) (Figure 2). For example, addition of 5 mol % of PCy_3 to the reaction mixture led to <10% conversion of substrate to product after 5 h, while 6.3 mol % of PCy_3 was sufficient to effect complete shutdown of the coupling reaction. In an effort to further gain insights of the role of additional phosphine, we monitored the reaction mixture of **26**, $C_6H_5CONEt_2$ with cyclopentene at 80 °C. A new Ru-H peak at δ -23.4 (t, $J_{PH} = 17.2$ Hz) and free benzene peak were observed by 1H NMR and a new single phosphine signal was detected at δ 49.3 ppm by $^{31}P\{^1H\}$ NMR spectroscopy at 80 °C. The hydride peak δ -23.4 ppm and the phosphine signal δ 49.3 ppm were assigned to a new cationic Ru-H complex which has two phosphine ligands, by comparing the spectroscopic data with a similar ruthenium complex $(PCy_3)_2(CO)RuHCl$ (**19**) (1H NMR δ -24.7 (t, $J_{PH} = 18$ Hz), $^{31}P\{^1H\}$ NMR δ 46.6).^{61b} The phosphine addition study indicated that η^6 -benzene ligands are easily dissociated by substrate compared to phosphine ligand under mild reaction conditions.

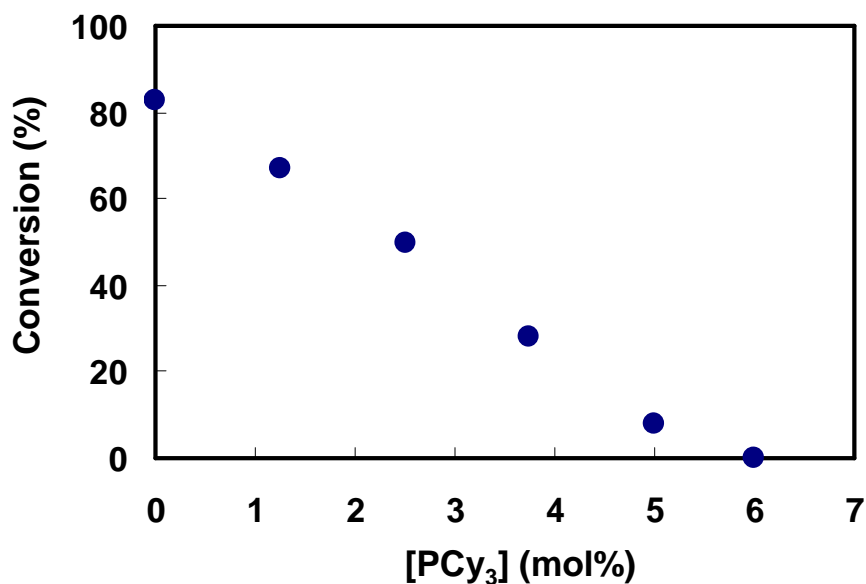
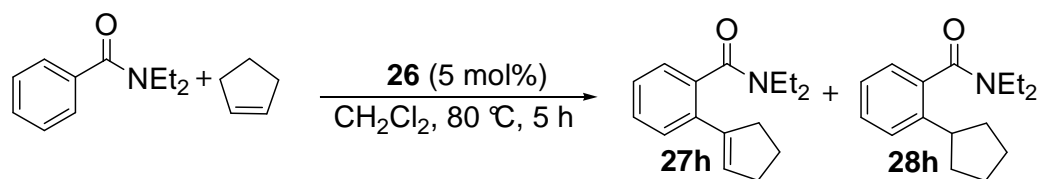
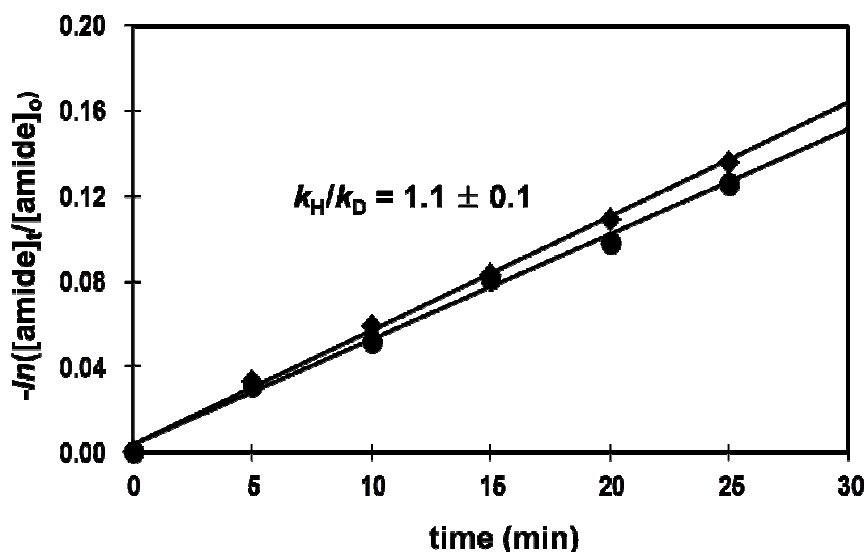
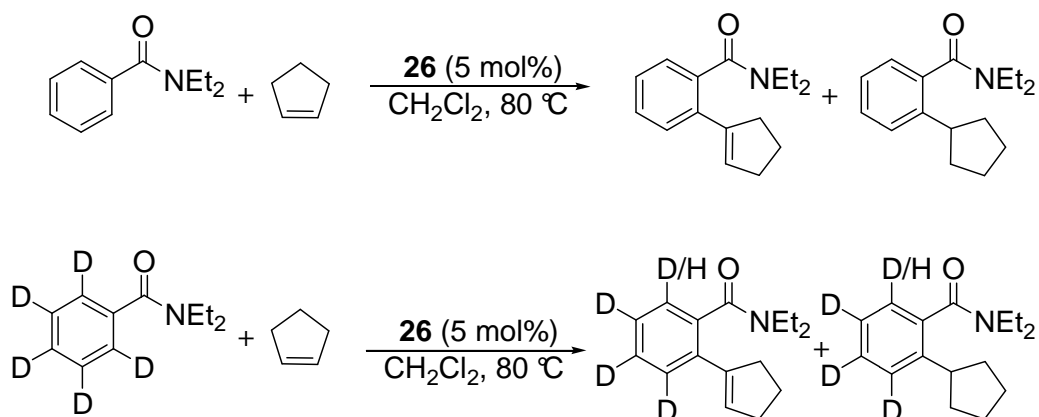


Figure 2. PCy₃ Inhibition Study for the Coupling Reaction of $\text{C}_6\text{H}_5\text{CONEt}_2$ with Cyclopentene Catalyzed by **26**.

2.3.2 Isotope Effect Study

A negligible deuterium isotope effect was observed for the reaction of $\text{C}_6\text{H}_5\text{CONEt}_2$ versus $\text{C}_6\text{D}_5\text{CONEt}_2$. The pseudo-first order plots for the catalytic reaction of both $\text{C}_6\text{H}_5\text{CONEt}_2$ and $\text{C}_6\text{D}_5\text{CONEt}_2$ with cyclopentene at $80\text{ }^\circ\text{C}$ gave $k_{\text{obs}} = 5.3 \times 10^{-3}\text{ min}^{-1}$ and $k_{\text{obs}} = 4.9 \times 10^{-3}\text{ min}^{-1}$, respectively, from which a negligible isotope effect of $k_{\text{H}}/k_{\text{D}} = 1.1 \pm 0.1$ was derived (Figure 3). These results indicate that cleavage of the aryl C-H bond is not the rate-limiting step for the coupling reaction.



◆ $C_6H_5CONEt_2$ ● $C_6D_5CONEt_2$

Figure 3. First-Order Plots of $-\ln([C_6H_5CONEt_2]_t/[C_6H_5CONEt_2]_0)$ vs Time for Coupling Reaction.

The carbon isotope effects of $C_6H_5CONEt_2$ were measured by ^{13}C NMR analysis following Singleton's carbon isotope measurement technique at natural abundance (eq 52).⁶² The virgin $C_6H_5CONEt_2$ was used as the standard. The ^{13}C NMR signal intensities were compared between virgin and recovered starting materials using *para*-carbon signal as an internal standard. The carbon isotope effect was observed on *ortho* carbon when the ^{13}C ratio of recovered $C_6H_5CONEt_2$ at 78-82% conversion was compared to that the virgin sample (average of 3 runs). As shown in eq 52, the relative proportions of the ^{13}C

isotope composition at *ortho* carbon was the most significantly increased by 2.3%. No other signals showed any significant changes in the ^{13}C isotopic composition. Using the equations of Melander and Saunder, the $^{12}\text{C}/^{13}\text{C}$ isotope effects are calculated and summarized in eq 52 and Table 4.⁶³ These isotope effects indicate that the rate-limiting step is the C-C bond formation with arylamides and alkenes.

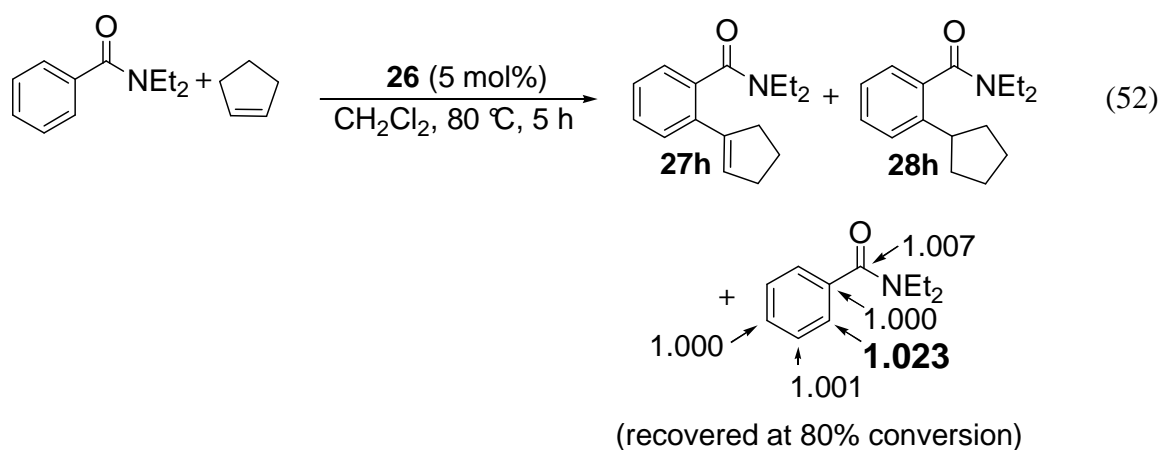


Table 4. Average ^{13}C Integration of the Recovered and Virgin Sample of $\text{C}_6\text{H}_5\text{CONEt}_2$.

C #	virgin	recovered (78 % conv.)	recovered/virgin	change (%)
1	1.034	1.041	1.007	0.70
2(ref)	1.000	1.000	1.000	0.00
3	1.975	2.020	1.023	2.27
4	1.986	1.985	0.999	-0.10
5	0.956	0.954	0.998	-0.20

C #	virgin	recovered (80 % conv.)	recovered/virgin	change (%)
1	1.034	1.041	1.007	0.70
2(ref)	1.000	1.000	1.000	0.00
3	1.975	2.024	1.023	2.48
4	1.986	1.984	0.999	-0.10
5	0.956	0.957	1.001	0.10

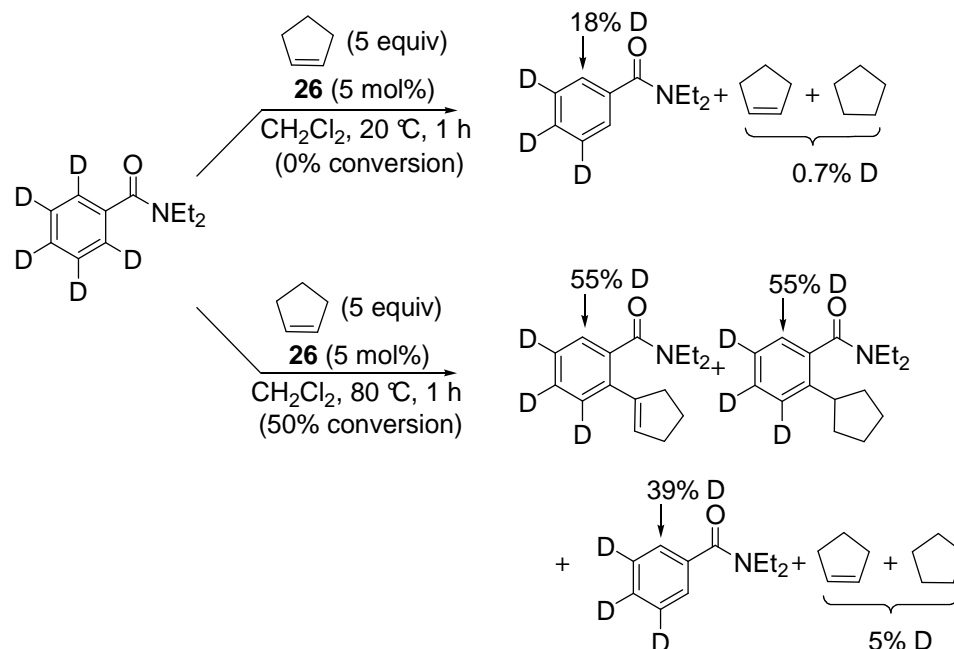
C #	virgin	recovered (82 % conv.)	recovered/virgin	change (%)
1	1.034	1.041	1.007	0.70
2(ref)	1.000	1.000	1.000	0.00
3	1.975	2.023	1.024	2.43
4	1.986	1.988	1.001	0.10
5	0.956	0.953	0.997	-0.30

2.3.3 Deuterium Labeling Study

The following deuterium labeling experiments were performed in order to understand about the reaction mechanism. The treatment of *N,N*-diethyl benzamide-*d*₅ (0.5 mmol) and cyclopentene (2.5 mmol) in the presence of **26** (5 mol %) in CH₂Cl₂ was monitored by ¹H and ²H NMR spectroscopy. Initially, a rapid and extensive H/D exchange was observed on the *ortho*-arene positions after 1 h at 20 °C. After 1 h at 80 °C, both the coupling products (55% D) along with both unreacted cyclopentene and the amide substrates evidenced significant deuterium incorporation (Scheme 14). The peak intensity at δ 7.02 ppm, which corresponds to the *ortho* position of the coupling products significantly increases due to rapid H/D exchange with cyclopentene (Figure 4 (a) and (b)). The decreased deuterium signal of *ortho* position of coupling products was further confirmed by ²H NMR spectroscopy.

Recovered starting materials showed the proton signal with strong intensities at *ortho*-arene positions in its ^1H NMR spectrum. Recovered cyclopentene and cyclopentane exhibited strong deuterium signals in their ^2H NMR spectrum due to intensive deuterium incorporation. Figure 5 (a) showed the ^1H NMR spectrum of *N,N*-diethyl benzamide- d_5 and while Figure 4 (b) shows the ^1H NMR spectrum of recovered *N,N*-diethyl benzamide- d_n . The peaks at δ 7.28 ppm, which are assignable to the aromatic protons of the arylamide substrate, considerably increased compared to virgin *N,N*-diethyl benzamide- d_5 . Rapid H/D exchange with cyclopentene in recovered *N,N*-diethyl benzamide- d_n was confirmed by ^2H NMR as indicated by the decreased intensities of deuterium signals (Figure 5 (c) and (d)). As shown in Figure 5 (e), significant amounts of deuterium were observed for cyclopentene- d_n and cyclopentane- d_n in the ^2H NMR spectrum of recovered cyclopentene and cyclopentane. These results indicate that C-H bond activation step is reversible at *ortho* position of aromatic ring in substrate.

Scheme 14



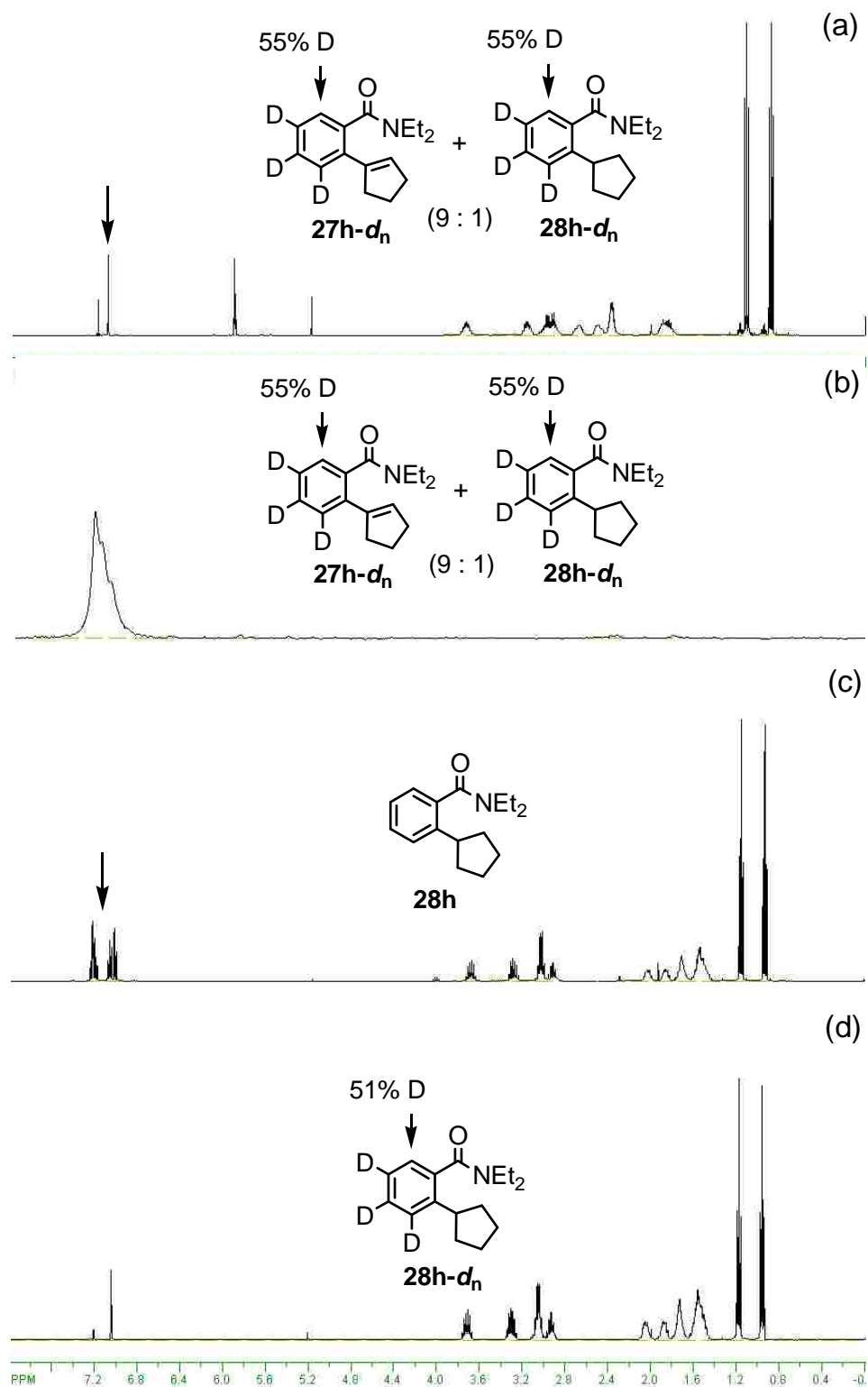


Figure 4. (a) ^1H NMR Spectrum of Mixture of **23h-d_n** and **24h-d_n**, (b) ^2H NMR Spectrum of Mixture of **23h-d_n** and **24h-d_n**, (c) ^1H NMR Spectrum **24h**, (d) ^1H NMR Spectrum of **24h-d_n**.

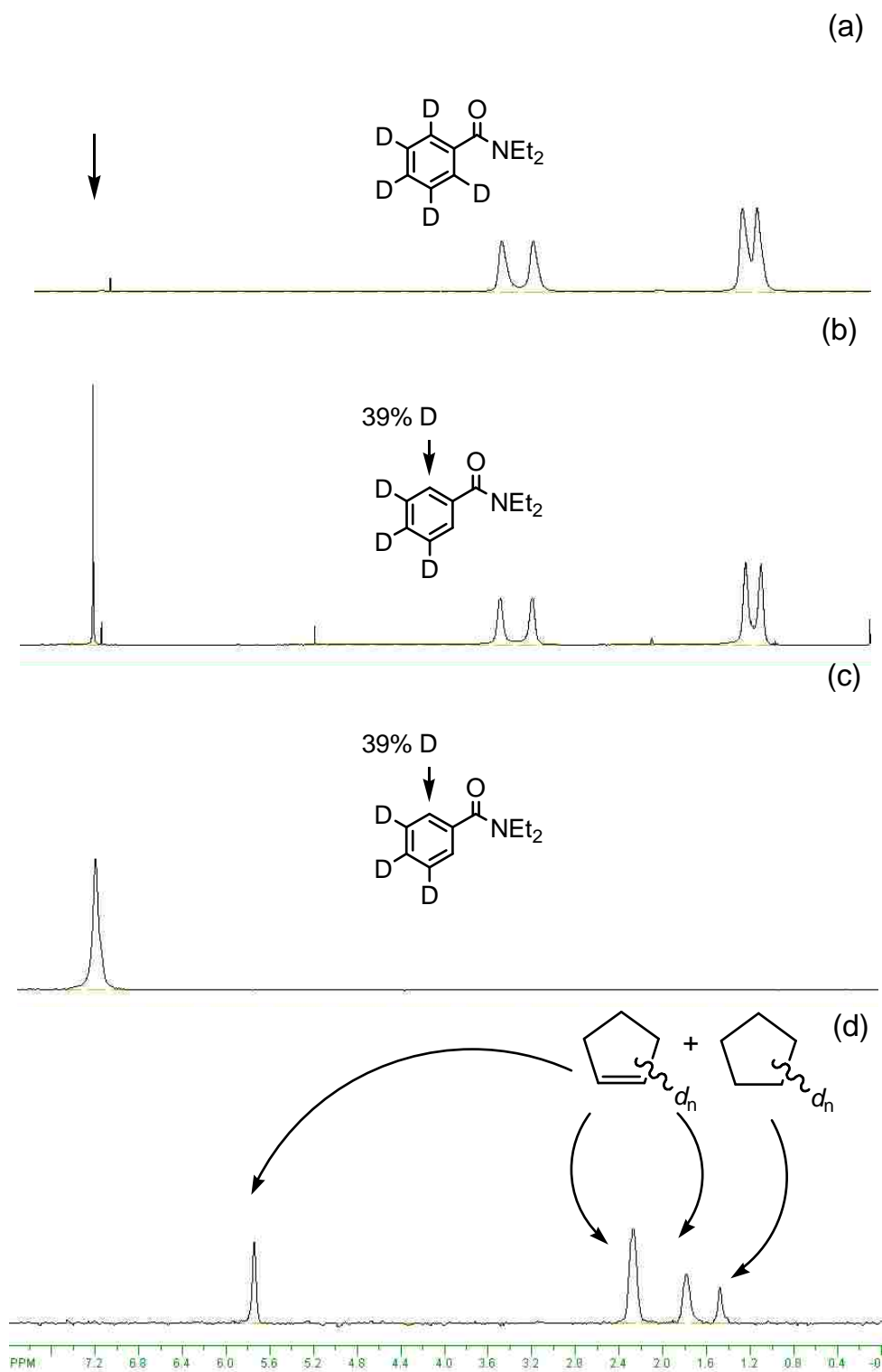
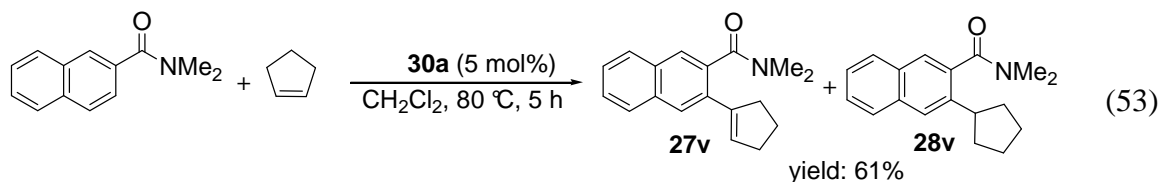


Figure 5. (a) ^1H NMR Spectrum of *N,N*-Diethyl Benzamide- d_5 , (b) ^1H NMR Spectrum of Recovered *N,N*-Diethyl Benzamide- d_n , (c) ^2H NMR Spectrum of Recovered *N,N*-Diethyl Benzamide- d_n , (d) ^2H NMR Spectrum of Recovered Cyclopentene- d_n and Cyclopentane- d_n .

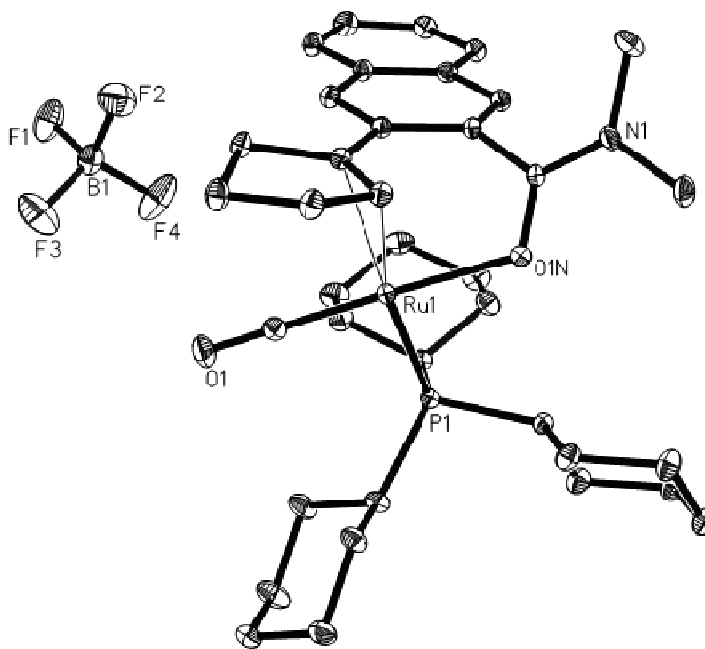
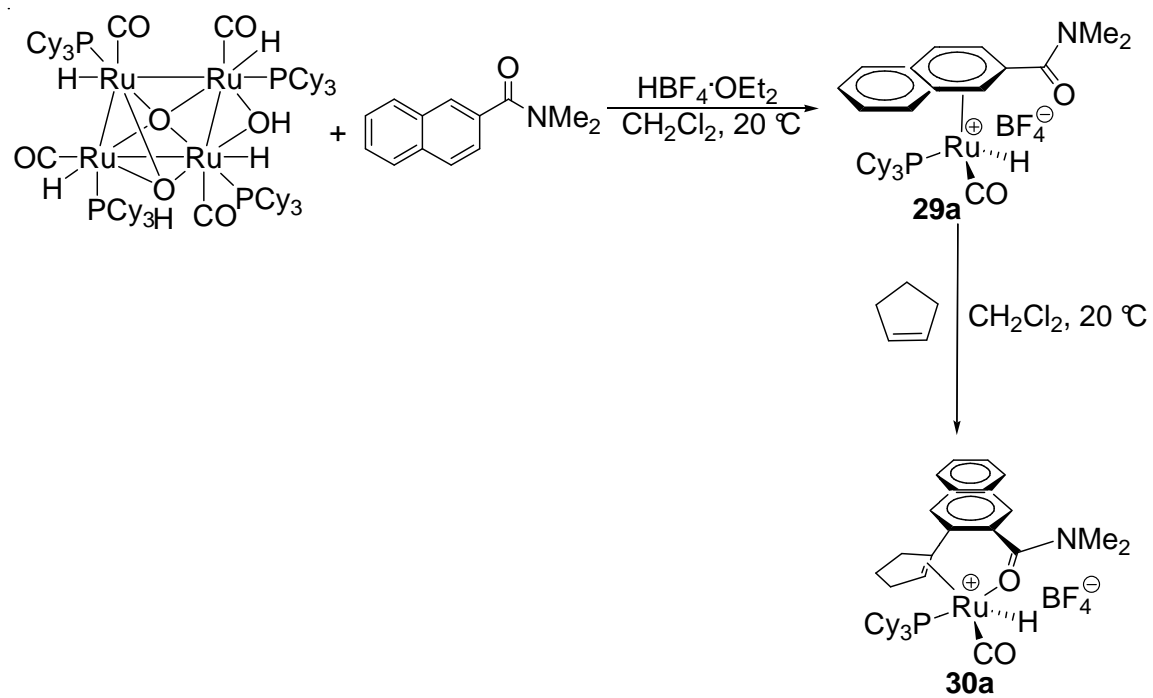
2.3.4 Isolation of Catalytically Relevant Species

In an effort to gain insights into the nature of the intermediate species, the reaction of tetrameric ruthenium complex **4** with amide were examined. The protonation reaction between tetrameric ruthenium complex **4** (200 mg, 0.12 mmol) and *N,N*-dimethyl-2-naphthamide (100 mg, 0.50 mmol) with HBF₄·OEt₂ (64 μL) in CH₂Cl₂ at room temperature cleanly afforded the cationic ruthenium-hydride complex [RuH(PCy₃)(CO)(η⁶-*N,N*-dimethyl-2-naphthamide)]BF₄ (**29a**), which was isolated as a green-colored solid in 80% yield (Scheme 15). The broad ruthenium-hydride signal was observed at δ -21.70 by ¹H NMR spectroscopy in CD₂Cl₂, and a broad single phosphine signal was detected at δ 74.4 ppm by ³¹P{¹H} NMR spectroscopy. Subsequently, the cationic ruthenium-hydride complex **30a** was formed by adding cyclopentene (5 equiv) to the cationic ruthenium-hydride complex **29a** in CH₂Cl₂ at room temperature. The new ruthenium-hydride signal appeared in the ¹H NMR of **30a** in CD₂Cl₂ at δ -19.58 (d, *J*_{PH} = 21.8 Hz) by and a new single phosphine signal exhibited at δ 65.4 ppm in its ³¹P{¹H} NMR spectrum.

The cationic ruthenium-hydride complex **30a** was isolated in 82% yield from a reaction of **29a** with cyclopentene in CH₂Cl₂, and its structure was established by X-ray crystallography (Figure 6). The molecular structure of **30a** showed a distorted square-pyramidal geometry with hydride ligand occupying an axial position. Amide group is *trans* arrangement to carbonyl and olefin group. The C₁₁-C₁₂ bond distance of the olefin group is 1.39 Å, which is comparable to cyclic olefin bond distance. Catalytic activities of the isolated complex **30a** for the coupling reaction of *N,N*-dimethyl-2-naphthamide with cyclopentene were found to be identical to that of **26** (eq 53).



Complex **30a** represents a rare example of a structurally characterized cationic ruthenium hydride species which is catalytically active for chelate-assisted C-H activation reactions. Though *ortho*-metalated complexes have been commonly invoked as the key species for chelate-assisted C-H activation chemistry,¹ structurally well-characterized metalated ruthenium complexes were often found to be catalytically inactive for the C-H insertion reactions.⁶⁴ More recently Kakiuchi and Yu independently reported the synthesis of catalytically active *ortho*-metalated Ru and Pd complexes and their activity for both C-O and C-H bond activation and insertion reactions of arene compounds, respectively.⁶⁵ It is also noteworthy that both Ru(0)-enone and Rh(I)-olefin complexes were found to be active for the C-H insertion of aryl ketones.⁶⁶ In our case, the successful isolation of **30a** further suggests that the coupling reaction could be inhibited by the products. Indeed, the coupling reaction $C_6H_5CONEt_2$ with cyclopentene in the presence of 2.5 equiv **27a** showed virtually no activity under otherwise similar conditions as stipulated in eq 49 ($\leq 3\%$ conversion).

Scheme 15**Figure 6.** Molecular Structure of 30a.

2.3.5 VT NMR Study

In an attempt to better understand the mechanism of the reaction, the reaction of complex **26** with different arylamides was monitored by NMR. The most noticeable change was observed in the reaction with *N,N*-dimethyl-2-naphthamide. In a heavy-walled J-Young NMR tube, *N,N*-dimethyl-2-naphthamide (87 μmol) was added into a CD_2Cl_2 solution containing complex **26** (50 mg, 87 μmol). When the mixture was monitored at room temperature, the formation of a new species was detected by ^{31}P NMR spectroscopy (δ 74.4), and this new species was found to exist as an equilibrium mixture with **26** (**26:29a** = 9:1) (eq 54). Since no other peak could be assigned, due to the presence of PCy_3 signals, the structure of new species was established from the protonation reaction between the tetrameric ruthenium complex **4** and *N,N*-dimethyl-2-naphthamide with $\text{HBF}_4 \cdot \text{OEt}_2$. Both ^{31}P NMR signals were identical and all of the spectroscopic data were consistent with the complex **29a**. The equilibrium constants between **26** and **29a** were estimated from VT ^{31}P NMR spectroscopy in the temperature range of 30 to 60 $^\circ\text{C}$. The van't Hoff analysis of these data led to the thermodynamic parameters of $\Delta H^\circ = 0.6 \pm 0.1$ kcal/mol and $\Delta S^\circ = -0.5 \pm 0.1$ eu for the equilibrium reaction (Figure 7). These results indicate that the ligand exchange between benzene and arylamides are very facile under the catalytic reaction condition.

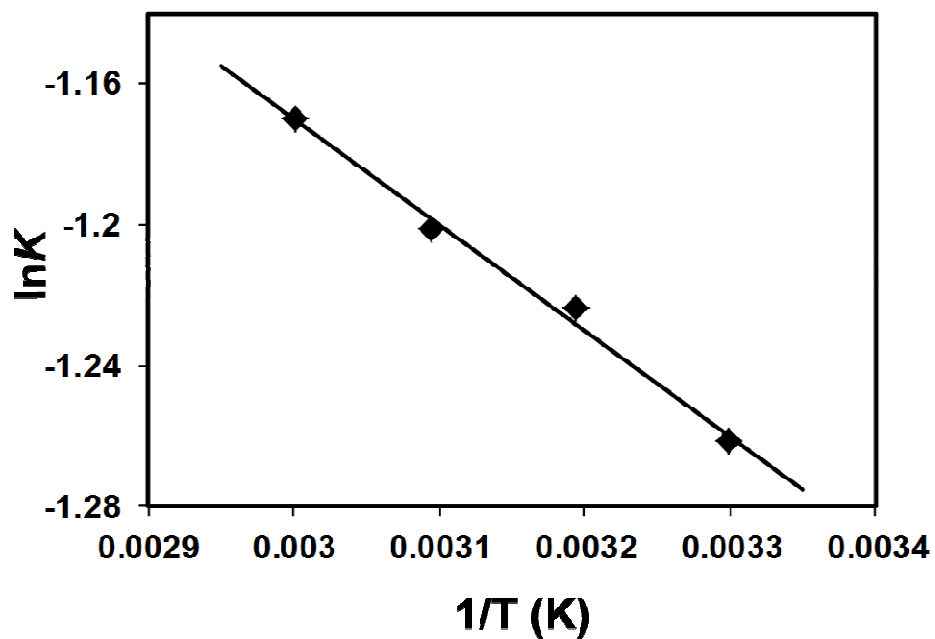
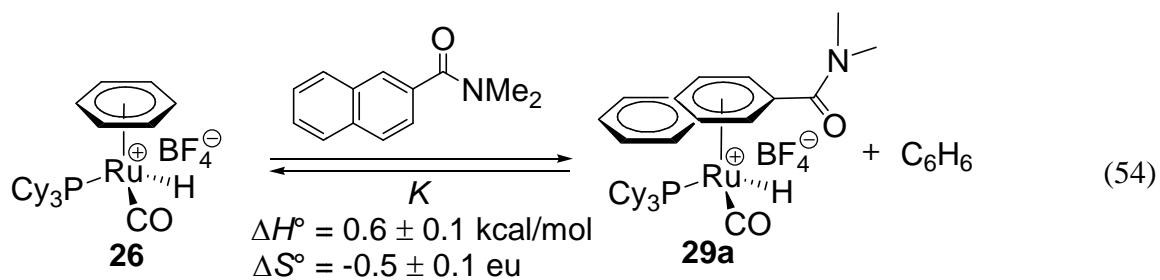


Figure 7. van't Hoff Plot of $\ln K$ vs $1/T$.

2.4 Proposed Mechanism

These results provide support for a mechanism involving vinyl C–H bond activation as depicted in Scheme 16. We propose that the initial arene exchange/ π -coordination of an arylamide from **26** would form the arene-coordinated cationic Ru–H species **29**. The equilibrium constants between **26** and **29a** were measured from VT NMR

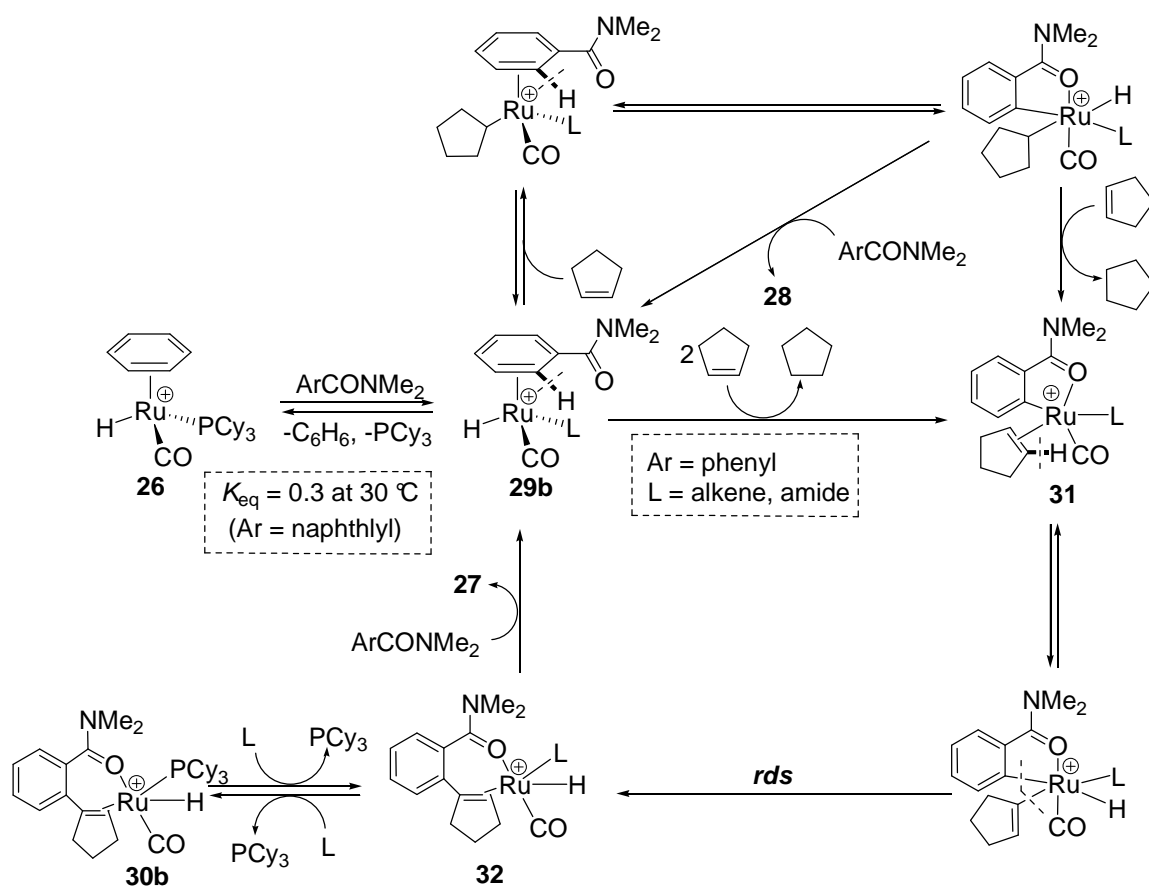
experiments using phosphorus signal for both complexes in different temperature ($K_{\text{eq}} = 0.3$ at 30 °C). The phosphine inhibition study implicates that the reactive species would be formed from a reversible dissociation of η^6 -benzene ligand. These results indicate that the reversible ligand exchange reaction of **26** with arylamides readily proceeds in the reaction mixture, which are consistent with our proposed mechanism.

Complex **29b** further undergoes chelate-directed *ortho*-C–H activation and dehydrogenation to form the *ortho*-metallated species **31**. The extensive H/D exchange at *ortho*-position of arylamide as well as deuterated cyclopentene and cyclopentane is observed by both ^1H and ^2H NMR. The negligible isotope effect of $k_{\text{H}}/k_{\text{D}} = 1.1 \pm 0.1$ is observed for the coupling reaction of $\text{C}_6\text{H}_5\text{CONEt}_2$ and $\text{C}_6\text{D}_5\text{CONEt}_2$ with cyclopentene. These mechanistic features indicate that the cleavage of aryl C–H bond is reversible and not the rate-limiting step for the coupling reaction. The subsequent vinyl C–H activation and the turnover limiting aryl-to-vinyl reductive elimination steps would form the cationic ruthenium-hydride species **32**. Both carbon isotope effect study which shows the most significantly increased ratio at *ortho* carbon by comparison with virgin sample. The successful isolation of the complex **30b**, which shows identical catalytic activity with respect to the coupling reaction in comparison with cationic ruthenium hydride complex **26**, provide the supporting evidence for the rate-limiting C–C bond formation step. The cationic Ru–H complex **32** would be easily converted to cationic Ru–H complex **29b** by dissociation of product/ π -coordination of an arylamide. On the other hand, the formation of the insertion product **28** can be readily explained by invoking a direct olefin insertion and the subsequent *ortho* C–H activation and reductive elimination subsequence from **29b**.

One of the major reasons the oxidative C–H coupling pathway is favored over the

Murai-type C-H insertion pathway may be due to the catalyst's ability to promote facile vinyl C-H activation. Cyclic alkenes are favor to form the metal-vinyl species instead of metal-alkyl species and generate the oxidative C-H coupling product predominantly. While the formation of metal-vinyl species has been well documented in the C–H bond activation literature,⁶⁷ its synthetic utility has been rarely exploited in catalytic coupling reactions.

Scheme 16



Conclusions

The cationic ruthenium-hydride complex **26** was found to be an effective catalyst for coupling reaction with arylamides and alkenes via C-H activation. The C-H bonds at *ortho* position of arylamides is selectively cleaved and added to alkenes. The olefination products were produced in high yield and high selectivity when unactivated cyclic alkenes such as cyclopentene, cyclohexane, cycloheptene and cyclooctene, were employed. A catalytically active cationic ruthenium-hydride complex **30** was isolated and characterized. A normal deuterium isotope effect ($k_{\text{CH}}/k_{\text{CD}} = 1.1 \pm 0.1$) and deuterium labeling studies showed that the C-H bond activation is not the rate-determining step. ^{13}C isotope effect results indicated that the rate determining step was C-C bond formation which was consistent with our proposed mechanism.

Chapter III

Stereoselective Catalytic Conjugate Addition and Oxidative Coupling Reaction of Simple Alkenes to α,β -Unsaturated Carbonyl Compounds

Considerable research to the development of the expeditious catalytic synthesis of tetrasubstituted olefins has in part been stimulated by growing demand for developing generally applicable methods for biologically active compounds such as tamoxifen **33** (drug for breast cancer) and rofecoxib **34** (nonsteroidal anti-inflammatory drug) as well as for light/electron responsive organic materials and molecular devices including sensors and switches (Figure 8).⁶⁸

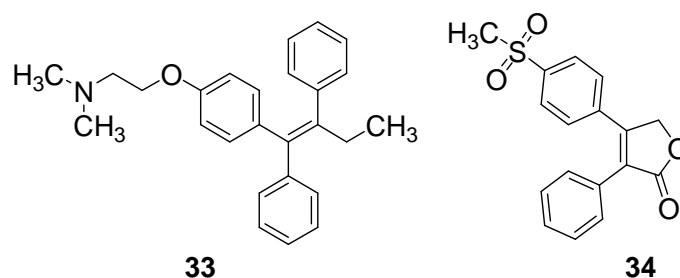


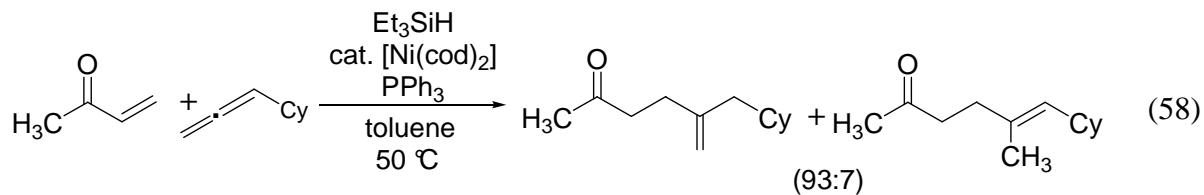
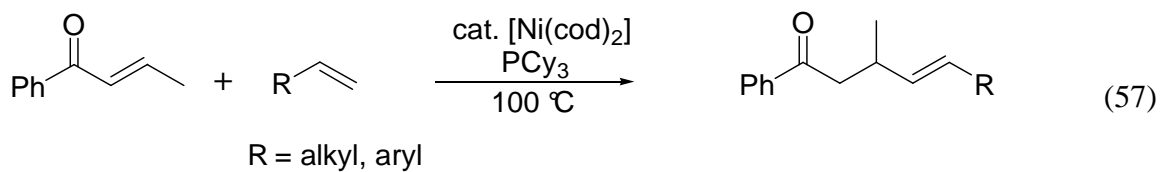
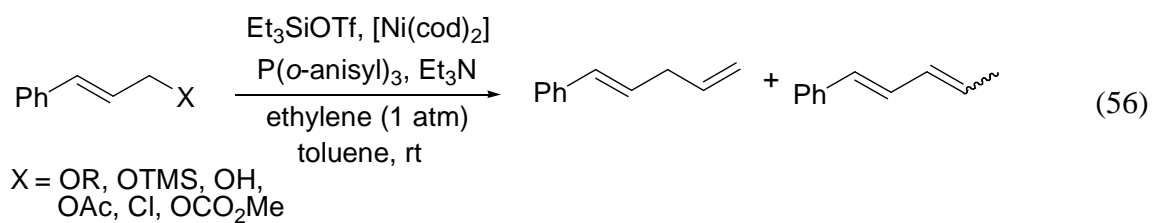
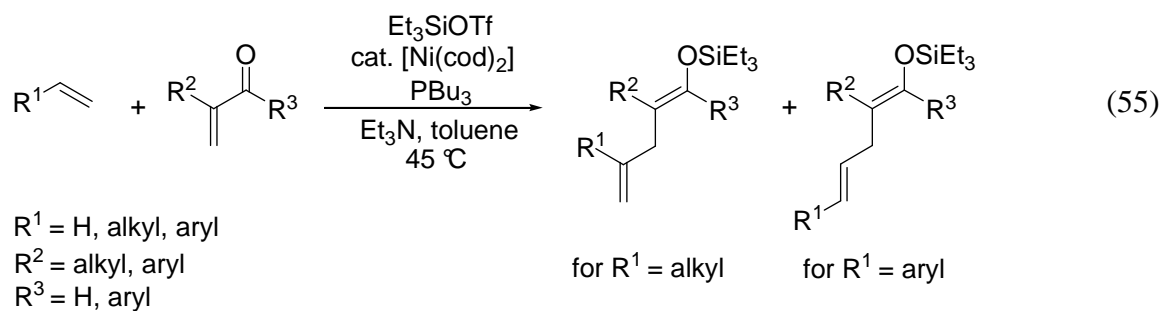
Figure 8. Structure of Tamoxifen **33** and Rofecoxib **34**.

Since classical olefination methods are generally not suitable for the synthesis of highly substituted olefins, extensive research has been devoted over the years to develop catalytic olefination methods that do not generate copious byproducts.^{4, 33-34, 68-75} Recent notable examples for the synthesis of tetrasubstituted olefins that utilize transition metal catalysis include: Suzuki-type Pd-catalyzed coupling reactions,⁶⁹ Ni- and Rh-catalyzed

exocyclization methods,⁷⁰ Ni- and Pd-catalyzed nucleophilic coupling reactions of silylacetylenes⁷¹ and of alkyne-to-arylboronic acids,⁷² Ti-catalyzed tandem alkyne-epoxide-ethyl acetate coupling,⁷³ and the ring-closing olefin metathesis by using Grubbs' catalyst.⁷⁴ Though chelate-assisted catalytic C–H insertion method to α,β -unsaturated carbonyl and imine compounds has successfully been utilized for the synthesis of tri- and tetrasubstituted olefins,^{4, 33-34} the general applicable catalytic conjugate addition of simple olefins to α,β -unsaturated carbonyl compounds has been largely elusive due to the lack of reactivity of alkene substrates and the formation of homocoupling and other byproducts. In this regard, the recently reported Ni-catalyzed enone-to-alkene cross coupling reaction and allylic substitution are a notable advance as described below.⁷⁵

Jamison has reported a nickel-catalyzed reaction of enones with alkenes in the presence of Et_3SiOTf and Et_3N to give enol silyl ethers, which is more straightforward method for introducing an alkenyl group at the β -position of enones (eq 55).^{75a} He has also described the catalytic intermolecular allylic substitution of unactivated, simple alkene catalyzed by nickel complex, which can accommodate a wide range of allylic alcohol derivatives and simple terminal alkenes (eq 56).^{75b} Ogoshi has developed a first example of a direct conjugate addition of simple alkenes to enones catalyzed by Ni(0) complex (eq 57).^{75c} This reaction is a powerful synthetic tool for the introduction of an alkenyl group at the β -position of enones without any pre-step, since the conventional conjugate addition method requires the preparation of alkenyl metals and its metal must be discarded after reaction. Recently, Montgomery has reported that regioselective catalytic reductive coupling of enones and terminal allenes provides the preparation of

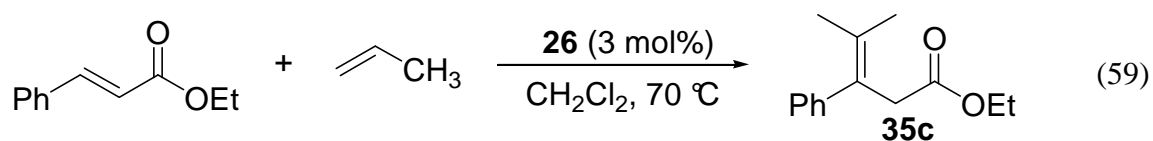
γ,δ -unsaturated carbonyls with 1,1-disubstituted alkenes, which are not generally available by other reductive coupling procedures (eq 58).^{75d}



Even though several research groups have reported notable advances for the catalytic synthesis of tetrasubstituted olefins, examples of generally applicable synthetic methods of tetrasubstituted olefins catalyzed by transition metal complexes are relatively rare.

Results and Discussion

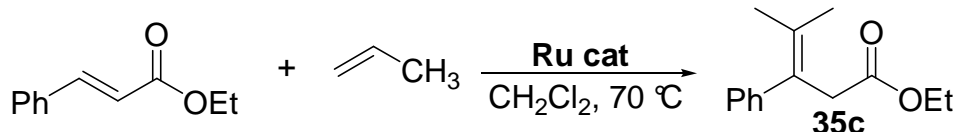
Inspired by recent reports on the C-C bond forming reactions catalyzed by late transition metal complexes,⁷⁶ we have begun to explore the synthetic utility of a well-defined cationic ruthenium hydride complex $[\eta^6\text{-}(\text{C}_6\text{H}_6)(\text{CO})(\text{PCy}_3)\text{RuH}]^+\text{BF}_4^-$ (**26**) for the coupling reaction of a variety of carbonyl compounds with simple alkenes.⁷⁷ As describe in Chapter 2, we recently discovered that the cationic ruthenium hydride complex **26** is a highly effective catalyst precursor for the oxidative coupling reaction of arylamides with simple alkenes.^{77c} While studying the ruthenium-catalyzed C-C bond forming reactions, we recently discovered that novel catalytic synthesis of tetrasubstituted olefins from the intermolecular and intramolecular conjugate addition reaction of simple olefins to α,β -unsaturated carbonyl compounds.⁷⁷ For example, propene (2.9 mmol) was added to a CH_2Cl_2 solution of (*E*)- $\text{C}_6\text{H}_5\text{CH}=\text{CHCO}_2\text{Et}$ (0.58 mmol) and a cationic ruthenium complex **26** (3 mol%) and the reaction mixture was stirred at 70 °C for 2 h to obtain stereoselective tetrasubstituted olefin product with 95% yield (eq 59). This catalytic method efficiently produces tetrasubstituted olefin products from the intermolecular coupling of α,β -unsaturated carbonyl compounds and simple alkenes without generating of any byproducts.



3.1 Catalyst Survey

Initial feasibility of the conjugate addition reaction was screened by using a cinnamic acid derivative and an α -olefin. Thus, the treatment of ethyl cinnamate (0.58 mmol) with propene (2.9 mmol) in the presence of a Ru catalyst (3 mol %) in CH_2Cl_2 was stirred at 70 °C for 2 h, after which the product conversion was analyzed by GC. Among the screened ruthenium catalysts, the complex **26**, both in isolated form and *in-situ* formed from the of the tetranuclear complex $\{[(\text{PCy}_3)(\text{CO})\text{RuH}]_4(\mu\text{-O})(\mu\text{-OH})_2\}$ (**4**) with $\text{HBF}_4 \cdot \text{OEt}_2$, exhibited uniquely high activity in yielding the coupling product **35c** (Table 5). $\text{RuH}_2(\text{CO})(\text{PPh}_3)_3$, which was reported by Muari and Trost for the alkylation of α,β -unsaturated carbonyl compounds with alkenes, did not proceed even in presence of an additive $\text{HBF}_4 \cdot \text{OEt}_2$ (entry 5). Other readily available ruthenium complexes such as $\text{RuCl}_2(\text{PPh}_3)_3$, $\text{RuCl}_3 \cdot 3\text{H}_2\text{O}$, $\text{Ru}_3(\text{CO})_{12}$ and $[\text{Ru}(p\text{-cymene})\text{Cl}_2]_2$ also showed no activity for this coupling reaction under the similar conditions.

Table 5. Catalyst Survey for the Coupling Reaction of (*E*)-C₆H₅CH=CHCO₂Et and Propene.^a



entry	catalyst	additive	conversion (%) ^b
1	[(η ⁶ -C ₆ H ₆)(CO)(PCy ₃)RuH] ⁺ BF ₄ ⁻ (26)	-	99
2	{[(PCy ₃)(CO)RuH] ₄ (μ-O)(μ-OH) ₂ } (4)	-	0
3	{[(PCy ₃)(CO)RuH] ₄ (μ-O)(μ-OH) ₂ } (4)	HBF ₄ ·OEt ₂	99
4	RuHCl(CO)(PCy ₃) ₂	-	0
5	RuH ₂ (CO)(PPh ₃) ₃	-	0
6	RuCl ₂ (PPh ₃) ₃	-	0
7	RuCl ₂ (PPh ₃) ₃	HBF ₄ ·OEt ₂	0
8	[RuH(CO)(PCy ₃) ₂ (S) ₂] ⁺ BF ₄ ⁻	-	0
9	RuCl ₃ ·3H ₂ O/HBF ₄ ·OEt ₂	HBF ₄ ·OEt ₂	0
10	Ru ₃ (CO) ₁₂	-	0
11	[Ru(<i>p</i> -cymene)Cl ₂] ₂	-	0
12	HBF ₄ ·OEt ₂	-	0

^a Reaction conditions: (*E*)-C₆H₅CH=CHCO₂Et (0.58 mmol), propene (2.9 mmol), catalyst (3 mol%), CH₂Cl₂ (2 mL), 70 °C, 2-5 h, ^b The conversion of (*E*)-C₆H₅CH=CHCO₂Et as determined by GC analysis using C₆Me₆ as an internal standard. ^c S = CH₃CN.

3.2 Reaction Scope

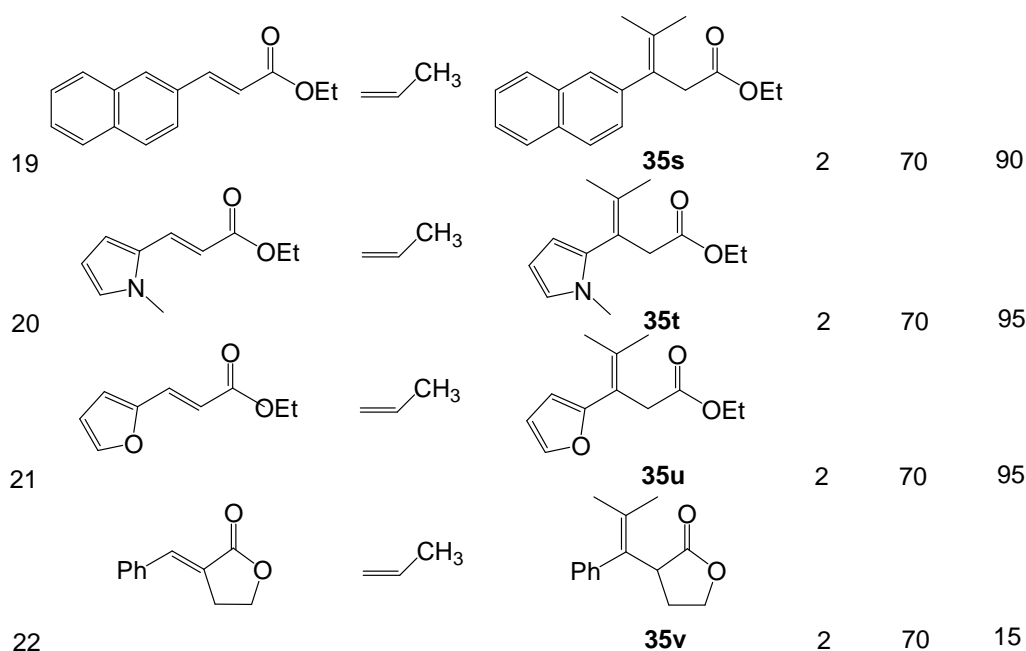
The scope of the coupling reaction of carbonyl compounds with alkenes was examined by using the catalyst **26**. Enones, α,β-unsaturated esters and amides were found to react smoothly with simple α-olefins to give the tetrasubstituted olefin products. Moreover, α-substituted α,β-unsaturated compounds and intramolecular compounds are also suitable substrates for the coupling reaction with high yield. In general, cinnamic esters and amides with *para*-electron donating group were found to promote the coupling reaction, but neither cyclic enones nor pyrrolinones gave the coupling products under the similar reaction conditions.

3.2.1 Coupling Reactions of α,β -Unsaturated Ester and Enones with Alkenes

The scope of the coupling reaction of enones and α,β -unsaturated esters with simple alkenes was examined by using the catalyst **26** (Table 6). Enones and α,β -unsaturated esters were found to react easily with a wide variety of simple olefins to yield the tetrasubstituted olefin products. The reaction of (*E*)-*p*-X-C₆H₄CH=CHCO₂Et (X = OEt, Me, H, F, Cl, CO₂Me, CF₃) with propene gave the coupling products **35** in high yields (entries 1-7). Both electron donating and withdrawing group at *para* position in enones and α,β -unsaturated esters gave corresponding tetrasubstituted olefin products in high yields under the similar reaction conditions. A mixture of *E/Z* olefin products were formed from the coupling reaction of α,β -unsaturated esters with ethylene or 1-pentene, while the coupling reaction with 1-butene and 2-butene gave the same product **35n** (entries 13-16). The coupling reaction with cyclopentene showed good activity but poor selectivity due to olefin isomerization (entry 17). A linear olefin products **35q** was produced with 4-chlorostyrene (entry 18). Heterocyclic compounds such as (*E*)-ethyl *N*-methyl-2-pyrroleacetate and (*E*)-ethyl-3-(furan-2-yl) acrylate were found to readily undergo the coupling reaction with propene to give the stereoselective product **35t** and **35u** (entries 20 and 21). A cyclic lactone with propene also gave the tetrasubstituted olefin coupling products **35v** with a low yield (entry 22).

Table 6. Conjugate Addition Reaction of Simple Olefins to α,β -Unsaturated Ester and Enones.^a

entry	substrate	alkene	product (s)	t (h)	temp (°C)	yield (%) ^b
1				2	70	95
2	X = OEt	R = Et	35a	2	70	95
3	X = Me	R = Et	35b	2	70	94
4	X = H	R = Et	35c	2	70	95
5	X = F	R = Et	35d	2	70	95
6	X = Cl	R = Et	35e	2	70	93
7	X = CO ₂ Me	R = Et	35f	2	70	94
8	X = CF ₃	R = Et	35g	2	70	93
9	X = H	R = Me	35h	2	70	95
9	X = H	R = Bz	35i	2	70	93
10				2	70	92
11	X = H	R = Me	35j	2	70	92
12	X = H	R = Ph	35k	2	70	92
12	X = Me	R = Me	35l	2	70	95
13			 (Z)/(E)-35m = 3:1	14	50	78
14				14	50	92
15				14	50	90
16			 35o/35p = 2:1	14	50	62
17				14	50	94
18 ^c				14	50	50



^a Reaction conditions: carbonyl compound (0.58 mmol), propene (2.9 mmol), catalyst (3 mol%), CH₂Cl₂ (2 mL), 70 °C, 2-14 h, ^b Isolated yield. ^c Less than 5% of branched olefin product is formed.

3.2.2 Coupling Reactions of α,β -Unsaturated Amides with Alkenes

In an effort to extend the scope, we next surveyed the conjugate addition of α,β -unsaturated amides with simple olefins (Table 7). The reaction of the primary amides such as (*E*)-C₆H₅CH=CHCONH₂ with propene gave a slightly lower yield of the coupling product compared to secondary and tertiary amides (entries 1-11). Steric and electronic environments on the amide group were found to be less important with propene in yielding stereoselective products **36** for these cases (entries 1-11). The fact that both 1- and 2-butenes gave the same product **36** suggested that the rate of olefin isomerization is much faster than the coupling reaction rate (entries 15, 16). It should be emphasized that the α -olefins with sterically non-demanding group were found to give similar (*Z*)-selective tetrasubstituted olefins (entries 17-20), whereas the coupling

reaction with cyclopentene afforded a highly diastereoselective formation of the coupling product **36t** (entry 21). The structure of **36t** was tentatively assigned on the basis of ^1H NMR spectroscopic data. Assignment of the signals for diastereotopic CH proton (H_1) was established by the magnitude of its vicinal coupling to H_2 (Figure 9). For activated olefins, a mixture of linear and branched olefin products **36u** and **36v** was produced with styrene (entry 22), while ethyl acrylate gave an exclusive formation of the (*Z*)-selective linear coupling product **36w** (entry 23). (*E*)-*N,N*-Dimethyl-(naphthalen-2-yl)-2-propenamide was also found to react smoothly with propene to give the corresponding tetrasubstituted olefin product **36x** (entry 24).

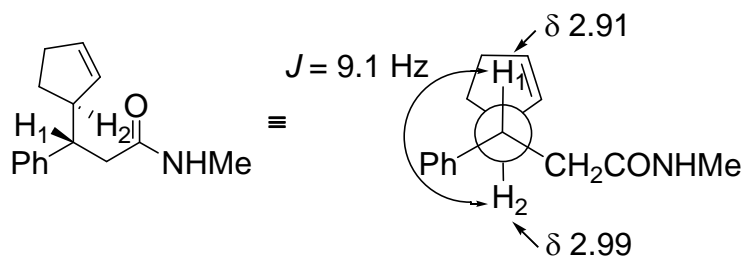
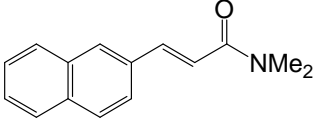
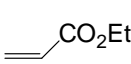
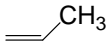
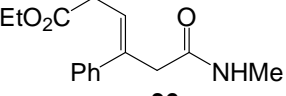
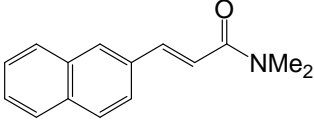
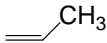
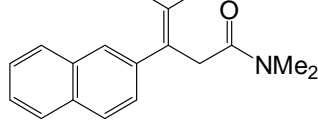


Figure 9. Newman Projection of Compound **36t**.

Table 7. Conjugate Addition Reaction of Simple Olefins to α,β -Unsaturated Amides.^a

entry	substrate	alkene	product (s)	t (h)	temp (°C)	yield (%) ^b
1	R = H, H		36a	2	70	75
2	R = H, Me		36b	2	70	93
3	R = Me, Me		36c	2	70	94
4	R = Et, Et		36d	2	70	95
5	R = <i>i</i> -Pr, <i>i</i> -Pr		36e	2	70	95
6	R = <i>n</i> -Bu, <i>n</i> -Bu		36f	2	70	95
7	R = H, <i>p</i> -Me-C ₆ H ₄		36g	2	70	94
8	R = H, Ph		36h	2	70	96
9	R = H, <i>p</i> -Cl-C ₆ H ₄		36i	2	70	94
10	R = H, Bz		36j	2	70	94
11	R = Me, Ph		36k	2	70	94
12	n = 1		36l	2	70	94
13	n = 2		36m	2	70	95
14			(Z)/(E)-36n = 3:1	14	50	78
15			36o	14	50	64
16			36o	14	50	65
17		R = (CH ₂) ₂ CH ₃	36p	14	50	90
18		R = (CH ₂) ₄ CH ₃	36q	14	50	81
19		R = Cy	36r	14	50	90
20		R = CH ₂ Ph	36s	14	50	85
21			36t	14	50	89
22			36u/36v = 3:2	14	50	70

23					14	50	50
24				2	70	95	

^a Reaction conditions: carbonyl compound (0.58 mmol), propene (2.9 mmol), catalyst (3 mol%), CH₂Cl₂ (2 mL), 70 °C, 2-14 h. ^b Isolated yield.

3.2.3 Coupling Reactions of α -Substituted α,β -Unsaturated Carbonyl Compounds with Alkenes

The scope of the coupling reaction of α -substituted α,β -unsaturated carbonyl compounds with simple olefins was explored by using the cationic ruthenium hydride complex **26** (Table 8). Generally, α -substituted α,β -unsaturated carbonyl compounds were found to undergo the coupling reaction with simple olefins to give tetrasubstituted olefin products. However, the tertiary cinnamides which are sterically demanding substrates showed no activity for the coupling reaction with alkenes. The reaction of α -phenyl α,β -unsaturated amide with propene gave slightly lower yield of the coupling product in comparison with α -methyl α,β -unsaturated amide substrates (entries 4-7). A mixture of *E/Z* olefin products was formed from α -substituted α,β -unsaturated amide with ethylene, while the coupling reaction with 1-butenes and 2-butenes gave the same product **37i** (entries 8-10). Sterically less demanding α -olefins such as 1-hexene and 4-phenyl-1-butene were found to give tetrasubstituted *Z*-olefins selectively **37j** and **37k**, while the coupling reaction with cyclopentene gave highly diastereoselective coupling products which have three different chiral centers (entries 11-13). The structures of the coupling products **37l** and **37m** were assigned from the ¹H NMR spectroscopic data.

Assignment of the ^1H NMR spectra for the diastereotopic CH protons was established by examining the coupling constants with their vicinal protons (Figure 10). Heterocyclic compound such (*E*)-ethyl-3-(furan-2-yl) 2-methylacrylate with propene yielded tetrasubstituted olefin product **33o** (entry 14).

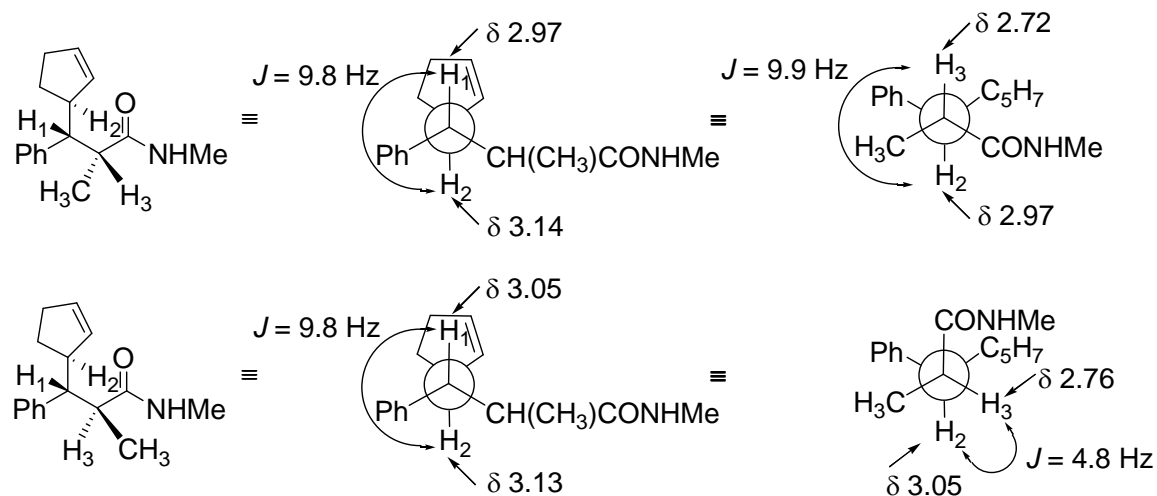


Figure 10. Newman Projection of Compounds **37l** and **37m**.

Table 8. Conjugate Addition Reaction of Simple Olefins to α -Substituted α,β -Unsaturated Compounds.^a

entry	substrate	alkene	product (s)	t (h)	temp (°C)	yield (%) ^b
1				14	70	91
2	X = H		37a	14	70	94
3	X = Me		37b	14	70	95
	X = Cl		37c	14	70	95
4				14	70	92
5	R = Me	R' = H, Me	37d	14	70	92
6	R = Me	R' = H, Bz	37e	14	70	95
7	R = Ph	R' = H, Me	37f	14	70	<5
	R = Me	R' = Me, Me	37g	14	70	<5
8				14	50	80
			(Z)/(E)- 37h = 2:1			
9				14	50	38
10			37i	14	50	37
11				14	50	80
			37j			
12				14	50	80
			37k			
13				14	20	89
			37l/37m = 7:2			
14				14	70	95
			37n			

^a Reaction conditions: carbonyl compound (0.58 mmol), propene (2.9 mmol), **26** (3 mol%), CH₂Cl₂ (2 mL), 70 °C, 2-14 h, ^b Isolated yield.

3.2.4 Oxidative Coupling Reactions of α -Substituted α,β -Unsaturated Carbonyl

Compounds with Aromatic Alkenes

The scope of the coupling reaction of α -substituted α,β -unsaturated carbonyl compounds with aromatic alkenes was further extended by using cationic ruthenium hydride complex **26** (Table 9). α -Methyl α,β -unsaturated esters (e.g. (*E*)-*p*-X-C₆H₄CH=C(CH₃)CO₂Et, X = Me, H, Cl) and α -methyl α,β -unsaturated amides with sterically demanding group were found to give <5% of the coupling products. In contrast, α -methyl α,β -unsaturated amide with less bulky alkyl group with styrene in the presence of **26** was found to easily afford oxidative coupling products under similar condition (entries 1-5). Styrene derivatives with electron donating groups were found to readily undergo the oxidative coupling reaction with (*E*)-C₆H₅CH=C(CH₃)CONHCH₃ to give tetrasubstituted diene products (entries 7 and 8). In contrast, aromatic olefins with electron withdrawing group gave low yields for the coupling reaction with (*E*)-C₆H₅CH=C(CH₃)CONHCH₃ (entries 6 and 9). 2-Vinylnaphthalene derivatives were also suitable substrates for the oxidative coupling reaction with (*E*)-C₆H₅CH=C(CH₃)CONHCH₃ to give oxidative coupling products (entries 10 and 11).

Table 9. Oxidative Coupling Reaction of Aromatic Olefins to α -Substituted α,β -Unsaturated Amides.^a

entry	substrate	alkene	product (s)	t (h)	temp (°C)	yield (%) ^b
1	X = H Z = OEt		38a	14	50	<5
2	X = Me Z = OEt		38b	14	50	<5
3	X = Cl Z = OEt		38c	14	50	<5
4	X = H Z = NMe ₂		38d	14	50	<5
5	X = H Z = NHMe		38e	14	50	51
6		Y = Cl	38f	14	50	14
7		Y = OMe	38g	14	50	62
8		Y = Me	38h	14	50	56
9		Y = Ph	38i	14	50	29
10		Y = H	38j	14	50	70
11		Y = OMe	38k	14	50	71

^a Reaction conditions: carbonyl compound (0.58 mmol), propene (2.9 mmol), catalyst (3 mol%), CH₂Cl₂ (2 mL), 70 °C, 2-14 h, ^b Isolated yield.

3.4.5 Intramolecular Coupling Reaction of α,β -Unsaturated Esters with Simple Olefins

To further extend the synthetic applicability of the coupling reaction, we next explored the intramolecular coupling reaction catalyzed by cationic ruthenium hydride complex **26** (Table 10). Thus, the treatment of (*E*)-methyl 3-(2-allylphenyl)acrylate with 5 mol% of **26** in CH₂Cl₂ at 80 °C led to the formation of 1,2-disubstituted indene product **39a** in 78% isolated yield (entry 1). Both intramolecular substrates, which have 1-butenyl and 2-butenyl-substituted appendages gave the same 1,2-disubstituted indene product **39b** respectively (entries 2 and 3). The result indicates that the olefin isomerization is faster than the cyclization reaction. On the other hand, cyclic olefin substrates were found to readily undergo the oxidative cyclization reaction to form fulvene products **39c-39h** (entries 4-9). Both seven- to eight-membered cyclic olefin substrates showed the similar activity for cyclization (entries 5, 6, 8 and 9), but six-membered cyclic olefin substrates with olefin group exhibited relatively low yield (entries 4 and 7). Even though reaction temperature was increased up to 100 °C, five-membered cyclic olefin substrates exhibited no activity for cyclization.

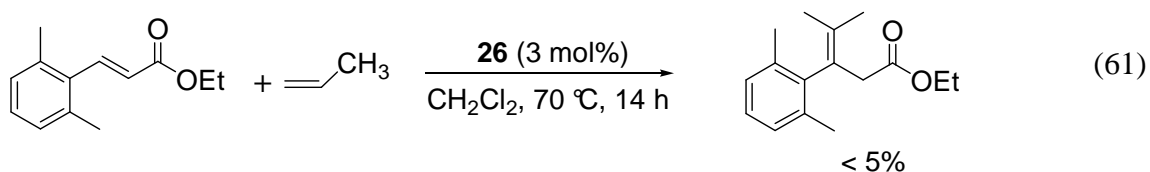
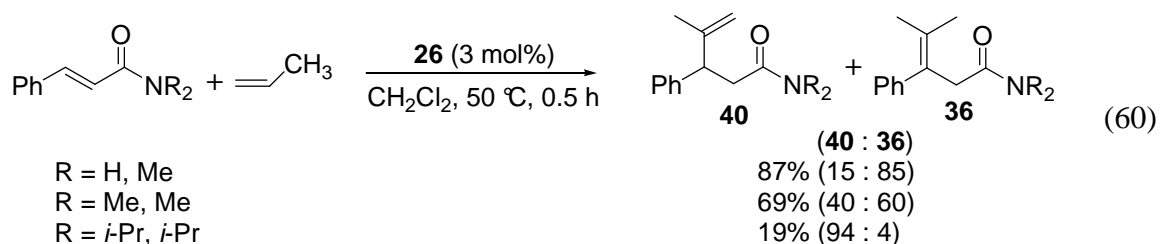
Table 10. Intramolecular Coupling Reaction of α,β -Unsaturated Esters with Simple Olefins Catalyzed by **26**.^a

entry	substrate	product	yield (%) ^b
1			78
2			76
3			75
4			51
5			71
6			83
7			70
8			82
9			88

^a Reaction conditions: carbonyl compound (0.58 mmol), catalyst (5 mol%), CH₂Cl₂ (2 mL), 80 °C, 24 h, ^b Isolated yield.

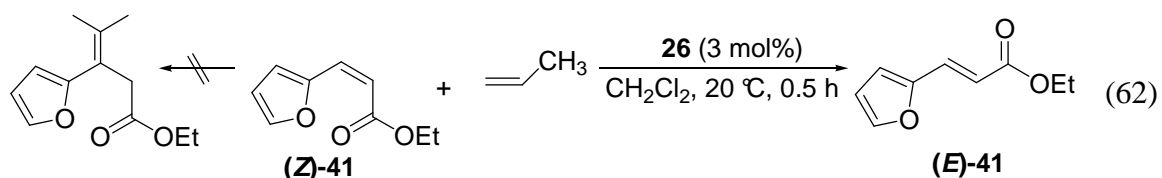
In order to investigate steric effects, we employed a series of cinnamide derivatives with sterically demanding alkyl groups (R = CH₃, (CH₃)₂, (*i*-Pr)₂) as the substrates for the coupling reaction. Increasing the steric bulk of amide nitrogen position

from methyl to isopropyl led to dramatically decreased yield after 0.5 h, but the coupling reactions with different alkyl groups at nitrogen site gave the comparable yield at 70 °C for 2 h (Eq 60). A sterically more demanding substrate (*E*)-ethyl-3-(2,6-dimethylphenyl)acrylate showed no activity under the similar reaction condition. 2,6-Dimethyl group inhibited the coupling reaction with propene due to steric repulsion by strongly blocking the substrate to coordinate to ruthenium center (eq 61). From these results, a steric effect toward active ruthenium species should play an important role in the coupling reaction.



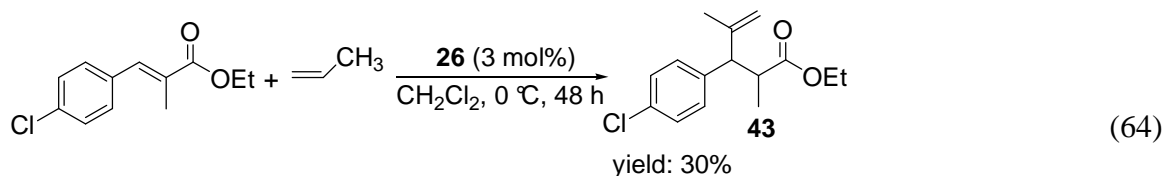
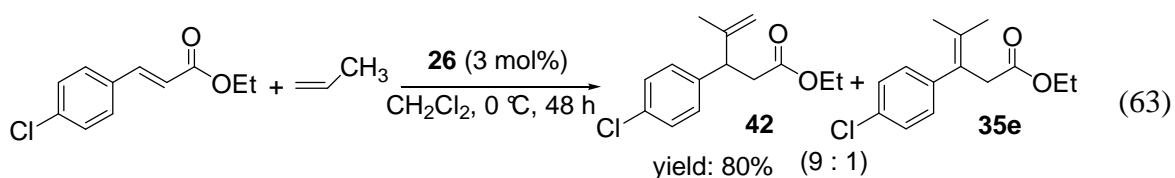
We next compared the reactivity pattern between *trans* and *cis* conformation of α,β -unsaturated carbonyl compounds. We hypothesized that the coupling reaction proceeds through *trans* conformation for the α,β -unsaturated carbonyl compound and complexation of cationic ruthenium hydride complex *syn* to the ene group on the carbonyl double bond. On the other hand, the *cis* conformation of substrate would disfavor for coupling reaction because chelation of ruthenium to oxygen atom in carbonyl

substrates is key step for coupling reaction. This seems to be true because the coupling reaction of ethyl *cis*-2-furanacrylate with propene in presence cationic ruthenium complex at 20 °C for 0.5 h led to a fast transition from *cis* to *trans* conformation without forming the coupling product (Eq 62). We rationalized that the *cis* conformation would disfavor the the coupling reaction because the sterically crowded *Z*-form substrate would be difficult to coordinate ruthenium center. These results indicate that the chelate-assisted insertion of the ruthenium into the carbonyl substrate is an important step for the coupling reaction.



As mentioned above, we found that the cationic ruthenium complex **26** is a highly effective catalyst for the intermolecular conjugate addition reaction of simple olefins to α,β -unsaturated carbonyl compounds.^{77d} The coupling reaction easily generates tetrasubstituted olefins after olefin isomerization step. We hypothesized that the coupling reaction of α,β -unsaturated carbonyl compounds with simple alkenes can easily produce 1,1-disubstituted olefin products. This reaction would be synthetically useful because chiral compounds which can be easily generated from the coupling reaction and 1,1-disubstituted alkenes derived from the conjugate addition reaction are powerful intermediates in synthesis of a diverse range of important compounds. Treatment of (*E*)-*p*-ClC₆H₄CH=CHCO₂Et with propene in the presence of a catalytic amount of cationic

ruthenium hydride complex **26** (3 mol%) in CH₂Cl₂ at 0 °C for 48 h gave the coupling products in 80% yield with high diastereoselectivity in the formation of 1,1-disubstituted olefin product (**42:35a** = 9:1) (eq 63). (*E*)-*p*-ClC₆H₄CH=C(CH₃)CO₂Et was found to react with propene in the presence of **26** at 0 °C for 48 h. The reaction showed high stereoselectivity for 1,1-disubstituted olefin product albeit with a moderate yield (30%) (eq 64).



3.3 Mechanistic Studies

3.3.1 Reaction Profile

In order to probe the reaction mechanism of the coupling reaction, the disappearance of starting material as well as the appearance of products was monitored by ¹H NMR for the reaction of (*E*)-*p*-CF₃C₆H₄CH=CHCO₂Et (**44**) with propene in the presence of **26** (2 mg, 3.5 μmol) at 60 °C. The compound **44** was rapidly converted to compound **45** within 5 min along with the insertion of propene. The signals due to the tetrasubstituted olefin product **35g** gradually appeared at the expense of the compound **45** by isomerization. Eventually, the formation of the tetrasubstituted olefin product **35g** was observed after heating at 60 °C for 3 h (Figure 11).

The kinetics of the conversion of **45** to the tetrasubstitute olefin product **35g** was followed by ^1H NMR. In a J-Young NMR tube, **44** (28 mg, 0.12 mmol), propene (5 equiv), and **26** (2.0 mg, 3.5 μmol) were dissolved in CD_2Cl_2 (0.5 mL). The appearance of **45** and **35g** was monitored by ^1H NMR at 60 $^\circ\text{C}$ in 5 min intervals. The experimental data were successfully fitted to the kinetic equation for two consecutive reaction kinetics by using nonlinear regression techniques for the conversion of **44** to **35g** (Sigma-plot Version 10). The rate constants $k_1 = 0.042 \text{ min}^{-1}$ and $k_2 = 0.011 \text{ min}^{-1}$ were calculated from this analysis.

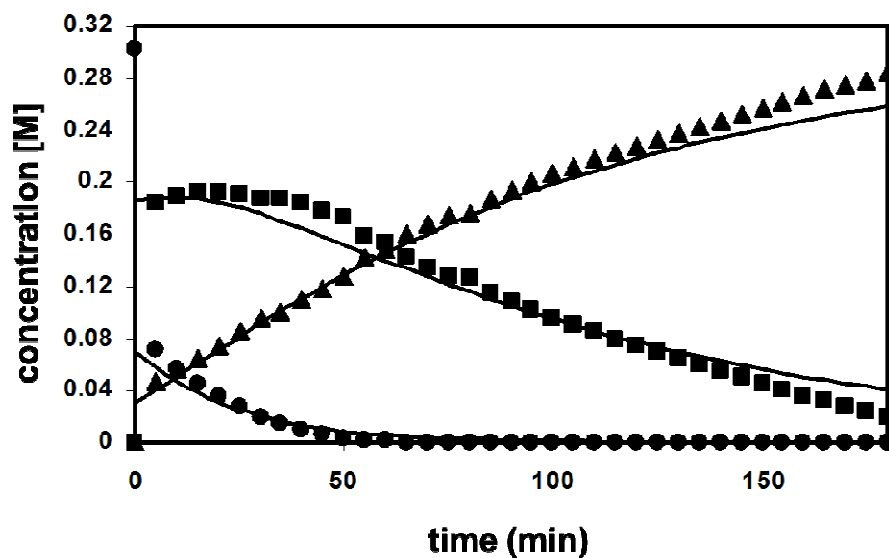
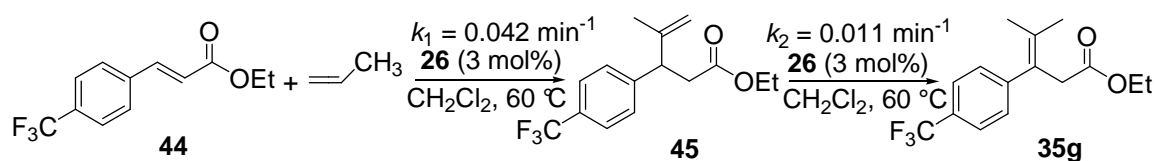


Figure 11. Kinetic Profile of the Conversion of **44** to **35g**. Notations: **44** (●), **45** (■), **35g** (▲).

3.3.2 Hammett Study

To discern the electronic effects on the product formation, Hammett ρ values were measured for the coupling reactions with different carbonyl compounds and alkenes. Thus, the correlation of relative rates with σ_p for series of *para*-substituted *p*-X-C₆H₄CH=CHCO₂Et (X = OCH₃, CH₃, H, F, Cl, CO₂Me, CF₃) with propene in presence of **26** (3 mol%) at 20 °C led to positive ρ value ($\rho = +1.1 \pm 0.1$) (Figure 12).

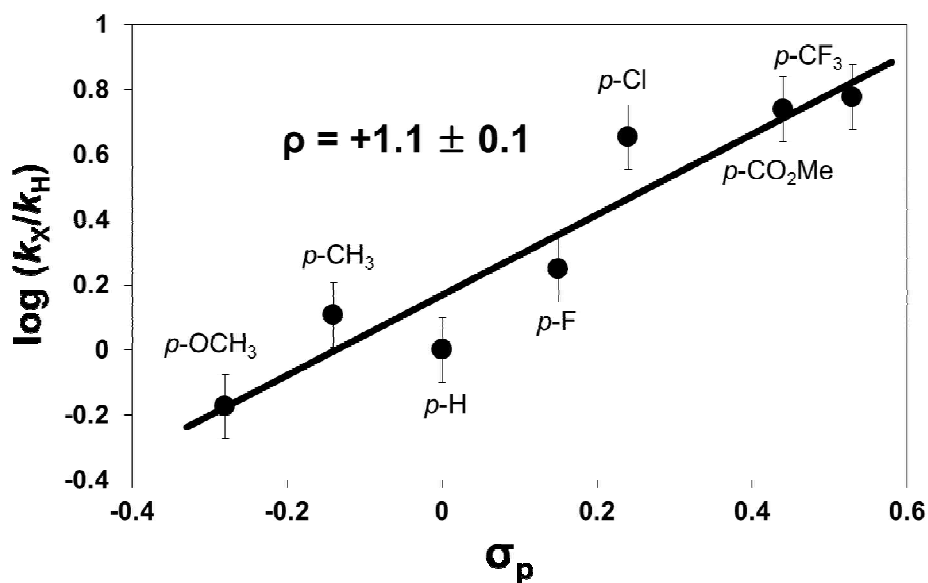
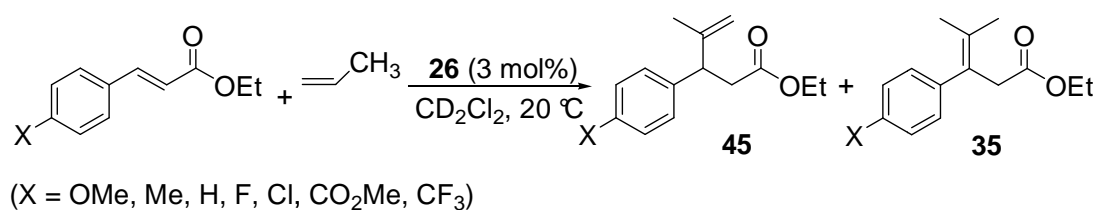


Figure 12. Hammett Plot of the Coupling Reaction of *para*-Substituted (*E*)-*p*-X-C₆H₄CH=CHCO₂Et (X = OCH₃, CH₃, H, F, Cl, CO₂Me, CF₃) with Propene.

An analogous correlation of the reaction rates of (*E*)-C₆H₅CH=CHCO₂Et with series of *para*-substituted styrene *p*-Y-C₆H₄CH=CH₂ (Y = OCH₃, CH₃, H, Cl, CF₃) also resulted in the positive ρ value ($\rho = +1.5 \pm 0.1$) in presence of **26** (5 mol%) at 50 °C in

CH_2Cl_2 (Figure 13). The reaction rates were found to be strongly accelerated by electron-withdrawing group of both cinnamate and styrene derivatives. The similar Hammett ρ values indicate the same mechanistic pathway for the coupling reaction of α,β -unsaturated carbonyl compounds and alkenes. The positive ρ values indicate that an excess electron density on the transition state is influenced by coordination of both substrates to the ruthenium center. The Hammett ρ value observed from the correlation of *para*-substituted $p\text{-X-C}_6\text{H}_4\text{CH=CHCO}_2\text{Et}$ in CD_2Cl_2 matches well with the chelate-directed regioselective alkene insertion, which is dictated by the nucleophilicity of a developing negative charge on the β -carbon of cinnamate derivatives.^{77(d)}

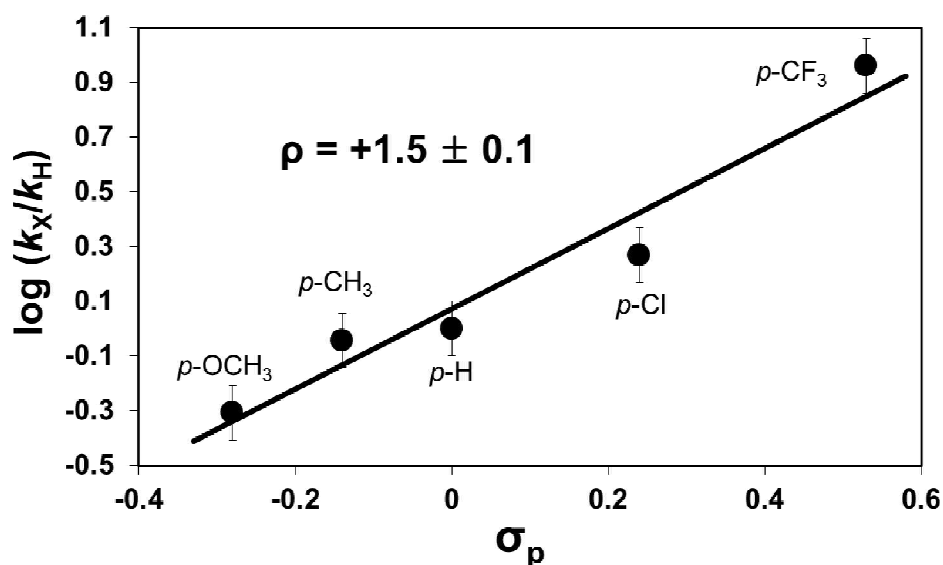
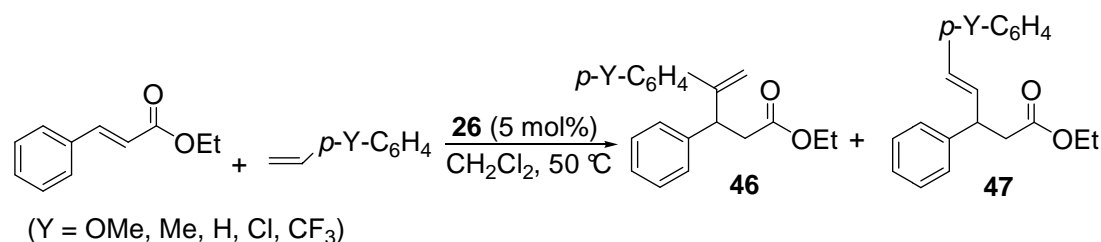


Figure 13. Hammett Plot of the Coupling Reaction of $(E)\text{-C}_6\text{H}_4\text{CH=CHCO}_2\text{Et}$ with *para*-Substituted Styrene $p\text{-Y-C}_6\text{H}_4\text{CH=CH}_2$ (Y = OCH_3 , CH_3 , H, Cl, CF_3).

For the coupling reaction of (*E*)-C₆H₅CH=C(CH₃)CONHCH₃ with *para*-substituted styrenes *p*-Y-C₆H₄CH=CH₂ (Y = OCH₃, CH₃, H, F, Cl, CF₃), a difference in the selectivity pattern was observed depending on the substitution (Scheme 16). The coupling reactions of (*E*)-C₆H₅CH=C(CH₃)CONHCH₃ with styrene derivatives with *para*-electron donating group (OCH₃, CH₃, H) gave the oxidative coupling products **39** predominantly (70 ~ 85 %). In contrast, the coupling reactions of (*E*)-C₆H₅CH=C(CH₃)CONHCH₃ with *p*-Y-C₆H₄CH=CH₂ (Y = F, Cl, CF₃) with *para*-electron withdrawing group were found to give a mixture of the branched and linear olefin products **48** and **49** as the major products (75 ~ 85%).

To understand the electronic effects on the product formation for *para*-substituted group of styrene derivatives, the Hammett ρ value was measured for the coupling reaction of (*E*)-C₆H₅CH=C(CH₃)CONHCH₃ with styrene derivatives in CH₂Cl₂. The correlation of the relative rates with σ_p for (*E*)-C₆H₅CH=C(CH₃)CONHCH₃ with a series of *para*-substituted styrene *p*-Y-C₆H₄CH=CH₂ (Y = OCH₃, CH₃, H, F, Cl, CF₃) in presence **26** (5 mol %) at 40 °C in CH₂Cl₂ led to the positive ρ values both electron donation and electron withdrawing groups (for electron donating groups: $\rho = +1.1 \pm 0.1$, for electron withdrawing groups: $\rho = +0.9 \pm 0.1$) (Scheme 16 and Figure 14). The reaction rate was found to be strongly accelerated by electron-withdrawing group of styrene derivatives, which is consistent with conjugate addition mechanism. The positive value of ρ indicates that there must be an excess of electron density built up at transition state which can be influenced by the substituent on the arene ring. These results also imply that the rate-limiting step is facilitated by electron withdrawing groups, but the

coupling reactions were operated by different mechanistic pathway depending substrate employed.

Scheme 16

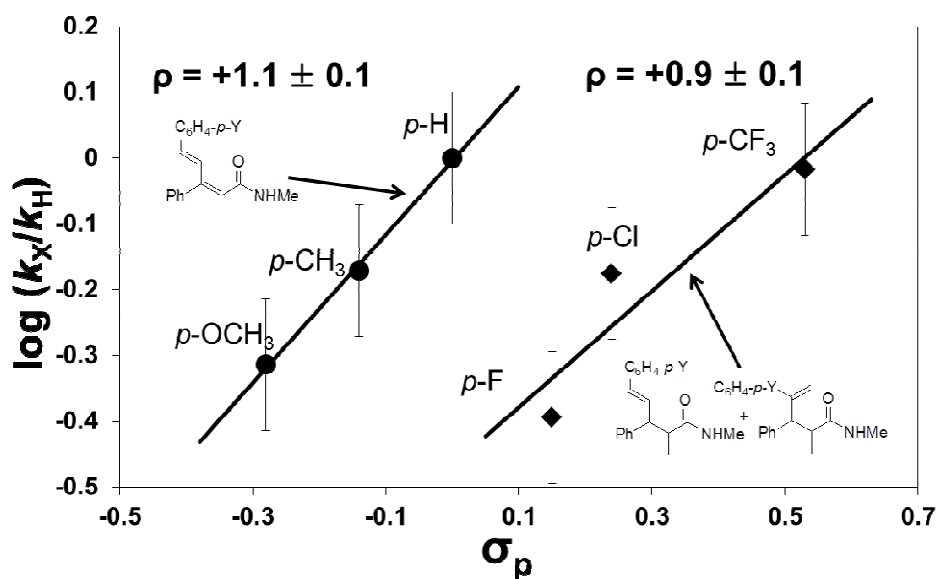
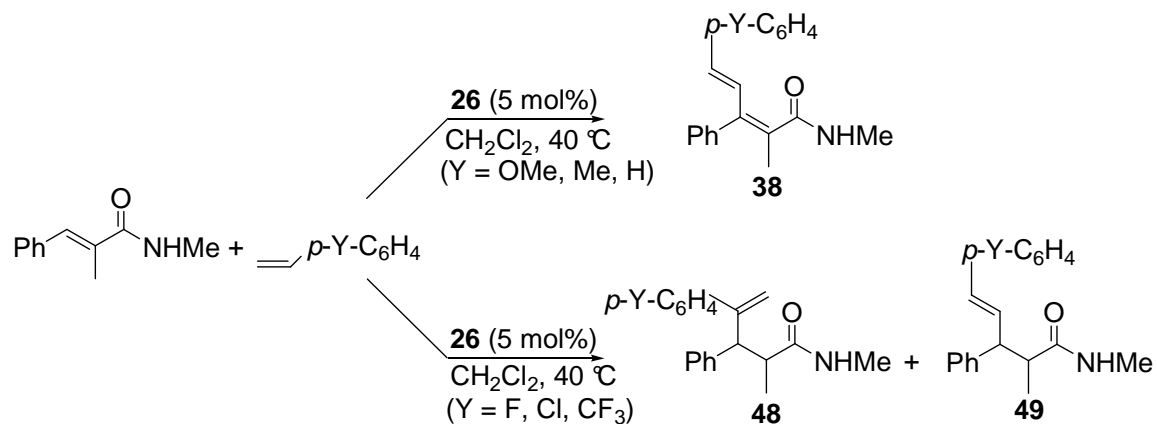
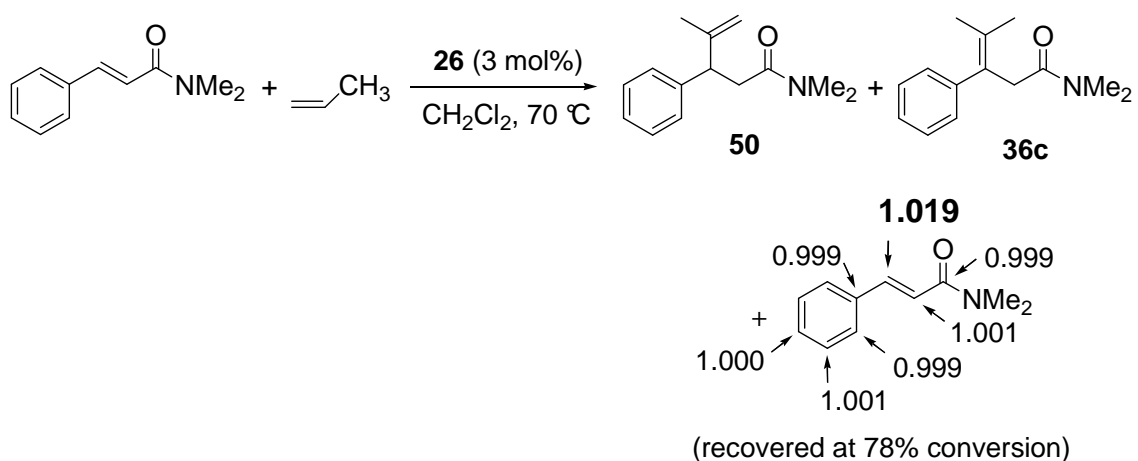


Figure 14. Hammett Plot of the Coupling Reaction of (E) - $\text{C}_6\text{H}_4\text{CH}=\text{C}(\text{CH}_3)\text{CONHCH}_3$ with p -Substituted Styrene $p\text{-Y}-\text{C}_6\text{H}_4\text{CH}=\text{CH}_2$ ($\text{Y} = \text{OCH}_3, \text{CH}_3, \text{H, F, Cl, CF}_3$).

3.3.3 Isotope Effect Studies

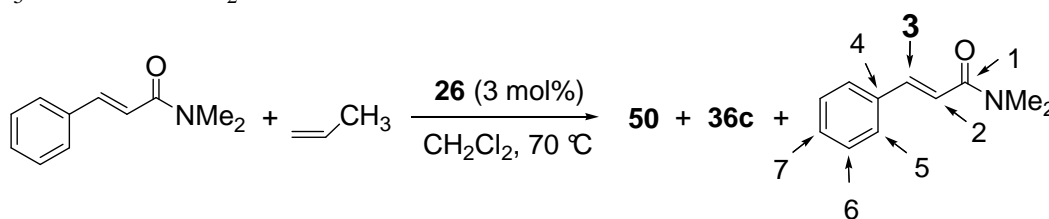
The following kinetic experiments were performed in order to gain detailed mechanistic insights on the coupling reaction. The carbon isotope effect of the coupling reaction was measured by employing Singleton's NMR technique at natural abundance.⁶² The ¹³C NMR signal intensities were compared between the recovered (*E*)-C₆H₅CH=CHCONMe₂ at 75 ~ 80% conversions and virgin sample by using aromatic C⁽⁷⁾H signal as an internal standard. As shown in Scheme 17, the most pronounced carbon isotope effect was observed on the β-carbon atom of (*E*)-C₆H₅CH=CHCONMe₂ when the ¹³C ratio of recovered substrate at 78% conversion was compared to that of the virgin sample (¹³C(recovered)/¹³C(virgin) at C_β = 1.019, average of three runs). Using the equations developed by Melander and Saunderson,⁶³ the ¹²C/¹³C isotope effects are calculated as summarized in Table 11. The results indicate that the olefin insertion to α,β-unsaturated carbonyl substrate is the rate-limiting step for the coupling reaction.

Scheme 17



In contrast, a negligible isotope effect of k_H/k_D was observed from ethylene and ethylene- d_4 with (*E*)- $C_6H_5CH=CHCO_2Et$ at 60 °C in CD_2Cl_2 . The pseudo-first-order plots of the catalytic reaction from both ethylene and ethylene- d_4 led to $k_{obs} = 8.3 \times 10^{-4} \text{ min}^{-1}$ and $k_{obs} = 7.3 \times 10^{-4} \text{ min}^{-1}$, respectively, which translated to a $k_H/k_D = 1.1 \pm 0.1$ (Figure 15). These results indicate that the C-C bond formation step is the rate-limiting step of coupling reaction of α,β -unsaturated carbonyl compounds with simple olefins and subsequent β -hydride elimination and isomerization steps are relatively facile.^{77d}

Table 11. Average ^{13}C Integration of the Recovered and Virgin Samples of (*E*)- $C_6H_5CH=CHCONEt_2$.



C #	virgin	recovered (75 % conv.)	recovered/virgin	change (%)
1	1.089	1.084	0.9952	-0.48
2	0.928	0.929	1.0011	0.11
3	1.035	1.054	1.0182	1.82
4	1.047	1.046	0.9990	-0.10
5	2.138	2.134	0.9980	-0.20
6	2.119	2.121	1.0010	0.10
7(ref)	1.000	1.000	1.0000	0.00

C #	virgin	recovered (78 % conv.)	recovered/virgin	change (%)
1	1.089	1.090	1.0005	0.05
2	0.928	0.929	1.0009	0.09
3	1.035	1.054	1.0186	1.86
4	1.047	1.047	0.9990	-0.10
5	2.138	2.139	1.0003	0.03
6	2.119	2.119	0.9999	-0.01
7(ref)	1.000	1.000	1.0000	0.00

C #	virgin	recovered (80 % conv.)	recovered/virgin	change (%)
1	1.089	1.090	1.0010	0.10
2	0.928	0.929	1.0011	0.11
3	1.035	1.055	1.0192	1.92
4	1.047	1.045	0.9984	-0.16
5	2.138	2.140	1.0010	0.10
6	2.119	2.121	1.0010	0.10
7(ref)	1.000	1.000	1.0000	0.00

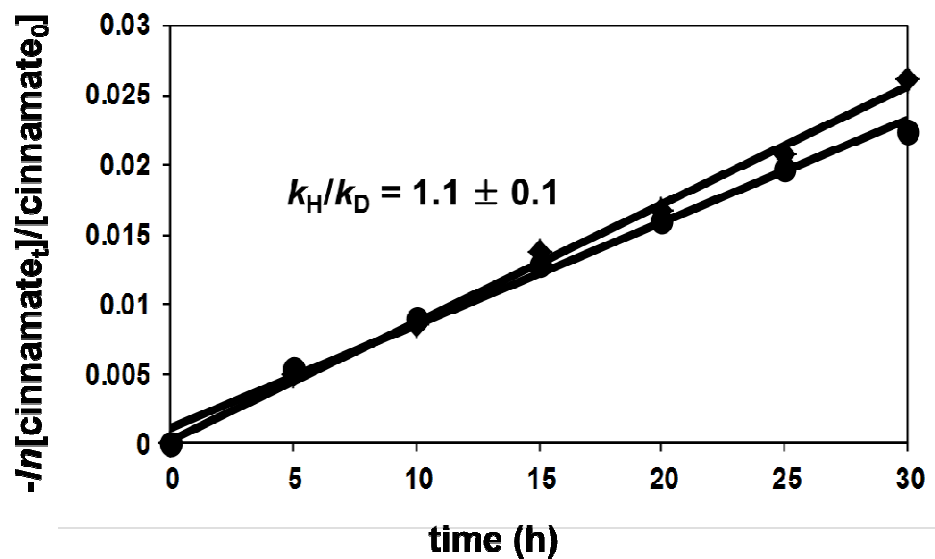
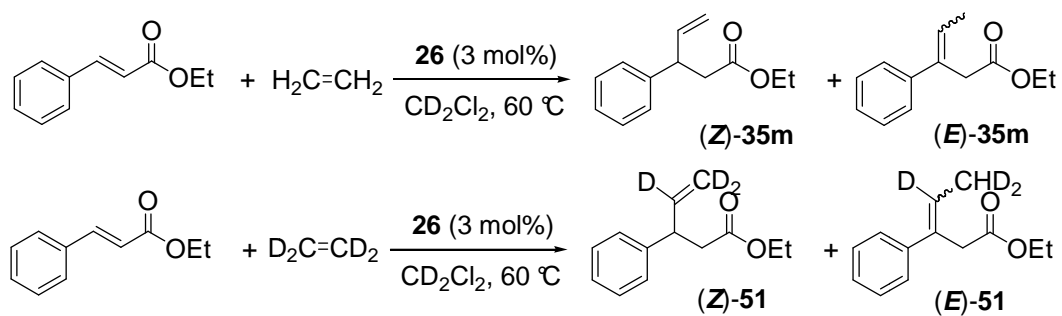


Figure 15. First-Order Plots of $-\ln[\text{cinnamate}]_t/[\text{cinnamate}]_0$ vs Time for the Coupling Reaction of (*E*)- $\text{C}_6\text{H}_5\text{CH}=\text{CHCO}_2\text{Et}$ with Ethylene (\blacklozenge) or Ethylene- d_4 (\bullet).

To discern the rate-limiting step of the coupling reaction of (*E*)- $C_6H_5CH=C(CH_3)CONHCH_3$ with styrene derivatives which can give different selectivity depending on *para*-substituted styrene derivatives, the carbon isotope effect of the coupling reactions of (*E*)- $C_6H_5CH=C(CH_3)CONHCH_3$ with 4-chlorostyrene were measured by employing Singleton's NMR technique at natural abundance. In this case, the most pronounced carbon isotope effect was observed on the β -carbon atom of (*E*)- $C_6H_5CH=C(CH_3)CONHCH_3$ when the ^{13}C ratio of recovered substrate at 81% conversion was compared to that of the virgin sample ($^{13}C(\text{recovered})/^{13}C(\text{virgin})$ at $C_\beta = 1.039$, average of two runs). These results indicate that the olefin insertion into an α -substituted α,β -unsaturated carbonyl compounds is the rate-limiting step of the coupling reaction which is consistent with previous case.^{77d} On the other hand, the negligible carbon isotope effect for coupling reaction of (*E*)- $C_6H_5CH=C(CH_3)CONHCH_3$ with styrene in yielding the oxidative coupling product **38e** was observed on β -carbon atom of (*E*)- $C_6H_5CH=C(CH_3)CONHCH_3$. The ^{13}C ratio of recovered substrate to that of the virgin sample [$^{13}C(\text{recovered})/^{13}C(\text{virgin})$] was $C_\beta = 0.998$ (average of 2 runs, at 70% conversion). These results of ^{13}C isotope effect studies are calculated and summarized in Table 12 and Table 13. These observations indicate that the C-C bond forming step is not the rate-limiting step for the coupling reaction of $C_6H_5CH=C(CH_3)CONHCH_3$ with styrene derivatives in forming oxidative product **38e**.

Scheme 18

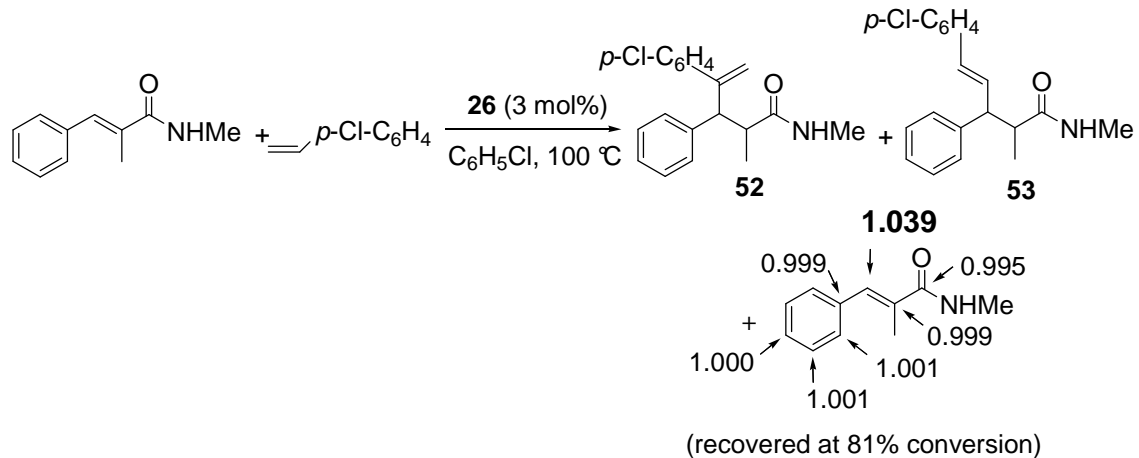
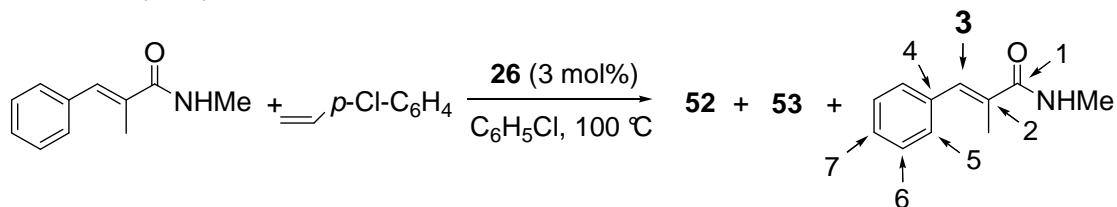


Table 12. Average ^{13}C Integration of the Recovered and Virgin Samples of (*E*)- $\text{C}_6\text{H}_5\text{CH}=\text{C}(\text{CH}_3)\text{CONHCH}_3$.



C #	virgin	recovered (80 % conv.)	recovered/virgin	change (%)
1	1.014	1.014	1.0000	0.00
2	0.969	0.967	1.0010	0.10
3	0.970	1.038	1.0381	3.81
4	0.955	0.958	1.0030	0.30
5	2.066	2.069	1.0015	0.15
6	1.992	1.996	1.0020	0.20
7(ref)	1.000	1.000	1.0000	0.00

C #	virgin	recovered (82 % conv.)	recovered/virgin	change (%)
1	1.014	1.013	0.9990	-0.10
2	0.969	0.968	0.9990	-0.10
3	0.970	1.009	1.0402	4.02
4	0.955	0.950	0.9950	-0.50
5	2.066	2.068	1.0010	0.10
6	1.992	1.991	0.9990	-0.10
7(ref)	1.000	1.000	1.0000	0.00

Scheme 19

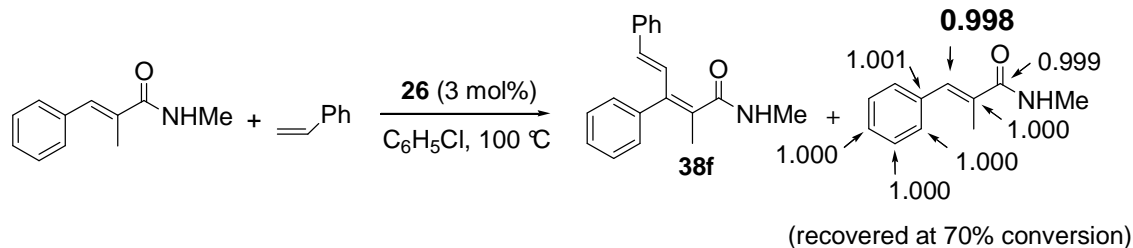
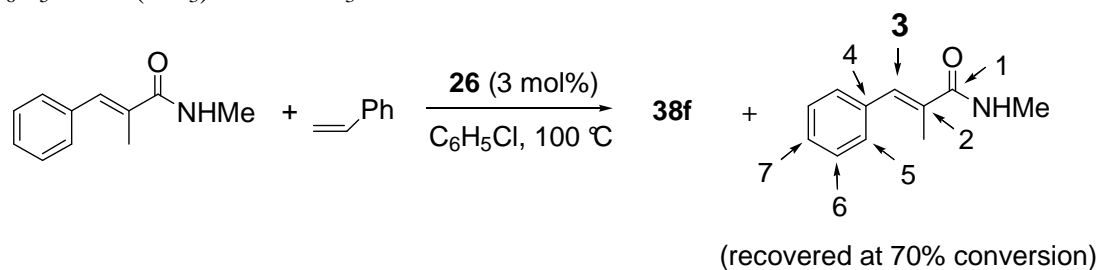


Table 13. Average ^{13}C Integration of the Recovered and Virgin Samples of (*E*)- $\text{C}_6\text{H}_5\text{CH}=\text{C}(\text{CH}_3)\text{CONHCH}_3$.



C #	virgin	recovered (65 % conv.)	recovered/virgin	change (%)
1	1.014	1.015	1.0009	0.09
2	0.969	0.969	0.9990	-0.10
3	0.970	0.975	1.0020	0.20
4	0.955	0.953	0.9980	-0.20
5	2.066	2.068	1.0010	0.10
6	1.992	1.991	0.9995	-0.05
7(ref)	1.000	1.000	1.0000	0.00

C #	virgin	recovered (67 % conv.)	recovered/virgin	change (%)
1	1.014	1.013	0.9990	-0.10
2	0.969	0.970	1.0010	0.10
3	0.970	0.967	0.9970	-0.30
4	0.955	0.958	1.0030	0.30
5	2.066	2.067	0.9995	-0.05
6	1.992	0.993	1.0005	0.05
7(ref)	1.000	1.000	1.0000	0.00

A normal deuterium isotope effect $k_{\text{H}}/k_{\text{D}} = 1.7 \pm 0.1$ was observed for coupling reaction of styrene and styrene- d_8 with (*E*)- $\text{C}_6\text{H}_5\text{CH}=\text{C}(\text{CH}_3)\text{CONHCH}_3$ at 40 °C in

CH_2Cl_2 . Also, a negligible isotope effect of $k_{\text{H}}/k_{\text{D}} = 1.1 \pm 0.1$ was observed from (*E*)- $\text{C}_6\text{H}_5\text{CH}=\text{C}(\text{CH}_3)\text{CONHCH}_3$ and (*E*)- $\text{C}_6\text{H}_5\text{CD}=\text{C}(\text{CH}_3)\text{CONHCH}_3$ with styrene under the similar reaction conditions. This result indicates that the cleavage of vinyl C-H bond of styrene is the rate-limiting step for oxidative coupling reaction, which means that this coupling reaction of (*E*)- $\text{C}_6\text{H}_5\text{CH}=\text{C}(\text{CH}_3)\text{CONHCH}_3$ with styrene derivatives which have electron donating groups has different mechanistic pathway in comparison with previous case.

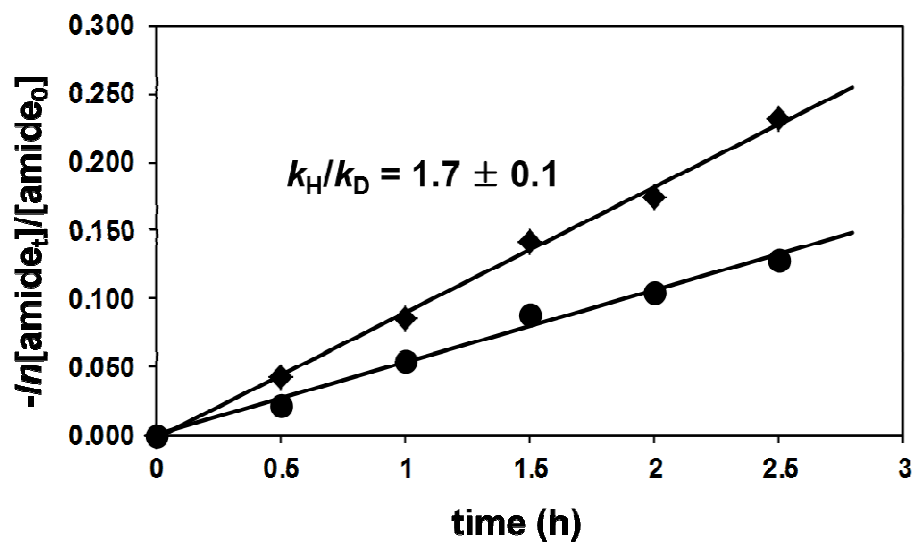
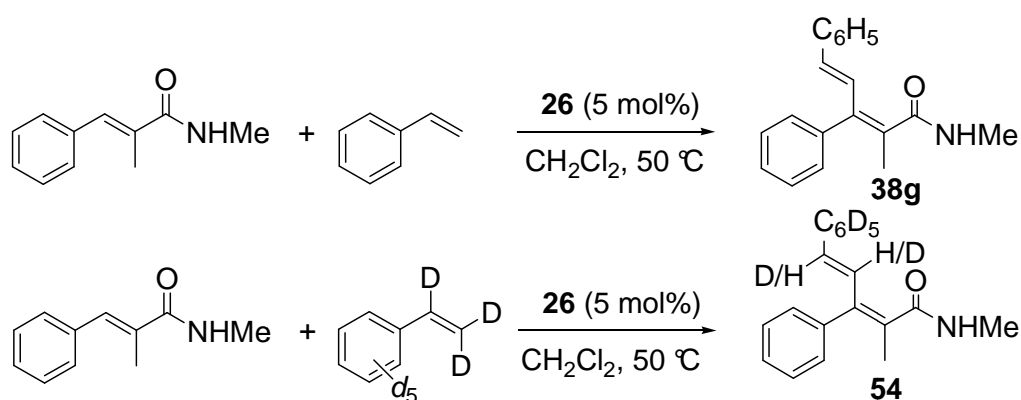


Figure 16. First-Order Plots of $-\ln([\text{cinnamide}]_t/[\text{cinnamide}]_0)$ vs Time for the Coupling Reaction of (*E*)- $\text{C}_6\text{H}_5\text{CH}=\text{C}(\text{CH}_3)\text{CONHCH}_3$ with Styrene (\blacklozenge) or Styrene- d_8 (\bullet).

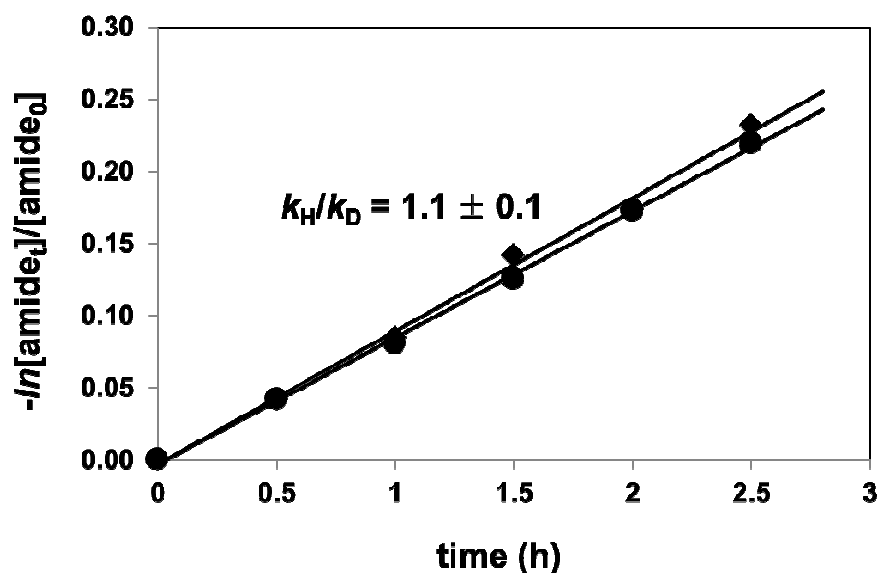
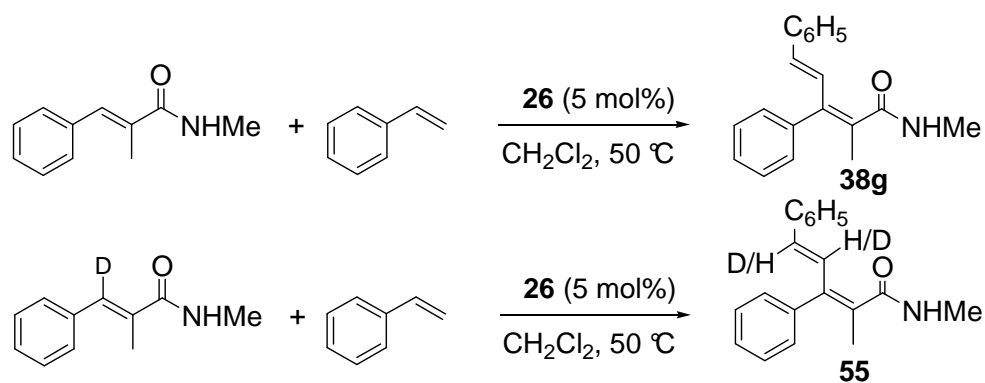


Figure 17. First-Order Plots of $-\ln([amide]_t/[amide]_0)$ vs Time for the Coupling Reaction of (*E*)- $C_6H_5CH=C(CH_3)CONHMe$ (♦) or (*E*)- $C_6H_5CD=C(CH_3)CONHMe$ (●) with Styrene.

3.3.4 Deuterium Labeling Studies

The following deuterium labeling studies were performed to learn more about the reaction mechanism. To examine H/D exchange pattern on the carbonyl substrate, the reaction mixture of (*E*)- $C_6D_5CD=CDCONMe_2$ (0.58 mmol) with propene (2.9 mmol) in the presence of **26** (3 mol %) in CH_2Cl_2 (2 mL) was stirred at 70 °C for 2 h. The isolated product **36c** was found to contain ~55% D on the α -methylene position, but with only 6%

of D on the δ -methyl positions (eq 65). Also, a significant deuterium incorporation was observed on unreacted propene.

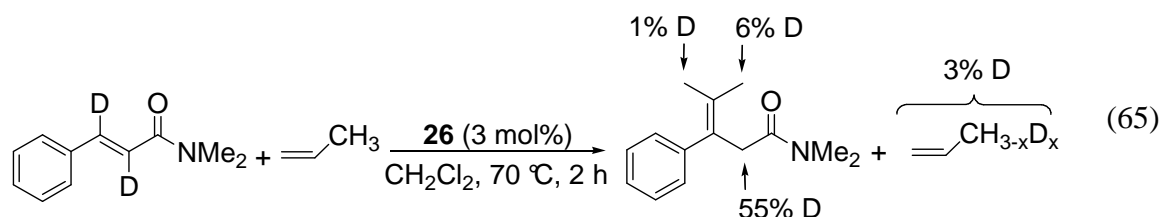


Figure 18(a) shows the ^1H NMR spectrum of the compound **36c-d_n**. The intensities of the peaks at δ 3.37 and 1.81 ppm which were assigned to methylene and methyl resonances, respectively, significantly decreased due to extensive deuterium incorporation. As shown in Figure 18(b), the existence of deuterium at each position was further confirmed by ^2H NMR. The recovered propene also observed an extensive deuterium incorporation on both vinyl and methyl positions (Figure 18(c)).

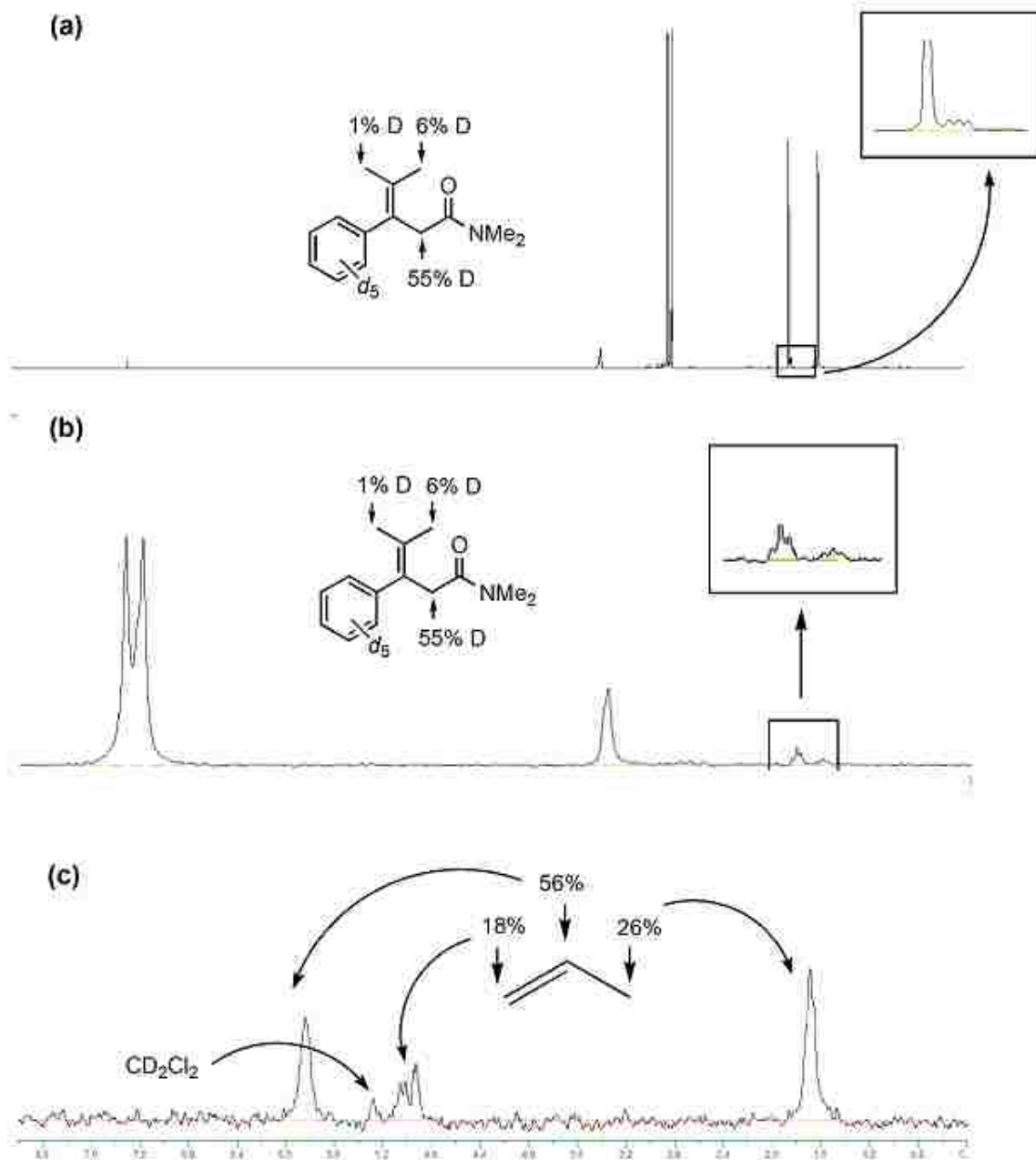


Figure 18. (a) ^1H NMR Spectrum of $36c-d_n$, (b) ^2H NMR Spectrum of $36c-d_n$, (c) ^2H NMR Spectrum of Recovered Propene.

To examine the H/D exchange pattern on the α -substituted carbonyl substrate, the treatment of (*E*)- $C_6H_5CD=C(CH_3)CONHCH_3$ (0.07 mmol) and styrene (5 equiv) in the presence of **26** (5 mol%) in CD_2Cl_2 was monitored by 1H and 2H NMR (eq 66). Initially, extensive H/D exchange was observed on both the β -position of carbonyl compound and vinyl position of styrene after 15 h at 20 °C without forming product. Such extensive H/D scrambling pattern is consistent with reversible C-H bond activation of β -position of (*E*)- $C_6H_5CD=C(CH_3)CONHCH_3$. These results indicate that vinyl C-H bond activation of α -substituted cinnamide substrates is not the rate limiting step of coupling reaction with styrene, for the styrenes with electron donating group at *para*-position.

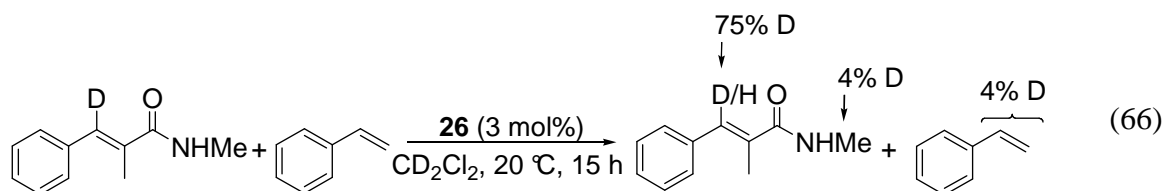


Figure 19(b) shows the 2H NMR spectrum of the coupling reaction mixture of (*E*)- $C_6H_5CD=C(CH_3)CONHCH_3$ with styrene in presence of **26** after 15 h at 20 °C. The intensity of the peak at δ 7.32 assigned to two vinyl resonance noticeably decreased due to extensive deuterium incorporation. As shown in Figure 19(b), new peaks due to styrene signals were observed by 2H NMR spectrum.

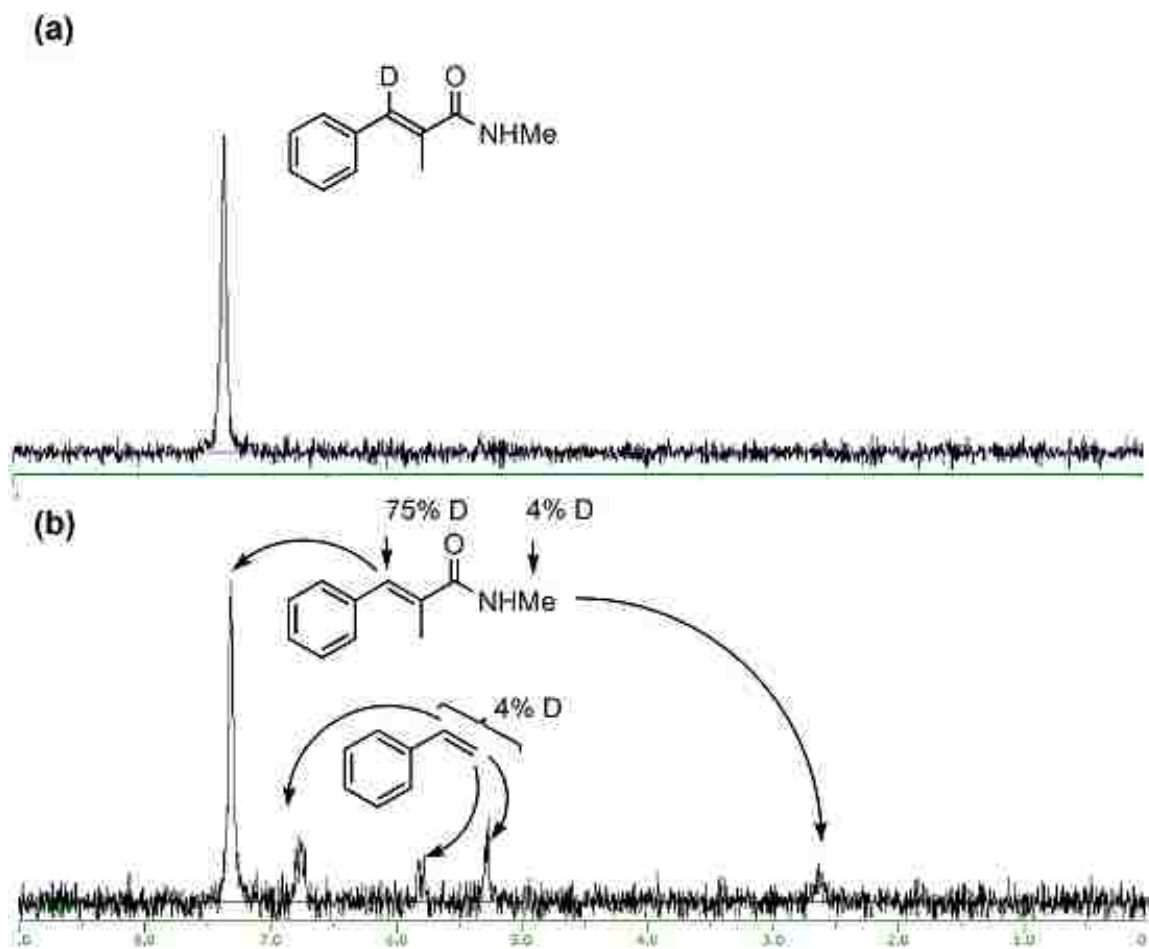


Figure 19. (a) ^2H NMR Spectrum of $(E)\text{-C}_6\text{H}_5\text{CD}=\text{C}(\text{CH}_3)\text{CONHCH}_3$, (b) ^2H NMR Spectrum of the Coupling Reaction Mixture of $(E)\text{-C}_6\text{H}_5\text{CD}=\text{C}(\text{CH}_3)\text{CONHCH}_3$ with Styrene.

3.3.5 Isolation of Catalytically Relevant Species

In an effort to trap/isolate catalytically relevant species, the reaction mixture of complex **26** (10 μmol) with a naphthyl-substituted amide (10 μmol), cyclopentene (5 equiv) and H_2O (10 equiv) in CD_2Cl_2 was followed by NMR (Scheme 20). The formation of the Ru-allyl complex **56** was detected after 5 h at room temperature. In a preparatory scale reaction, the complex **56** was most conveniently isolated from the reaction mixture of the tetrameric ruthenium complex $\{[(\text{PCy}_3)(\text{CO})\text{RuH}]_4(\mu\text{-O})(\mu\text{-OH})_2\}$ (**4**) with the amide (0.1 mmol), $\text{HBF}_4\cdot\text{OEt}_2$ (4 equiv) and cyclopentene (20 equiv) in wet CH_2Cl_2 , and its structure was unequivocally established by X-ray crystallography (Figure 20). The X-ray crystal structure of **56** showed that ruthenium atom has a distorted octahedral coordination. The cation complex is totally disordered (in a 2:1 ratio) over non-crystallographic mirror plane. The $\text{Ru}_1\text{-C}_{11}$, $\text{Ru}_1\text{-C}_{11}$ and $\text{Ru}_1\text{-C}_{11}$ distances for the complex **56** are 2.22 Å, 2.17 Å and 2.14 Å, respectively. The bond lengths of $\text{Ru}_1\text{-O}_2$ are 1.98 Å. The $\text{O}_{1w}\text{-Ru}_1\text{-O}_1$ angles are 87° and $\text{O}_2\text{-Ru}_1\text{-C}_{11}$ angles are 83° .

The complex **56** was found to exhibit virtually identical activity as **26** in mediating the coupling reaction of (*E*)- $\text{C}_6\text{H}_5\text{CD}=\text{CHCONHCH}_3$ and propene under the conditions stipulated in eq 59; the reaction gave **36b** in > 90% yield after 2 h. When this reaction was performed in the presence of 1.5 equiv of H_2O , a substantially lower product conversion (75% after 2 h) was observed. To further establish the catalytic relevance of the complex **56**, the exchange reaction of **56** with (*E*)- $\text{PhCH}=\text{CHCONHMe}$ (1 equiv) was monitored by ^1H NMR. The reversible coordination of the amide substrate was observed at room temperature to form a 2:1 ratio of **56** and carbonyl-coordinated complex, but no new Ru-H species has been detected even after heating at 60°C . Though more careful

study is needed to establish the reaction step for converting catalytically active species, these results suggest that the Ru-allyl complex **56** would be converted to catalytically active Ru-H species by ligand exchange with substrate and H₂O.

Scheme 20

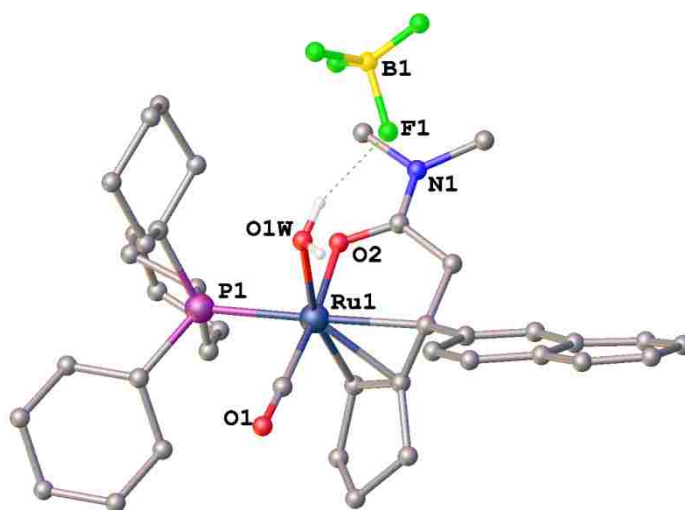
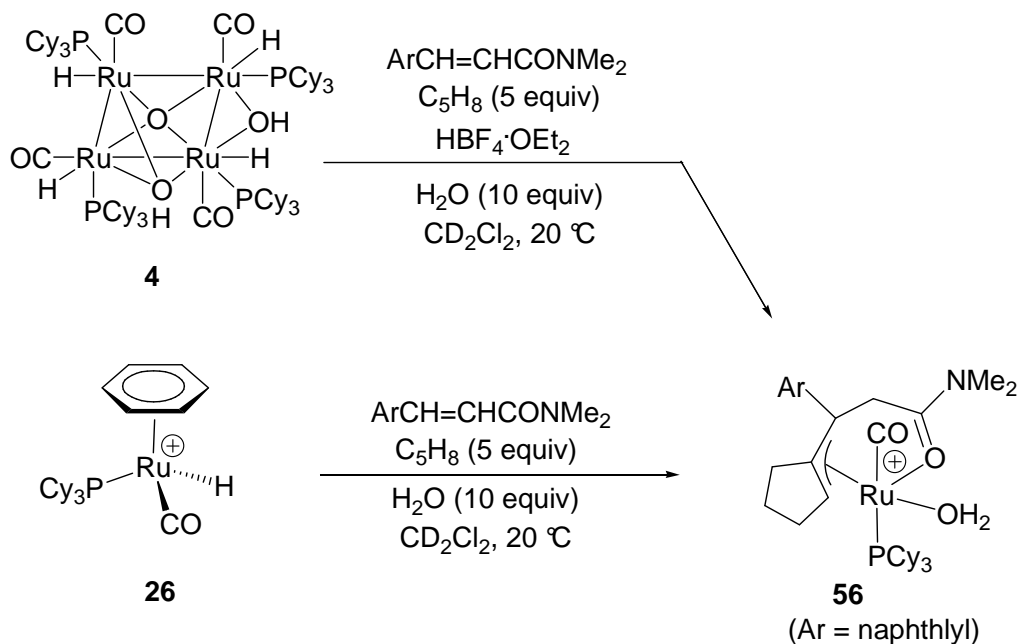


Figure 20. Molecular Structure of **56**.

3.4 Empirical Rate Law Derivation

The kinetics of the catalytic coupling reaction of (*E*)-ethyl cinnamate with propene was measured. The treatment of (*E*)-C₆H₅CH=CHCO₂Et (0.07 mmol) and propene (5 equiv) in the presence of **26** (5 mol%) in CD₂Cl₂ at 20 °C was monitored by ¹H NMR. Initially, the rate was measured by monitoring the ¹H integration of (*E*)-C₆H₅CH=CHCO₂Et (OCH₂CH₃ (1.21 ppm)) and the product (OCH₂CH₃ (1.16 ppm)) signals, and these were normalized against the solvent resonance. The kinetic plot for the reaction rate as a function of catalyst concentration indicates that reaction rate is first-order (Figure 21). The kinetic data revealed that the rate of coupling reaction is independent of the propene concentration (Figure 22). In contrast, the plot of kinetic data indicates that the rate of coupling reaction is inverse first-order of substrate concentration (Figure 23). The empirical rate law is given in eq 67.

$$v = k[\mathbf{26}]^1[\text{propene}]^0[\text{cinnamate}]^{-1} \quad (67)$$

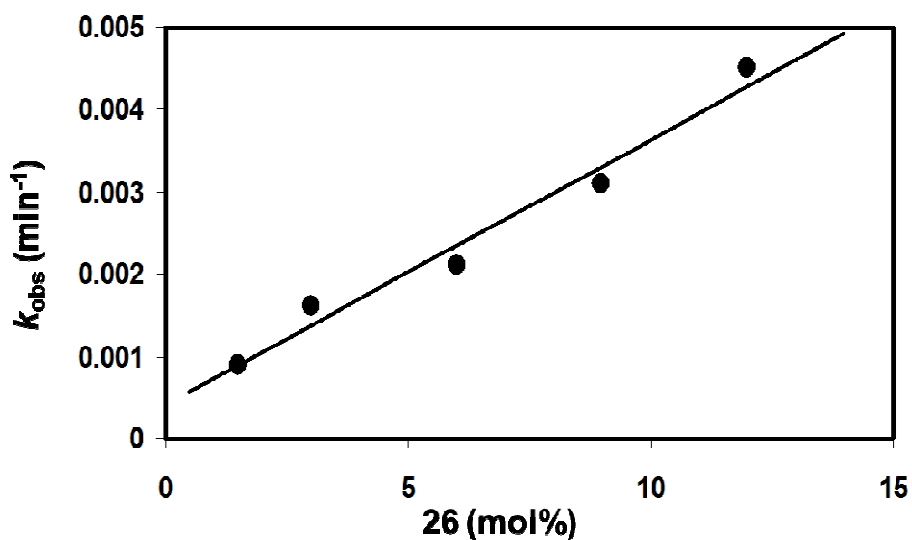


Figure 21. Plot of Observed Reaction Rate vs Catalyst Concentration for the Coupling Reaction.

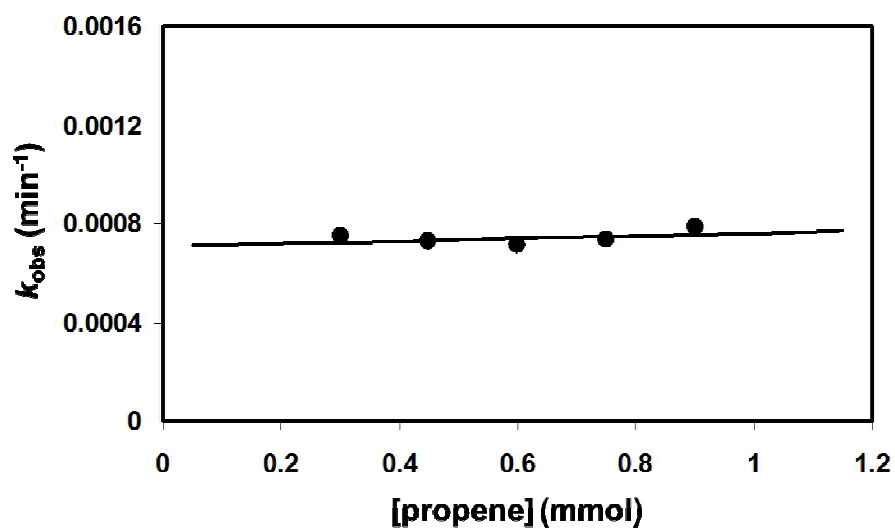


Figure 22. Plot of Observed Reaction Rate vs Propene Concentration for the Coupling Reaction.

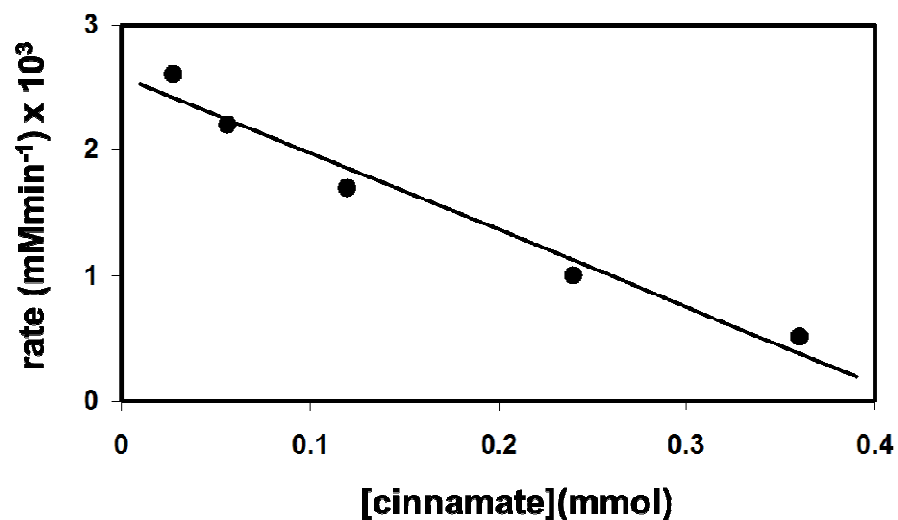


Figure 23. Plot of Observed Reaction Rate vs (*E*)-C₆H₅CH=CHCO₂Et Concentration for the Coupling Reaction.

3.5 Thermodynamic Parameters

The temperature dependence on the coupling reaction of (*E*)-C₆H₄CH=CHCO₂Et with propene mediated by **26** was monitored by ¹H NMR. Both catalyst concentration

and the cinnamate molar ratio were fixed as the coupling reaction conditions. The excess propene concentration not only maintains approximately zero-order conditions throughout the reaction but also minimizes cinnamate inhibition. Standard Eyring (Figure 24) and Arrhenius analysis (Figure 25) derived from the kinetic data resulted the following activation parameters: $\Delta H^\ddagger = 20.3$ kcal/mol, $\Delta S^\ddagger = -42.1$ eu, and $E_a = 20.9$ kcal/mol. A large, negative ΔS^\ddagger value suggests that the transition state is highly organized.

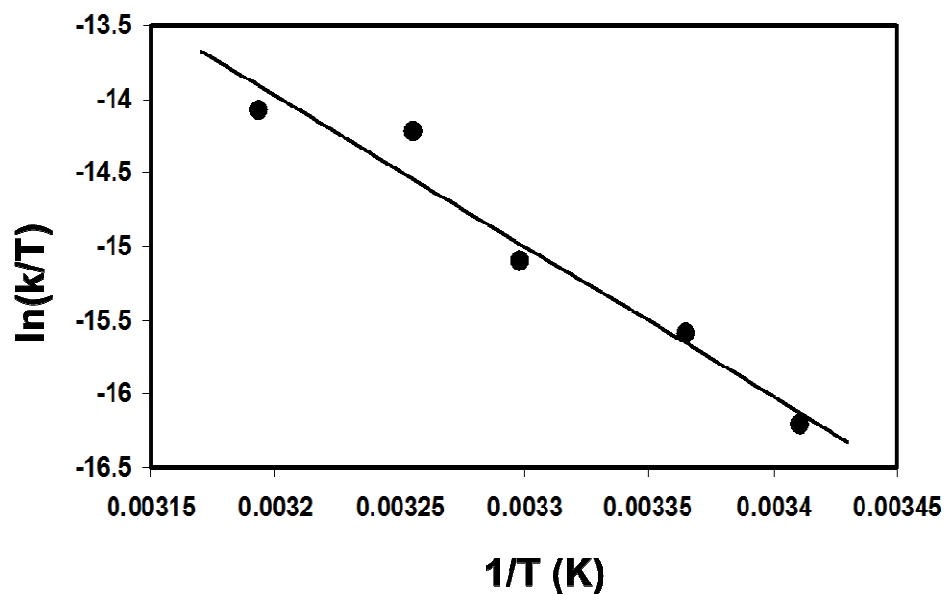


Figure 24. Eyring Plot for the Coupling Reaction of (*E*)- $C_6H_5CH=CHCO_2Et$ with Propene.

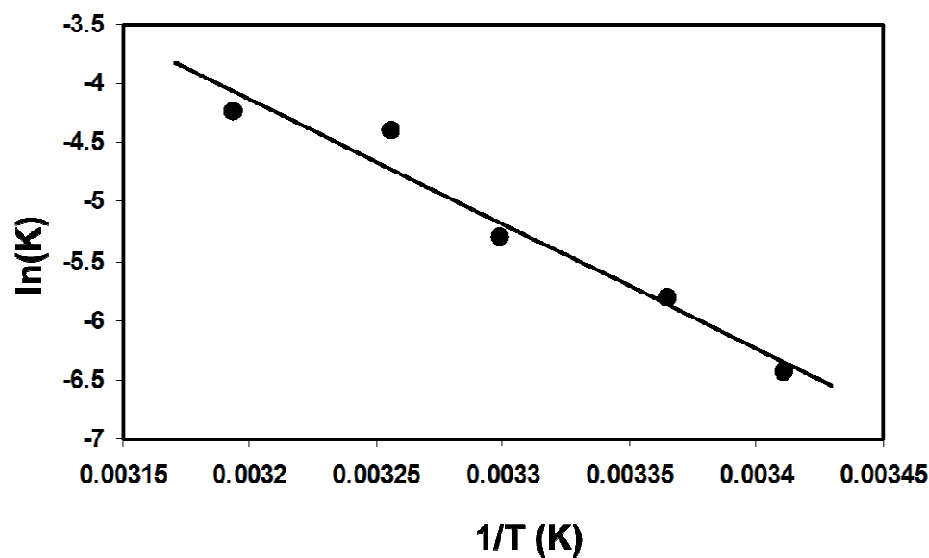


Figure 25. Arrhenius Plot for the Coupling Reaction of (*E*)-C₆H₅CH=CHCO₂Et with Propene.

3.6 Proposed Mechanism

We propose three different mechanistic pathways to explain the coupling reactions of α,β -unsaturated carbonyl compounds with alkenes. The plausible mechanism of the conjugate addition reaction involves the cationic Ru-H species **57**, which is initially formed from the ligand exchange step of **26** with the carbonyl substrate (Scheme 21).^{11d} The key features of this mechanistic pathway are the chelate-directed regioselective alkene insertion and β -hydride elimination steps to form the cationic Ru/alkene/hydride species **58**.^{77d} Both the observation of the carbon isotope effect on β -carbon (¹³C ratio of recovered sample/virgin sample: C _{β} = 1.019) and a negligible isotope effect of $k_{\text{H}}/k_{\text{D}} = 1.1 \pm 0.1$ with ethylene and ethylene-*d*₄ support the rate-limiting olefin insertion step (Table 14). The positive Hammett ρ values for both carbonyl compounds and alkenes are also consistent with the formation of the carbonyl-chelated species **58**

followed by the regioselective olefin insertion and β -hydride elimination. The insertion step is dictated by the nucleophilicity of a developing negative charge on the β -carbon of cinnamate derivatives. In light of the recent deuterium labeling study on the alkene dimerization and isomerization reactions,^{77c} the subsequent olefin isomerization step is expected to be facile in forming the tetrasubstituted olefin products with the regeneration of **57**. The successful isolation of the catalytically relevant species **56** suggests complex **57** as a possible intermediate, which can undergo dehydrogenation and then trapping by a water molecule.^{77d} The catalytically relevant species **56** would be converted to catalytically active species **57** by ligand exchange with hydrogen from water.

Table 14. Kinetics and Isotope Effects for the Coupling Reaction of α,β -Unsaturated Carbonyl Compounds with Alkene.

	Conjugate Addition Reaction	Oxidative Coupling Reaction
Hammett ρ value	$\rho = + 1.12^a$ $\rho = +1.47^b$	$\rho = + 1.12^c$ $\rho = + 0.88^d$
¹³ C Isotope Effect	$C_\beta = 1.018^e$	$C_\beta = 0.998^f$
Deuterium Kinetic Isotope Effect	$k_H/k_D = 1.1 \pm 0.1^g$	$k_H/k_D = 1.7 \pm 0.1^h$
Rate Limiting Step	Alkene Insertion	Vinyl C-H Activation

^a Hammett ρ value ((*E*)-*p*-X-C₆H₄CH=CHCO₂Et with propene). ^b Hammett ρ value ((*E*)-C₆H₄CH=CHCO₂Et with Y-*p*-C₆H₄CH=CH₂). ^c Hammett ρ value ((*E*)-C₆H₅CH=CH(CH₃)CONHMe with Y-*p*-C₆H₄CH=CH₂ (Y=OCH₃, CH₃ H)). ^d Hammett ρ value ((*E*)-C₆H₅CH=CH(CH₃)CONHMe with Y-*p*-C₆H₄CH=CH₂ (Y=F, Cl, CF₃)). ^e ¹³C ratio (recovered/virgin) ((*E*)-C₆H₄CH=CHCON(CH₃)₂ with propene). ^f ¹³C ratio (recovered/virgin) ((*E*)-C₆H₄CH=CH(CH₃)CONHMe with styrene). ^g Kinetic isotope effect ((*E*)-C₆H₄CH=CHCO₂Et with ethylene/ethylene-*d*₄). ^h Kinetic isotope effect ((*E*)-C₆H₄CH=CH(CH₃)CONHCH₃ with styrene/styrene-*d*₈).

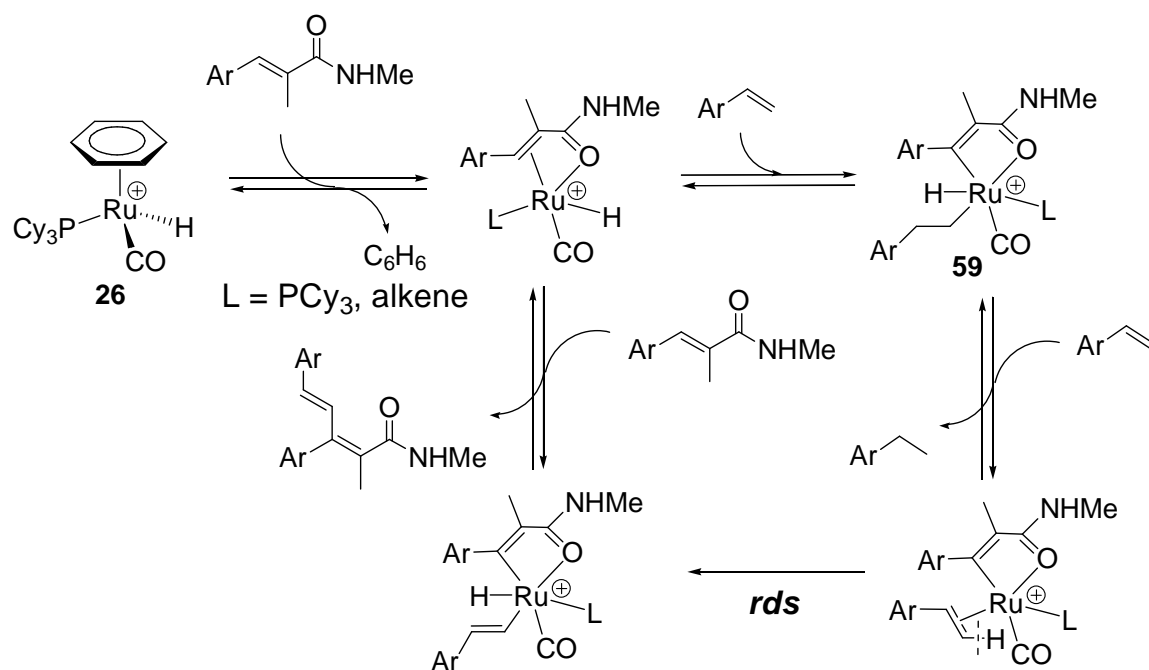
The formation of oxidative coupling products **38** can be explained by a mechanistic pathway involving vinyl C-H bond activation of arylalkenes (Scheme 22). The insertion of arylalkenes to the electrophilic ruthenium center followed by the ligand exchange reaction of **26** with carbonyl substrate and the β C-H bond activation of (*E*)- $\text{C}_6\text{H}_5\text{CH}=\text{C}(\text{CH}_3)\text{CONHCH}_3$ would form the ruthenium hydride species **59**. Subsequent vinyl C-H activation of arylalkenes and reductive elimination would give *E* selectivity for oxidative coupling products.

We performed a variety of kinetic experiments to elucidate the mechanism of the coupling reaction. Both the normal deuterium kinetic isotope effect of $k_{\text{H}}/k_{\text{D}} = 1.7 \pm 0.1$ with styrene and styrene- d_8 and negligible isotope effect of $k_{\text{H}}/k_{\text{D}} = 1.1 \pm 0.1$ with (*E*)- $\text{C}_6\text{H}_5\text{CH}=\text{C}(\text{CH}_3)\text{CONHCH}_3$ and (*E*)- $\text{C}_6\text{H}_5\text{CD}=\text{C}(\text{CH}_3)\text{CONHCH}_3$ are consistent with the vinyl C-H bond cleavage rate-limiting step. These results indicate that the different rate-limiting step compared to the conjugate addition reaction (Table 14). Both negligible carbon isotope effect from the coupling reaction with styrene and deuterium labeling study also provide supporting evidences for the rate-limiting vinyl C-H bond activation step. The reaction rate and product selectivity were found to be increased by styrene containing electron donating groups, depending on electron donating abilities of *para* functional group.

In contrast, the coupling reaction of (*E*)- $\text{C}_6\text{H}_5\text{CH}=\text{C}(\text{CH}_3)\text{CONHCH}_3$ with styrene containing electron withdrawing groups gave a mixture of the branched and linear olefin insertion products predominantly which were similar fashions with alkene insertion pathway.^{11d} This phenomenon indicates that the coupling reaction depending on the substrate used exhibits different product selectivity. The most pronounced carbon isotope

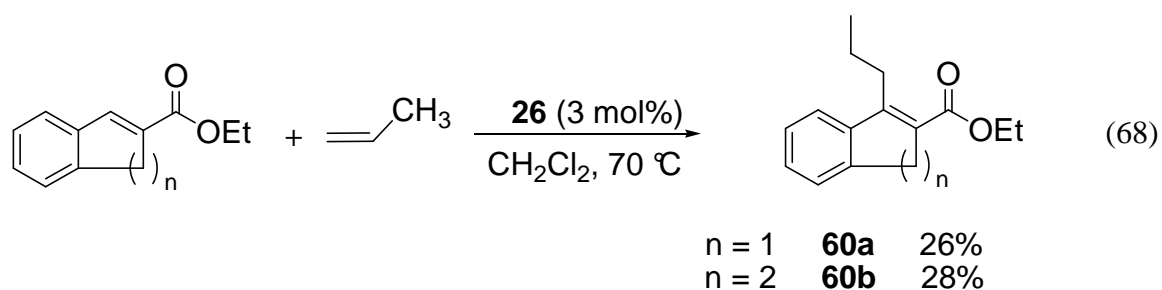
effect was observed on the β carbon atom of (E) - $C_6H_5CH=C(CH_3)CONHCH_3$ with 4-chlorostyrene. These results also indicate that the formation of C-C bond via olefin insertion into a carbonyl substrate is the rate-limiting step, and are consistent with alkene insertion pathway instead of the oxidative coupling pathway. These results suggest that two different reaction mechanisms are competing operational dependent on the substrate employed due to electron effect.

Scheme 22

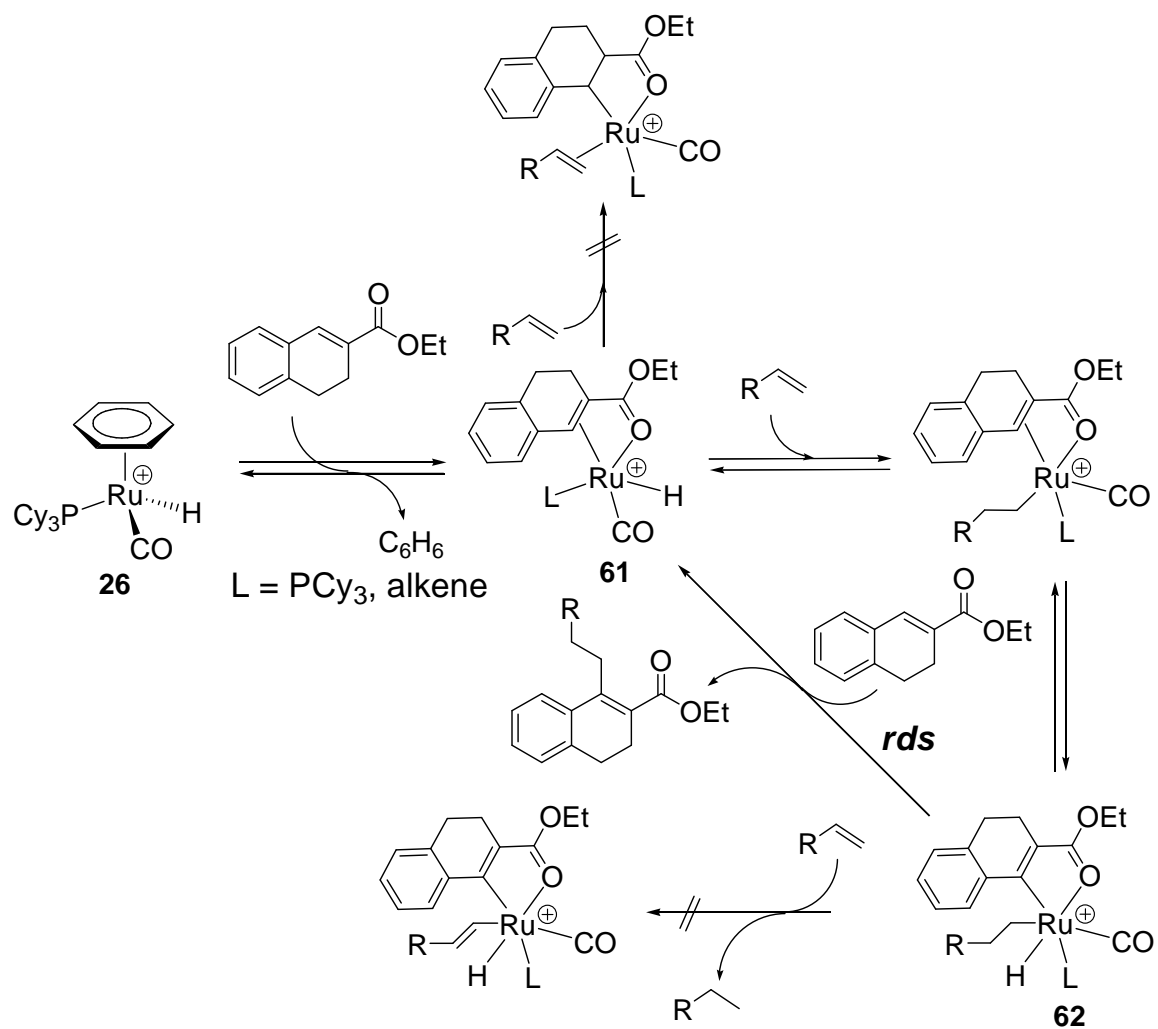


In case of the coupling reaction of cyclic cinnamic acid derivatives with propene, we observed the formation of tetrasubstituted olefin products via a direct C-H bond

cleavage (eq 68). Initially, the cationic Ru-H complex **61** is formed from the ligand exchange reaction of **26** with cyclic α,β -unsaturated compounds. The chelate-assisted insertion of the ruthenium center into β -position by C-H bond cleavage gives the cationic Ru-H species **62** after hydrometallation of **61**. Reductive elimination from **62** provides products **60a** and **60b**, regenerating the catalytically active species **62**. The stereochemistry around the double bond is retained in each step. Trost and Murai also reported that the Ru-catalyzed coupling reactions of 1-acetylcyclohexene and α,β -unsaturated esters with alkenes such as silylethylenes and styrene by direct C-H bond cleavage.⁸ The apparent lack of the formation of conjugate addition products or oxidative products can be readily explained by the rigidity of the cyclic moieties, which would prohibit the insertion of the α,β -unsaturated ester by hydride migration or vinyl C-H activation of alkenes.



Scheme 23



Conclusions

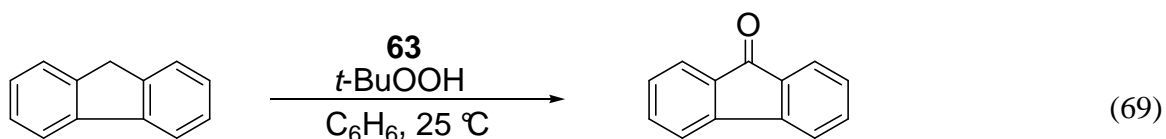
An effective catalytic conjugate addition reaction protocol has been developed for the synthesis of tetrasubstituted olefin products. The kinetic and spectroscopic data are consistent with three different mechanistic pathways depending on the substrate employed. The reaction of an α,β -unsaturated carbonyl compound with simple olefins predominantly gives the tetrasubstituted olefin products. The mechanistic studies suggest that the olefin insertion into an α,β -unsaturated carbonyl substrate is the rate-limiting step for conjugate addition reaction. In contrast, the coupling reaction of (*E*)- $\text{C}_6\text{H}_5\text{CH}=\text{C}(\text{CH}_3)\text{CONHCH}_3$ with aromatic alkenes gives oxidative coupling products. The mechanistic results support the different mechanistic pathway, which involves the rate-limiting vinyl C-H activation step, in comparison with the conjugate addition reaction. This synthetic methodology promises to provide a straightforward route to the valuable organic compounds such as tetrasubstituted olefins which are difficult to synthesize by using traditional synthetic methods.

Chapter IV

Aqueous Phase C-H Bond Oxidation Reaction of Arylalkanes Catalyzed by a Water-Soluble Cationic Ru(III) Pymox Complex

C-H oxidation reactions play an important role in organic chemistry and there is an increasing demand for selective and mild oxidation methods in modern organic synthesis. Saturated hydrocarbon compounds account for the largest sources of natural petroleum feedstock materials, which traditionally have been used as fuels, lubricants, and solvents. During the past few decades, there has been an extensive research devoted on the catalytic oxidation of inexpensive hydrocarbons to more commercially valuable products such as pharmaceuticals, flavors, fragrances, plasticizers, and polymer precursors.⁷⁸ Many methods for catalytic oxidations with transition metal catalysts have been investigated extensively because of their particular importance in view of synthetic, mechanistic, and industrial aspects.⁷⁹ A number of transition metal catalyzed reaction have been extensively investigated including iron-catalyzed oxidation of alkanes called Gif systems.

The ruthenium catalysts have been used to be oxidation of hydrocarbons with *t*-BuOOH to give corresponding ketones and alcohols efficiently. $\text{RuCl}_2(\text{PPh}_3)_3$ (**63**) was reported to be effective catalyst for oxidation of the benzylic position of hydrocarbons. For example, the catalytic oxidation of fluorine gives fluorenone in 87% (eq 69).⁸⁰



The mechanism of this reaction has been studied by Murahashi. Hammett ρ value showed -1.39 which was similar to those obtained for the oxidation with cytochrome P450 (-1.6)⁸¹ and Fe(TPP)Cl-PhIO (-1.69)⁸² but the observed ρ value (-1.39) is quite different from the $t\text{-BuO}\cdot$ radical (-0.4)⁸³ and the $t\text{-BuOO}\cdot$ radicals (-0.6)⁸⁴ (Table 1). These kinetic data implicate the existence of a metal-dependent species such as oxo-ruthenium, which is similar to $\text{Fe}^{\text{V}}=\text{O}$ of cytochrome P450, rather than $t\text{-BuO}\cdot$ and $t\text{-BuOO}\cdot$ intermediates. The intramolecular deuterium isotope effect ($k_{\text{H}}/k_{\text{D}}$) was examined. The $k_{\text{H}}/k_{\text{D}}$ value was determined to be 9.0 and this value was similar to that obtained for oxidation with cytochrome P450 ($k_{\text{H}}/k_{\text{D}} = 11$),⁸⁵ This data indicates that the C-H bond breaking is the rate determining step. Furthermore, the intermolecular isotope effect of the oxidation of cyclohexanes was determined to be 9.2. This is contrast to the smaller isotope effect ($k_{\text{H}}/k_{\text{D}} = 4.2$) which was obtained from the reaction with $t\text{-BuO}\cdot$ (Table 15).⁸⁶

The kinetic results, isotope effects, and other studies indicate that the oxidation is not due to $t\text{-BuO}\cdot$ or $t\text{-BuOO}\cdot$ radical but due to the oxo ruthenium species derived from low valent ruthenium and $t\text{-BuOOH}$ (Scheme 24). The ruthenium(II) complex **A** reacts with $t\text{-BuOOH}$ to give the alkylperoxoruthenium(II) complex **B**, which subsequently undergoes heterolytic cleavage of the O-O bond to give oxo-ruthenium(IV) species **C**. The reaction with $t\text{-BuO}\cdot$ or $t\text{-BuOO}\cdot$ is unlikely, because the oxidation of alkanes proceeds efficiently even in the presence of radical scavengers such as 2,6-di-*tert*-butyl-

4-methylphenol. Abstraction of a hydrogen atom from an alkane by intermediate **C** would form the caged complex **D**, bearing an alkyl radical and a hydroxo-ruthenium(III) species. Transfer of the hydroxyl ligand to the caged alkyl radical (path **A**) would afford an alcohol and the Ru(II) intermediate **F** to complete the catalytic cycle. Further oxidation of secondary alcohol formed the corresponding ketones under the reaction conditions. When the alkyl radical **D** has low oxidation potential, fast single-electron transfer would take place to give cation **E** (path **B**), which undergoes reaction with the second molecule of *t*-BuOOH to give the corresponding *t*-butylperoxy product and water. From all data such as ρ values, k_H/k_D ratios, and relative oxidation rates in the various substrates, they proposed mechanism for $\text{RuCl}_2(\text{PPh}_3)_3/t\text{-BuOOH}$ system which was containing the oxo-ruthenium species (Scheme 24).

Table 15. Kinetics, Intra- and Intermolecular Deuterium Isotope Effects for the Ruthenium Catalyzed Oxidation of Hydrocarbons with *t*-BuOOH.

system	ρ	k_H/k_D^a	k_H/k_D^b
$\text{RuCl}_2(\text{PPh}_3)_3/t\text{-BuOOH}^c$	-1.39	9.0	9.2
cytochrome P450	-1.6 ^d	11 ^e	
$[\text{Ru}(\text{dmp})_2(\text{OH}_2)_2][[\text{PF}_6]_2/\text{H}_2\text{O}_2$			4.0 ^f
$[\text{Ru}(6,6'\text{-Cl}_2\text{bpy})_2(\text{OH}_2)_2][\text{CF}_3\text{SO}_3]_2/t\text{-BuOOH}^g$			4.8
<i>t</i> -BuO•	-0.4 ^h		4.2
<i>t</i> -BuOO•	-0.6 ⁱ		

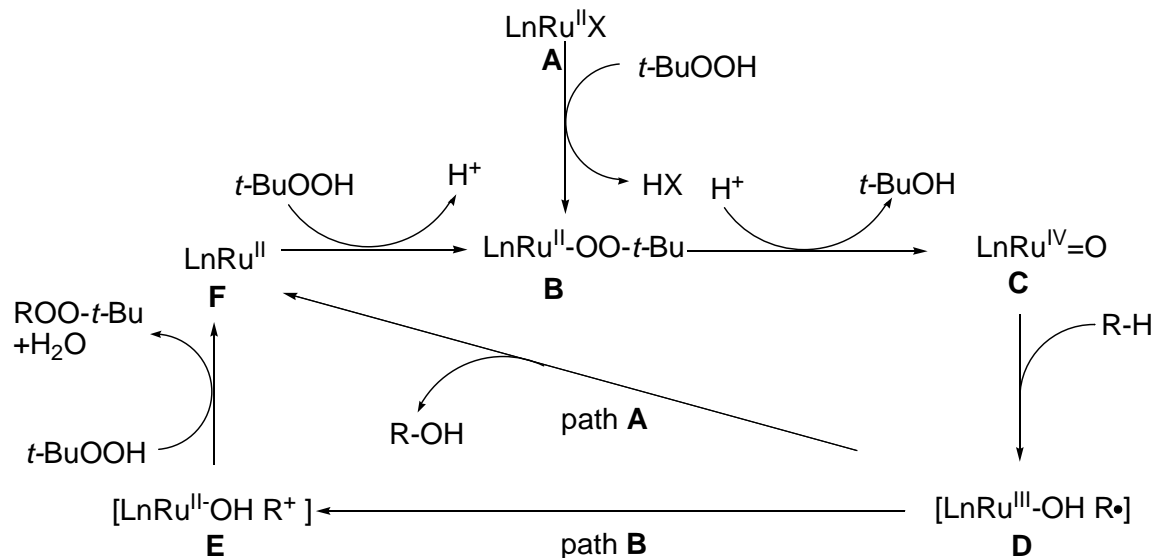
^a Intramolecular isotope effect for the oxidation of 1,1-dideuterio-1,3-diphenylpropane.

^b Intermolecular isotope effect for the oxidation of cyclohexane/cyclohexane-*d*₁₂.

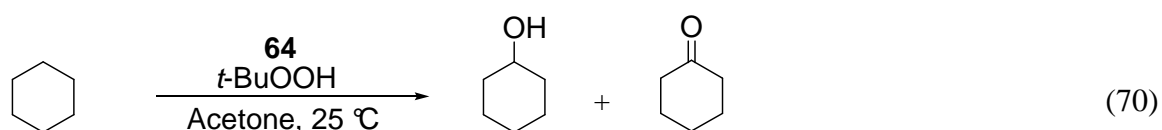
^c Reference 80. ^d Reference 81. ^e Reference 85. ^f Reference 88. ^g Reference 87.

^h Reference 83. ⁱ Reference 84.

Scheme 24



In contrast, Che reported that the ruthenium(II) complex *cis*-[Ru(6,6'-Cl₂bpy)₂(OH₂)₂][CF₃SO₃], (**64**) is a robust catalyst for C-H bond oxidations of hydrocarbons. They proposed different mechanism in the reaction which was called to be a free radical system.⁸⁷ *cis*-[Ru(6,6'-Cl₂bpy)₂(OH₂)₂][SF₃SO₃]₂, (**64**) was found to efficient catalyst for oxidation of the alkanes, including linear alkanes such as *n*-hexane. Typically, the catalytic oxidation of cyclohexane gives cyclohexanol and cyclohexanone in 85% yield (ratio = 1:1.6) (eq 70).

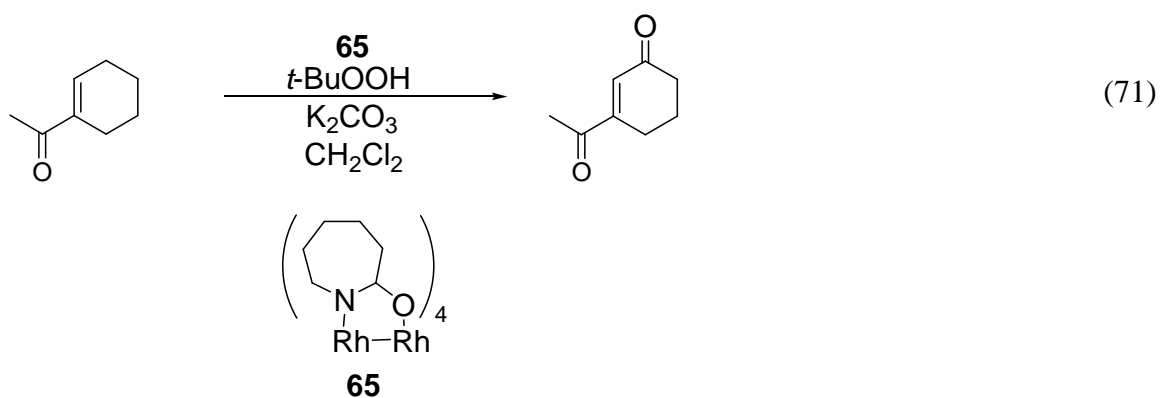


A smaller kinetic isotope effect ($k_{\text{H}}/k_{\text{D}} = 4.8$) and tertiary to secondary C-H bond relative reactivities ($k_{\text{tert}}/k_{\text{sec}} = 7.4$) have been observed in the catalytic cyclohexane and

adamantine oxidations, respectively. Also Drago and coworkers found very similar data for the catalytic $[\text{Ru}(\text{dmp})_2(\text{OH}_2)_2][\text{PF}_6]_2/\text{H}_2\text{O}_2$ system ($k_{\text{H}}/k_{\text{D}} = 4.0$ for cyclohexane; $k_{\text{tert}}/k_{\text{sec}} = 7.1$ for adamantane; $\text{dmp} = 2,9\text{-dimethyl-}1,10\text{-phenanthroline}$).⁸⁸ From the results of cyclohexane oxidation, they suggested that the active species has substantial radical character: (a) addition of 2,6-di-*tert*-butyl-4-methylphenol as a radical trap suppressed the catalytic oxidation; (b) a substantial amount of cyclohexyl chloride was produced in the presence of CCl_4 ; (c) when the terminal oxidant was changed from *t*-BuOOH to cumene hydroperoxide, the product profile is dominated by acetophenone, which is generated by β -scission of cumyloxy radicals. Following these kinetic and mechanistic data, they proposed a free-radical process mechanism which generates active alkyl radical from metal-oxo intermediate.

It is remarkable that the allylic positions of hydrocarbons were oxidized selectively by dirhodium caprolactamate ($\text{Rh}_2(\text{cap})_4$), (**65**) with *t*-BuOOH (eq 71).⁸⁹ Most of cyclohexene and their derivatives were rapidly converted to enones in 1 h with 0.1 mol%

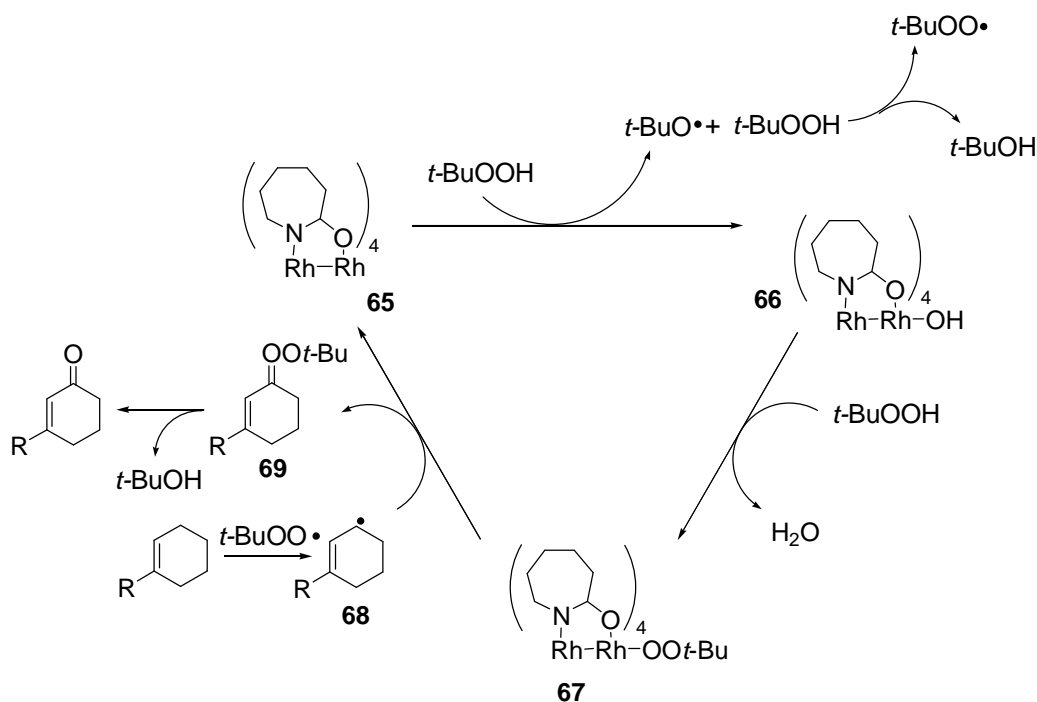
65.



Mechanistically, **65** undergoes a 1-electron oxidation in the presence of *t*-BuOOH to form a Rh^{5+} species **66** which can be converted under the reaction conditions to

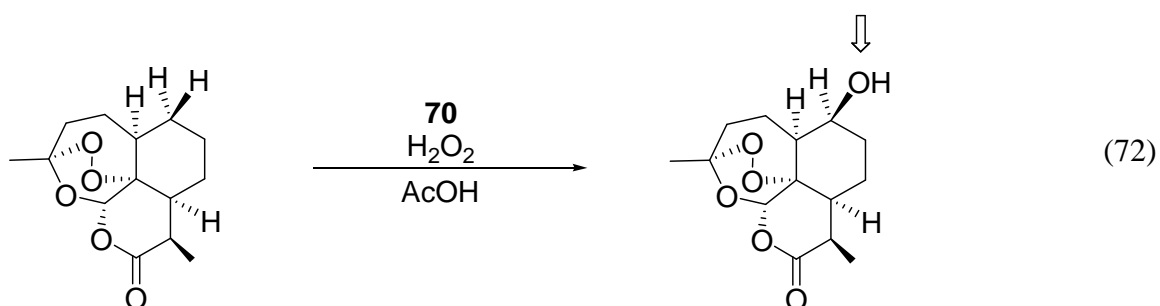
dirhodium alkylperoxo species **67** (Scheme 25). Furthermore, evolution of oxygen during the course of the reaction was observed and is consistent with the formation of $t\text{-BuOO}\cdot$ radical which is known to di-*tert*-butyltetraoxide⁹⁰ and it is able for selective hydrogen atom abstraction to produce radical **68**. Ligand transfer of the metal-bound peroxide to the carbon-centered radical forms the mixed peroxide **69** and regenerates the catalyst. This proposed sequence thus constitutes a redox chain catalytic cycle.⁹¹ Finally, rapid decomposition of **55** yields products.

Scheme 25

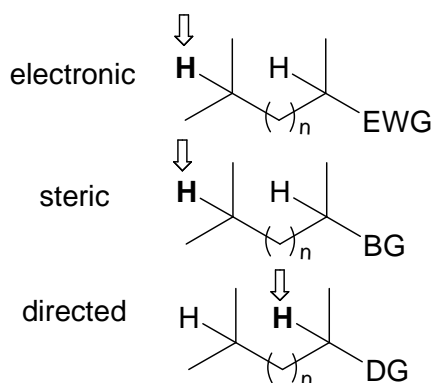
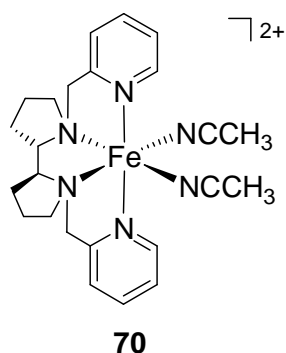


Recently, White and coworkers have reported that an iron-based catalyst ($[\text{Fe}(\text{S},\text{S}\text{-PDP})(\text{CH}_3\text{CN})_2][\text{SbF}_6]_2$), (**70**) that reacts selectively with C-H bonds which has traditionally used to add directing groups, require extra steps.³³ The iron-based catalyst makes it possible to oxidize the unreactive aliphatic C-H bonds at tertiary carbons in

complex molecules without the need for directing or activating groups. Predictable selectivity is achieved solely based on the electronic and steric properties of the C-H bonds, without the need for directing groups. Three modes of selectivity enable the predictable oxidation of complex natural products and their derivatives such as (+)-aremisinin at specific C-H bonds with preparatively useful yields (eq 72). This type of general and predictable reactivity stands to enable aliphatic C-H oxidation to streamline the process of complex molecule synthesis.



Predictable C-H Oxidation

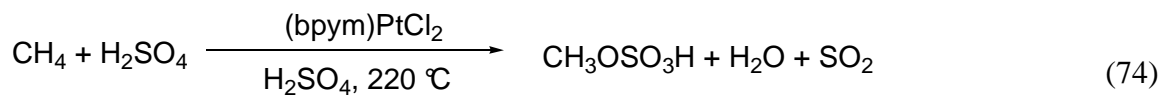
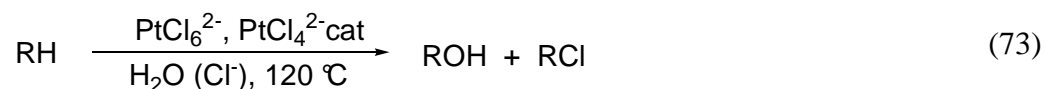
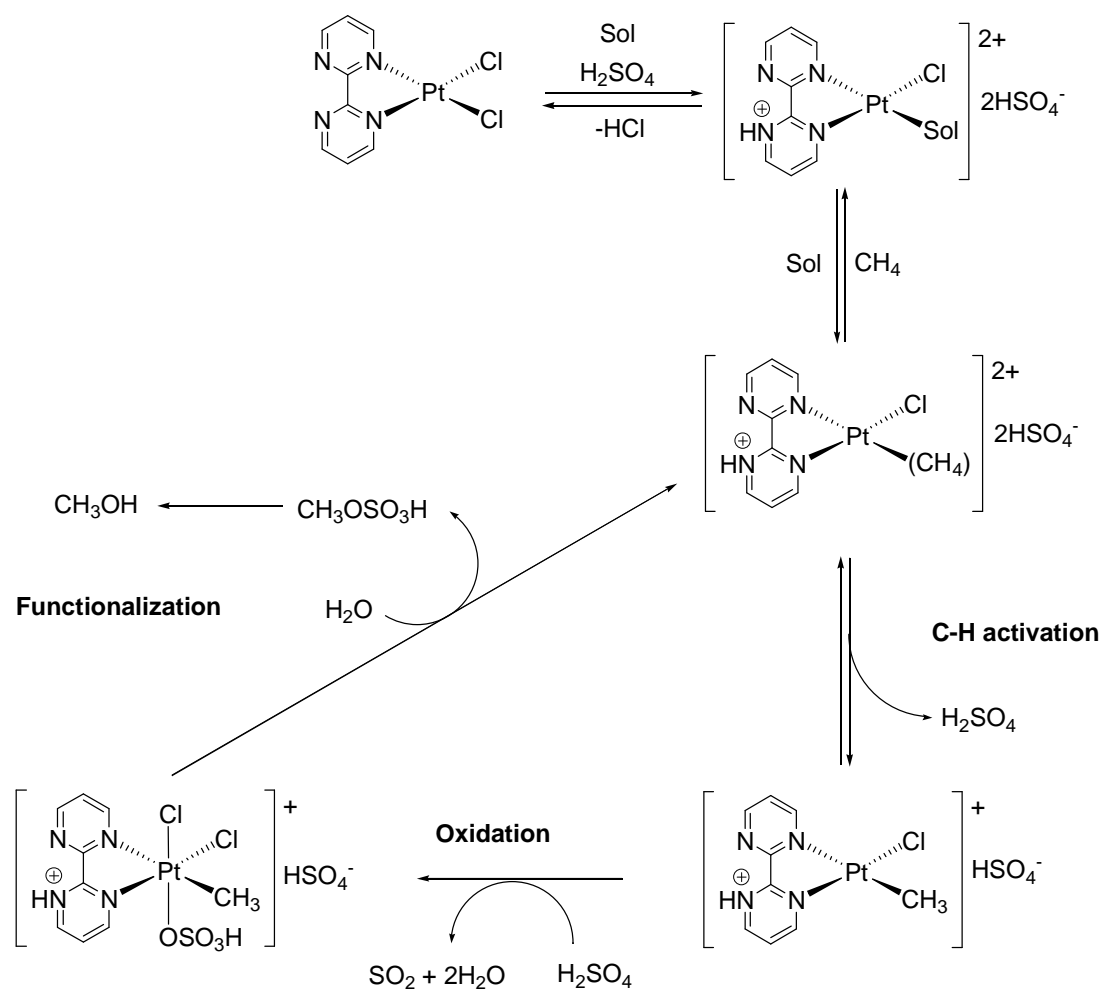


EWG : electronic withdrawing group
BG : bulky group
DG : directing group

Figure 26. Selectivity for catalyzed C-H bond oxidation by [Fe(*S,S*-PDP)(CH₃CN)₂][SbF₆]₂, **70**.

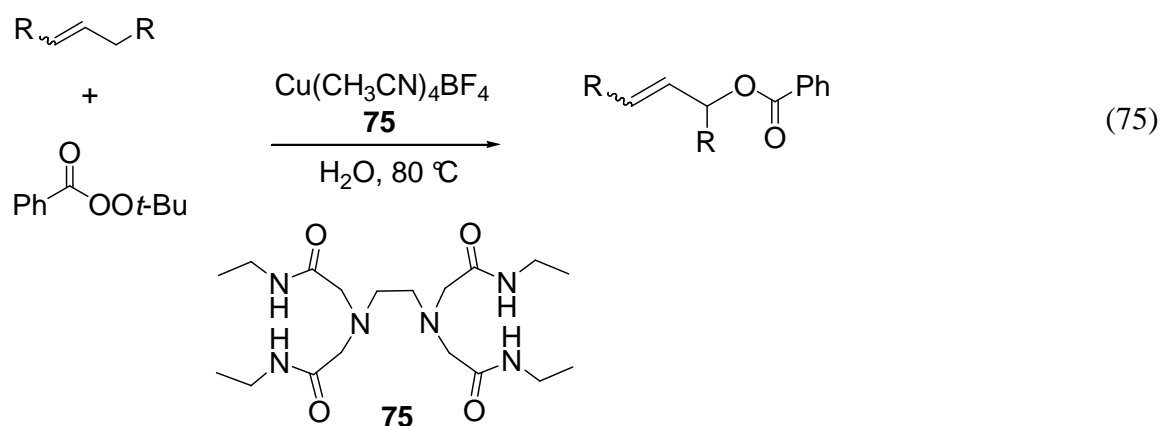
The use of transition metals for catalyzing reactions is of growing importance in modern organic chemistry.⁹³ From economic and environmental points of view, the development of novel organic transformation systems in aqueous solution has become one of the most attractive research topics in modern chemistry.⁹⁴ Generally, transition metal catalysis is carried out under an inert gas atmosphere and the exclusion of moisture has been essential. The reason could be that water as a ligand often occupies metals' coordination sites. On the other hand, metal-carbon bonds are easily attacked by water either via proton transfer or via the oxygen (nucleophilic reaction). However, recent studies have shown that, in water, such catalysts are both facilitated and can be operated in open air.⁹⁵ Another predictable advantage of these water soluble catalysts can be reused after separation from water insoluble organic products.

In the 1970s Shilov et al. developed a catalytic oxidation in which methane was converted to methanol and chloromethane in acidic aqueous solution (eq 73).⁹⁶ Since Shilov's pioneering report on methane oxidation catalyzed by PtCl_4^{2-} under mild conditions, a number of well-defined, transition metal catalytic systems have been shown to catalyze methane functionalization. Notable recent example of methane oxidation have been reported by Periana using $(\text{bpym})\text{PtCl}_2$ ($\text{bpym} = 2,2'$ -bipyrimidine).⁹⁷ Periana system converts methane to methyl bisulfate in concentrated sulfuric acid, a potential precursor for methanol (eq 74). The conversion of methane to methyl bisulfate is greater than 70% based on methane and the selectivity is also over 90%. This system accomplishes C-H activation, oxidation, and functionalization in the best way so far achieved for a homogeneous system (Scheme 26).⁹⁷

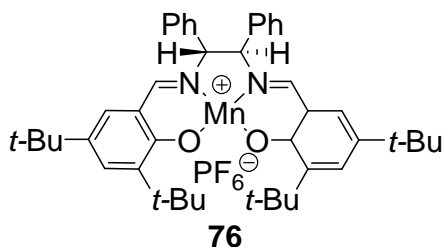
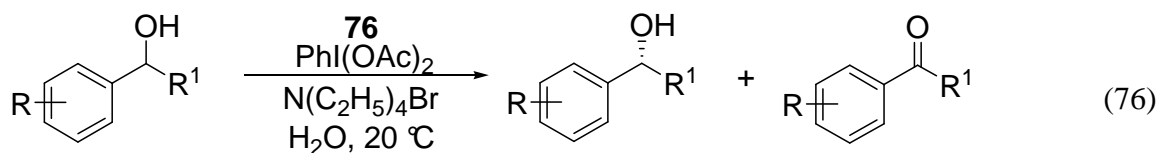
**Scheme 26**

Muzart reported an efficient and recyclable water-soluble system to promote the allylic oxidation of olefins with organic peroxyesters in water.⁹⁸ The mixture of the

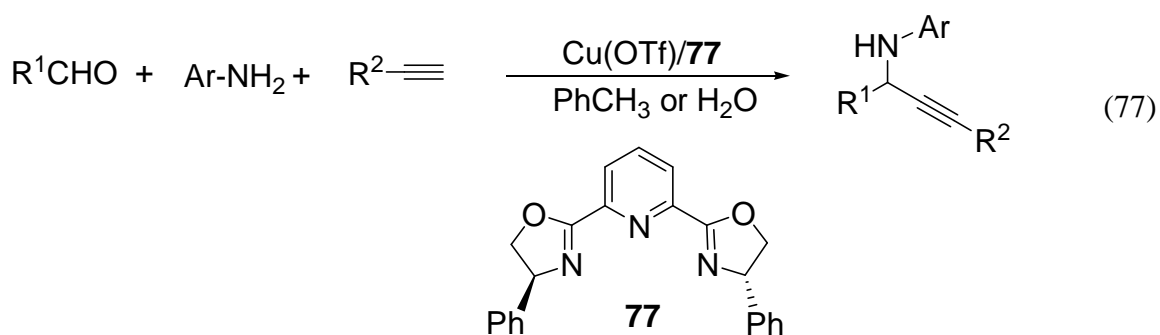
hydrophilic nitrogen donor ligand with $\text{Cu}(\text{CH}_3\text{CN})_4\text{BF}_4$ in water led to an efficient and reusable catalytic system for the allylic oxidation of olefins with *tert*-butyl perbenzoate (eq 75). The aqueous phase recovered after extraction of the reaction products remained catalytically active, and oxidation of cyclohexene was repeated four times with the same aqueous phase without a drop in the yield.



Xia found that Mn(salen) complex (**76**) was effective catalysts for the oxidation of secondary alcohols to ketones in the presence of the co-oxidant diacetoxyiodobenzene ($\text{PhI}(\text{OAc})_2$) under aqueous condition (eq 76).⁹⁹ To increase the substrate and catalyst's solubility in water, the phase-transfer catalyst ($\text{N}(\text{C}_2\text{H}_5)_4\text{Br}$) was included in the aqueous system and the product was formed with a high 84.1% ee in 62.5% yield.

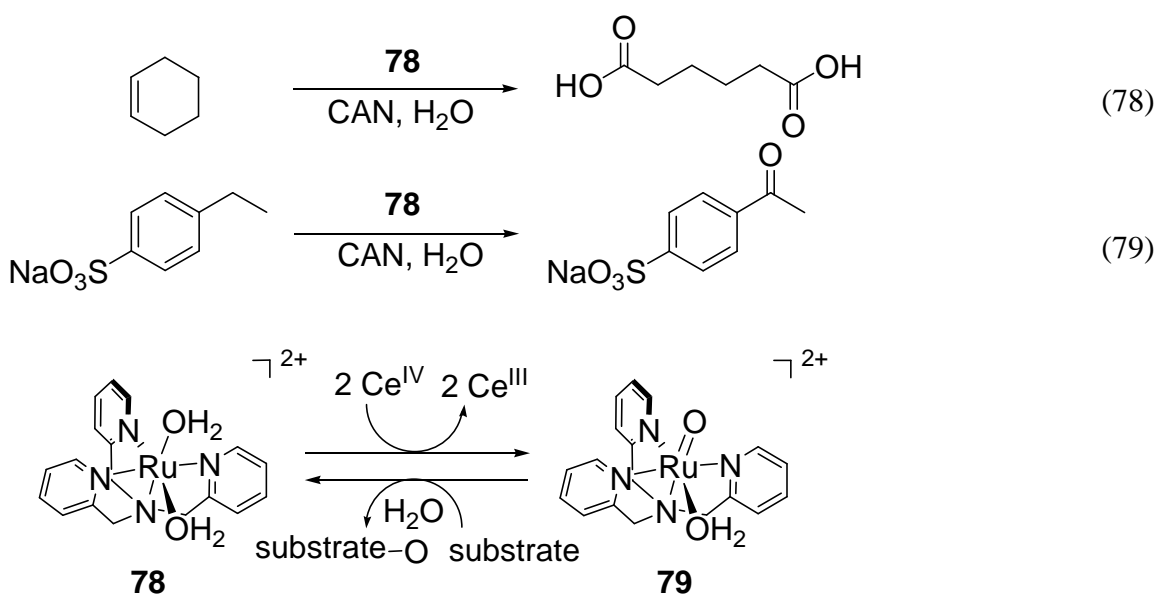


Recently, Li and coworkers reported an efficient asymmetric aldehyde-alkyne-amine coupling reaction in water (eq 77).¹⁰⁰ Use of the tridentate bis(oxazolinyl)pyridines, **77** with Cu(OTf) afforded the product with both high yield (48-93%) and enantioselectivity in organic solvent (up to 99.6% ee) and in water (up to 84% ee). In most cases, imines were formed *in situ* and the addition was very simple: mixing an aldehyde, aniline, and alkyne with the catalyst in one pot.



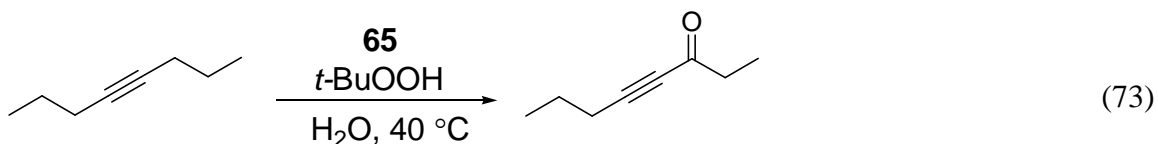
Fukuzumi have recently reported that the formation of novel ruthenium(IV)-oxo complex and its reactivity toward efficient and selective catalytic oxygenation and

oxidation reaction of various hydrocarbons in water, which can be used as an oxygen source.¹⁰¹ In this system, water is not only the solvent but also the sole oxygen source in the efficient oxidation of organic compounds catalyzed by a Ru(II)-pyridylamine-aqua complex, **78** with Ce(IV) as the oxidant. An intermediate-spin Ru(IV)-oxo complex, **79** is formed as the reactive species.¹⁰¹ This catalytic system has been shown high turnover numbers for various substrates: cyclohexane is converted into the corresponding dicarboxylic acid and the water soluble sodium 4-sulfonate-1-ethylbenzene forms the corresponding acetophenone derivative selectively (eqs 78-79).



Doyle reported that Rh₂(cap)₄, **65** with *t*-BuOOH can effectively catalyze allylic,⁸⁹ benzylic oxidation.¹⁰² They have recently reported the oxidation of alkynes to α,β -acetylenic ketones by *t*-BuOOH, catalyzed by **65** with water as the reaction solvent.¹⁰³ The catalytic oxidation of 4-octyne by **65** with *t*-BuOOH in water afforded the

corresponding ynone with high yield (89%) and short reaction time (1 h) (eq 80). The aqueous phase recovered after extraction of the reaction products can be used to another reaction, and oxidation of other substrate was repeated three times with the same aqueous phase without decreasing catalytic activity.



Results and Discussion

The catalytic C-H bond oxidation of alkanes under mild conditions is of central importance in view of synthetic and industrial aspects.⁷⁸ Generally, catalytic oxidation of alkanes under mild conditions is quite difficult, because of the lack of the reactivity of alkanes, which stems from their high C-H bond dissociation energy. Efficient metal catalysts are required for unactivated C-H bond oxidation in organic synthesis. Recently, transition metal catalyzed oxidations have been reported; ruthenium and iron complexes with chelating nitrogen ligands have been shown to exhibit high activity and selectivity for oxidative reactions under organic and aqueous condition,^{87,92,101,104} but selective catalytic oxidation of alkane under mild condition are relatively rare.

From environmental and economic points of view, the development of organic transformations in aqueous media has become one of the major advantages in modern chemistry.¹⁰⁵ Following the general trend, the design of novel transition-metal catalysts for organic reaction in water has arisen a growing interest in recent years, disclosing up to

date a wide variety of highly efficient and selective synthetic approaches.⁹⁵ Recently, Fukuzumi and co-workers has reported highly efficient and selective catalytic oxygenation and oxidation reaction by $[\text{Ru}(\text{tpa})(\text{H}_2\text{O})_2](\text{PF}_6)_2$ which contain tetradentate nitrogen based ligand under aqueous condition.¹⁰¹ Even though catalytic reaction under aqueous condition has a lot of advantages, it is difficult to use water as solvent in metal catalyzed chemical reactions because the majority of transition metal catalysts are unstable and insoluble in aqueous condition.

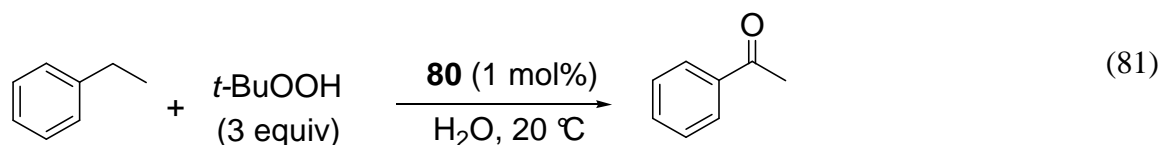
Since the first reports of the use of chiral oxazoline-based ligands in asymmetric catalysis,¹⁰⁶ a diverse range of oxazoline ring-based ligands with transition metals have been developed as catalysts in a wide range of chemical reactions, such as cyclopropanation, epoxidation, alcohol oxidation. Initially we thought that oxazoline ligands are suitable candidates for highly active and selective catalytic oxidation because of their readily accessibility, modular nature, and applicability in a wide range of metal catalyzed transformations.^{106,107} We have recently developed cationic ruthenium (III) complex $[(\text{pymox-Me}_2)_2\text{RuCl}_2]^+\text{BF}_4^-$ (**80**) ($\text{pymox-Me}_2 = 4,4\text{-dimethyl-2-(2-pyridyl)oxazoline}$). We have discovered that **80** was found to be efficient catalyst for C-H oxidation reaction of arylalkanes in water. In this chapter, we describe the synthesis and characterization of **80** and their applications for C-H oxidation reactions in aqueous condition.

4.1 Synthesis of Water-Soluble Ruthenium Pymox Complexes

As part of an ongoing effort to develop ruthenium-catalyzed C-H bond activation reactions, we initially screened several chelating nitrogen ligands to synthesize water

soluble ruthenium catalysts. Thus, the treatment of $[(\text{COD})\text{RuCl}_2]_x$ with 1.2 equivalents of pymox-Me_2 ligand in 1,2-dichloroethane at 50 °C produced an orange-yellow colored complex $(\text{pymox-Me}_2)\text{Ru}(\text{COD})\text{Cl}_2$ (**81**), which was isolated in 65% yield after recrystallization in *n*-hexanes/ CH_2Cl_2 (Scheme 27). The treatment of **81** (0.4 mmol) with pymox-Me_2 (1.9 mmol) in 1,2-dichloroethane at 100 °C led to the isolation of a deep blue-purple colored complex $(\text{pymox-Me}_2)_2\text{RuCl}_2$ (**82**) in 55% yield. Alternatively, the complex **82** could be directly produced from the treatment of $[(\text{COD})\text{RuCl}_2]_x$ with excess amount of pymox-Me_2 in 1,2-dichloroethane at 100 °C with 65% yield.

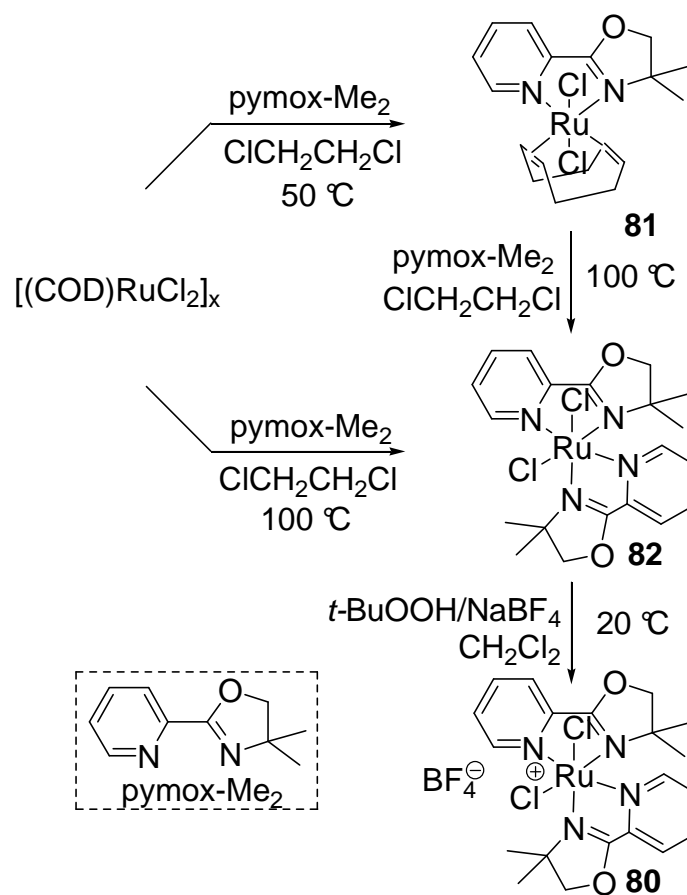
The subsequent treatment of **82** with NaBF_4 and *t*-BuOOH in CH_2Cl_2 led to the cationic Ru(III) complex $[(\text{pymox-Me}_2)_2\text{RuCl}_2]^+\text{BF}_4^-$ (**80**) in 73% isolated yield. The structure of these ruthenium complexes was completely established by both spectroscopic and X-ray crystallographic methods. The molecular structure of both **82** and **80** showed an octahedral geometry with *cis* coordination of the chloride and anti-pyridine ligands. The average Ru-Cl bond distance of the cationic Ru(III) complex **80** (2.33 Å) was found to be considerably shorter than the neutral complex **82** (2.41 Å). The magnetic moment of **80** ($\mu_{\text{eff}} = 1.55 B_M$) as determined by using the Evans NMR method was also consistent with a paramagnetic Ru(III) complex.



In a strikingly different reactivity pattern, only complex **80** was found to exhibit high catalytic activity for C-H bond oxidation reaction in aqueous solution, even though

both **82** and **80** are soluble in water. Thus, the treatment of ethylbenzene (1.0 mmol) with *t*-BuOOH (3 mmol, 70 wt% in aqueous solution) in the presence of 1 mol% of **80** in water (3 mL) cleanly produced acetophenone in >95% conversion within 16 h at room temperature (eq 81).

Scheme 27



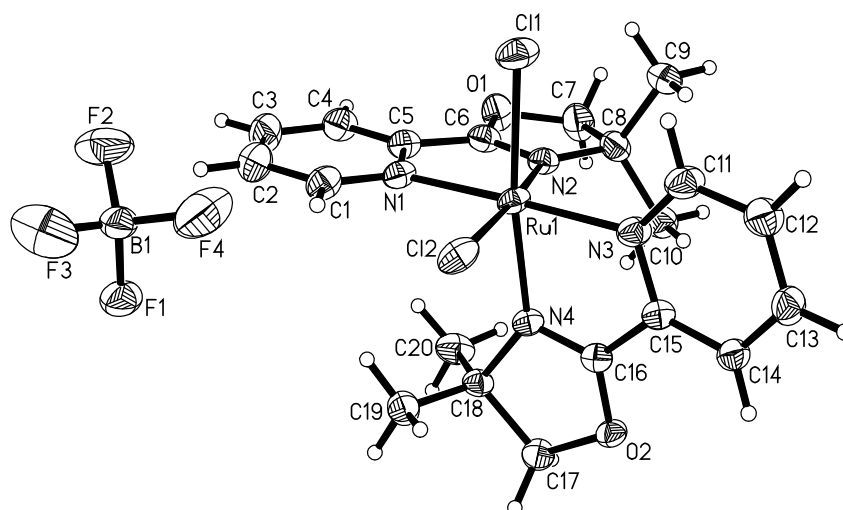


Figure 27. Molecular Structure of Complex 80.

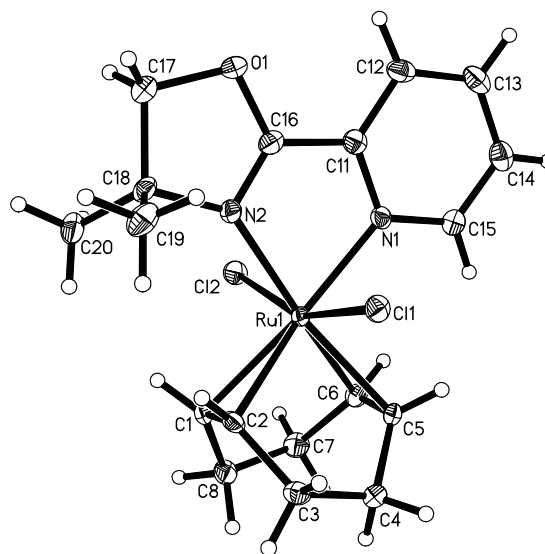


Figure 28. Molecular Structure of Complex 81.

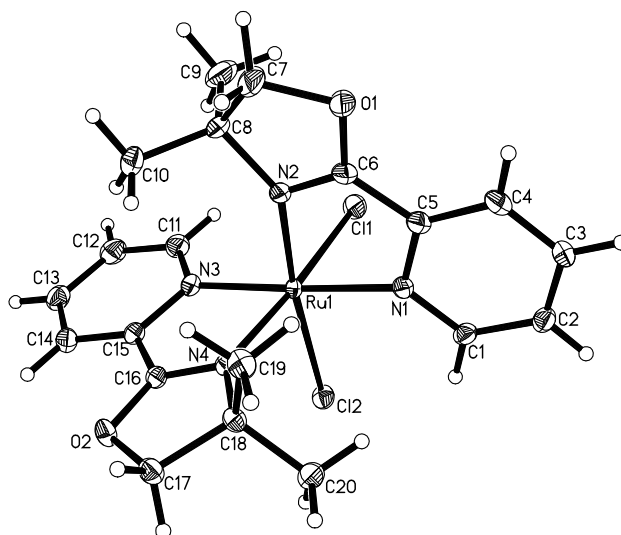


Figure 29. Molecular Structure of Complex **82**.

4.2 Optimization Studies for C-H Oxidation Reaction of Arylalkanes

4.2.1 Catalyst Survey

Initially, we used the reaction of ethylbenzene with *t*-BuOOH as an oxidizing agent to survey the catalytic activity of ruthenium complexes. However, commonly available ruthenium complexes such as $\text{RuCl}_2(\text{PPh}_3)_3$, RuO_2 , $\text{RuCl}_3 \cdot 3\text{H}_2\text{O}$, (*p*-cymene) RuCl_2 and $\text{Bu}_4\text{N}^+\text{RuO}_4^-$ were not soluble in aqueous solution. Thus, catalytic activity could not be directly compared to the complex **80** under the similar reaction condition.

Ethylbenzene was readily oxidized to acetophenone by **80** at 20 °C in aqueous condition giving 71% yield in 5 h at 20 °C and over 95% yield in 16 h. On the other hand, oxidation of ethylbenzene with 1.0 mol% $\text{RuCl}_2(\text{PPh}_3)_3$ (**83**) and *t*-BuOOH in benzene at

20 °C for 2 h afforded acetophenone in only 53% yield.⁸⁰ Che reported that the reaction was performed at 20 °C for 24 h in the presence of *cis*-[Ru(6,6'-Cl₂bpy)₂(OH₂)₂][SF₃SO₃]₂ (bpy = 2,2'-bipyridine) (**84**) (0.1 mol%) with *t*-BuOOH in acetone and obtained in 71% yield.⁸⁷ Doyle and coworker obtained that ethylbenzene is reacted with dirhodium caprolactamate (Rh₂(cap)₄) (**65**), *t*-BuOOH and NaBF₄ in DMF at 40 °C for 16 h and gave its corresponding product in 20% yield.¹⁰² Even though our catalytic system could not be directly compared with these catalytic systems, our system was comparable to or better than the reported catalytic systems (Table 16).

Table 16. Catalyst Survey for Oxidation Reaction of Ethylbenzene with *t*-BuOOH.

entry	cat	solvent	t (h)	yield (%)
1 ^a	none	H ₂ O	5	0
2 ^b	80	H ₂ O	5	71
3 ^c	83	C ₆ H ₆	2	53
4 ^d	84	acetone	24	71
5 ^e	65	DMF	16	20

Reaction Conditions: ^a *t*-BuOOH (3.0 equiv). ^b **80** (1 mol%), *t*-BuOOH (3.0 equiv). ^c **83** (1 mol%), *t*-BuOOH (4.0 equiv), reference 18. ^d **84** (0.1 mol%), *t*-BuOOH (3.2 equiv), reference 25. ^e **65** (1.0 mol%), *t*-BuOOH (3.2 equiv), NaBF₄ (0.5 equiv), reference 31.

4.2.2 Survey of Oxidizing Agents

A variety of oxidizing agents was examined in order to optimize the reaction condition. The reaction of ethylbenzene (1.0 mmol) with an oxidizing agent (3.0 mmol) in the presence of the complex **80** was performed in a variety of oxidizing agents and the yield of oxidizing products was determined by GC. It was found that the nature of oxidizing agents significantly affected the efficiency of the oxidation of arylalkanes.

Table 17. Oxidizing Agent and Additive Effects on Oxidation of Ethylbenzene.^a

entry	[ox]	additive(s)	conversion ^b (%)
1	O ₂	none	9
2	O ₂	NaBF ₄	10
3 ^c	O ₂	CH ₃ CHO	18
4 ^c	O ₂	CH ₃ CHO + NaBF ₄	20
5	NaIO ₄	none	0
6	NaIO ₄	NaBF ₄	2
7	<i>m</i> -CPBA	none	18
8	<i>m</i> -CPBA	NaBF ₄	22
9	H ₂ O ₂	none	21
10	H ₂ O ₂	NaBF ₄	23
11	CH ₃ CO ₃ H	none	35
12	CH ₃ CO ₃ H	NaBF ₄	38
13	<i>t</i>-BuOOH	none	>95
14	<i>t</i>-BuOOH	NaBF ₄	>95

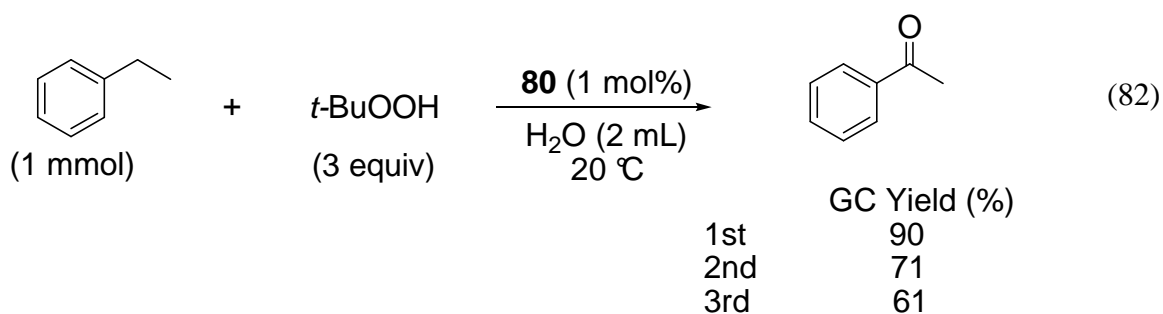
^a Reaction conditions: ethylbenzene (1 mmol), [ox] (3.0 equiv), additive (3 mol%), **80** (1 mol%), H₂O (3 mL), 20 °C, 16 h. ^b Determined by GC. ^c Acetaldehyde (0.1 equiv).

t-BuOOH was found to be the best oxidizing agent for this reaction (Table 17). As in the case of molecular oxygen, low yields were obtained (entry 1). In the presence of additives such as NaBF₄, acetaldehyde which generates peracetic acid *in situ* with molecular oxygen, or both NaBF₄ and acetaldehyde, product yield was increased to a little bit higher compared with no additive (entry 2-4). Sodium periodate (NaIO₄) showed no reaction with complex **80** under the similar reaction condition (entry 5-6). 3-Chloroperoxybenzoic acid (*m*-CPBA) only or with NaBF₄ as additive also led to low yields (entry 7-8). Hydrogen peroxide (H₂O₂) gave low yields. Addition of NaBF₄ to H₂O₂ reaction gave similar yield (entry 9 and 10). Peracetic acid (CH₃CO₃H) was found to be slightly increase activity compared to other oxidants, but in lower yield compared to *t*-BuOOH (entry 11-12). When *t*-BuOOH was used as oxidizing agent in this reaction, it exhibited highest activity with complex **80** under similar reaction condition. When NaBF₄ was added as additive, product yield was not changed compared to the case of catalyst only. From these results, *t*-BuOOH was the best oxidizing agent with complex **80** in aqueous solution and oxidation reaction with *t*-BuOOH in presence of **80** was not affected from NaBF₄.

4.2.3 Reusability of the Cationic Ruthenium Complex in Aqueous Solution

Salient features of water-soluble catalyst **80** are that it retains significant activity after repeated runs, and it can be readily separated from the reaction mixture by simple extraction. In this series of oxidations, ethylbenzene was treated under standard conditions (1.0 mol% of **80**, 3.0 mol% NaBF₄, 3.0 equiv of *t*-BuOOH, in 3.0 mL water) to afford their corresponding oxidizing products in 90% yield (eq 82). Following

extraction of products with diethyl ether, the aqueous layer from the first reaction was reused with additional substrate and oxidizing agent. The second and third reactions were performed with the similar reaction condition and these reaction gave comparable yields (2nd: 71%, 3rd: 61%). Subsequently, we found that resultant aqueous layer from the second reaction was able to catalyze another oxidation. Even though the yields of second and third time were diminished, the oxidation of ethylbenzene by complex **80** in aqueous condition showed reusability of the catalyst.



4.3 Reaction Scope

The scope of the oxidation of alkanes was explored in order to demonstrate the synthetic utility of complex **80**. We examined various benzylic compounds and cyclic alkanes by using these optimized conditions. In general, the C-H bond oxidation of benzylic compounds occurred smoothly at room temperature to give the ketone products (Table 18).

Ethylbenzene and its derivatives are oxidized at the benzylic C-H bonds to give acetophenone and its derivatives selectively (entry 1-3). Propylbenzene was converted to

its corresponding α -position ketone **85d** with good yield (entry 4). The formation of C-C bond cleavage product for isobutylbenzene is reminiscent of the oxidation reaction promoted by transition metal complexes (entry 5), where benzyloxy radical species has been implicated for the C-C bond cleavage reactions of alkylbenzenes.¹⁰ The oxidation of tertiary benzylic C-H bond is favored over the primary ones to give the alcohol products (entry 6). 2-Ethyl-naphthalene produced to their corresponding ketone in higher yield than ethylbenzene and their derivatives (entry 7). Indan was oxidized with high conversion and converted selectively to their corresponding ketones, which are 1-indanone and 2,3-dihydro-3-hydroxyindan-1-one, with moderate yield in 2 h (entry 8). Fluorene and diphenylmethane can be readily converted into the corresponding ketones in high yield in short reaction time (entries 9 and 11).

In contrast, the dehydrogenation product **85i** was favored over the oxidation product **85m** for the 9,10-anthracene case (entry 10). Functionalized alkylated arene such as xanthene was also oxidized with 95% yield (entry 12). The oxidation of cyclic alkenes was found to be sluggish, giving only modest conversions under the similar reaction conditions (entries 13-15).

Table 18. Aqueous Phase C-H Bond Oxidation of Arylalkanes.^a

entry	substrate	products	t (h)	convn (%)	yield (%) ^b	
1			85a X = H	16	95	83(90)
2			86b X = OMe	16	97	87(95)
3			85c X = Cl	16	87	77(83)
4			85d	16	88	72(80)
5			85e	24	56	41(47)
6			85f:85g = (3:1)	16	90	74(80) ^c
7			85h	16	94	89(90)
8			85i:85j = (8.5:1)	2	>99	80(90) ^d
9 ^e			85k	2	93	86(92)
10 ^e			85l:85fm = (4:1)	2	>99	88(95)
11			85n	2	90	82(88)
12 ^e			85o	2	>99	87(95)
13			85p:85q = (3:1)	24	33	--(29) ^f
14			85r:85s = (1:1)	24	31	--(28) ^f
15			85t:85u = (15:1)	24	66	54(62)

^a Reaction conditions: substrate (1.0 mmol), *t*-BuOOH (3.0 mmol, 70 wt% in water), **80** (1.0 mol%), H₂O (3 mL), 20-22 °C. ^b Isolated product yields. The GC product yields are listed in parenthesis. ^c Less than 5% of benzaldehyde derivative is formed. ^d Five percent of 1,3-indandione is formed. ^e Substrate was dissolved in 1 mL of CH₂Cl₂. ^f Products were not isolated due to low conversion and difficulty in separation.

4.4 Mechanistic Studies

4.4.1 Isotope Effect Study

As mention in above, the k_H/k_D value between radical-caged and free radical mechanism showed different feature (Table 15). The radical-caged mechanism was usually obtained by higher isotope effect (k_H/k_D) than free radical mechanism. But, both mechanisms indicate that the C-H bond breaking is the rate determining step. To learn more about the isotope effect of our system, the oxidation of ethylbenzene with *t*-BuOOH and ethylbenzene-*d*₁₀ with *t*-BuOOH were performed separately, and the reaction rates were determined by GC. A significant isotope effect was observed for the C-H bond oxidation reaction of ethylbenzene and ethylbenzene-*d*₁₀. The pseudo-first order plots of the catalytic reaction of both ethylbenzene and ethylbenzene-*d*₁₀ with *t*-BuOOH, at room temperature led to a $k_{\text{obs}} = 2.1 \times 10^{-2} \text{ h}^{-1}$ and $k_{\text{obs}} = 1.5 \times 10^{-3} \text{ h}^{-1}$, respectively, from which a $k_H/k_D = 14 \pm 0.1$ was obtained (Figure 30). This result indicates that the cleavage of the C-H bond is the rate-limiting step in the overall reaction mechanism and this value is similar with radical caged mechanism.

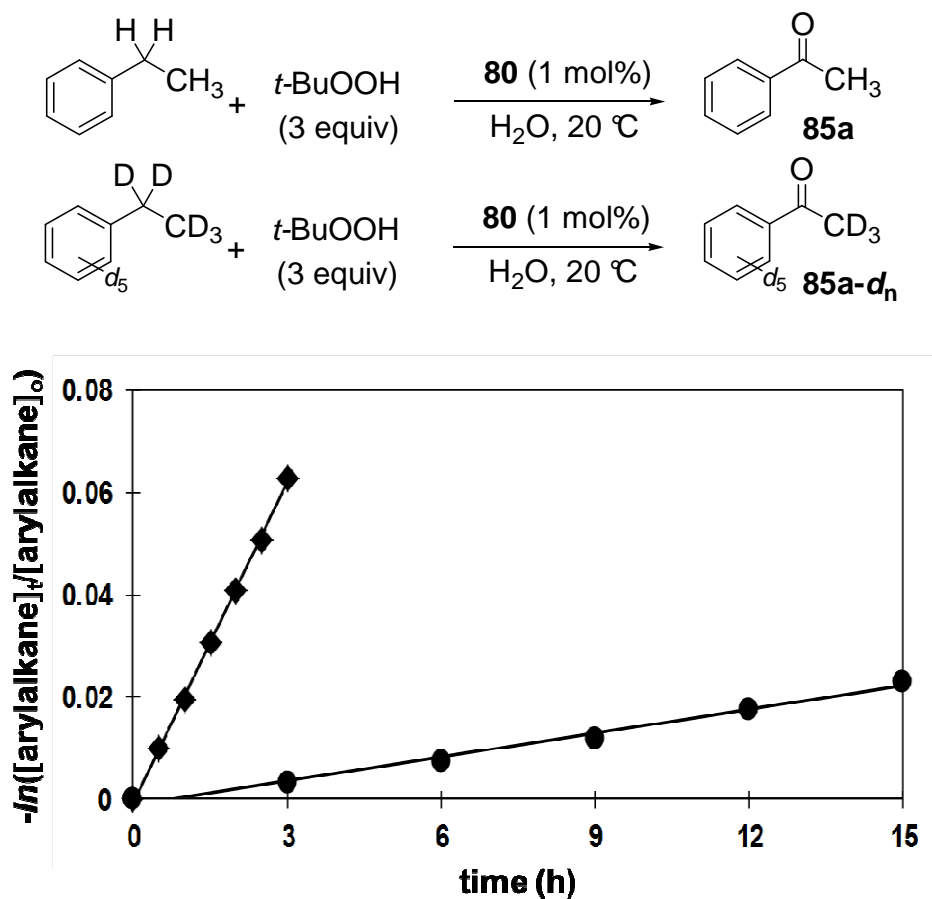


Figure 30. First-Order Plots of $-\ln([\text{ethylalkane}]_t/[\text{ethylalkane}]_0)$ vs Time for C-H Bond Oxidation Reaction of Ethylbenzene (♦) or Ethylbenzene- d_{10} (●) with $t\text{-BuOOH}$.

4.4.2 Hammett Study

Hammett studies of *para*-substituted ethylbenzene substrates were performed to determine the electronic effects on arylalkane substrate during C-H bond oxidation reaction. The reaction rate was found to be considerably accelerated by ethylbenzene containing electron donating groups. The Hammett correlation of *para*-substituted ethylbenzene substrates $p\text{-X-C}_6\text{H}_4\text{CH}_2\text{CH}_3$ (X = OMe, CH₃, H, F, Cl) led to $\rho = -1.1 \pm 0.1$ (Figure 31). The negative value of ρ indicates considerable cationic character in the transition state. The observed ρ value is substantially higher than the oxidation reaction catalyzed by free radical species such as $t\text{-BuO}\cdot$ and $t\text{-BuOO}\cdot$ ($\rho = -0.4$ to -0.6), but

somewhat lower than the ones catalyzed by $(\text{PPh}_3)_2\text{RuCl}_2/t\text{-BuOOH}$ and cytochrome P-450 and their synthetic model systems ($\rho = -1.3$ to -1.6).¹² A relatively high $-\rho$ value suggested of a substantial charge transfer from a metal-oxo species to the substrate during the C-H bond cleavage step.

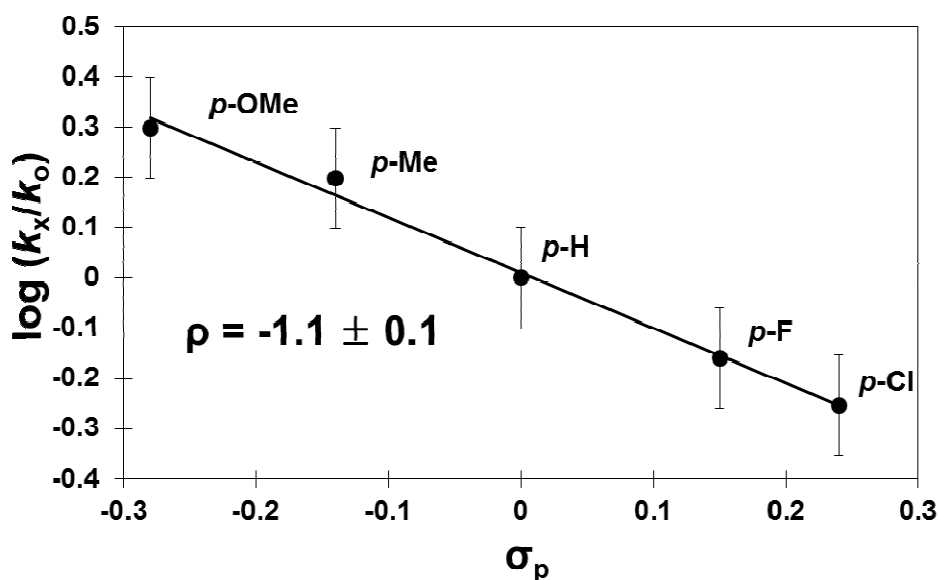
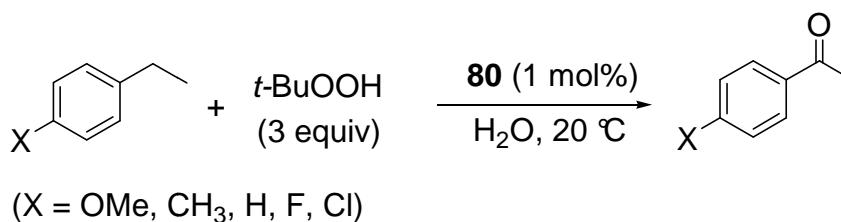


Figure 31. Hammett plot of the C-H Bond Oxidation Reaction of *para*-Substituted Ethylbenzene Substrates $p\text{-X-C}_6\text{H}_4\text{CH}_2\text{CH}_3$ (X = OMe, CH₃, H, F, Cl) with *t*-BuOOH.

4.4.3 Detection of Catalytically Active Species

The initially inactive neutral ruthenium complex **82** became an active catalyst upon addition of NaBF_4 for the oxidation reaction. This fact and a relatively low Ru(II)/Ru(III) redox potential ($E_0 = +0.22$ V) clearly indicate that the cat

ionic Ru(III) complex **80** is catalytically active species for the oxidation reaction (Figure.30).¹⁰⁸

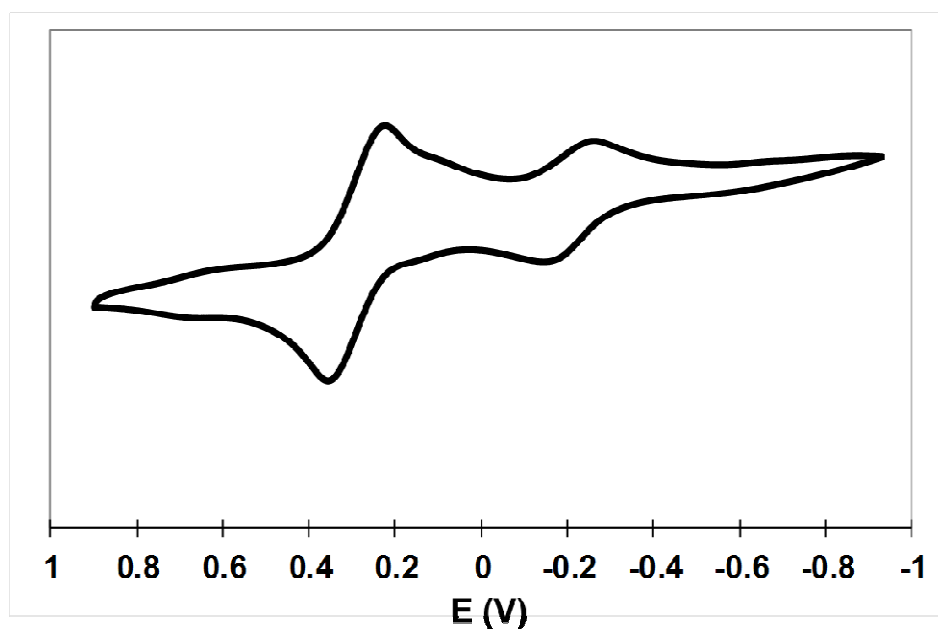


Figure 32. Cyclic Voltammogram of **80** in CH₂Cl₂.

The observation of a strong metal-to-ligand charge transfer (MLCT) band at 360 nm ($d\pi-\pi^*$) from the reaction mixture of **82** with *t*-BuOOH and NaBF₄ also supports the formation of a Ru(III) species which gives similar metal-to-ligand charge transfer band at 360 nm ($d\pi-\pi^*$) (Figure 33). The data are most consistent with a “solvent-charged” oxygen rebound mechanism of rate-limiting C-H oxidation step from a Ru(IV)-oxo species.^{80,87,108} From UV-vis spectra and relatively low redox potential, we expected that when complex **82** was added in the reaction solution with *t*-BuOOH and NaBF₄, complex **80** was generated *in situ* from **82** and cationic Ru(III) complex **80** acted as catalyst precursor in oxidation of alkanes.

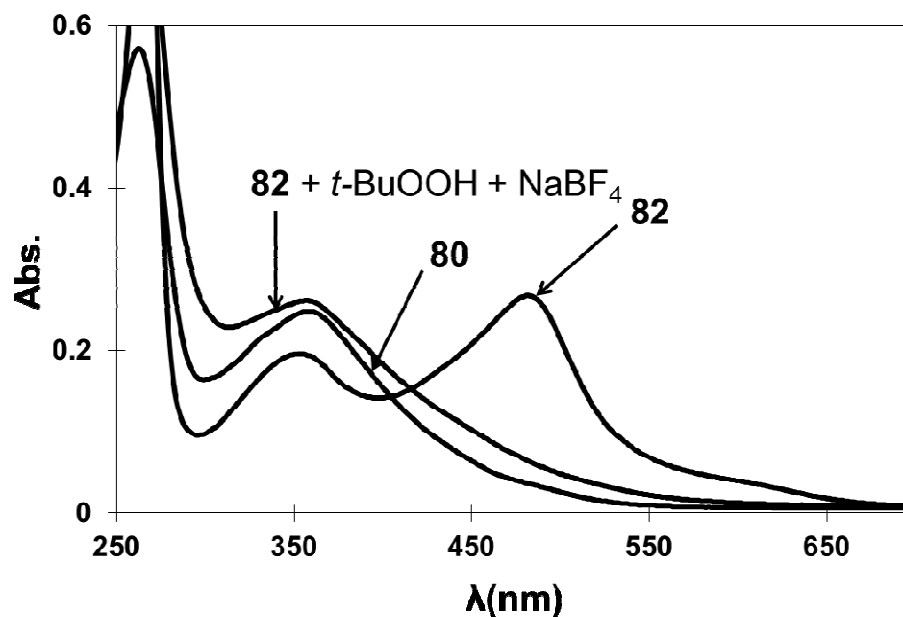


Figure 33. UV-vis spectra of **82** (20 μM), **82** (20 μM)/*t*-BuOOH (30 equiv)/NaBF₄, and **80** (20 μM) in water.

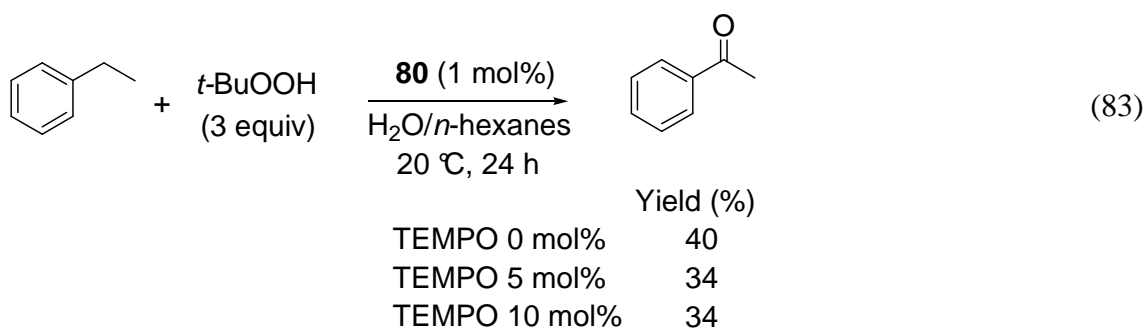
4.5 Proposed Mechanism

Regarding ongoing controversy surrounding the reaction mechanism of Gif-type oxidations, pathways involving metal-oxo species or oxygenated free radicals have been proposed. It is difficult to differentiate these two mechanistic possibilities, partly because many reports describing the relative reactivity of discrete metal-oxo complexes toward different saturated C-H bonds. For our catalytic system, we proposed that ruthenium-oxo species **87** which is similar with Gif-type metal oxo species, generated from alkylperoxo-Ru(III) complex **86** by heterolytic cleavage of the O-O bond, is the active species for C-H bond oxidation of alkanes. This mechanism is similar with Murahashi's RuCl₂(PPh₃)₃'s mechanism.¹⁸ Another possibility is concerted mechanism without formation of radical intermediate based on proton tunneling. But, former mechanism is widely accepted in the literature.

While the detailed reaction mechanism for the oxidation of alkanes catalyzed by **80** still remains unclear at this stage, a plausible mechanism is compiled as shown in Scheme 28. Initially, the reaction of Ru(II) complex **82** with *t*-BuOOH and NaBF₄ led to generation of catalytically active cationic Ru(III) complex **80**. We were able to isolate cationic Ru(III) complex **80** from the oxidation reaction and confirmed their molecular structure by X-ray diffraction analysis. These results indicate that cationic Ru(III) complex **80** is an active catalyst for the C-H bond oxidation reaction.

We propose that the Ru(III) complex **80** would react with *t*-BuOOH to give the alkylperoxo-Ru(III) complex **86**. This is consistent with previous cases containing alkylperoxo-metals which can promote oxidation of hydrocarbons and are viable intermediate in catalytic oxidation of hydrocarbons with ROOH.^{18,71} Alkylperoxo-Ru(III) complex **86** subsequently undergoes heterolytic cleavage of the O-O bond to give Ru(IV)-oxo species **87**. The deuterium isotope effect was examined for oxidation of ethylbenzene and ethylbenzene-*d*₁₀ catalyzed by **80**. The k_H/k_D value was determined to be 14 ± 0.1 by means of GC analysis and this value indicates that C-H bond breaking is the rate-determining step. This large k_H/k_D value is similar to that obtained for the oxidation with cytochrome P450 and Murahashi system (Table 15). Hammett value ($\rho = -1.1$) is slightly lower than the ones catalyzed by (PPh₃)RuCl₂/*t*-BuOOH and cytochrome P-450 and their synthetic model systems ($\rho = -1.3$ to -1.6), but substantially higher than the oxidation reaction catalyzed by free radical species such as *t*-BuO• and *t*-BuOO• ($\rho = -0.4$ to -0.6) (Table 15).¹² A relatively high $-\rho$ value suggested of a substantial charge transfer from a metal-oxo species to the substrate during the C-H bond cleavage step. These proposed mechanisms invoked metal-oxo complexes as reactive intermediates in

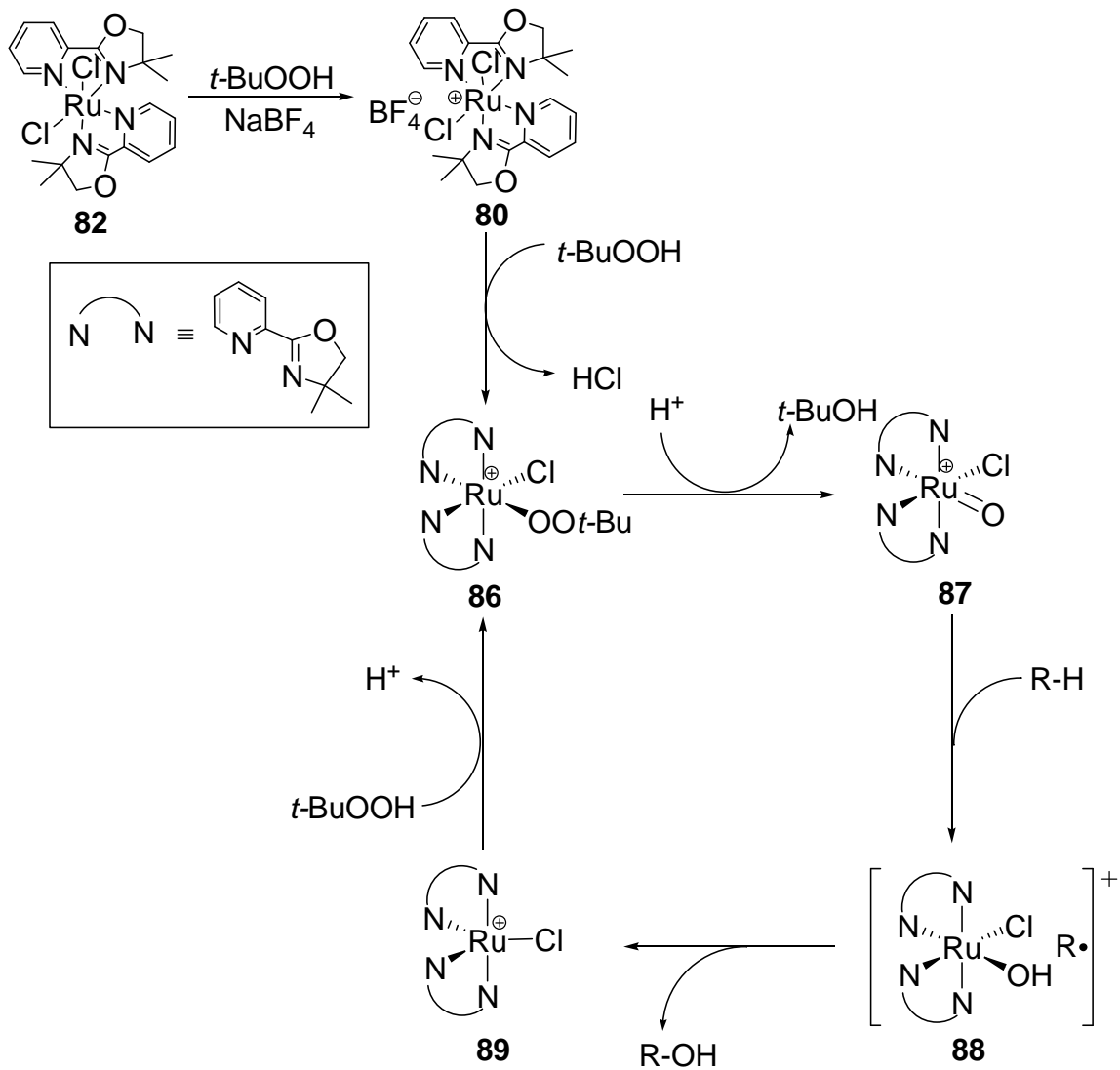
oxidation of hydrocarbons. Abstraction of a hydrogen atom from an alkane by the intermediate **87** would form the caged complex **88**, bearing an alkyl radical and a hydroxo-Ru(IV) intermediate **88**. The fact that a radical scavenger TEMPO (10 mol%) did not significantly affected the rate of the oxidation reaction also supports the notion of a solvent-caged mechanism (eq 83).



ROO*t*-Bu which is usually generated at free radical mechanism was not detected from oxidation of alkanes catalyzed by **80**.³⁰ Transfer of the hydroxyl ligand to the caged alkyl radical would afford an alcohol and the ruthenium(II) species **89** to complete the catalytic cycle. Further oxidation of secondary alcohol thus formed gives the corresponding ketones under the reaction condition. From these data, we suggest that the active species of the **80**/*t*-BuOOH system is oxo-ruthenium species, not free radical species.

The detailed reaction mechanism for the oxidation of alkanes catalyzed by **80** still remains to be established. Detailed mechanistic studies of these reactions study are currently underway.

Scheme 28



5. Conclusions

We have successfully synthesized ruthenium complexes containing oxazoline ligands which have been fully characterized both spectroscopically and analytically. The cationic Ru(III) complex **80** was found to be an effective catalyst for the oxidation of saturated C-H bonds in aqueous condition. While high valent metal-oxo species have been invoked in both nonheme and Gif-type oxidation, catalytic C-H bond oxidation reactions mediated by well-defined cationic Ru(III) complexes have been rarely reported.¹³ Efforts to extend the scope of oxidation reaction as well as the nature of active species are currently underway.

Chapter V

Experimental Section

General Information. All operations were carried out in an inert-atmosphere glove box or by using standard high vacuum and Schlenk techniques unless otherwise noted. Tetrahydrofuran, benzene, hexanes and Et₂O were distilled from purple solutions of sodium and benzophenone immediately prior to use. The NMR solvents were dried from activated molecular sieves (4 Å). All organic substrates were received from commercial sources and used without further purification. The ¹H, ²H, ¹³C and ³¹P NMR spectra were recorded on a Varian 300 or 400 MHz FT-NMR spectrometer. Mass spectra were recorded from a Agilent 6850 GC/MS spectrometer. The conversion of organic products was measured from a Hewlett-Packard HP 6890 GC spectrometer. FT-IR spectra were recorded on Perkin Elmer Spectrum 100. High resolution EI mass spectrum was obtained at the Center of Mass Spectrometry, Washington University, St. Louis, MO. Elemental analysis was performed at the Midwest Microlab, Indianapolis, IN.

For Chapter 2

Representative Procedure of the Catalytic Reaction. In a glove box, complex **26** (15 mg, 25 μmol), an arylamide (0.5 mmol) and an alkene (2.5 mmol) were dissolved in CH₂Cl₂ (2 mL) in a 25 mL Schlenk tube equipped with a Teflon screw cap stopcock and a magnetic stirring bar. The tube was brought out of the box, and was stirred for 5 h in an oil bath set at 80 °C. After the tube was cooled to room temperature, the solution was filtered through a short silica plug (hexanes/EtOAc = 2:1) in air, and the filtrate was analyzed by GC. Typically, the product mixture of **27** and **28** was not separable by column chromatography, and was subjected to the hydrogenation reaction to obtain isolated yield of the products. The treatment of the crude product mixture with H₂ (1 atm) in the presence of **26** (15 mg, 5 mol %) in chlorobenzene at 110 °C for 2 h led to the

clean formation of the hydrogenated product **28**. Analytically pure organic product was isolated after a column chromatography on silica gel (hexanes/EtOAc).

Synthesis of 29. In a glove box, the tetrameric ruthenium complex $\{[(PCy_3)(CO)RuH]_4(\mu-O)(\mu-OH)_2\}$ (**4**) (200 mg, 0.12 mmol) and *N,N*-dimethyl-2-naphthamide were dissolved in CH_2Cl_2 (5 mL) in a 25 mL Schlenk tube equipped with a Teflon screw cap stopcock and a magnetic stirring bar. The tube was brought out of the box, and $HBF_4 \cdot OEt_2$ (64 μ L, 0.48 mmol) was added under N_2 stream. The color of the solution was changed from dark red to green immediately. After stirring for 1 h at room temperature, the solvent was removed under vacuum, and the residue was crashed by adding hexanes (10 mL). Filtering the resulting solid through a fritted funnel and recrystallization from CH_2Cl_2 /hexanes yielded the product as a light green powder (210 mg, ca. 60% yield, estimated purity by 1H NMR ~80%; contained 2 other minor isomers (~20%)).

Spectroscopic data for the major isomer of **29**: 1H NMR (CD_2Cl_2 , 400 MHz) δ 7.9-7.4 (m, 7H, Ar), 3.18 and 3.02 (s, 3H, $N(CH_3)_2$), 2.0-1.2 (m, PCy_3), -21.2 (br, Ru-H); $^{13}C\{^1H\}$ NMR (CD_2Cl_2 , 100.5 MHz) δ 197.6 (d, $J_{CP} = 18.2$ Hz, Ru-CO), 178.7 ($CON(CH_3)_2$), 134.8, 132.9, 129.6, 129.2, 128.9, 128.4, 128.0 and 123.9 (Ar), 38.9 ($N(CH_3)_2$), 38.6 (CH), 35.1 ($N(CH_3)_2$), 32.1, 30.9, 30.4, 29.9, 28.0, 26.8, 26.2 (CH_2); $^{31}P\{^1H\}$ NMR (CD_2Cl_2 , 161.8 MHz) δ 74.4 (PCy_3); IR (CD_2Cl_2) $\nu_{CO} = 1930, 1585$ cm^{-1} .

Synthesis of 30a. In a glove box, complex **29** (100 mg, 0.14 mmol) and cyclopentene (100 mg, 1.5 mmol) were dissolved in CH_2Cl_2 (5 mL) in a 25 mL Schlenk tube equipped with a Teflon screw cap stopcock and a magnetic stirring bar. The color of the solution was changed from green to orange immediately. After stirring for 1 h at room temperature, the solvent was removed under vacuum, and *n*-hexanes (10 mL) was added to the residue. The resulting solid was filtered through a fritted funnel and recrystallized

from CH₂Cl₂/hexanes to yield the product as a pale yellow powder (90 mg, 82% yield). Single crystals of **30a** suitable for X-ray crystallography were obtained from CH₂Cl₂/*n*-pentane solution.

For **30a**: ¹H NMR (CD₂Cl₂, 400.0 MHz) δ 8.45 (s, 1H, Ar), 8.06 (m, 1H, Ar), 7.94 (m, 2H, Ar), 7.72 (m, 2H, Ar), 5.46 (s, CCHCH₂) 3.38 (s, 3H, N(CH₃)₂), 3.31 (m, 1H, CH₂), 3.17 (s, 3H, N(CH₃)₂), 3.08 (m, 1H, CH₂), 2.81 (m, 2H, CH₂), 2.0-1.8 (br, 6H, PCy₃), 1.82 (m, 2H, CH₂), 1.8-0.6 (br, 27H, PCy₃), -19.6 (d, *J*_{PH} = 21.8 Hz, Ru-H); ¹³C{¹H} NMR (CD₂Cl₂, 100.5 MHz) δ 201.2 (d, *J*_{CP} = 15.4 Hz, Ru-CO), 174.3 (CON(CH₃)₂), 136.4, 135.2, 132.4, 130.7, 130.5, 130.3, 129.4, 129.2, 128.3 and 117.8 (Ar), 115.5 (d, *J*_{CP} = 5.1 Hz, Ru-C), 104.7 (d, *J*_{CP} = 11.6 Hz, Ru-C), 42.4 (N(CH₃)₂), 37.6 and 37.5 (CH₂), 37.3(N(CH₃)₂), 34.6 and 34.4 (CH), 30.4, 30.0, 28.1, 28.0, 27.9, 27.8, 26.4 and 21.0 (CH₂); ³¹P{¹H} NMR (CD₂Cl₂, 161.8 MHz) δ 65.4 (PCy₃); IR (CD₂Cl₂) ν_{CO} = 1948, 1600 cm⁻¹; Anal. Calcd for C₃₈H₅₅BCl₂F₄NO₂PRu: C, 53.85; H, 6.54. Found: C, 53.51; H, 6.48.

Phosphine Inhibition Study. In a glove box, complex **26** (15 mg, 25 μmol), an C₆H₅CONEt₂ (0.5 mmol) and an alkene (2.5 mmol) were dissolved in CH₂Cl₂ (2.0 mL) in a 25 mL Schlenk tube equipped with a Teflon screw cap stopcock and a magnetic stirring bar. For phosphine inhibition study, PCy₃ (0 ~ 6.3 mol%) was added to the reaction mixture. The tube was brought out of the box, and was stirred for 5 h in an oil bath set at 80 °C. After the tube was cooled to room temperature, the solution was filtered through a short silica plug (hexanes/EtOAc = 2:1) in air, and the filtrate was analyzed by GC.

Deuterium Isotope Effect Study. In a glove box, complex **26** (17 mg, 30 μmol), C₆H₅CONEt₂ (177 mg, 1.0 mmol) or C₆D₅CONEt₂ (182 mg, 1.0 mmol) and cyclopentene (0.09 g, 5 mmol) were dissolved in CH₂Cl₂ (5.0 mL) in a 25 mL Schlenk tube equipped with a Teflon screw cap stopcock and a magnetic stirring bar. After the solution was

stirred at room temperature for 10 min, an equal amount of the solution (1.4 mL) was divided and placed in 5 different Schlenk tubes. The tubes were brought out of the box, and were stirred for 25 min in an oil bath set at 80 °C. Each reaction tube was taken out from the oil bath in 5 min intervals, and was immediately cooled in a dry ice/acetone bath. After filtering through a small silica gel column (hexanes/EtOAc = 2:1), the solution was analyzed by GC. The k_{obs} was determined from a first-order plot of $\ln[27\mathbf{h} + 28\mathbf{h}]$ vs time as measured by the appearance of the products **27h** and **28h** by GC.

Deuterium Labeling Study. In a glove box, complex **26** (15 mg, 25 μmol), *N,N*-diethyl benzamide- d_5 ($\text{C}_6\text{H}_5\text{CONEt}_2$, 91 mg, 0.50 mmol) and cyclopentene (0.17 g, 2.5 mmol) were dissolved in CH_2Cl_2 (2 mL) in a 25 mL Schlenk tube equipped with a Teflon screw cap stopcock and a magnetic stirring bar. The tube was brought out of the box, and was stirred for 1 h in an oil bath set at 80 °C. The tube was immediately cooled and was open to air. After filtering through a short silica gel column (hexanes/EtOAc = 2:1), the conversion was determined by GC. Both unreacted cyclopentene- d_n and cyclopentane- d_n were collected separately via a vacuum transfer. The product mixture of **27h**- d_n and **28h**- d_n and unreacted *N,N*-diethyl benzamide- d_n was separated by a column chromatography on silica gel (hexanes/EtOAc), and each was analyzed by both ^1H and ^2H NMR.

Carbon Isotope Effect Study. In a glove box, complex **26** (0.23 g, 0.4 mmol), $\text{C}_6\text{H}_5\text{CONEt}_2$ (1.4 g, 8.0 mmol) and cyclopentene (2.72 g, 0.04 mol) were dissolved in CH_2Cl_2 (32 mL) in a 100 mL Schlenk tube equipped with a Teflon screw cap stopcock and a magnetic stirring bar. The tube was brought out of the box, and was stirred in an oil bath at 80 °C for 5 h. The tube was cooled to room temperature and was open to air. After filtering through a small silica column (hexanes/EtOAc = 2:1), the conversion was determined by GC (78%, 80% and 82% conversion). Unreacted $\text{C}_6\text{H}_5\text{CONEt}_2$ was separated by a column chromatography on silica gel (hexanes/EtOAc) for $^{13}\text{C}\{^1\text{H}\}$ NMR

analysis.

The ^{13}C NMR analysis of the recovered and virgin samples of $\text{C}_6\text{H}_5\text{CONEt}_2$ was performed by following Singleton's ^{13}C NMR method (ref. 9 in the main text). The NMR sample of virgin and recovered $\text{C}_6\text{H}_5\text{CONEt}_2$ was prepared identically by dissolving $\text{C}_6\text{H}_5\text{CONEt}_2$ (100 mg) in $\text{DMSO-}d_8$ (0.5 mL) in a 5 mm high precision NMR tube. The $^{13}\text{C}\{^1\text{H}\}$ NMR spectra were recorded with H-decoupling and 45 degree pulses. A 60 s delay between pulses was imposed to minimize T_1 variations (d1 = 60 s, at = 5.0 s, np = 245098, nt = 706).

VT NMR Study for the Reaction of **26 with *N,N*-dimethyl-2-naphthamide.** In a glove box, complex **26** (50 mg, 87 μmol) and *N,N*-dimethyl-2-naphthamide (17 mg, 87 μmol) were dissolved in CD_2Cl_2 (0.5 mL) in a thick wall J-Young NMR tube. The tube was allowed to equilibrate for 30 min before the NMR analysis. The sample tube was inserted into the NMR probe. The equilibrium constants were determined from the phosphorus integration of **26** and **29** by ^{31}P NMR in the temperature range 30 to 60 $^\circ\text{C}$ (10 $^\circ\text{C}$ intervals). The sample was allowed to equilibrate for 10-15 min before the data acquisition at each temperature.

Characterization Data of Organic Products

For **28a**: ^1H NMR (400 MHz, CDCl_3) δ 7.2-7.0 (m, 4H, Ar), 3.04 (s, 3H, $\text{N}(\text{CH}_3)_2$), 2.90 (m, 1H, ArCH), 2.72 (s, 3H, $\text{N}(\text{CH}_3)_2$), 2.0-1.4 (br, 8H, CH_2); $^{13}\text{C}\{^1\text{H}\}$ NMR (100 MHz, CDCl_3) δ 171.7 (CO), 142.8, 136.4, 128.9, 126.3, 125.7 and 125.4 (Ar), 42.3 (ArCH), 38.9 ($\text{N}(\text{CH}_3)_2$), 35.4 (CH_2), 34.5 (CH_2), 34.4 ($\text{N}(\text{CH}_3)_2$), 25.7 (CH_2); GC-MS m/z = 217 (M^+); Anal. Calcd for $\text{C}_{14}\text{H}_{19}\text{NO}$: C, 77.38; H, 8.81. Found: C, 77.49; H, 8.70.

For **28b**: ^1H NMR (400 MHz, CDCl_3) δ 7.2-6.9 (m, 3H, Ar), 3.08 (s, 3H, $\text{N}(\text{CH}_3)_2$), 2.91 (m, 1H, CH_2CHCH_2), 2.78 (s, 3H, $\text{N}(\text{CH}_3)_2$), 2.25 (s, 3H, CH_3), 1.7-1.3 (br, 8H, CH_2); $^{13}\text{C}\{^1\text{H}\}$ NMR (100 MHz, CDCl_3) δ 171.9 (CO), 139.6, 136.4, 135.3, 129.7, 126.3 and 125.9 (Ar), 42.1 (CH_2CHCH_2), 38.9 ($\text{N}(\text{CH}_3)_2$), 35.5 (CH_2), 34.5 (CH_2), 34.4 ($\text{N}(\text{CH}_3)_2$), 25.6 (CH_2), 20.8 (CH_3); GC-MS $m/z = 231$ (M^+); Anal. Calcd for $\text{C}_{14}\text{H}_{18}\text{ClNO}$: C, 77.88; H, 9.15. Found: C, 78.57; H, 9.32.

For **28c**: ^1H NMR (400 MHz, CDCl_3) δ 7.2-7.0 (m, 3H, Ar), 3.03 (s, 3H, $\text{N}(\text{CH}_3)_2$), 2.85 (m, 1H, CH_2CHCH_2), 2.75 (s, 3H, $\text{N}(\text{CH}_3)_2$), 2.1-1.4 (br, 8H, CH_2); $^{13}\text{C}\{^1\text{H}\}$ NMR (100 MHz, CDCl_3) δ 170.1 (CO), 141.5, 138.0, 134.4, 129.0, 128.1 and 125.4 (Ar), 41.9 (CH_2CHCH_2), 38.9 ($\text{N}(\text{CH}_3)_2$), 35.5 (CH_2), 34.6 ($\text{N}(\text{CH}_3)_2$), 34.5 (CH_2), 25.7 (CH_2); GC-MS $m/z = 251$ (M^+); Anal. Calcd for $\text{C}_{14}\text{H}_{18}\text{ClNO}$: C, 66.79; H, 7.21. Found: C, 67.20; H, 7.34.

For **28d**: ^1H NMR (400 MHz, CDCl_3) δ 7.0-6.6 (m, 3H, Ar), 3.70 (s, 3H, OCH_3), 3.02 (s, 3H, $\text{N}(\text{CH}_3)_2$), 2.92 (m, 1H, ArCH), 2.74 (s, 3H, $\text{N}(\text{CH}_3)_2$), 1.9-1.4 (br, 8H, CH_2); $^{13}\text{C}\{^1\text{H}\}$ NMR (100 MHz, CDCl_3) δ 171.6 (CO), 159.8, 144.8, 129.0, 126.8, 112.0 and 110.6 (Ar), 55.0 (OCH_3), 42.3 (ArCH), 38.9 ($\text{N}(\text{CH}_3)_2$), 35.0 (CH_2), 34.5 ($\text{N}(\text{CH}_3)_2$), 34.4 (CH_2), 25.6 (CH_2); GC-MS $m/z = 247$ (M^+); Anal. Calcd for $\text{C}_{15}\text{H}_{21}\text{NO}_2$: C, 72.84; H, 8.56. Found: C, 72.68; H, 8.55.

For **28e**: ^1H NMR (400 MHz, CDCl_3) δ 7.2-7.0 (m, 3H, Ar), 3.02 (s, 3H, $\text{N}(\text{CH}_3)_2$), 2.91 (m, 1H, ArCH), 2.72 (s, 3H, $\text{N}(\text{CH}_3)_2$), 2.0-1.4 (br, 8H, CH_2); $^{13}\text{C}\{^1\text{H}\}$ NMR (100 MHz, CDCl_3) δ 170.5 (CO), 145.5, 134.8, 134.6, 126.9, 126.6 and 125.8 (Ar), 42.1 (ArCH), 38.7 ($\text{N}(\text{CH}_3)_2$), 35.2 (CH_2), 34.4 ($\text{N}(\text{CH}_3)_2$), 34.3 (CH_2), 25.6 (CH_2); GC-MS $m/z = 251$ (M^+); Anal. Calcd for $\text{C}_{14}\text{H}_{18}\text{ClNO}$: C, 66.79; H, 7.21. Found: C, 66.83; H, 7.30.

For **28f**: ^1H NMR (400 MHz, CDCl_3) δ 7.2-7.0 (m, 4H, Ar), 6.73 and 5.98 (s, NH_2), 3.32 (m, 1H, CH_2CHCH_2), 2.0-1.4 (br, 8H, CH_2); $^{13}\text{C}\{^1\text{H}\}$ NMR (100 MHz, CDCl_3) δ 173.6 (CO), 144.4, 136.2, 130.1, 126.7, 126.5 and 125.5 (Ar), 41.8 (CH_2CHCH_2), 35.3 (CHCH_2), 25.9 (CH_2); GC-MS $m/z = 189$ (M^+); Anal. Calcd for $\text{C}_{12}\text{H}_{15}\text{NO}$: C, 76.16; H, 7.99. Found: C, 76.31; H, 7.88.

For **28g**: ^1H NMR (400 MHz, CDCl_3) δ 7.2-7.0 (m, 4H, Ar), 6.28 (d, $J = 3.9$ Hz, 1H, NH), 3.18 (m, 1H, ArCH), 2.71 (d, $J = 4.9$ Hz, NHCH_3), 2.0-1.4 (br, 8H, CH_2); $^{13}\text{C}\{^1\text{H}\}$ NMR (100 MHz, CDCl_3) δ 171.5 (CO), 144.3, 140.0, 129.7, 126.41, 126.40 and 125.4 (Ar), 41.8 (ArCH), 35.1 (CHCH_2), 26.5 (NCH_3), 25.8 (CH_2); GC-MS $m/z = 203$ (M^+); Anal. Calcd for $\text{C}_{13}\text{H}_{17}\text{NO}$: C, 76.81; H, 8.43. Found: C, 76.58; H, 8.18.

For **28h**: ^1H NMR (400 MHz, CDCl_3) δ 7.2-7.0 (m, 4H, Ar), 3.68 (m, 1H, $\text{N}(\text{CH}_2\text{CH}_3)_2$), 3.37 (m, 1H, $\text{N}(\text{CH}_2\text{CH}_3)_2$), 3.03 (m, 2H, $\text{N}(\text{CH}_2\text{CH}_3)_2$), 2.92 (m, 1H, ArCH), 2.0-1.4 (br, 8H, CH_2), 1.15 (t, $J = 6.8$ Hz, 3H, CH_2CH_3), 0.93 (t, $J = 6.8$ Hz, 3H, CH_2CH_3); $^{13}\text{C}\{^1\text{H}\}$ NMR (100 MHz, CDCl_3) δ 170.9 (CO), 142.6, 136.8, 128.7, 126.1, 125.5, and 125.1 (Ar), 42.7 ($\text{N}(\text{CH}_2\text{CH}_3)_2$), 42.2 (ArCH), 38.4 ($\text{N}(\text{CH}_2\text{CH}_3)_2$), 35.5 (CH_2), 34.4 (CH_2), 25.8 (CH_2), 25.6 (CH_2), 13.8 ($\text{N}(\text{CH}_2\text{CH}_3)_2$), 12.6 ($\text{N}(\text{CH}_2\text{CH}_3)_2$); GC-MS $m/z = 245$ (M^+); Anal. Calcd for $\text{C}_{16}\text{H}_{22}\text{NO}$: C, 78.32; H, 9.45. Found: C, 78.10; H, 9.23.

For **28i**: ^1H NMR (400 MHz, CDCl_3) δ 7.3-7.1 (Ar), 6.97 (m, 1H, Ar), 6.35 (br, 1H, NH), 4.38 (m, 2H, NHCH_2Ar), 3.17 (m, ArCH), 1.9-1.3 (br, 8H, CH_2); $^{13}\text{C}\{^1\text{H}\}$ NMR (100 MHz, CDCl_3) δ 170.5 (CO), 144.2, 138.3, 136.8, 129.8, 128.6, 127.7, 127.4, 126.5, 126.4 and 125.4 (Ar), 43.6 (CH_2Ar), 41.8 (ArCH), 35.1 (CH_2), 25.7 (CH_2); GC-MS $m/z = 279$ (M^+); Anal. Calcd for $\text{C}_{19}\text{H}_{21}\text{NO}$: C, 81.68; H, 7.58. Found: C, 81.72; H, 7.38.

For **28j**: ^1H NMR (400 MHz, CDCl_3) δ 7.66 (s, 1H, NH), 7.4-7.0 (m, 10H, Ar), 3.30 (m, 1H, ArCH), 1.98 (br, 2H, CH_2), 1.7-1.5 (br, 6H, CH_2); $^{13}\text{C}\{^1\text{H}\}$ NMR (100 MHz, CDCl_3) δ 168.8 (CO), 144.8, 138.2, 137.1, 130.4, 129.2, 126.9, 126.5, 125.7, 124.5 and 119.9 (Ar), 42.0 (ArCH), 35.3 (CH_2), 25.9 (CH_2); GC-MS $m/z = 265$ (M^+); Anal. Calcd for $\text{C}_{18}\text{H}_{19}\text{NO}_2$: C, 81.47; H, 7.22. Found: C, 81.61; H, 7.11.

For **28k**: ^1H NMR (400 MHz, CDCl_3) δ 7.4-6.8 (m, 9H, Ar), 7.35 (br, 1H, NH), 3.73 (s, 3H, OCH_3), 3.34 (m, 1H, ArCH), 2.05 (br, 2H, CH_2), 1.78-1.5 (br, 6H, CH_2); $^{13}\text{C}\{^1\text{H}\}$ NMR (100 MHz, CDCl_3) δ 168.7 (CO), 156.7, 144.9, 137.2, 131.3, 130.4, 127.0, 126.5, 125.8, 121.8 and 114.4 (Ar), 55.5 (OCH_3), 42.0 (ArCH), 35.4 (CH_2), 26.0 (CH_2); GC-MS $m/z = 295$ (M^+); Anal. Calcd for $\text{C}_{19}\text{H}_{21}\text{NO}_2$: C, 77.26; H, 7.17. Found: C, 77.05; H, 7.02.

For **28l**: ^1H NMR (400 MHz, CDCl_3) δ 7.87 (s, 1H, NH), 7.4-7.2 (m, 9H, Ar), 7.05 (m, 1H, Ar), 3.25 (m, 1H, ArCH), 1.94 (br, 2H, CH_2), 1.72-1.5 (br, 6H, CH_2); $^{13}\text{C}\{^1\text{H}\}$ NMR (100 MHz, CDCl_3) δ 169.1 (CO), 144.7, 136.8, 136.6, 130.4, 129.3, 129.0, 126.9, 126.4, 125.7 and 121.3 (Ar), 42.0 (ArCH), 35.2 (CH_2), 25.9 (CH_2); GC-MS $m/z = 299$ (M^+); Anal. Calcd for $\text{C}_{18}\text{H}_{18}\text{ClNO}$: C, 72.11; H, 6.05. Found: C, 71.84; H, 6.10.

For **28m**: ^1H NMR (400 MHz, CDCl_3) δ 7.3-7.0 (m, 4H, Ar), 3.11 (s, 3H, $\text{N}(\text{CH}_3)_2$), 2.79 (s, 3H, $\text{N}(\text{CH}_3)_2$), 2.47 (m, 1H, CH_2CHCH_2), 1.9-1.2 (br, 10H, CH_2); $^{13}\text{C}\{^1\text{H}\}$ NMR (100 MHz, CDCl_3) δ 171.7 (CO), 144.1, 136.1, 128.9, 126.7, 126.0 and 125.8 (Ar), 41.5 (CH_2CHCH_2), 39.0 ($\text{N}(\text{CH}_3)_2$), 34.8 (CH_2), 34.7 ($\text{N}(\text{CH}_3)_2$), 34.0 (CH_2), 27.1 (CH_2), 26.9 (CH_2), 26.2 (CH_2); GC-MS $m/z = 231$ (M^+); Anal. Calcd for $\text{C}_{15}\text{H}_{21}\text{NO}$: C, 77.88; H, 9.15. Found: C, 77.84; H, 9.01.

For **28n**: ^1H NMR (400 MHz, CDCl_3) δ 7.3-7.0 (m, 4H, Ar), 3.11 (s, 3H, $\text{N}(\text{CH}_3)_2$), 2.77 (s, 3H, $\text{N}(\text{CH}_3)_2$), 2.58 (m, 1H, CH_2CHCH_2), 1.9-1.4 (br, 12H, CH_2); $^{13}\text{C}\{^1\text{H}\}$ NMR (100

MHz, CDCl₃) δ 171.7 (CO), 146.0, 135.3, 129.1, 126.7, 125.7 and 125.6 (Ar), 43.3 (CH₂CHCH₂), 38.9 (N(CH₃)₂), 37.1 (CH₂), 36.0 (CH₂), 34.6 (N(CH₃)₂), 28.2 (CH₂), 27.7 (CH₂), 27.3 (CH₂); GC-MS m/z = 245 (M⁺); Anal. Calcd for C₁₆H₂₃NO: C, 78.32; H, 9.45. Found: C, 78.10; H, 9.23.

For **28o**: ¹H NMR (400 MHz, CDCl₃) δ 7.2-7.0 (m, 10H, Ar), 6.17 (br, 1H, NH), 4.45 (d, J = 6.0 Hz, 2H, NHCH₂Ar), 2.95 (m, 1H, ArCH), 1.73 (m, 2H, CH₂), 1.6-1.3 (m, 10H, CH₂); ¹³C{¹H} NMR (100 MHz, CDCl₃) δ 170.5 (CO), 147.6, 138.5, 135.5, 130.0, 128.8, 128.0, 127.6, 126.9, 126.4 and 125.4 (Ar), 43.8 (CH₂Ar), 42.3 (ArCH), 36.9 (CH₂), 27.8 (CH₂), 27.4 (CH₂); GC-MS m/z = 307 (M⁺); Anal. Calcd for C₁₈H₂₁NO: C, 82.04; H, 8.20. Found: C, 82.01; H, 7.99.

For **28p**: ¹H NMR (400 MHz, CDCl₃) δ 7.3-7.0 (m, 4H, Ar), 3.07 (s, 3H, N(CH₃)₂), 2.77 (s, 3H, N(CH₃)₂), 2.74 (m, 1H, ArCH), 1.8-1.5 (br, 14H, CH₂); ¹³C{¹H} NMR (100 MHz, CDCl₃) δ 171.7 (CO), 146.4, 135.3, 128.9, 126.9, 125.6 and 125.4 (Ar), 40.0 (ArCH), 38.8 (N(CH₃)₂), 35.3 (CH₂), 34.5 (N(CH₃)₂), 26.8 (CH₂), 26.7 (CH₂), 26.6 (CH₂), 26.5 (CH₂), 25.6 (CH₂); GC-MS m/z = 259 (M⁺); Anal. Calcd for C₁₇H₂₅NO: C, 78.72; H, 9.71. Found: C, 78.67; H, 9.67.

For **28q**: ¹H NMR (400 MHz, CDCl₃) δ 7.3-7.0 (m, 4H, Ar), 3.02 (s, 3H, N(CH₃)₂), 2.71 (s, 3H, N(CH₃)₂), 2.41 (br, 2H, CH₂CH(CH₃)₂), 1.81 (m, 1H, CH₂CH(CH₃)₂), 0.80 (d, J = 6.7 Hz, 6H, CH₃); ¹³C{¹H} NMR (100 MHz, CDCl₃) δ 171.4 (CO), 138.0, 136.6, 130.1, 128.5, 126.0, and 125.8 (Ar), 42.2 (CH₂CH(CH₃)₂), 38.7 (N(CH₃)₂), 34.5 (N(CH₃)₂), 29.3 (CH₂CH(CH₃)₂), 22.6 (CH₂CH(CH₃)₂); GC-MS m/z = 205 (M⁺); Anal. Calcd for C₁₃H₁₉NO: C, 76.06; H, 9.33. Found: C, 75.82; H, 9.34.

For **28r**: ^1H NMR (400 MHz, CDCl_3) δ 7.3-7.0 (m, 9H, Ar), 3.12 (br, 2H, $\text{CH}_2\text{CH}(\text{CH}_3)\text{Ph}$), 3.01 (br, 3H, $\text{N}(\text{CH}_3)_2$), 2.77 (t, $J = 6.5$ Hz, 1H, $\text{CH}_2\text{CH}(\text{CH}_3)\text{Ph}$), 2.65 (br, 3H, $\text{N}(\text{CH}_3)_2$), 1.21 (d, $J = 6.5$ Hz, 3H, $\text{CH}_2\text{CHCH}_3(\text{Ph})$); $^{13}\text{C}\{^1\text{H}\}$ NMR (100 MHz, CDCl_3) δ 171.0 (CO), 146.6, 137.2, 136.3, 130.2, 128.3, 128.1, 126.8, 126.0, 125.9 and 125.8 (Ar), 41.9 ($\text{CH}_2\text{CHCH}_3(\text{Ph})$), 40.8 ($\text{CH}_2\text{CHCH}_3(\text{Ph})$), 38.3 ($\text{N}(\text{CH}_3)_2$), 34.3 ($\text{N}(\text{CH}_3)_2$), 21.4 (CH_3); GC-MS $m/z = 267$ (M^+); Anal. Calcd for $\text{C}_{18}\text{H}_{21}\text{NO}$: C, 80.86; H, 7.92. Found: C, 80.57; H, 7.90.

For **28s**: ^1H NMR (400 MHz, CDCl_3) δ 7.2-7.0 (m, 4H, Ar), 3.04 (s, 3H, $\text{N}(\text{CH}_3)_2$), 2.73 (s, 3H, $\text{N}(\text{CH}_3)_2$), 2.47 (br, 2H, CH_2), 1.5-1.3 (br, 2H, CH_2), 0.82 (s, 9H, $\text{C}(\text{CH}_3)_3$); $^{13}\text{C}\{^1\text{H}\}$ NMR (100 MHz, CDCl_3) δ 171.4 (CO), 139.6, 136.4, 129.5, 128.8, 125.9, and 125.8 (Ar), 45.7 ($\text{CH}_2\text{CH}_2\text{C}(\text{CH}_3)_2$), 38.8 ($\text{N}(\text{CH}_3)_2$), 34.5 ($\text{N}(\text{CH}_3)_2$), 30.5 ($\text{CH}_2\text{CH}_2\text{C}(\text{CH}_3)_3$), 29.2 ($\text{CH}_2\text{CH}_2\text{C}(\text{CH}_3)_3$), 28.4 ($\text{CH}_2\text{CH}_2\text{C}(\text{CH}_3)_2$); GC-MS $m/z = 233$ (M^+); Anal. Calcd for $\text{C}_{15}\text{H}_{23}\text{NO}$: C, 77.21; H, 9.93. Found: C, 76.97; H, 10.08.

For **28t**: ^1H NMR (400 MHz, CDCl_3) δ 7.6-7.3 (m, 6H, Ar), 3.04 (s, 3H, $\text{N}(\text{CH}_3)_2$), 2.68 (s, 3H, $\text{N}(\text{CH}_3)_2$), 2.47 (br, 2H, $\text{CH}_2\text{CH}(\text{CH}_3)_2$), 1.86 (m, 1H, $\text{CH}_2\text{CH}(\text{CH}_3)_2$), 0.81 (d, $J = 6.6$ Hz, 6H, $\text{CH}_2\text{CH}(\text{CH}_3)_2$); $^{13}\text{C}\{^1\text{H}\}$ NMR (100 MHz, CDCl_3) δ 170.9 (CO), 135.4, 135.0, 132.9, 131.1, 128.4, 127.3, 127.0, 126.3, 125.5 and 125.2 (Ar), 42.3 ($\text{CH}_2\text{CH}(\text{CH}_3)_2$), 38.5 ($\text{N}(\text{CH}_3)_2$), 34.3 ($\text{N}(\text{CH}_3)_2$), 28.8 (CH_2), 22.4 (CH_3); GC-MS $m/z = 257$ (M^+); Anal. Calcd for $\text{C}_{17}\text{H}_{21}\text{NO}$: C, 79.96; H, 8.29. Found: C, 79.41; H, 8.11.

For **28u**: ^1H NMR (400 MHz, CDCl_3) δ 7.6-7.3 (m, 6H, Ar), 2.99 (s, 3H, $\text{N}(\text{CH}_3)_2$), 2.66 (s, 3H, $\text{N}(\text{CH}_3)_2$), 2.57 (br, 2H, CH_2), 1.5-1.3 (br, 2H, CH_2), 0.84 (s, 9H, $\text{C}(\text{CH}_3)_3$); $^{13}\text{C}\{^1\text{H}\}$ NMR (100 MHz, CDCl_3) δ 171.0 (CO), 137.2, 135.2, 133.4, 131.1, 127.7, 127.5, 127.1, 126.4, 125.6 and 125.2 (Ar), 45.6 ($\text{CH}_2\text{CH}_2\text{C}(\text{CH}_3)_3$), 38.7 ($\text{N}(\text{CH}_3)_2$), 34.4 ($\text{N}(\text{CH}_3)_2$), 29.1 ($\text{CH}_2\text{CH}_2\text{C}(\text{CH}_3)_3$), 28.3 ($\text{CH}_2\text{CH}_2\text{C}(\text{CH}_3)_3$), 28.4 ($\text{CH}_2\text{CH}_2\text{C}(\text{CH}_3)_3$);

GC-MS $m/z = 283$ (M^+); Anal. Calcd for $C_{19}H_{25}NO$: C, 80.52; H, 8.89. Found: C, 79.92; H, 8.63.

For **28v**: 1H NMR (400 MHz, $CDCl_3$) δ 7.6-7.4 (m, 6H, Ar), 3.09 (s, 3H, $N(CH_3)_2$), 3.05 (m, 1H, ArCH), 2.77 (s, 3H, $N(CH_3)_2$), 2.2-1.6 (br, 8H, CH_2); $^{13}C\{^1H\}$ NMR (100 MHz, $CDCl_3$) δ 171.8 (CO), 140.9, 135.7, 133.7, 131.5, 127.7, 127.6, 126.6, 125.9, 125.1 and 125.0 (Ar), 42.5 (ArCH), 39.3 ($N(CH_3)_2$), 34.9 (CH_2), 34.8 ($N(CH_3)_2$), 34.7 (CH_2), 25.7 (CH_3); GC-MS $m/z = 267$ (M^+); Anal. Calcd for $C_{18}H_{21}NO$: C, 80.86; H, 7.92. Found: C, 79.90; H, 7.90.

For **28w**: 1H NMR (400 MHz, $CDCl_3$) δ 7.4-7.0 (m, 10H, Ar), 6.22 (t, $J = 5.6$ Hz, 1H, NH), 4.52 (d, $J = 6.0$ Hz, 2H, $NHCH_2Ar$), 2.44 (d, $J = 7.8$ Hz, 2H, $CH_2CH(CH_3)_2$), 1.89 (m, 1H, $CH_2CH(CH_3)_2$), 0.84 (d, $J = 6.4$ Hz, 6H, $CH_2CH(CH_3)_2$); $^{13}C\{^1H\}$ NMR (100 MHz, $CDCl_3$) δ 169.9 (CO), 138.3, 138.0, 137.8, 128.7, 128.5, 128.1, 127.6 and 127.3 (Ar), 43.8 (CH_2Ar), 42.4 (CH_2CHCH_2), 29.7 (CH_2), 22.6 (CH_3); GC-MS $m/z = 267$ (M^+); Anal. Calcd for $C_{18}H_{21}NO$: C, 80.86; H, 7.92. Found: C, 80.72; H, 8.08.

For **28x**: 1H NMR (400 MHz, $CDCl_3$) δ 7.3-7.1 (m, 10H, Ar), 6.33 (t, $J = 4.9$ Hz, 1H, NH), 4.54 (d, $J = 5.9$ Hz, 2H, $NHCH_2Ar$), 2.71 (m, 2H, $CH_2CH_2C(CH_3)_3$), 1.42 (m, 2H, $CH_2CH_2C(CH_3)_3$), 0.94 (s, 9H, $CH_2CH_2C(CH_3)_3$); $^{13}C\{^1H\}$ NMR (100 MHz, $CDCl_3$) δ 170.1 (CO), 141.7, 138.4, 136.4, 130.2, 129.9, 128.8, 128.0, 127.6, 126.9 and 125.7 (Ar), 46.6 ($CH_2CH_2C(CH_3)_3$), 43.9 (CH_2Ar), 30.7 ($CH_2CH_2C(CH_3)_3$), 29.3 ($CH_2CH_2C(CH_3)_3$), 28.7 ($CH_2CH_2C(CH_3)_3$); GC-MS $m/z = 295$ (M^+); Anal. Calcd for $C_{20}H_{25}NO$: C, 81.31; H, 8.53. Found: C, 81.09; H, 8.26.

For **28y**: 1H NMR (400 MHz, $CDCl_3$) δ 7.3-7.0 (m, 4H, Ar), 3.78 (m, 1H, NCH_2CH_2), 3.56 (m, 1H, NCH_2CH_2), 3.05 (m, 2H, CH_2), 2.93 (m, 1H, CH_2CHCH_2), 2.0-1.7 (br, 4H,

CH₂), 1.64 (m, 6H, CH₂), 1.39 (m, 2H, CH₂); ¹³C{¹H} NMR (100 MHz, CDCl₃) δ 170.0 (CO), 142.9, 136.5, 128.8, 126.4, 125.7, and 125.3 (Ar), 48.2 (CH₂CHCH₂), 42.3 (N(CH₂)₂), 35.5 (CH₂), 34.9 (CH₂), 28.4 (CH₂), 25.9 (CH₂), 25.8 (CH₂), 25.7 (CH₂), 24.5 (CH₂); GC-MS *m/z* = 257 (M⁺); Anal. Calcd for C₁₇H₂₃NO: C, 79.33; H, 9.01. Found: C, 78.99; H, 9.01.

For **28z**: ¹H NMR (400 MHz, CDCl₃) δ 6.4-6.3 (m, 2H, Ar), 3.73 (m, 1H, CH₂CHCH₂), 3.58 (s, 3H, NCH₃), 2.36 (s, 3H, COCH₃), 1.9-1.6 (br, 8H, CH₂); ¹³C{¹H} NMR (100 MHz, CDCl₃) δ 194.4 (CO), 142.1, 121.4, 121.0 and 110.8 (Ar), 36.2 (NCH₃), 35.1 (COCH₃), 30.5 (CH₂), 28.9 (CH), 26.7 (CH₂); GC-MS *m/z* = 295 (M⁺); Anal. Calcd for C₁₂H₁₇NO: C, 75.35; H, 8.96. Found: C, 75.35; H, 8.87.

For Chapter 3

Representative Procedure of the Catalytic Reaction. In a glove box, complex **26** (10.0 mg, 17.4 μmol), carbonyl compound (0.58 mmol) and alkene (2.90 mmol) were dissolved in CH₂Cl₂ (2.0 mL) in a 25 mL Schlenk tube equipped with a Teflon stopcock and a magnetic stirring bar. The tube was brought out of the box, and was stirred for 2 h in an oil bath which was preset at 70 °C. Reaction tube was taken out of the oil bath, and was immediately cooled in a dry ice/acetone bath. After filtering through a small silica gel column (hexanes/EtOAc = 2:1), the solution was analyzed by GC. Analytically pure products were isolated after a simple column chromatography on silica gel (hexanes/EtOAc = from 20:1 to 4:1).

Synthesis of 56. In a glove box, tetrameric ruthenium complex, {[(PCy₃)(CO)RuH]₄(μ₄-O)(μ₃-OH)(μ₂-OH)} (**4**) (200 mg, 0.09 mmol) and (*E*)-*N,N*-dimethyl-3-(naphthalene-2-yl)-2-propenamide (80 mg, 3.5 mmol) were dissolved in dichloromethane (5 mL) in a 25 mL Schlenk tube equipped with a Teflon screw cap stopcock and a magnetic stirring bar.

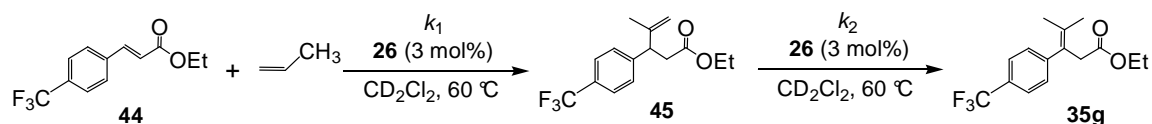
The tube was brought out of the box, and $\text{HBF}_4 \cdot \text{OEt}_2$ (48 μL , 0.36 mmol) was added and then cyclopentene (250 mg, 3.6 mmol) and water (66 mg, 3.6 mmol) were added under N_2 stream. The color of the solution was changed from dark red to orange. After stirring for 24 h at room temperature, the solvent was removed under vacuum, and the residue was crashed by adding hexanes (10 mL). Filtering the resulting solid through a fritted funnel and recrystallization from CH_2Cl_2 /hexanes yielded the product as a orange powder (260 mg, 82% yield). Single crystals of **56** suitable for X-ray crystallography were obtained from CH_2Cl_2 /pentane solution.

For **56**: ^1H NMR (CD_2Cl_2 , 400.0 MHz) δ 8.0-7.5 (m, 7H, Ar), 3.57 (d, $J = 18.3$ Hz, CH_2), 3.25 (dd, $J = 18.3, 4.7$ Hz, CH_2), 3.02 (s, 3H, $\text{N}(\text{CH}_3)_2$), 3.01 (s, 3H, $\text{N}(\text{CH}_3)_2$), 2.68 (m, CCHCH_2), 2.54 (s, CCH_2CO), 2.51 (s, H_2O), 2.37 (br m, 3H, PCy_3), 2.16 (dd, $J = 16.0, 8.0$ Hz, CH_2), 2.1-1.9 (m, 8H, PCy_3), 1.88 (dd, $J = 16.0, 8.0$ Hz, CHCH_2), 1.7-1.3 (m, 21H, PCy_3), 1.27 (br, CH_2); $^{13}\text{C}\{^1\text{H}\}$ NMR (CD_2Cl_2 , 100.5 MHz), δ 207.1 (d, $J_{\text{CP}} = 15.6$ Hz, Ru-CO), 185.4 (d, $J_{\text{CP}} = 7.8$ Hz, $\text{CON}(\text{CH}_3)_2$), 143.5 (d, $J_{\text{CP}} = 2.7$ Hz, $\text{ArC}(\text{CH}_2)\text{C}$), 133.9, 133.7, 128.8, 128.4, 128.0, 127.6, 127.5, 127.4, 126.9 and 126.5 (Ar) 115.6 (ArCCCH), 59.3 (ArCCCH), 41.2 and 41.1 (CH_2), 40.0 ($\text{N}(\text{CH}_3)_2$), 37.5 ($\text{N}(\text{CH}_3)_2$), 36.2 and 36.1 (CH), 35.1, 33.8, 29.7, 29.4, 28.9, 28.8, 28.3, 28.2, 26.8 and 22.1 (PCy_3); $^{31}\text{P}\{^1\text{H}\}$ NMR (CD_2Cl_2 , 161.8 MHz) δ 37.3 (s, PCy_3); IR (CD_2Cl_2) $\nu_{\text{CO}} = 1931, 1603 \text{ cm}^{-1}$; Anal. Calcd for $\text{C}_{40}\text{H}_{59}\text{BCl}_2\text{F}_4\text{NO}_3\text{PRu}$: C, 53.88; H, 6.67. Found: C, 53.58; H, 6.60.

Kinetic Profile Experiment. In a glove box, **26** (2 mg, 3.5 μmol) and (*E*)-*p*- $\text{CF}_3\text{-C}_6\text{H}_4\text{CH=CHCO}_2\text{Et}$ (28 mg, 0.12 mmol) were dissolved in CD_2Cl_2 (0.4 mL) in a thick wall J-Young NMR tube with a Teflon screw cap. The tube was cooled in a liquid nitrogen bath, and excess propene (0.6 mmol) was condensed via a vacuum line transfer. The tube was gradually warmed to room temperature. The sample was inserted into the NMR probe which was preset at 60 $^\circ\text{C}$. The appearance and disappearance of the proton

signals for **44** (δ 6.55, CH), **45** (δ 2.88, CH₂), and **35g** (δ 3.37 CH₂) were monitored by ¹H NMR at 60 °C in 5 min intervals. The rate of the product formation was determined by measuring the integration of the product peaks against the disappearance of **44**. By using a nonlinear regression technique (Sigmaplot Version 10), the experimental data were globally fitted to the kinetic equation. The rate constants $k_1 = 0.042 \text{ min}^{-1}$ and $k_2 = 0.011 \text{ min}^{-1}$ were obtained from this analysis

Derivation of the Kinetic Equation of the Conversion of **44** to **35g**



The derivation for two consecutive first-order reaction was followed the method described in: Moore, J. W.; Pearson, R. G. Kinetics and Mechanism, 3rd Ed.; Wiley: New York, 1981, pp290-296.

$$d[\mathbf{44}]/dt = -k_1[\mathbf{44}]$$

$$d[\mathbf{45}]/dt = k_1[\mathbf{44}] - k_2[\mathbf{45}]$$

$$d[\mathbf{35g}]/dt = k_2[\mathbf{45}]$$

$$[\mathbf{44}] = [\mathbf{44}]_0 e^{-k_1 t}$$

$$d[\mathbf{45}]/dt = k_1[\mathbf{44}]_0 e^{-k_1 t} - k_2[\mathbf{45}]$$

$$[\mathbf{45}] = [\mathbf{44}]_0 k_1 (e^{-k_1 t} - e^{-k_2 t}) / (k_2 - k_1) - [\mathbf{45}]_0 e^{-k_2 t}$$

$$d[\mathbf{44}]/dt + d[\mathbf{45}]/dt + d[\mathbf{35g}]/dt = 0$$

Since

$$[\mathbf{44}] + [\mathbf{45}] + [\mathbf{35g}] = [\mathbf{44}]_0$$

$$[\mathbf{35g}] = [\mathbf{44}]_0 - [\mathbf{44}] - [\mathbf{45}]$$

$$= [\mathbf{44}]_0(1 + (k_1e^{-k_2t} - k_2e^{-k_1t})/(k_2 - k_1)) + [\mathbf{45}]_0(1 - e^{-k_2t}) + [\mathbf{35g}]_0$$

$$d[\mathbf{35g}]/dt = [\mathbf{44}]_0k_1k_2(e^{-k_2t} - e^{-k_1t})/(k_1 - k_2) - [\mathbf{45}]_0k_2e^{-k_2t}$$

The experimental data was globally fitted to the kinetic equation by using non-linear regression techniques (Sigmaplot V. 10). The rate constants $k_1 = 0.042 \text{ min}^{-1}$ and $k_2 = 0.011 \text{ min}^{-1}$ were obtained and from this analysis.

$$d[\mathbf{35g}]/dt = [\mathbf{44}]_0 \times 0.042 \times 0.011 \times (e^{-0.011t} - e^{-0.042t})/(0.042 - 0.011) - [\mathbf{45}]_0 \times 0.011 \times e^{-0.011t}$$

$$= [\mathbf{44}]_0 \times 0.015 \times (e^{-0.011t} - e^{-0.042t}) - [\mathbf{45}]_0 \times 0.011 \times e^{-0.011t}$$

Hammett Study: Reaction in CD_2Cl_2 . In a glove box, *para*-substituted *p*-X- $\text{C}_6\text{H}_4\text{CH}=\text{CHCO}_2\text{Et}$ (X = OCH_3 , CH_3 , H, F, Cl, CO_2Me , CF_3) (0.12 mmol) and complex **26** (2 mg, 3.5 μmol) were dissolved in CD_2Cl_2 (0.4 mL) in a thick wall J-Young NMR tube with a Teflon screw cap. The tube was cooled in a liquid nitrogen bath, and excess propene (0.6 mmol) was condensed via a vacuum line transfer. The tube was gradually warmed to room temperature. The sample was inserted into the NMR probe which was preset at 20 °C. The rate was measured by monitoring the ^1H NMR in 5 min intervals. The k_{obs} was estimated from a first-order plot of $-\ln([\text{(E)-C}_6\text{H}_5\text{CH}=\text{CHCO}_2\text{Et}]_t/[\text{(E)-C}_6\text{H}_5\text{CH}=\text{CHCO}_2\text{Et}]_0)$ vs time by measuring the ^1H integration of starting material (δ 1.24, OCH_2CH_3) and product (δ 1.12, OCH_2CH_3) signals, which was normalized against and internal standard (solvent resonance).

Reaction in CH_2Cl_2 . In a glove box, complex **26** (20 mg, 35 μmol), (*E*)- $\text{C}_6\text{H}_5\text{CH}=\text{C}(\text{CH}_3)\text{CONHCH}_3$ (122 mg, 0.7 mmol) or (*E*)- $\text{C}_6\text{H}_5\text{CH}=\text{CHCO}_2\text{Et}$ (0.7 mmol) and *para*-substituted *p*-Y- $\text{C}_6\text{H}_4\text{CH}=\text{CH}_2$ (X = OCH_3 , CH_3 , H, F, Cl, CF_3) (3.5 mmol) were dissolved in CH_2Cl_2 (8.0 mL) in a 25 mL Schlenk tube equipped with a Teflon

screw cap stopcock and a magnetic stirring bar. After the solution was stirred at room temperature for 10 min, an equal amount of the solution (1.0 mL) was divided and placed in 5 different Schlenk tubes. The tubes were brought out of the box, and were stirred for 150 min in an oil bath set at 50 °C. Each reaction tube was taken out from the oil bath in 30 min intervals, and was immediately cooled in a dry ice/acetone bath. After filtering through a small silica gel column (hexanes/EtOAc = 2:1), the solution was analyzed by GC with internal standard. The k_{obs} was determined from a first-order plot of $-\ln([\text{starting material}]_t/[\text{starting material}]_0)$ vs time.

Deuterium Isotope Effect Study: Reaction in CD_2Cl_2 . In a glove box, complex **26** (2 mg, 3.5 μmol) and (*E*)- $\text{C}_6\text{H}_5\text{CH}=\text{CHCO}_2\text{Et}$ (20 mg, 0.12 mmol) were dissolved in CD_2Cl_2 (0.4 mL) in a thick wall J-Young NMR tube with a Teflon screw cap. The tube was cooled in a liquid nitrogen bath, and excess ethylene and ethylene- d_4 (0.6 mmol) was condensed via a vacuum line transfer. The tube was gradually warmed to room temperature. The sample was inserted into the NMR probe which was preset at 60 °C. The rate was measured by monitoring the ^1H integration of starting material (δ 1.22 OCH_2CH_3) and product (δ 1.16, OCH_2CH_3) signals in 5 min intervals, and these were normalized against an internal standard (solvent resonance). The k_{obs} was estimated from a first-order plot of $-\ln([\text{E}]\text{-C}_6\text{H}_5\text{CH}=\text{CHCO}_2\text{Et}]_t/[\text{E}]\text{-C}_6\text{H}_5\text{CH}=\text{CHCO}_2\text{Et}]_0)$ vs time.

Reaction in CH_2Cl_2 . In a glove box, complex **26** (20 mg, 35 μmol), (*E*)- $\text{C}_6\text{H}_5\text{CH}=\text{C}(\text{CH}_3)\text{CONHCH}_3$ (122 mg, 0.7 mmol) or $\text{C}_6\text{H}_5\text{CD}=\text{C}(\text{CH}_3)\text{CONHCH}_3$ (122 mg, 0.7 mmol) and styrene or styrene- d_{10} (0.36 g, 35 mmol) were dissolved in CH_2Cl_2 (8.0 mL) in a 25 mL Schlenk tube equipped with a Teflon screw cap stopcock and a

magnetic stirring bar. After the solution was stirred at room temperature for 10 min, an equal amount of the solution (1.0 mL) was divided and placed in 5 different Schlenk tubes. The tubes were brought out of the box, and were stirred for 150 min in an oil bath set at 50 °C. Each reaction tube was taken out from the oil bath in 30 min intervals, and was immediately cooled in a dry ice/acetone bath. After filtering through a small silica gel column (hexanes/EtOAc = 2:1), the solution was analyzed by GC with internal standard. The k_{obs} was determined from a first-order plot of $-\ln([\text{cinnamide}]_t/[\text{cinnamide}]_0)$ vs time.

Carbon Isotope Effect Study. In a glove box, complex **26** (164 mg, 0.28 mmol), carbonyl compound (5.7 mmol) and alkene (5~10 equiv) were dissolved in CH₂Cl₂ (10 mL) in two or three separate 100 mL Schlenk tubes equipped with a Teflon screw cap stopcock and a magnetic stirring bar. The tubes were brought out of the box, and stirred for 14 h, respectively, in an oil bath which was preset at 50 °C. Unreacted carbonyl compound was collected separately after filtering through a small silica gel column (hexanes/EtOAc = 2:1), and the solution was analyzed by GC (60-82% conversion).

The ¹³C{¹H} NMR analysis of the recovered and virgin samples of carbonyl compound was performed by following Singleton's NMR method (ref. 11 in the main text). The NMR sample of virgin and recovered carbonyl compound was prepared identically by dissolving carbonyl compound (100 mg) in CDCl₃ (0.5 mL) in a 5 mm high precision NMR tube. The ¹³C{¹H} NMR spectra were recorded with H-decoupling and 45 degree pulses. A 60 s delay between pulses was imposed to minimize T_1 variations (d1 = 60 s, at = 5.0 s, np = 245098, nt = 704).

Deuterium Labeling Study: In a glove box, complex **26** (10.0 mg, 17.4 μmol) and (*E*)- $\text{C}_6\text{D}_5\text{CD}=\text{CDCON}(\text{CH}_3)_2$ (106 mg, 0.58 mmol) were dissolved in CH_2Cl_2 (2.0 mL) in a 25 mL Schlenk tube equipped with a Teflon screw cap stopcock and a magnetic stirring bar. The tube was brought out of the box, and was stirred for 2 h in an oil bath set at 70 $^\circ\text{C}$. The tube was immediately cooled and was open to air. After filtering through a small silica column (hexanes/EtOAc = 2:1), the conversion was determined by GC. Unreacted propylene- d_n was collected separately via vacuum transfer. The product was separated by column chromatography on silica gel (hexanes/EtOAc), and each was analyzed by both ^1H and ^2H NMR.

In a glove box, complex **26** (4 mg, 6.0 μmol), (*E*)- $\text{C}_6\text{H}_5\text{CD}=\text{C}(\text{CH}_3)\text{CONHMe}$ (20 mg, 0.12 mmol) and styrene (63 mg, 0.60 mmol) were dissolved in CD_2Cl_2 and CH_2Cl_2 (0.4 mL) in a thick wall J-Young NMR tube with a Teflon screw cap. The thick wall J-Young NMR tubes were brought out of the box. The reaction mixture was monitored by both ^1H and ^2H NMR in 5 h intervals for 15 h, and these were normalized against an internal standard (solvent resonance). The deuterium incorporation of each substrate was estimated by both ^1H and ^2H NMR spectrum.

General Procedure for Empirical Rate Law Derivation. In a glove box, complex **26** (2 mg, 3.5 μmol) and (*E*)- $\text{C}_6\text{H}_5\text{CH}=\text{CHCO}_2\text{Et}$ (20 mg, 0.12 mmol) were dissolved in CD_2Cl_2 (0.4 mL) in a thick wall J-Young NMR tube with a Teflon screw cap. The tube was cooled in a liquid nitrogen bath, and excess propylene (0.6 mmol) was condensed via a vacuum line transfer. The tube was gradually warmed to room temperature. The sample

was inserted into the NMR probe which was preset at 20-40 °C. The rate was measured by monitoring the ^1H integration of starting material (δ 1.24, OCH_2CH_3) and product (δ 1.16 OCH_2CH_3) signals in 5 min intervals, and these were normalized against an internal standard (solvent resonance). The k_{obs} was estimated from a first-order plot of $-\ln([\text{(E)-C}_6\text{H}_5\text{CH=CHCO}_2\text{Et}]_t/[\text{(E)-C}_6\text{H}_5\text{CH=CHCO}_2\text{Et}]_0)$ vs time.

Characterization Data of Organic Products

For **35a**: ^1H NMR (400 MHz, CDCl_3) δ 7.1-7.0 (m, 2H, Ar), 6.9-6.8 (m, 2H, Ar), 4.07 (q, $J = 7.2$ Hz, OCH_2CH_3), 3.98 (q, $J = 7.0$ Hz, $\text{ArOCH}_2\text{CH}_3$), 3.34 (s, CH_2), 1.82 (s, 3H, $=\text{C}(\text{CH}_3)_2$), 1.62 (s, 3H, $=\text{C}(\text{CH}_3)_2$), 1.38 (t, $J = 7.0$ Hz, $\text{ArOCH}_2\text{CH}_3$), 1.16 (t, $J = 7.2$ Hz, OCH_2CH_3); $^{13}\text{C}\{^1\text{H}\}$ NMR (100 MHz, CDCl_3) δ 169.9 (CO), 155.4 (Ar), 133.4 ($=\text{C}(\text{CH}_3)_2$), 130.0 and 127.9 (Ar), 125.4 ($\text{C}=\text{C}(\text{CH}_3)_2$), 111.9 (Ar), 61.9 ($\text{ArOCH}_2\text{CH}_3$), 58.4 (OCH_2CH_3), 38.3 (CH_2), 20.3 and 18.7 ($=\text{C}(\text{CH}_3)_2$), 12.9 ($\text{ArOCH}_2\text{CH}_3$), 12.2 (OCH_2CH_3); GC-MS $m/z = 262$ (M^+); Anal. Calcd for $\text{C}_{16}\text{H}_{22}\text{O}_3$: C, 73.25; H, 8.45. Found: C, 73.40; H, 8.33.

For **35b**: ^1H NMR (400 MHz, CDCl_3) δ 7.1-7.0 (m, 4H, Ar), 4.07 (q, $J = 7.3$ Hz, OCH_2CH_3), 3.37 (s, CH_2), 2.33 (s, ArCH_3), 1.85 (s, 3H, $=\text{C}(\text{CH}_3)_2$), 1.65 (s, 3H, $=\text{C}(\text{CH}_3)_2$), 1.18 (t, $J = 7.2$ Hz, OCH_2CH_3); $^{13}\text{C}\{^1\text{H}\}$ NMR (100 MHz, CDCl_3) δ 171.8 (CO), 140.2 ($=\text{C}(\text{CH}_3)_2$), 135.7, 132.1 and 128.7 (Ar), 127.5 ($\text{C}=\text{C}(\text{CH}_3)_2$), 60.4 (OCH_2CH_3), 40.3 (CH_2), 22.3 (ArCH_3), 21.1 and 20.7 ($=\text{C}(\text{CH}_3)_2$), 14.2 (OCH_2CH_3); GC-MS $m/z = 232$ (M^+); The ^1H and ^{13}C NMR spectral data are in good agreement with the literature data.¹⁰⁹

For **35c**: ^1H NMR (400 MHz, CDCl_3) δ 7.3-7.1 (m, 4H, Ar), 4.07 (q, $J = 7.1$ Hz, 2H, OCH_2CH_3), 3.39 (s, 2H, CH_2), 1.85 (s, 3H, $=\text{C}(\text{CH}_3)_2$), 1.64 (s, 3H, $=\text{C}(\text{CH}_3)_2$), 1.16 (t, $J = 7.1$ Hz, 3H, OCH_2CH_3); $^{13}\text{C}\{^1\text{H}\}$ NMR (100 MHz, CDCl_3) δ 171.2 (CO), 143.2 ($=\text{C}(\text{CH}_3)_2$), 132.1, 128.8 and 127.9 (Ar), 127.8 ($\text{C}=\text{C}(\text{CH}_3)_2$), 126.2 (Ar), 60.3 (OCH_2CH_3), 40.1 (CH_2), 22.2 and 20.6 ($=\text{C}(\text{CH}_3)_2$), 14.1 (OCH_2CH_3); GC-MS $m/z = 218$ (M^+); The ^1H and ^{13}C NMR spectral data are in good agreement with the literature data.¹⁰⁹

For **35d**: ^1H NMR (400 MHz, CDCl_3) δ 7.3-7.0 (m, 4H, Ar), 4.06 (q, $J = 7.2$ Hz, 2H, OCH_2CH_3), 3.33 (s, 2H, CH_2), 1.81 (s, 3H, $=\text{C}(\text{CH}_3)_2$), 1.58 (s, 3H, $=\text{C}(\text{CH}_3)_2$), 1.14 (t, $J = 7.2$ Hz, 3H, OCH_2CH_3); $^{13}\text{C}\{^1\text{H}\}$ NMR (100 MHz, CDCl_3) δ 162.5 (CO), 160.1 (Ar), 139.0 ($=\text{C}(\text{CH}_3)_2$), 132.8 and 130.4 (Ar), 126.8 ($\text{C}=\text{C}(\text{CH}_3)_2$), 114.9 (Ar), 60.4 (OCH_2CH_3), 40.1 (CH_2), 22.1 and 20.6 ($=\text{C}(\text{CH}_3)_2$), 14.1 (OCH_2CH_3); GC-MS $m/z = 252$ (M^+); Anal. Calcd for $\text{C}_{14}\text{H}_{17}\text{FO}_2$: C, 71.16; H, 7.25. Found: C, 70.99; H, 7.21.

For **35e**: ^1H NMR (400 MHz, CDCl_3) δ 7.3-7.0 (m, 4H, Ar), 4.06 (q, $J = 7.2$ Hz, 2H, OCH_2CH_3), 3.34 (s, 2H, CH_2), 1.83 (s, 3H, $=\text{C}(\text{CH}_3)_2$), 1.61 (s, 3H, $=\text{C}(\text{CH}_3)_2$), 1.18 (t, $J = 7.0$ Hz, 3H, OCH_2CH_3); $^{13}\text{C}\{^1\text{H}\}$ NMR (100 MHz, CDCl_3) δ 171.6 (CO), 141.7 ($=\text{C}(\text{CH}_3)_2$), 133.2, 132.1, 130.4 and 128.3 (Ar), 126.8 ($\text{C}=\text{C}(\text{CH}_3)_2$), 60.6 (OCH_2CH_3), 40.1 (CH_2), 22.3 and 20.8 ($=\text{C}(\text{CH}_3)_2$), 14.2 (OCH_2CH_3); GC-MS $m/z = 236$ (M^+); The ^1H and ^{13}C NMR spectral data are in good agreement with the literature data.¹⁰⁹

For **35f**: ^1H NMR (400 MHz, CDCl_3) δ 7.9-7.2 (m, 4H, Ar), 3.98 (q, $J = 7.2$ Hz, 2H, OCH_2CH_3), 3.30 (s, 2H, CH_2), 1.77 (s, 3H, $=\text{C}(\text{CH}_3)_2$), 1.54 (s, 3H, $=\text{C}(\text{CH}_3)_2$), 1.10 (t, $J = 7.2$ Hz, 3H, OCH_2CH_3); $^{13}\text{C}\{^1\text{H}\}$ NMR (100 MHz, CDCl_3) δ 171.2 and 166.8 (CO), 148.1 ($=\text{C}(\text{CH}_3)_2$), 133.4, 129.3, 128.9 and 128.0 (Ar), 127.0 ($\text{C}=\text{C}(\text{CH}_3)_2$), 60.4 (OCH_2CH_3), 51.8 (OCH_3), 39.7 (CH_2), 22.1 and 20.7 ($=\text{C}(\text{CH}_3)_2$), 14.0 (OCH_2CH_3); GC-

MS $m/z = 276$ (M^+); Anal. Calcd for $C_{16}H_{20}O_4$: C, 69.54; H, 7.30. Found: C, 70.01; H, 7.44.

For **35g**: 1H NMR (400 MHz, $CDCl_3$) δ 7.6-7.5 (m, 2H, Ar), 7.3-7.2 (m, 2H, Ar), 4.07 (q, $J = 7.2$ Hz, 2H, OCH_2CH_3), 3.37 (s, 2H, CH_2), 1.86 (s, 3H, $=C(CH_3)_2$), 1.62 (s, 3H, $=C(CH_3)_2$), 1.17 (t, $J = 7.0$ Hz, 3H, OCH_2CH_3); $^{13}C\{^1H\}$ NMR (100 MHz, $CDCl_3$) δ 171.6 (CO), 147.2 (q, $J = 1.2$ Hz, CCF_3), 134.0 ($=C(CH_3)_2$), 129.5 (Ar), 126.9 ($C=C(CH_3)_2$), 125.2 (q, $J = 3.7$ Hz, CCF_3), 60.7 (OCH_2CH_3), 40.1 (CH_2), 22.4 and 20.9 ($=C(CH_3)_2$), 14.3 (OCH_2CH_3); GC-MS $m/z = 286$ (M^+); Anal. Calcd for $C_{15}H_{17}F_3O_2$: C, 62.93; H, 5.99. Found: C, 63.23; H, 5.99.

For **35h**: 1H NMR (400 MHz, $CDCl_3$) δ 7.3-7.2 (m, 5H, Ar), 3.58 (s, 3H, OCH_3), 3.41 (s, 2H, CH_2), 1.85 (s, 3H, $=C(CH_3)_2$), 1.64 (s, 3H, $=C(CH_3)_2$); $^{13}C\{^1H\}$ NMR (100 MHz, $CDCl_3$) δ 171.9 (CO), 143.1 ($=C(CH_3)_2$), 132.2, 128.7 and 127.9 (Ar), 127.6 ($C=C(CH_3)_2$), 126.2 (Ar), 51.4 (OCH_3), 39.8 (CH_2), 22.1 and 20.5 ($=C(CH_3)_2$); GC-MS $m/z = 204$ (M^+); The 1H and ^{13}C NMR spectral data are in good agreement with the literature data.¹¹⁰

For **35i**: 1H NMR (400 MHz, $CDCl_3$) δ 7.4-7.1 (m, 10H, Ar), 5.11 (s, 2H, $ArCH_2$), 3.51 (s, CH_2), 1.91 (s, 3H, $=C(CH_3)_2$), 1.69 (s, 3H, $=C(CH_3)_2$); $^{13}C\{^1H\}$ NMR (100 MHz, $CDCl_3$) δ 171.7 (CO), 143.2 ($=C(CH_3)_2$), 136.1, 132.7, 129.0, 128.6 and 128.2 (Ar), 127.7 ($C=C(CH_3)_2$), 126.4 (Ar), 66.4 ($ArCH_2$), 40.3 (CH_2), 22.4 and 20.9 ($=C(CH_3)_2$); GC-MS $m/z = 280$ (M^+); Anal. Calcd for $C_{19}H_{20}O_2$: C, 81.40; H, 7.19. Found: C, 81.62; H, 7.26.

For **35j**: 1H NMR (400 MHz, $CDCl_3$) δ 7.3-7.1 (m, 5H, Ar), 3.46 (s, 2H, CH_2), 2.02 (s, 3H, $C(O)CH_3$), 1.78 (s, 3H, $=C(CH_3)_2$), 1.64 (s, 3H, $=C(CH_3)_2$); $^{13}C\{^1H\}$ NMR (100 MHz, $CDCl_3$) δ 206.4 (CO), 143.2 ($=C(CH_3)_2$), 132.4 ($C=C(CH_3)_2$), 128.7, 128.1 and

126.3 (Ar), 50.0 (CH₂), 29.5 (C(O)CH₃), 22.2 and 20.8 (=C(CH₃)₂); GC-MS m/z = 188 (M⁺); The ¹H and ¹³C NMR spectral data are in good agreement with the literature data.¹¹¹

For **35k**: ¹H NMR (400 MHz, CDCl₃) δ 7.9 (m, 2H, Ar), 7.5-7.2 (m, 8H, Ar), 4.12 (s, 2H, CH₂), 1.87 (s, 3H, =C(CH₃)₂), 1.74 (s, 3H, =C(CH₃)₂); ¹³C{¹H} NMR (100 MHz, CDCl₃) δ 197.3 (CO), 143.7 (=C(CH₃)₂), 137.1 and 132.9 (Ar), 132.4 (C=C(CH₃)₂), 128.6, 128.6, 128.4 and 126.2 (Ar), 44.8 (CH₂), 22.3 and 20.9 (=C(CH₃)₂); GC-MS m/z = 250 (M⁺); Anal. Calcd for C₁₈H₁₈O: C, 86.36; H, 7.25. Found: C, 86.22; H, 7.27.

For **35l**: ¹H NMR (400 MHz, CDCl₃) δ 7.1-7.0 (m, 4H, Ar), 3.48 (s, 2H, CH₂), 2.32 (s, ArCH₃), 2.05 (s, 3H, C(O)CH₃), 1.81 (s, 3H, =C(CH₃)₂), 1.67 (s, 3H, =C(CH₃)₂); ¹³C{¹H} NMR (100 MHz, CDCl₃) δ 206.9 (CO), 140.3 (=C(CH₃)₂), 135.8, 132.3, 128.9 and 128.7 (Ar), 127.9 (C=C(CH₃)₂), 50.3 (CH₂), 29.6 (C(O)CH₃), 22.3 (=C(CH₃)₂), 21.2 (ArCH₃), 20.9 (=C(CH₃)₂); GC-MS m/z = 202 (M⁺); Anal. Calcd for C₁₄H₁₈O: C, 83.12; H, 8.97. Found: C, 83.11; H, 8.93.

For (**Z**)-**35m**: ¹H NMR (400 MHz, CDCl₃) δ 7.4-7.2 (m, 4H, Ar), 6.01 (q, J = 7.0 Hz, 1H, =CHCH₃), 4.09 (q, J = 7.1 Hz, 2H, OCH₂CH₃), 3.46 (s, CH₂), 1.82 (d, J = 6.9 Hz, =CHCH₃), 1.17 (t, J = 7.1 Hz, 3H, OCH₂CH₃): NOESY δ 3.46 ↔ 1.82 (↔ denotes NOE correlation); ¹³C{¹H} NMR (100 MHz, CDCl₃) δ 171.1 (CO), 140.9 (=C(CH₃)₂), 132.5 (Ar), 130.0 (=CHCH₃), 129.1, 128.3 and 127.1 (Ar), 60.7 (OCH₂CH₃), 35.6 (CH₂), 14.6 (OCH₂CH₃), 14.1 (=CHCH₃); GC-MS m/z = 238 (M⁺); Anal. Calcd for C₁₃H₁₅ClO₂: C, 65.41; H, 6.33. Found: C, 65.66; H, 6.57.

For (**E**)-**35m**: ¹H NMR (400 MHz, CDCl₃) δ 7.4-7.2 (m, 4H, Ar), 5.72 (q, J = 6.9 Hz, 1H, =CHCH₃), 4.03 (q, J = 7.1 Hz, 2H, OCH₂CH₃), 3.30 (s, 2H, CH₂), 1.60 (d, J = 6.9 Hz,

3H, =CHCH₃), 1.15 (t, $J = 7.1$ Hz, OCH₂CH₃); ¹³C{¹H} NMR (100 MHz, CDCl₃) δ 171.4 (CO), 143.1 (=C(CH₃)₂), 132.5 and 133.3 (Ar), 132.5 (=CHCH₃), 128.2 and 127.2 (Ar), 60.6 (OCH₂CH₃), 44.3 (CH₂), 14.9 (OCH₂CH₃), 14.1 (=CHCH₃); GC-MS $m/z = 238$ (M⁺); Anal. Calcd for C₁₃H₁₅ClO₂: C, 65.41; H, 6.33. Found: C, 65.66; H, 6.57.

For **35n**: ¹H NMR (400 MHz, CDCl₃) δ 7.2-7.0 (m, 4H, Ar), 4.03 (q, $J = 7.2$ Hz, 2H, OCH₂CH₃), 3.29 (s, CH₂), 1.88 (q, $J = 7.6$ Hz, 2H, =C(CH₃)CH₂CH₃), 1.78 (s, 3H, =C(CH₃)CH₂CH₃), 1.14 (t, $J = 7.2$ Hz, OCH₂CH₃), 0.89 (t, $J = 7.6$ Hz, 3H, =C(CH₃)CH₂CH₃); ¹³C{¹H} NMR (100 MHz, CDCl₃) δ 171.6 (CO), 141.6 (=C(CH₃)CH₂CH₃), 138.6, 130.1, 128.3 and 128.2 (Ar), 126.6 (C=C(CH₃)CH₂CH₃), 60.4 (OCH₂CH₃), 40.2 (CH₂), 28.4 (=C(CH₃)CH₂CH₃), 17.6 (=C(CH₃)CH₂CH₃), 14.2 (OCH₂CH₃), 13.0 (=C(CH₃)CH₂CH₃); GC-MS $m/z = 266$ (M⁺); Anal. Calcd for C₁₅H₁₉ClO₂: C, 67.54; H, 7.18. Found: C, 67.72; H, 6.78.

For **35o**: ¹H NMR (400 MHz, CDCl₃) δ 7.3-7.0 (m, 4H, Ar), 4.04 (q, $J = 7.2$ Hz, 2H, OCH₂CH₃), 3.30 (s, 2H, CH₂), 1.87 (m, 2H, =C(CH₃)CH₂CH₂CH₃), 1.70 (s, 3H, =C(CH₃)CH₂CH₂CH₃), 1.29 (m, 2H, =C(CH₃)CH₂CH₂CH₃), 1.07 (t, $J = 7.2$ Hz, 3H, OCH₂CH₃), 0.65 (t, $J = 7.2$ Hz, 3H, =C(CH₃)CH₂CH₂CH₃); ¹³C{¹H} NMR (100 MHz, CDCl₃) δ 171.4 (CO), 141.8 (=C(CH₃)CH₂CH₂CH₃), 137.1, 132.1, 130.3 and 128.3 (Ar), 127.3 (C=C(CH₃)CH₂CH₂CH₃), 60.5 (OCH₂CH₃), 40.4 (=C(CH₃)CH₂CH₂CH₃), 37.3 (CH₂), 21.4 (=C(CH₃)CH₂CH₂CH₃), 17.9 (=C(CH₃)CH₂CH₂CH₃), 14.2 (OCH₂CH₃), 13.8 (=C(CH₃)CH₂CH₂CH₃); GC-MS $m/z = 280$ (M⁺); Anal. Calcd for C₁₆H₂₁ClO₂: C, 68.44; H, 7.54. Found: C, 68.27; H, 7.38.

For **35p**: ¹H NMR (400 MHz, CDCl₃) δ 7.3-7.0 (m, 4H, Ar), 4.00 (q, $J = 7.2$ Hz, OCH₂CH₃), 3.34 (s, CH₂), 2.15 (m, 2H, =C(CH₃)CH₂CH₂CH₃), 1.47 (s, 3H, =C(CH₃)CH₂CH₂CH₃), 1.41 (m, , =C(CH₃)CH₂CH₂CH₃), 1.05 (t, $J = 7.2$ Hz, 3H,

OCH₂CH₃), 0.94 (t, $J = 7.2$ Hz, 3H, CCH₂CH₂CH₃); ¹³C{¹H} NMR (100 MHz, CDCl₃) δ 171.6 (CO), 141.7 (=C(CH₃)CH₂CH₂CH₃), 137.0, 132.0, 130.4 and 128.3 (Ar), 127.5 (C=C(CH₃)CH₂CH₂CH₃), 60.5 (OCH₂CH₃), 39.7 (=C(CH₃)CH₂CH₂CH₃), 36.5 (CH₂), 21.3 (=C(CH₃)CH₂CH₂CH₃), 19.9 (=C(CH₃)CH₂CH₂CH₃), 14.2 (OCH₂CH₃), 14.1 (=C(CH₃)CH₂CH₂CH₃); GC-MS $m/z = 280$ (M⁺); Anal. Calcd for C₁₆H₂₁ClO₂: C, 68.44; H, 7.54. Found: C, 68.27; H, 7.38.

For **35q**: ¹H NMR (400 MHz, CDCl₃) δ 7.2-7.0 (m, 5H, Ar), 3.92 (q, $J = 7.1$ Hz, 2H, OCH₂CH₃), 2.83 (td, $J = 10.2, 4.6$ Hz, 1H, ArCH), 2.73 (dd, $J = 15.0, 4.6$ Hz, 1H ArCHCH₂), 2.50 (dd $J = 15.0, 10.5$ Hz, 1H, ArCHCH₂), 1.97 (m, 1H, ArCHCH), 1.90-1.14 (br, 8H, CH₂), 1.04 (t, $J = 7.1$ Hz, 3H, OCH₂CH₃); ¹³C{¹H} NMR (100 MHz, CDCl₃) δ 172.2 (CO), 142.7, 131.9, 129.2 and 128.3 (Ar), 60.2 (OCH₂CH₃), 47.7 and 46.2 (CH), 40.7, 31.5, 31.3, 25.3 and 24.9 (CH₂), 14.1 (OCH₂CH₃); GC-MS $m/z = 280$ (M⁺); Anal. Calcd for C₁₆H₂₁ClO₂: C, 68.44; H, 7.54. Found: C, 68.50; H, 7.62.

For **35r**: ¹H NMR (400 MHz, CDCl₃) δ 7.2-7.0 (m, 8H, Ar), 6.25 (AB, $J_{AB} = 15.9$ Hz, 2H, CH=CHAr), 4.01 (q, $J = 7.2$ Hz, 2H, OCH₂CH₃), 3.91 (q, $J_X = 7.4$ Hz, 1H, ArCH(CH)CH₂), 2.70 (t, $J = 7.1$ Hz, 2H, ArCH(CH)CH₂), 1.11 (t, $J = 7.2$ Hz, 3H, OCH₂CH₃); NOESY δ 6.25 \leftrightarrow 2.70 (\leftrightarrow denotes NOE correlation); ¹³C{¹H} NMR (100 MHz, CDCl₃) δ 171.6 (CO), 141.0 and 135.6 (Ar), 132.3 (CH=CHAr), 130.0 (Ar), 129.5 (CH=CHAr), 129.4, 129.2, 129.0, 128.9 and 127.7 (Ar), 60.8 (OCH₂CH₃), 44.6 (ArCHCH₂), 40.7 (ArCHCH₂), 14.4 (OCH₂CH₃); GC-MS $m/z = 349$ (M⁺); Anal. Calcd for C₁₉H₁₈Cl₂O₂: C, 65.34; H, 5.19. Found: C, 65.54; H, 5.35.

For **35s**: ¹H NMR (400 MHz, CDCl₃) δ 7.9-7.4 (m, 7H, Ar), 4.08 (q, $J = 7.1$ Hz, 2H, OCH₂CH₃), 3.51 (s, CH₂), 1.93 (s, 3H, =C(CH₃)₂), 1.71 (s, 3H, =C(CH₃)₂), 1.18 (t, $J = 7.1$ Hz, 3H, OCH₂CH₃); ¹³C{¹H} NMR (100 MHz, CDCl₃) δ 171.9 (CO), 140.9

(=C(CH₃)₂), 133.5 and 133.0 (Ar), 132.2 (C=C(CH₃)₂), 128.0, 127.80, 127.77, 127.73, 127.70, 127.50, 126.0 and 125.6 (Ar), 60.6 (OCH₂CH₃), 40.4 (CH₂), 22.5 and 21.0 (=C(CH₃)₂), 14.3 (OCH₂CH₃); GC-MS *m/z* = 268 (M⁺); Anal. Calcd for C₁₈H₂₀O₂: C, 80.56; H, 7.51. Found: C, 80.62; H, 7.72.

For **35t**: ¹H NMR (400 MHz, CDCl₃) δ 6.58 (dd, *J* = 2.6, 1.8 Hz, 1H, Ar), 6.10 (dd, *J* = 3.4, 2.6 Hz, 1H, Ar), 5.88 (dd, *J* = 3.4, 1.8 Hz, 1H, Ar), 4.09 (q, *J* = 7.2 Hz, 2H, OCH₂CH₃), 3.39 (s, 3H, NCH₃), 3.35 (s, 2H, CH₂), 1.87 (s, 3H, =C(CH₃)₂), 1.60 (s, 3H, =C(CH₃)₂), 1.22 (t, *J* = 7.2 Hz, 3H, OCH₂CH₃); ¹³C{¹H} NMR (100 MHz, CDCl₃) δ 171.6 (CO), 137.4 (=C(CH₃)₂), 134.4 (Ar), 120.7 (C=C(CH₃)₂), 119.5, 107.1 and 106.6 (Ar), 60.5 (OCH₂CH₃), 40.3 (NCH₃), 33.7 (CH₂), 22.4 and 20.5 (=C(CH₃)₂), 14.2 (OCH₂CH₃); GC-MS *m/z* = 221 (M⁺); Anal. Calcd for C₁₃H₁₉NO₃: C, 70.56; H, 8.65. Found: C, 70.85; H, 8.65.

For **35u**: ¹H NMR (400 MHz, CDCl₃) δ 7.31 (q, *J* = 0.7 Hz, 1H, Ar), 6.35 (p, *J* = 1.7 Hz, 1H, Ar), 6.19 (d, *J* = 3.4 Hz, 1H, Ar), 4.09 (q, *J* = 7.2 Hz, 2H, OCH₂CH₃), 3.44 (s, CH₂), 1.98 (s, 3H, =C(CH₃)₂), 1.87 (s, 3H, =C(CH₃)₂), 1.19 (t, *J* = 7.2 Hz, 3H, OCH₂CH₃); ¹³C{¹H} NMR (100 MHz, CDCl₃) δ 171.7 (CO), 154.5 (=C(CH₃)₂), 140.5 and 135.0 (Ar), 118.3 (CC(CH₃)₂), 110.8 and 108.2 (Ar), 60.4 (OCH₂CH₃), 36.8 (CH₂), 23.0 and 22.1 (=C(CH₃)₂), 14.3 (OCH₂CH₃); GC-MS *m/z* = 208 (M⁺); Anal. Calcd for C₁₂H₁₆O₃: C, 69.21; H, 7.74. Found: C, 68.98; H, 7.64.

For **35v**: ¹H NMR (400 MHz, CDCl₃) δ 7.3-7.0 (m, 5H, Ar), 4.21 (m, 1H, CH), 3.92 (m, 2H, CHCH₂CH₂O), 2.29 (m, 1H, CHCH₂), 2.03 (m, 1H, CHCH₂), 1.91 (s, 3H, =C(CH₃)₂), 1.53 (s, 3H, =C(CH₃)₂); ¹³C{¹H} NMR (100 MHz, CDCl₃) δ 177.7 (CO), 140.3 (=C(CH₃)₂), 134.2 and 129.8 (Ar), 129.7 (C=C(CH₃)₂), 128.5 and 127.0 (Ar), 66.9

(CH₂CO), 43.5 (CH), 27.5 (CH₂), 22.8 and 20.5 (=C(CH₃)₂); GC-MS *m/z* = 216 (M⁺); Anal. Calcd for C₁₄H₁₆O₂: C, 77.75; H, 7.49. Found: C, 77.67; H, 7.53.

For **36a**: ¹H NMR (400 MHz, CDCl₃) δ 7.3-7.1 (m, 5H, Ar), 6.61 (br, 1H, NH₂), 5.78 (br, 1H, NH₂), 3.29 (s, 2H, CH₂), 1.85 (s, 3H, =C(CH₃)₂), 1.67 (s, 3H, =C(CH₃)₂); ¹³C{¹H} NMR (100 MHz, CDCl₃) δ 174.1 (CO), 142.7 (=C(CH₃)₂), 133.6 (Ar), 129.0 (C=C(CH₃)₂), 128.7, 128.3 and 126.7 (Ar), 42.3 (CH₂), 22.4 and 21.0 (=C(CH₃)₂); GC-MS *m/z* = 189 (M⁺); Anal. Calcd for C₁₂H₁₅NO: C, 76.16; H, 7.99. Found: C, 77.47; H, 7.78.

For **36b**: ¹H NMR (400 MHz, CDCl₃) δ 7.3-7.1 (m, 5H, Ar), 5.88 (br, 1H, NHCH₃), 3.28 (s, 2H, CH₂), 2.70 (d, *J* = 4.9 Hz, 3H, NHCH₃), 1.82 (s, 3H, =C(CH₃)₂), 1.64 (s, 3H, =C(CH₃)₂); ¹³C{¹H} NMR (100 MHz, CDCl₃) δ 171.3 (CO), 142.8 (=C(CH₃)₂), 133.6 (Ar), 129.0 (C=C(CH₃)₂), 128.7, 128.3 and 126.5 (Ar), 42.6 (CH₂), 26.4 (NHCH₃), 22.5 and 21.0 (=C(CH₃)₂); GC-MS *m/z* = 203 (M⁺); Anal. Calcd for C₁₃H₁₇NO: C, 76.81; H, 8.43. Found: C, 76.38; H, 8.19.

For **36c**: ¹H NMR (400 MHz, CDCl₃) δ 7.3-7.1 (m, 5H, Ar), 3.37 (s, 2H, CH₂), 2.79 (s, 3H, N(CH₃)₂), 2.76 (s, 3H, N(CH₃)₂), 1.81 (s, 3H, =C(CH₃)₂), 1.57 (s, 3H, =C(CH₃)₂); ¹³C{¹H} NMR (100 MHz, CDCl₃) δ 168.8 (CO), 141.4 (=C(CH₃)₂), 129.4 and 126.8 (Ar), 126.7 (C=C(CH₃)₂), 125.9 and 124.1 (Ar), 37.1 (CH₂), 35.3 (N(CH₃)₂), 33.4 (N(CH₃)₂), 20.2 and 18.6 (=C(CH₃)₂); GC-MS *m/z* = 217 (M⁺); Anal. Calcd for C₁₄H₁₉NO: C, 77.38; H, 8.81. Found: C, 76.96; H, 8.76.

For **36d**: ¹H NMR (400 MHz, CDCl₃) δ 7.2-7.0 (m, 5H, Ar), 3.30 (s, 2H, CH₂), 3.20 (q, *J* = 7.1 Hz, 2H, N(CH₂CH₃)₂), 3.03 (q, *J* = 7.1 Hz, 2H, N(CH₂CH₃)₂), 1.78 (s, 3H, =C(CH₃)₂), 1.53 (s, 3H, =C(CH₃)₂), 0.93 (t, *J* = 7.2 Hz, 2H, N(CH₂CH₃)₂), 0.87 (t, *J* = 7.1

Hz, 2H, N(CH₂CH₃)₂); ¹³C{¹H} NMR (100 MHz, CDCl₃) δ 169.7 (CO), 143.0 (=C(CH₃)₂), 130.9 (Ar), 129.0 (C=C(CH₃)₂), 128.7, 127.7 and 125.9 (Ar), 41.7 and 39.9 (N(CH₂CH₃)₂), 38.7 (CH₂), 22.0 and 20.4 (=C(CH₃)₂), 14.0 and 12.6 (N(CH₂CH₃)₂); GC-MS *m/z* = 245 (M⁺); Anal. Calcd for C₁₆H₂₃NO: C, 78.32; H, 9.45. Found: C, 77.86; H, 9.56.

For **36e**: ¹H NMR (400 MHz, CDCl₃) δ 7.3-7.1 (m, 5H, Ar), 3.81 (p, *J* = 6.7 Hz, 1H, N(CH(CH₃)₂)₂), 3.35 (s, 2H, CH₂), 3.31 (br, 1H, N(CH(CH₃)₂)₂), 1.84 (s, 3H, =C(CH₃)₂), 1.58 (s, 3H, =C(CH₃)₂), 1.27 (d, *J* = 6.8 Hz, 3H, N(CH(CH₃)₂)₂), 0.96 (d, *J* = 6.7 Hz, 3H, N(CH(CH₃)₂)₂); ¹³C{¹H} NMR (100 MHz, CDCl₃) δ 169.9 (CO), 143.4 (=C(CH₃)₂), 131.1 (Ar), 129.5 (C=C(CH₃)₂), 129.1, 128.0 and 126.2 (Ar), 48.9 (N(CH(CH₃)₂)₂), 45.8 (N(CH(CH₃)₂)₂), 40.7 (CH₂), 22.3 and 20.9 (=C(CH₃)₂), 20.8 (N(CH(CH₃)₂)₂), 20.7 (N(CH(CH₃)₂)₂); GC-MS *m/z* = 273 (M⁺); Anal. Calcd for C₁₈H₂₇NO: C, 79.07; H, 9.95. Found: C, 79.04; H, 9.74.

For **36f**: ¹H NMR (400 MHz, CDCl₃) δ 7.3-7.1 (m, 5H, Ar), 3.34 (s, 2H, CH₂), 3.16 (dd, *J* = 7.6 Hz, 2H, N(CH₂(CH₂)₂CH₃)₂), 2.98 (dd, *J* = 7.7 Hz, 2H, N(CH₂(CH₂)₂CH₃)₂), 1.82 (s, 3H, =C(CH₃)₂), 1.56 (s, 3H, =C(CH₃)₂), 1.33 (m, 4H, N(CH₂(CH₂)₂CH₃)₂), 1.16 (m, 4H, N(CH₂(CH₂)₂CH₃)₂), 0.83 (t, *J* = 7.3, 3H, N(CH₂(CH₂)₂CH₃)₂), 0.81 (t, *J* = 7.3, 3H, N(CH₂(CH₂)₂CH₃)₂); ¹³C{¹H} NMR (100 MHz, CDCl₃) δ 170.3 (CO), 143.2 (=C(CH₃)₂), 131.1 (Ar), 129.2 (C=C(CH₃)₂), 128.9, 127.9 and 126.1 (Ar), 47.7 and 45.8 (N(CH₂(CH₂)₂CH₃)₂), 40.7 (CH₂), 31.1 and 29.7 (N(CH₂(CH₂)₂CH₃)₂), 22.1 and 20.7 (=C(CH₃)₂), 20.2 and 20.0 (N(CH₂(CH₂)₂CH₃)₂), 13.9 and 13.8 (N(CH₂(CH₂)₂CH₃)₂); GC-MS *m/z* = 301 (M⁺); Anal. Calcd for C₂₀H₃₁NO: C, 79.68; H, 10.36. Found: C, 79.46; H, 10.11.

For **36g**: ^1H NMR (400 MHz, CDCl_3) δ 7.59 (br, 1H, NHAr), 7.4-6.9 (m, 9H, Ar), 3.48 (s, 2H, CH_2), 2.30 (s, 3H, Ar CH_3), 1.94 (s, 3H, $=\text{C}(\text{CH}_3)_2$), 1.75 (s, 3H, $=\text{C}(\text{CH}_3)_2$); $^{13}\text{C}\{^1\text{H}\}$ NMR (100 MHz, CDCl_3) δ 168.9 (CO), 142.8 ($=\text{C}(\text{CH}_3)_2$), 135.4 and 134.2 (Ar), 133.9 ($\text{C}=\text{C}(\text{CH}_3)_2$), 129.5, 128.8, 128.5, 126.8 and 120.0 (Ar), 43.7 (CH_2), 22.5 ($=\text{C}(\text{CH}_3)_2$), 21.1 (Ar CH_3), 20.9 ($=\text{C}(\text{CH}_3)_2$); GC-MS $m/z = 279$ (M^+); Anal. Calcd for $\text{C}_{19}\text{H}_{21}\text{NO}$: C, 81.68; H, 7.58. Found: C, 81.23; H, 7.61.

For **36h**: ^1H NMR (400 MHz, CDCl_3) δ 7.54 (br, 1H, NPh), 7.4-7.0 (m, 10H, Ar), 3.51 (s, 2H, CH_2), 1.94 (s, 3H, $=\text{C}(\text{CH}_3)_2$), 1.75 (s, 3H, $=\text{C}(\text{CH}_3)_2$); $^{13}\text{C}\{^1\text{H}\}$ NMR (100 MHz, CDCl_3) δ 169.0 (CO), 142.7 ($=\text{C}(\text{CH}_3)_2$), 137.9, 134.5, 129.0 and 128.8 (Ar), 128.7 ($\text{C}=\text{C}(\text{CH}_3)_2$), 128.6, 126.9, 124.3 and 120.0 (Ar), 43.9 (CH_2), 22.6 and 21.2 ($=\text{C}(\text{CH}_3)_2$); GC-MS $m/z = 265$ (M^+); Anal. Calcd for $\text{C}_{18}\text{H}_{19}\text{NO}$: C, 81.47; H, 7.22. Found: C, 81.70; H, 6.93.

For **36i**: ^1H NMR (400 MHz, CDCl_3) δ 7.69 (br, 1H, NHAr), 7.3-7.0 (m, 9H, Ar), 3.47 (s, 2H, CH_2), 1.92 (s, 3H, $=\text{C}(\text{CH}_3)_2$), 1.72 (s, 3H, $=\text{C}(\text{CH}_3)_2$); $^{13}\text{C}\{^1\text{H}\}$ NMR (100 MHz, CDCl_3) δ 169.3 (CO), 142.6 ($=\text{C}(\text{CH}_3)_2$), 136.5, 134.4, 129.0, 128.8 and 128.48 (Ar), 128.4 ($\text{C}=\text{C}(\text{CH}_3)_2$), 126.9 and 121.3 (Ar), 43.6 (CH_2), 22.6 and 21.1 ($=\text{C}(\text{CH}_3)_2$); GC-MS $m/z = 299$ (M^+); Anal. Calcd for $\text{C}_{18}\text{H}_{18}\text{ClNO}$: C, 72.11; H, 6.05. Found: C, 71.61; H, 5.95.

For **36j**: ^1H NMR (400 MHz, CDCl_3) δ 7.4-7.1 (m, 10H, Ar), 6.09 (br, 1H, NHBz), 4.38 (d, $J = 5.8$, 2H, NHCH_2Ar), 3.39 (s, 2H, CH_2), 1.88 (s, 3H, $=\text{C}(\text{CH}_3)_2$), 1.67 (s, 3H, $=\text{C}(\text{CH}_3)_2$); $^{13}\text{C}\{^1\text{H}\}$ NMR (100 MHz, CDCl_3) δ 170.1 (CO), 142.6 ($=\text{C}(\text{CH}_3)_2$), 138.3, 133.8, 128.9, 128.7, 128.4 and 127.6 (Ar), 128.9 ($\text{C}=\text{C}(\text{CH}_3)_2$), 126.7 (Ar), 43.6 (NCH_2), 42.7 (CH_2), 22.5 and 21.2 ($=\text{C}(\text{CH}_3)_2$); GC-MS $m/z = 279$ (M^+); Anal. Calcd for $\text{C}_{19}\text{H}_{21}\text{NO}$: C, 81.68; H, 7.58. Found: C, 81.76; H, 7.52.

For **36k**: ^1H NMR (400 MHz, CDCl_3) δ 7.4-6.9 (m, 10H, Ar), 3.16 (s, 3H, $\text{N}(\text{CH}_3)\text{Ph}$), 3.15 (s, 2H, CH_2), 1.73 (s, 3H, $=\text{C}(\text{CH}_3)_2$), 1.55 (s, 3H, $=\text{C}(\text{CH}_3)_2$); $^{13}\text{C}\{^1\text{H}\}$ NMR (100 MHz, CDCl_3) δ 171.0 (CO), 144.1 ($=\text{C}(\text{CH}_3)_2$), 143.4 and 131.3 (Ar), 129.6 ($\text{C}=\text{C}(\text{CH}_3)_2$), 128.9, 127.9, 127.3 and 126.0 (Ar), 39.6 (CH_2), 37.3 ($\text{N}(\text{CH}_3)\text{Ph}$), 22.5 and 20.6 ($=\text{C}(\text{CH}_3)_2$); GC-MS m/z = 279 (M^+); Anal. Calcd for $\text{C}_{19}\text{H}_{21}\text{NO}$: C, 81.68; H, 7.58. Found: C, 81.74; H, 7.49.

For **36l**: ^1H NMR (400 MHz, CDCl_3) δ 7.2-7.0 (m, 5H, Ar), 3.28 (t, J = 6.8 Hz, 2H, NCH_2), 3.27 (s, 2H, CH_2), 3.09 (t, J = 6.5 Hz, 2H, NCH_2), 1.78 (s, 3H, $=\text{C}(\text{CH}_3)_2$), 1.66 (m, 4H, CH_2), 1.52 (s, 3H, $=\text{C}(\text{CH}_3)_2$); $^{13}\text{C}\{^1\text{H}\}$ NMR (100 MHz, CDCl_3) δ 169.2 (CO), 143.3 ($=\text{C}(\text{CH}_3)_2$), 131.2 and 128.6 (Ar), 128.4 ($\text{C}=\text{C}(\text{CH}_3)_2$), 127.7 and 125.9 (Ar), 46.3 (NCH_2), 45.4 (NCH_2), 40.4, 25.9 and 24.1 (CH_2), 21.9 and 20.5 ($=\text{C}(\text{CH}_3)_2$); GC-MS m/z = 243 (M^+); Anal. Calcd for $\text{C}_{16}\text{H}_{21}\text{NO}$: C, 78.97; H, 8.70. Found: C, 78.72; H, 8.58.

For **36m**: ^1H NMR (400 MHz, CDCl_3) δ 7.3-7.1 (m, 5H, Ar), 3.42 (dd, J = 5.6 Hz, 2H, NCH_2), 3.39 (s, 2H, CH_2), 3.17 (dd, J = 5.6 Hz, 2H, NCH_2), 1.84 (s, 3H, $=\text{C}(\text{CH}_3)_2$), 1.58 (s, 3H, $=\text{C}(\text{CH}_3)_2$), 1.49 (m, 2H, CH_2), 1.40 (m, 2H, CH_2), 1.27 (m, 2H, CH_2); $^{13}\text{C}\{^1\text{H}\}$ NMR (100 MHz, CDCl_3) δ 169.3 (CO), 143.3 ($=\text{C}(\text{CH}_3)_2$), 131.4 and 129.0 (Ar), 128.9 ($\text{C}=\text{C}(\text{CH}_3)_2$), 128.0 and 126.2 (Ar), 46.8 and 42.7 (NCH_2), 38.9, 26.2, 25.6 and 24.5 (CH_2), 22.3 and 20.7 ($=\text{C}(\text{CH}_3)_2$); GC-MS m/z = 257 (M^+); Anal. Calcd for $\text{C}_{17}\text{H}_{23}\text{NO}$: C, 79.33; H, 9.01. Found: C, 79.33; H, 9.14.

For (**Z**)-**36n**: ^1H NMR (400 MHz, CDCl_3) δ 7.3-7.1 (m, 5H, Ar), 6.11 (q, J = 7.0 Hz, 1H, $=\text{CHCH}_3$), 6.09 (s, 1H, NHCH_3), 3.39 (s, 2H, CH_2), 2.67 (d, J = 4.9 Hz, 3H, NHCH_3), 1.79 (d, J = 7.0 Hz, 3H, $=\text{CHCH}_3$): NOESY δ 3.39 \leftrightarrow 1.79 (\leftrightarrow denotes NOE correlation); $^{13}\text{C}\{^1\text{H}\}$ NMR (100 MHz, CDCl_3) δ 170.7 (CO), 141.5 (Ar), 134.2

(C=CHCH₃), 128.4 and 127.2 (Ar), 127.1 (C=CHCH₃), 125.4 (Ar), 37.6 (CH₂), 26.3 (NHCH₃), 14.5 (C=CHCH₃); GC-MS m/z = 189 (M⁺); Anal. Calcd for C₁₂H₁₅NO: C, 76.16; H, 7.99. Found: C, 75.99; H, 7.92.

For (*E*)-**36n**: ¹H NMR (400 MHz, CDCl₃) δ 7.3-7.1 (m, 5H, Ar), 5.88 (s, 1H, NHCH₃), 5.75 (qt, J = 5.3, 0.5 Hz, 1H, =CHCH₃), 3.25 (s, CH₂), 2.71 (d, J = 4.9 Hz, NHCH₃), 1.65 (dt, J = 6.9, 1.0 Hz, 3H, =CHCH₃); ¹³C{¹H} NMR (100 MHz, CDCl₃) δ 171.7 (CO), 139.4 (Ar), 135.5 (C=CHCH₃), 128.5, 128.4 and 127.3 (Ar), 127.2 (C=CHCH₃), 47.1 (CH₂), 26.5 (NHCH₃), 15.2 (C=CHCH₃); GC-MS m/z = 189 (M⁺); Anal. Calcd for C₁₂H₁₅NO: C, 76.16; H, 7.99. Found: C, 75.99; H, 7.92.

For **36o**: ¹H NMR (400 MHz, CDCl₃) δ 7.3-7.1 (m, 5H, Ar), 5.82 (br, 1H, NHCH₃), 3.26 (s, 2H, CH₂), 2.71 (d, J = 3.8 Hz, 3H, NHCH₃), 1.96 (q, J = 7.5 Hz, 2H, =C(CH₃)CH₂CH₃), 1.82 (s, 3H, =C(CH₃)CH₂CH₃), 0.94 (t, J = 7.4 Hz, 3H, =C(CH₃)CH₂CH₃); NOESY δ 3.26 ↔ 1.81 (↔ denotes NOE correlation); ¹³C{¹H} NMR (100 MHz, CDCl₃) δ 171.2 (CO), 142.9 (Ar), 139.1 (C=C(CH₃)C₂H₅), 129.0 (=C(CH₃)C₂H₅), 128.5, 128.4 and 126.6 (Ar), 43.0 (CH₂), 28.6 (NHCH₃), 26.5 (CH₂), 17.9 and 13.3 (CH₃); GC-MS m/z = 217 (M⁺); Anal. Calcd for C₁₄H₁₉NO: C, 77.38; H, 8.81. Found: C, 76.91; H, 8.76.

For **36p**: ¹H NMR (400 MHz, CDCl₃) δ 7.3-7.0 (m, 5H, Ar), 5.82 (br, 1H, NHCH₃), 3.34 (s, 2H, CH₂), 2.79 (d, J = 4.9 Hz, 3H, NHCH₃), 2.04 (dd, J = 7.3 Hz, 2H, =C(CH₃)CH₂(CH₂)₂CH₃), 1.88 (s, 3H, =C(CH₃)CH₂(CH₂)₂CH₃), 1.41 (m, 2H, =C(CH₃)CH₂(CH₂)₂CH₃), 1.19 (m, 2H, =C(CH₃)CH₂(CH₂)₂CH₃), 0.82 (t, J = 7.3 Hz, 3H, =C(CH₃)CH₂(CH₂)₂CH₃); NOESY δ 3.34 ↔ 1.87 (↔ denotes NOE correlation); ¹³C{¹H} NMR (100 MHz, CDCl₃) δ 171.3 (CO), 143.0 (C=C(CH₃)CH₂(CH₂)₂CH₃), 138.1 (Ar), 129.5 (=C(CH₃)CH₂(CH₂)₂CH₃), 128.6, 128.4 and 126.4 (Ar), 43.1, 35.3 and

30.8 (CH₂), 26.6 (NHCH₃), 22.7 (CH₂), 18.4 and 14.1 (CH₃); GC-MS *m/z* = 245; Anal. Calcd for C₁₆H₂₃NO: C, 78.32; H, 9.45. Found: C, 78.30; H, 9.30.

For **36q**: ¹H NMR (400 MHz, CDCl₃) δ 7.3-7.0 (m, 5H, Ar), 5.88 (br, 1H, NHCH₃), 3.25 (s, 2H, CH₂), 2.70 (d, *J* = 4.8 Hz, 3H, NHCH₃), 1.95 (dd, *J* = 7.7 Hz, 2H, =C(CH₃)CH₂(CH₂)₄CH₃), 1.80 (s, 3H, =C(CH₃)CH₂(CH₂)₄CH₃), 1.33 (m, 2H, =C(CH₃)CH₂(CH₂)₄CH₃), 1.21 (m, 2H, =C(CH₃)CH₂(CH₂)₄CH₃), 1.09 (m, 4H, =C(CH₃)CH₂(CH₂)₄CH₃), 0.79 (t, *J* = 7.0 Hz, 3H, =C(CH₃)CH₂(CH₂)₄CH₃); NOESY δ 3.25 ↔ 1.80 (↔ denotes NOE correlation); ¹³C{¹H} NMR (100 MHz, CDCl₃) δ 171.2 (CO), 142.9 (C=C(CH₃)CH₂(CH₂)₄CH₃), 137.8 (Ar), 129.4 (=C(CH₃)CH₂(CH₂)₄CH₃), 128.5, 128.3 and 126.5 (Ar), 42.9, 35.4, 31.6, 29.2 and 28.3 (CH₂), 26.4 (NHCH₃), 22.6 (CH₂), 18.3 and 14.1 (CH₃); GC-MS *m/z* = 273; Anal. Calcd for C₁₆H₂₃NO: C, 79.07; H, 9.95. Found: C, 78.37; H, 9.87.

For **36r**: ¹H NMR (400 MHz, CDCl₃) δ 7.3-7.0 (m, 5H, Ar), 5.88 (br, 1H, NHCH₃), 3.24 (s, 2H, CH₂), 2.68 (d, *J* = 4.8 Hz, 3H, CH₃), 1.87 (d, *J* = 7.3 Hz, 2H, CH₂), 1.78 (s, 3H, CH₃), 1.6-1.5 (br, 5H, CH₂), 1.42 (m, 1H, CH), 1.10 (m, 2H, CH₂), 1.07 (m, 1H, CH₂), 0.62 (m, 2H, CH₂); NOESY δ 3.24 ↔ 1.78 (↔ denotes NOE correlation); ¹³C{¹H} NMR (100 MHz, CDCl₃) δ 171.2 (CO), 143.1 (C=C(CH₃)C₇H₁₃), 136.0 (Ar), 130.4 (=C(CH₃)C₇H₁₃), 128.9, 128.2 and 126.4 (Ar), 43.1 and 42.8 (CH₂), 36.1 (CH), 33.1 and 26.4 and 26.3 (CH₂), 18.3 (CH₃); GC-MS *m/z*: 285; Anal. Calcd for C₁₉H₂₇NO: C, 79.95; H, 9.53. Found: C, 79.80; H, 9.30.

For **36s**: ¹H NMR (400 MHz, CDCl₃) δ 7.3-6.9 (m, 10H, Ar), 5.64 (br, 1H, NHCH₃), 3.23 (s, 2H, CH₂), 2.71 (t, *J* = 7.4 Hz, 2H, =C(CH₃)CH₂CH₂Ph), 2.62 (d, *J* = 4.8 Hz, 3H, NHCH₃), 2.36 (t, *J* = 7.4 Hz, 2H, =C(CH₃)CH₂CH₂Ph), 1.87 (s, 3H, =C(CH₃)CH₂CH₂Ph); NOESY δ 3.23 ↔ 1.87 (↔ denotes NOE correlation); ¹³C{¹H}

NMR (100 MHz, CDCl₃) δ 170.8 (CO), 142.7 and 141.4 (Ar), 136.1 (C=C(CH₃)CH₂CH₂Ph), 131.0 (=C(CH₃)CH₂CH₂Ph), 128.5, 128.3, 128.2, 128.1, 126.6 and 126.0 (Ar), 43.0, 36.5 and 34.0 (CH₂), 26.4 (NHCH₃), 18.0 (CH₃); GC-MS m/z : 293; Anal. Calcd for C₁₆H₂₃NO: C, 81.87; H, 7.90. Found: C, 81.65; H, 7.70.

For **36t**: ¹H NMR (400 MHz, CDCl₃) δ 7.3-7.1 (m, 5H, Ar), 6.71 (br s, NHCH₃), 5.67 (m, CH), 5.27 (m, 1H, CH), 3.02 (m, 2H, CH₂), 2.58 (dd, J = 13.9, 4.0 Hz, 1H, CHCH₂), 2.46 (d, J = 5.1 Hz, 3H, NHCH₃), 2.39 (dd, J = 14.0, 9.1 Hz, 1H, CHCH₂), 2.17 (m, CH₂), 2.09 (m, 1H, CH), 1.63 (m, 1H, CH); ¹³C{¹H} NMR (100 MHz, CDCl₃) δ 172.7 (CO), 143.6 (Ar), 133.0 and 131.7 (CH), 128.4, 128.0 and 126.5 (Ar), 51.5 (CH), 48.2 (CH), 42.1 (CHCH₂), 32.3 (CH₂), 26.2 (NHCH₃); HRMS (m/z): calcd for C₁₅H₁₉NO (M+H)⁺, 230.1539; Found: 230.1504.

For **36u**: ¹H NMR (400 MHz, CDCl₃) δ 7.3-7.0 (m, 5H, Ar), 5.4 (t, J = 0.6 Hz, 1H, CC(Ph)=CH₂), 5.2 (br, 1H, NHCH₃), 5.1 (dd, J = 0.7 Hz, J = 1.4 Hz, 1H, CC(Ph)=CH₂), 4.4 (t, J = 7.8 Hz, ArCH), 2.7 (dd, J = 6.5 Hz, J = 14.1 Hz, 1H, ArCHCH₂), 2.6 (d, J = 4.8 Hz, NHCH₃), 2.5 (dd, J = 8.6 Hz, J = 14.1 Hz, 1H, ArCHCH₂); ¹³C{¹H} NMR (100 MHz, CDCl₃) δ 171.8 (CO), 151.0 (CHC(Ph)=CH₂), 143.1, 137.3, 128.9, 128.6, 127.8 and 126.4 (Ar), 113.4 (CHC(Ph)=CH₂), 45.5 (ArCHCH₂), 43.5 (ArCHCH₂), 26.5 (NHCH₃); GC-MS m/z = 265 (M⁺); Anal. Calcd for C₁₈H₁₉NO: C, 81.47; H, 7.22. Found: C, 81.84; H, 7.42.

For **36v**: ¹H NMR (400 MHz, CDCl₃) δ 7.3-7.0 (m, 5H, Ar), 6.3 (AB, J_{AB} = 16.0 Hz, 2H, ArCH=CHPh), 5.3 (br, 1H, NHCH₃), 4.0 (q, J_X = 7.3 Hz, ArCHCH₂), 2.6 (dd, J = 7.7 Hz, J = 14.1 Hz, 1H, ArCHCH₂), 2.6 (d, J = 4.8 Hz, NHCH₃), 2.5 (dd, J = 7.5 Hz, J = 14.0 Hz, 1H, ArCHCH₂); ¹³C{¹H} NMR (100 MHz, CDCl₃) δ 172.1 (CO), 142.2, 141.8, 132.4, 130.4, 128.4 and 128.1 (Ar), 127.6 (ArCH=CHPh), 127.1 and 127.0 (Ar), 126.8

(ArCHCHPh) 46.7 (ArCHCH₂), 43.0 (ArCHCH₂), 26.5 (NHCH₃); GC-MS m/z = 265 (M⁺); Anal. Calcd for C₁₈H₁₉NO: C, 81.47; H, 7.22. Found: C, 81.84; H, 7.42.

For **36w**: ¹H NMR (400 MHz, CDCl₃) δ 7.4-7.2 (m, 5H, Ar), 6.4 (br, 1H, NHCH₃), 6.2 (t, J = 7.7 Hz, C=CHCH₂), 4.2 (q, J = 7.2 Hz, 2H, CO₂CH₂CH₃), 3.5 (s, 2H, CH₂), 3.3 (d, J = 7.7 Hz, 2H, C=CHCH₂), 2.7 (d, J = 4.8 Hz, 3H, NHCH₃), 1.3 (t, J = 7.2, 3H, CO₂CH₂CH₃); ¹³C{¹H} NMR (100 MHz, CDCl₃) δ 172.0 and 170.2 (CO), 140.8 (Ar), 137.6 (C=CHCH₂), 128.8 (Ar), 128.0 (C=CHCH₂), 126.1 and 123.6 (Ar), 61.5 (CO₂CH₂CH₃), 38.6 (C=CHCH₂), 34.6 (ArCCH₂), 26.6 (NHCH₃), 14.4 (CO₂CH₂CH₃); GC-MS m/z = 261 (M⁺); Anal. Calcd for C₁₅H₁₉NO₃: C, 68.94; H, 7.33. Found: C, 68.85; H, 7.21.

For **36x**: ¹H NMR (400 MHz, CDCl₃) δ 7.3-7.3 (m, 7H, Ar), 3.48 (s, 2H, CH₂), 2.82 (s, 3H, N(CH₃)₂), 2.77 (s, 3H, N(CH₃)₂), 1.90 (s, 3H, =C(CH₃)₂), 1.67 (s, 3H, =C(CH₃)₂); ¹³C{¹H} NMR (100 MHz, CDCl₃) δ 170.8 (CO), 140.9 (=C(CH₃)₂), 133.3 and 132.0 (Ar), 128.6 (C=C(CH₃)₂), 127.8, 127.7, 127.5, 127.4, 127.2, 125.7 and 125.4 (Ar), 39.1 (CH₂), 37.3 (N(CH₃)₂), 35.4 (N(CH₃)₂), 22.3 and 20.7 (=C(CH₃)₂); GC-MS m/z = 267 (M⁺); Anal. Calcd for C₁₈H₂₁NO: C, 80.86; H, 7.92. Found: C, 80.55; H, 7.86.

For **37a**: ¹H NMR (400 MHz, CDCl₃) δ 7.1-6.9 (m, 4H, Ar), 4.08 (m, 2H, OCH₂CH₃), 3.80 (q, J = 7.1 Hz, 1H, CHCH₃), 2.34 (s, 3H, ArCH₃) 1.88 (s, 3H, =C(CH₃)₂), 1.51 (s, 3H, =C(CH₃)₂), 1.24 (t, J = 7.2 Hz, 3H, OCH₂CH₃) 1.16 (d, J = 7.1 Hz, 3H, CHCH₃); ¹³C{¹H} NMR (100 MHz, CDCl₃) δ 174.8 (CO), 137.9 (=C(CH₃)₂), 135.8 and 133.9 (Ar), 130.9 (C=C(CH₃)₂), 129.5 and 128.7 (Ar), 60.5 (OCH₂CH₃), 42.8 (CH), 22.8 (ArCH₃), 21.3 and 20.3 (=C(CH₃)₂), 15.9 (CH₃), 14.2 (OCH₂CH₃); GC-MS m/z = 246 (M⁺); Anal. Calcd for C₁₆H₂₂O₂: C, 78.01; H, 9.00. Found: C, 77.75; H, 8.94.

For **37b**: ^1H NMR (400 MHz, CDCl_3) δ 7.3-7.0 (m, 4H, Ar), 4.07 (m, 2H, OCH_2CH_3), 3.80 (q, $J = 7.1$ Hz, 1H, CHCH_3), 1.87 (s, 3H, $=\text{C}(\text{CH}_3)_2$), 1.49 (s, 3H, $=\text{C}(\text{CH}_3)_2$), 1.20 (t, $J = 7.1$ Hz, 3H, OCH_2CH_3), 1.15 (d, $J = 7.1$ Hz, 3H, CHCH_3); $^{13}\text{C}\{^1\text{H}\}$ NMR (100 MHz, CDCl_3) δ 174.7 (CO), 141.0 ($=\text{C}(\text{CH}_3)_2$), 134.0 (Ar), 131.0 ($\text{C}=\text{C}(\text{CH}_3)_2$), 129.7, 127.9 and 126.5 (Ar), 60.5 (OCH_2CH_3), 42.8 (CH), 22.7 and 20.3 ($=\text{C}(\text{CH}_3)_2$), 15.9 (CH_3), 14.1 (OCH_2CH_3); GC-MS $m/z = 232$ (M^+); Anal. Calcd for $\text{C}_{15}\text{H}_{20}\text{O}_2$: C, 77.55; H, 8.68. Found: C, 77.09; H, 8.62.

For **37c**: ^1H NMR (400 MHz, CDCl_3) δ 7.2-6.9 (m, 4H, Ar), 4.05 (m, 2H, OCH_2CH_3), 3.77 (q, $J = 7.1$ Hz, 1H, CHCH_3), 1.84 (s, 3H, $=\text{C}(\text{CH}_3)_2$), 1.45 (s, 3H, $=\text{C}(\text{CH}_3)_2$), 1.18 (t, $J = 7.1$ Hz, 3H, OCH_2CH_3) 1.09 (d, $J = 7.1$ Hz, 3H, CHCH_3); $^{13}\text{C}\{^1\text{H}\}$ NMR (100 MHz, CDCl_3) δ 174.5 (CO), 139.3 ($=\text{C}(\text{CH}_3)_2$), 132.8 (Ar), 132.4 ($\text{C}=\text{C}(\text{CH}_3)_2$), 131.9, 131.1 and 128.1 (Ar), 60.5 (OCH_2CH_3), 42.5 (CH), 22.7 and 20.3 ($=\text{C}(\text{CH}_3)_2$), 15.9 (CH_3), 14.2 (OCH_2CH_3); GC-MS $m/z = 252$ (M^+); Anal. Calcd for $\text{C}_{15}\text{H}_{19}\text{ClO}_2$: C, 67.54; H, 7.18. Found: C, 67.64; H, 7.20.

For **37d**: ^1H NMR (400 MHz, CDCl_3) δ 7.2-6.9 (m, 5H, Ar), 5.88 (br, 1H, NHCH_3), 3.62 (q, $J = 7.2$ Hz, 1H, CHCH_3), 2.66 (d, $J = 4.8$ Hz, 3H, NHCH_3), 1.79 (s, 3H, $=\text{C}(\text{CH}_3)_2$), 1.43 (s, 3H, $=\text{C}(\text{CH}_3)_2$), 1.01 (d, $J = 7.2$ Hz, 3H, CHCH_3); $^{13}\text{C}\{^1\text{H}\}$ NMR (100 MHz, CDCl_3) δ 174.4 (CO), 140.5 ($=\text{C}(\text{CH}_3)_2$), 135.1 (Ar), 131.2 ($\text{C}=\text{C}(\text{CH}_3)_2$), 129.2, 127.7 and 126.2 (Ar), 43.2 (CHCH_3), 26.2 (NHCH_3), 22.6 and 21.2 ($=\text{C}(\text{CH}_3)_2$), 15.4 (CH_3); GC-MS $m/z = 217$ (M^+); Anal. Calcd for $\text{C}_{14}\text{H}_{19}\text{NO}$: C, 76.38; H, 8.81. Found: C, 77.17; H, 8.73.

For **37e**: ^1H NMR (400 MHz, CDCl_3) δ 7.2-6.8 (m, 15H, Ar), 6.01 (t, $J = 5.8$ Hz, 1H, NH), 4.89 (s, 1H, CHPh), 4.13 (dd, $J = 6.0, 5.2$ Hz, 2H, NHCH_2Ar), 1.71 (s, 3H,

=C(CH₃)₂, 1.43 (s, 3H, =C(CH₃)₂); ¹³C{¹H} NMR (100 MHz, CDCl₃) δ 172.1 (CO), 141.5 (=C(CH₃)₂), 138.3, 138.2 and 133.5 (Ar), 133.0 (C=C(CH₃)₂), 130.1, 129.6, 128.6, 128.4, 127.8, 127.7, 127.0 and 126.3 (Ar), 57.5 (CHPh), 43.7 (NCH₂), 23.2 and 21.1 (=C(CH₃)₂); GC-MS *m/z* = 355 (M⁺); calcd for C₂₅H₂₅NO (M+H)⁺, 356.4851; Found: 356.4864.

For **37f**: ¹H NMR (400 MHz, CDCl₃) δ 7.47 (br, 1H, NHPh), 7.4-6.9 (m, 10H, Ar), 3.79 (q, *J* = 7.0 Hz, 1H, CHCH₃), 1.90 (s, 3H, =C(CH₃)₂), 1.53 (s, 3H, =C(CH₃)₂), 1.10 (d, *J* = 7.0 Hz, 3H, CHCH₃); ¹³C{¹H} NMR (100 MHz, CDCl₃) δ 173.6 (CO), 140.5 (=C(CH₃)₂), 138.5 and 135.0 (Ar), 131.7 (C=C(CH₃)₂), 129.4, 128.6, 127.9, 127.8, 127.3 and 126.4 (Ar), 43.6 (CHCH₃), 22.7 and 20.4 (=C(CH₃)₂), 15.6 (CH₃); GC-MS *m/z* = 279 (M⁺); Anal. Calcd for C₁₉H₂₁NO: C, 81.68; H, 7.58. Found: C, 81.97; H, 7.71.

For **37g**: ¹H NMR (400 MHz, CDCl₃) 7.2-6.8 (m, 10H, Ar), 6.15 (t, *J* = 5.5 Hz, 1H, NHBz), 4.27 (dd, *J* = 5.9, 2.6 Hz, 2H, NHCH₂Ar), 3.62 (q, *J* = 7.2 Hz, 1H, CHCH₃), 1.75 (s, 3H, =C(CH₃)₂), 1.39 (s, 3H, =C(CH₃)₂), 1.01 (d, *J* = 7.2 Hz, 3H, CHCH₃); ¹³C{¹H} NMR (100 MHz, CDCl₃) δ 173.7 (CO), 140.6 (=C(CH₃)₂), 138.6 and 135.1 (Ar), 132.0 (C=C(CH₃)₂), 129.4, 128.6, 127.9, 127.8, 127.3 and 126.4 (Ar), 43.6 (CHCH₃), 22.7 and 20.4 (=C(CH₃)₂), 15.6 (CH₃); GC-MS *m/z* = 279 (M⁺); Anal. Calcd for C₁₉H₂₁NO: C, 81.68; H, 7.58. Found: C, 81.97; H, 7.71.

For (**Z**)-**37h**: ¹H NMR (400 MHz, CDCl₃) δ 7.4-7.1 (m, 5H, Ar), 5.99 (s, 1H, NHCH₃), 5.81 (q, *J* = 6.8 Hz, 1H, =CHCH₃), 3.31 (q, *J* = 7.0 Hz, 1H, CHCH₃), 2.71 (d, *J* = 4.9 Hz, 3H, NHCH₃), 1.62 (d, *J* = 6.8 Hz, 3H, =CHCH₃), 1.32 (d, *J* = 7.0 Hz, 3H, CHCH₃): NOESY δ 3.31 ↔ 1.62 (↔ denotes NOE correlation); ¹³C{¹H} NMR (100 MHz, CDCl₃) δ 174.7 (CO), 141.7 (Ar), 139.6 (C=CHCH₃), 128.7 and 127.3 (Ar), 126.9 (=CHCH₃),

124.0 (Ar), 49.3 (CHCH₃), 26.4 (NHCH₃), 16.4 (=CHCH₃), 15.0 (CHCH₃); GC-MS m/z = 203 (M⁺); Anal. Calcd for C₁₃H₁₇NO: C, 76.81; H, 8.43. Found: C, 76.76; H, 8.27.

For (*E*)-**37h**: ¹H NMR (400 MHz, CDCl₃) δ 7.4-7.1 (m, 5H, Ar), 5.86 (s, 1H, NHCH₃), 5.83 (q, J = 6.8 Hz, 1H, =CHCH₃), 3.30 (q, J = 7.0 Hz, 1H, CHCH₃), 2.78 (d, J = 4.9 Hz, 3H, NHCH₃), 1.63 (d, J = 6.8 Hz, 3H, =CHCH₃), 1.29 (d, J = 7.0 Hz, 3H, CHCH₃): NOESY δ 5.83 ↔ 1.63 (↔ denotes NOE correlation); ¹³C{¹H} NMR (100 MHz, CDCl₃) δ 174.7 (CO), 141.8 (Ar), 139.6 (C=CHCH₃), 128.8 and 127.3 (Ar), 127.0 (=CHCH₃), 124.1 (Ar), 49.4 (CHCH₃), 26.5 (NHCH₃), 16.4 (=CHCH₃), 15.0 (CHCH₃); GC-MS m/z = 203 (M⁺); Anal. Calcd for C₁₃H₁₇NO: C, 76.81; H, 8.43. Found: C, 76.60; H, 8.27.

For **37i**: ¹H NMR (400 MHz, CDCl₃) δ 7.2-6.9 (m, 5H, Ar), 5.72 (br, 1H, NHCH₃), 3.59 (q, J = 7.1 Hz, 1H, CHCH₃), 2.71 (d, J = 4.8 Hz, 3H, NHCH₃), 1.82 (s, 3H, =C(CH₃)CH₂CH₃), 1.75 (q, J = 7.5 Hz, 2H, =C(CH₃)CH₂CH₃), 1.01 (d, J = 7.1 Hz, 3H, CHCH₃), 0.84 (t, J = 7.5 Hz, 3H, =C(CH₃)CH₂CH₃); NOESY δ 3.59 ↔ 1.82 (↔ denotes NOE correlation); ¹³C{¹H} NMR (100 MHz, CDCl₃) δ 174.4 (CO), 140.4 (Ar), 137.3 (C=C(CH₃)CH₂CH₃), 137.3 (Ar), 135.3 (=C(CH₃)CH₂CH₃), 129.3, 128.2 and 126.6 (Ar), 43.0 (CHCH₃), 29.2 (CH₂), 26.6 (NHCH₃), 17.6 (CHCH₃), 15.5 and 13.3 (CH₃); GC-MS m/z = 231 (M⁺); calcd for C₂₅H₂₅NO (M+H)⁺, 232.3460; Found: 232.3487.

For **37j**: ¹H NMR (400 MHz, CDCl₃) δ 7.3-7.0 (m, 5H, Ar), 5.78 (br, 1H, NHCH₃), 3.66 (q, J = 7.2 Hz, 1H, CHCH₃), 2.78 (d, J = 4.9 Hz, 3H, NHCH₃), 1.86 (s, 3H, =C(CH₃)CH₂(CH₂)₂CH₃), 1.82 (m, 2H, =C(CH₃)CH₂(CH₂)₂CH₃), 1.30 (m, 2H, =C(CH₃)CH₂(CH₂)₂CH₃), 1.11 (m, 2H, =C(CH₃)CH₂(CH₂)₂CH₃), 1.06 (d, J = 7.2 Hz, 3H, CHCH₃), 0.75 (t, J = 7.5 Hz, 3H, =C(CH₃)CH₂(CH₂)₂CH₃); NOESY δ 3.66 ↔ 1.86 (↔ denotes NOE correlation); ¹³C{¹H} NMR (100 MHz, CDCl₃) δ 174.4 (CO), 140.5 (C=C(CH₃)CH₂(CH₂)₂CH₃), 136.1 (Ar), 135.8 (=C(CH₃)CH₂(CH₂)₂CH₃), 129.5, 128.4,

128.0 and 126.6 (Ar), 43.8 (CHCH₃), 35.8 and 30.7 (CH₂), 26.6 (NHCH₃), 22.7 (CH₂), 18.1 (CHCH₃), 15.6 and 14.1 (CH₃); GC-MS *m/z* = 259; Anal. Calcd for C₁₇H₂₅NO: C, 78.72; H, 9.71. Found: C, 78.84; H, 9.55.

For **37k**: ¹H NMR (400 MHz, CDCl₃) δ 7.2-6.8 (m, 10H, Ar), 5.48 (br, 1H, NHCH₃), 3.59 (q, *J* = 7.0 Hz, 2H, CHCH₃), 2.67 (t, *J* = 7.4 Hz, 2H, =C(CH₃)CH₂CH₂Ph), 2.64 (d, *J* = 4.8 Hz, 3H, NHCH₃), 2.33 (m, 1H, =C(CH₃)CH₂CH₂Ph), 2.16 (m, 1H, =C(CH₃)CH₂CH₂Ph), 1.89 (s, 3H, CH₃), 1.01 (d, *J* = 7.0 Hz, 3H, =C(CH₃)CH₂CH₂Ph); NOESY δ 3.23 ↔ 1.87 (↔ denotes NOE correlation); ¹³C{¹H} NMR (100 MHz, CDCl₃) δ 174.1 (CO), 141.5 and 140.1 (Ar), 136.1 (C=C(CH₃)CH₂CH₂Ph), 131.0 (=C(CH₃)CH₂CH₂Ph), 129.4, 128.6, 128.3, 128.0, 126.7 and 126.1 (Ar), 43.0 (CHCH₃), 37.0 and 34.0 (CH₂), 26.6 (NHCH₃), 17.8 (CHCH₃), 15.3 (CH₃); GC-MS *m/z*: 307; Anal. Calcd for C₂₁H₂₅NO: C, 82.04; H, 8.20. Found: C, 81.65; H, 8.03.

For **37l**: ¹H NMR (400 MHz, CDCl₃) δ 7.3-7.1 (m, 5H, Ar), 6.61 (br, 1H, NHCH₃), 5.71 (m, 1H, =CH), 5.69 (m, 1H, =CH), 3.14 (m, 1H, CH), 2.97 (dd, *J* = 9.9, 9.8 Hz, 1H, CH), 2.85 (d, *J* = 4.8 Hz, NHCH₃), 2.72 (m, 1H, CH), 2.10 (m, 1H, CH₂), 2.01 (m, 1H, CH₂), 1.83 (m, 1H, CH₂), 1.51 (m, 1H, CH₂), 0.94 (d, *J* = 6.8 Hz, 3H, CHCH₃); ¹³C{¹H} NMR (100 MHz, CDCl₃) δ 177.1 (CO), 140.8 (Ar), 132.5 and 132.2 (CH), 129.6, 127.9 and 126.3 (Ar), 53.6 (CH), 48.8 (CHCH₃), 45.2 (CH), 32.0 and 28.4 (CH₂), 26.4 (NHCH₃), 16.6 (CHCH₃); HRMS (*m/z*): calcd for C₁₆H₂₁NO (M+H)⁺, 244.3570; Found: 244.3534.

For **37m**: ¹H NMR (400 MHz, CDCl₃) δ 7.3-7.1 (m, 5H, Ar), 6.16 (br, 1H, NHCH₃), 5.66 (m, 1H, =CH), 5.58 (m, 1H, =CH), 3.13 (m, 1H, CH), 3.05 (dd, *J* = 9.9, 4.8 Hz, 1H, CH), 2.79 (d, *J* = 4.8 Hz, NHCH₃), 2.76 (m, 1H, CH), 2.10 (m, 1H, CH₂), 2.01 (m, 1H, CH₂), 1.83 (m, 1H, CH₂), 1.51 (m, 1H, CH₂), 0.96 (d, *J* = 7.2 Hz, 3H, CHCH₃); ¹³C{¹H} NMR (100 MHz, CDCl₃) δ 176.8 (CO), 141.8 (Ar), 130.1 and 130.0 (CH), 129.1, 128.2 and

126.4 (Ar), 53.5 (CH), 45.7 (CHCH₃), 45.1 (CH), 37.9 and 37.0 (CH₂), 31.7 (NHCH₃), 15.0 (CHCH₃); HRMS (*m/z*): calcd for C₁₆H₂₁NO (M+H)⁺, 244.3570; Found: 244.3534.

For **37n**: ¹H NMR (400 MHz, CDCl₃) δ 7.30 (dd, *J* = 1.8, 1.1 Hz, 1H, Ar), 6.32 (dd, *J* = 3.2, 1.8 Hz, 1H, Ar), 6.10 (dd, *J* = 3.2, 0.8 Hz, 1H, Ar), 4.10 (m, 2H, OCH₂CH₃), 3.74 (q, *J* = 7.1 Hz, 1H, CHCH₃), 1.87 (s, 3H, =C(CH₃)₂), 1.80 (s, 3H, =C(CH₃)₂), 1.22 (d, *J* = 7.1 Hz, 3H, CHCH₃), 1.15 (t, *J* = 7.1 Hz, OCH₂CH₃); ¹³C{¹H} NMR (100 MHz, CDCl₃) δ 174.6 (CO), 152.9 (=C(CH₃)₂), 140.7 and 135.7 (Ar), 125.2 (CC(CH₃)₂), 110.3 and 108.5 (Ar), 60.5 (OCH₂CH₃), 41.8 (CHCH₃), 23.3 and 22.1 (=C(CH₃)₂), 15.7 (CHCH₃), 14.73 (OCH₂CH₃); GC-MS *m/z* = 222 (M⁺); Anal. Calcd for C₁₃H₁₈O₃: C, 70.24; H, 8.16. Found: C, 70.45; H, 7.97.

For **38e**: ¹H NMR (400 MHz, CDCl₃) δ 7.4-7.1 (m, 10H, Ar), 7.32 (d, *J* = 15.9 Hz, 1H, CH), 6.02 (d, *J* = 15.9 Hz, 1H, CH), 5.97 (br, 1H, NHCH₃), 3.00 (d, *J* = 4.9 Hz, 3H, NHCH₃), 1.79 (s, 3H, CH₃); ¹³C{¹H} NMR (100 MHz, CDCl₃) δ 172.2 (CO), 140.4 (C=C(CH₃)CO), 138.2 and 137.2 (Ar), 133.7 (CH), 133.3 (C=C(CH₃)CO), 129.5, 128.7 and 128.6 (Ar), 128.3 (CH), 127.9, 127.5 and 126.8 (Ar), 26.6 (NHCH₃), 18.6 (CH₃); GC-MS *m/z* = 277 (M⁺); Anal. Calcd for C₁₉H₁₉NO: C, 82.28; H, 6.90. Found: C, 81.98; H, 7.04.

For **38f**: ¹H NMR (400 MHz, CDCl₃) δ 7.4-7.1 (m, 9H, Ar), 7.31 (d, *J* = 15.8 Hz, 1H, CH), 5.96 (d, *J* = 15.9 Hz, 1H, CH), 5.94 (br, 1H, NHCH₃), 2.99 (d, *J* = 4.9 Hz, 3H, NHCH₃), 1.78 (s, 3H, CH₃); ¹³C{¹H} NMR (100 MHz, CDCl₃) δ 171.9 (CO), 140.2 (C=C(CH₃)CO), 137.9 and 135.6 (Ar), 133.5 (CH), 133.3 (C=C(CH₃)CO), 129.3 (Ar), 128.8 (CH), 128.7, 128.6, 128.5, 127.8 and 127.5 (Ar), 26.6 (NHCH₃), 18.5 (CH₃); GC-MS *m/z* = 311 (M⁺); Anal. Calcd for C₁₉H₁₈ClNO: C, 73.19; H, 5.82. Found: C, 73.27; H, 6.00.

For **38g**: ^1H NMR (400 MHz, CDCl_3) δ 7.4-6.8(m, 9H, Ar), 7.18 (d, $J = 15.9$ Hz, 1H, CH), 6.09 (d, $J = 15.9$ Hz, 1H, CH), 5.96 (br, 1H, NHCH_3), 3.75 (s, 3H, OCH_3), 2.98 (d, $J = 4.9$ Hz, 3H, NHCH_3), 1.77 (s, 3H, CH_3); $^{13}\text{C}\{^1\text{H}\}$ NMR (100 MHz, CDCl_3) δ 172.3 (CO), 159.5 (Ar), 140.6 ($\text{C}=\text{C}(\text{CH}_3)\text{CO}$), 138.4 (CH), 133.2, 132.1, 129.5, 128.5 and 128.0 (Ar), 127.4 (CH), 126.3 ($\text{C}=\text{C}(\text{CH}_3)\text{CO}$), 114.1 (Ar), 55.4 (OCH_3), 26.5 (NHCH_3), 18.5 (CH_3); GC-MS $m/z = 307$ (M^+); Anal. Calcd for $\text{C}_{20}\text{H}_{21}\text{NO}_2$: C, 78.15; H, 6.89. Found: C, 77.91; H, 7.02.

For **38h**: ^1H NMR (400 MHz, CDCl_3) δ 7.4-7.0 (m, 9H, Ar), 7.29 (d, $J = 15.9$ Hz, 1H, CH), 6.02 (d, $J = 15.9$ Hz, 1H, CH), 5.92 (br, 1H, 3H, NHCH_3), 3.00 (d, $J = 4.9$ Hz, NHCH_3), 2.30 (s, 3H, PhCH_3), 1.79 (s, 3H, CH_3); $^{13}\text{C}\{^1\text{H}\}$ NMR (100 MHz, CDCl_3) δ 172.3 (CO), 140.6 ($\text{C}=\text{C}(\text{CH}_3)\text{CO}$), 138.3 and 137.9 (Ar), 133.8 (CH), 132.7 ($\text{C}=\text{C}(\text{CH}_3)\text{CO}$), 129.6, 129.5, 128.6 and 127.5 (Ar), 127.4 (CH), 126.7 (Ar), 26.6 (NHCH_3), 21.4 (PhCH_3), 18.6 (CH_3); GC-MS $m/z = 291$ (M^+); Anal. Calcd for $\text{C}_{20}\text{H}_{21}\text{NO}$: C, 82.44; H, 7.26. Found: C, 82.04; H, 7.29.

For **38i**: ^1H NMR (400 MHz, CDCl_3) δ 7.4-7.1 (m, 14H, Ar), 7.31 (d, $J = 15.9$ Hz, 1H, CH), 5.98 (d, $J = 15.9$ Hz, 1H, CH), 5.80 (br, 1H, NHCH_3), 2.93 (d, $J = 4.9$ Hz, NHCH_3), 1.73 (s, 3H, CH_3); $^{13}\text{C}\{^1\text{H}\}$ NMR (100 MHz, CDCl_3) δ 172.2 (CO), 140.7, 140.6 and 140.5 (Ar), 138.2 ($\text{C}=\text{C}(\text{CH}_3)\text{CO}$), 136.3 (Ar), 133.73 (CH), 129.6, 129.1, 129.0 and 128.6 (Ar), 128.4 ($\text{C}=\text{C}(\text{CH}_3)\text{CO}$), 127.6 (CH), 127.5, 127.3, 127.2 and 127.0 (Ar), 26.7 (NHCH_3), 18.7 (CH_3); GC-MS $m/z = 353$ (M^+); Anal. Calcd for $\text{C}_{25}\text{H}_{23}\text{NO}$: C, 84.95; H, 6.56. Found: C, 84.59; H, 6.77.

For **38j**: ^1H NMR (400 MHz, CDCl_3) δ 7.7-7.2 (m, 12H, Ar), 7.39 (d, $J = 15.9$ Hz, 1H, CH), 6.20 (d, $J = 15.9$ Hz, 1H, CH), 6.09 (br, 1H, NHCH_3), 3.01 (d, $J = 4.9$ Hz, 3H,

NHCH₃), 1.82 (s, 3H, CH₃); ¹³C{¹H} NMR (100 MHz, CDCl₃) δ 172.2 (CO), 140.5 (C=C(CH₃)CO), 138.2, 134.7, 133.8 and 133.6 (Ar), 133.3 (CH), 133.1, 129.5, 128.3, 128.1 and 127.7 (Ar), 127.5 (CH), 127.2 and 126.4 (Ar), 126.1 (C=C(CH₃)CO), 123.5 (Ar), 26.6 (NHCH₃), 18.7 (CH₃); GC-MS *m/z* = 327 (M⁺); Anal. Calcd for C₂₃H₂₁NO: C, 84.37; H, 6.46. Found: C, 84.68; H, 6.50.

For **38k**: ¹H NMR (400 MHz, CDCl₃) δ 7.6-7.0 (m, 11H, Ar), 7.41 (d, *J* = 15.9 Hz, 1H, CH), 6.18 (d, *J* = 15.9 Hz, 1H, CH), 5.92 (br, 1H, NHCH₃), 3.98 (s, 3H, OCH₃), 3.05 (d, *J* = 4.9 Hz, 3H, NHCH₃), 1.82 (s, 3H, CH₃); ¹³C{¹H} NMR (100 MHz, CDCl₃) δ 172.3 (CO), 158.0 (Ar), 140.8 (C=C(CH₃)CO), 138.4 and 134.4 (Ar), 134.1 (CH), 132.7, 132.6, 129.7 and 129.6 (Ar), 129.1 (C=C(CH₃)CO), 128.6 (Ar), 127.7 (CH), 127.5, 127.3 and 127.1 (Ar), 55.5 (OCH₃), 26.7 (NHCH₃), 18.7 (CH₃); GC-MS *m/z* = 357 (M⁺); Anal. Calcd for C₂₄H₂₃NO₂: C, 80.64; H, 6.49. Found: C, 80.55; H, 6.59.

For **39a**: ¹H NMR (400 MHz, CDCl₃) δ 7.4-7.2 (m, 4H, Ar), 3.72 (s, 3H, OCH₃), 3.60 (s, 2H, CH₂), 3.39 (s, 2H, CH₂), 2.18 (s, 3H, CH₃); ¹³C{¹H} NMR (100 MHz, CDCl₃) δ 171.7 (CO), 146.0 (C), 142.3 and 142.2 (Ar), 129.8 (C), 126.4, 124.1, 123.4 and 118.5 (Ar), 52.2 (OCH₃), 42.9 and 31.5 (CH₂), 14.3 (CH₃); GC-MS *m/z* = 202 (M⁺); Anal. Calcd for C₁₃H₁₄O₂: C, 77.20; H, 6.98. Found: C, 77.61; H, 6.37.

For **39b**: ¹H NMR (400 MHz, CDCl₃) δ 7.5-7.2 (m, 4H, Ar), 3.73 (s, 3H, OCH₃), 3.60 (s, 2H, CH₂), 3.42 (s, 2H, CH₂), 2.60 (q, *J* = 7.6 Hz, 2H, CH₂), 1.22 (t, *J* = 7.6 Hz, 3H, CH₃); ¹³C{¹H} NMR (100 MHz, CDCl₃) δ 171.7 (CO), 148.3 and 146.0 (Ar), 142.3 and 129.0 (C), 126.4, 124.2, 123.5 and 118.7 (Ar), 52.2 (OCH₃), 40.1, 31.4 and 22.0 (CH₂), 14.3 (CH₃); GC-MS *m/z* = 216 (M⁺); Anal. Calcd for C₁₄H₁₆O₂: C, 77.75; H, 7.46. Found: C, 77.61; H, 7.37.

For **39c**: ^1H NMR (400 MHz, CDCl_3) δ 7.59 (s, 1H, CH), 6.92 (s, 1H, CH), 4.34 (q, $J = 7.1$ Hz, 2H, OCH_2CH_3), 2.91 (d, $J = 7.2$ Hz, 2H, CH_2), 2.76 (m, 4H, CH_2), 2.07 (m, 1H, CH), 1.80 (m, 4H, CH_2), 1.65 (m, 4H, CH_2), 1.53 (m, 4H, CH_2), 1.38 (t, $J = 7.1$ Hz, 3H, OCH_2CH_3); $^{13}\text{C}\{^1\text{H}\}$ NMR (100 MHz, CDCl_3) δ 168.4 (CO), 141.3, 140.8 and 138.5 (C), 132.2 and 131.0 (CH), 127.1 (C), 60.7 (OCH_2CH_3), 42.2 (CH_2), 39.7 (CH), 36.8, 36.3, 33.7, 28.5, 28.4 and 25.0 (CH_2), 14.5 (OCH_2CH_3); HRMS (m/z): calcd for $\text{C}_{20}\text{H}_{28}\text{O}_2$ (M) $^+$, 286.4146; Found: 286.4167.

For **39d**: ^1H NMR (400 MHz, CDCl_3) δ 7.53 (s, 1H, CH), 6.882 (s, 1H, CH), 4.26 (q, $J = 7.1$ Hz, 2H, OCH_2CH_3), 2.84 (d, $J = 7.2$ Hz, 2H, CH_2), 2.70 (m, 4H, CH_2), 1.96 (m, 1H, CH), 1.66 (m, 2H, CH_2), 1.57 (m, 4H, CH_2), 1.43 (m, 4H, CH_2), 1.35 (m, 4H, CH_2), 1.31 (t, $J = 7.1$ Hz, 3H, OCH_2CH_3); $^{13}\text{C}\{^1\text{H}\}$ NMR (100 MHz, CDCl_3) δ 168.2 (CO), 141.6, 140.7, 134 (C), 132.2 and 131.4 (CH), 127.3 (C), 60.7 (OCH_2CH_3), 42.1 (CH_2), 39.8 (CH), 32.7, 29.6, 29.0, 25.0, 23.3 and 23.2 (CH_2), 14.3 (OCH_2CH_3); HRMS (m/z): calcd for $\text{C}_{20}\text{H}_{28}\text{O}_2$ (M) $^+$, 300.4415; Found: 300.4457.

For **39e**: ^1H NMR (400 MHz, CDCl_3) δ 7.62 (s, 1H, CH), 6.96 (s, 1H, CH), 4.34 (q, $J = 7.2$ Hz, 2H, OCH_2CH_3), 2.94 (d, $J = 7.1$ Hz, 2H, CH_2), 2.75 (m, 4H, CH_2), 2.06 (m, 1H, CH), 1.68 (m, 4H, CH_2), 1.64 (m, 4H, CH_2), 1.35 (t, $J = 7.1$ Hz, 3H, OCH_2CH_3), 1.19 (m, 4H, CH_2); $^{13}\text{C}\{^1\text{H}\}$ NMR (100 MHz, CDCl_3) δ 168.5 (CO), 145.5, 141.9 and 135.6 (C), 132.4 and 131.3 (CH), 127.7 (C), 60.7 (OCH_2CH_3), 42.2 (CH_2), 39.9 (CH), 34.2, 32.7, 32.4, 32.3, 32.0, 26.1, 25.9 and 25.0 (CH_2), 14.6 (OCH_2CH_3); HRMS (m/z): calcd for $\text{C}_{21}\text{H}_{30}\text{O}_2$ (M) $^+$, 314.4684; Found: 314.4723.

For **39f**: ^1H NMR (400 MHz, CDCl_3) δ 7.60 (s, 1H, CH), 7.4-7.3 (m, 5H, Ar), 7.08 (s, 1H, CH), 4.09 (q, $J = 7.1$ Hz, 2H, OCH_2CH_3), 2.83 (m, 4H, CH_2), 1.85 (m, 4H, CH_2), 1.00 (t, $J = 7.1$ Hz, 3H, OCH_2CH_3); $^{13}\text{C}\{^1\text{H}\}$ NMR (100 MHz, CDCl_3) δ 169.0 (CO), 141.9,

140.9, 140.9 and 136.4 (C), 131.5 (CH), 130.8, 128.6, 128.4 and 128.0 (Ar), 126.9 (CH), 60.8 (OCH₂CH₃), 29.5, 29.1, 23.3 and 23.2 (CH₂), 13.8 (OCH₂CH₃); HRMS (*m/z*): calcd for C₁₉H₂₀O₂ (M)⁺, 280.3670; Found: 280.3562.

For **39g**: ¹H NMR (400 MHz, CDCl₃) δ 7.50 (s, 1H, CH), 7.3-7.2 (m, 5H, Ar), 7.01 (s, 1H, CH), 3.98 (q, *J* = 7.1 Hz, 2H, OCH₂CH₃), 2.77 (m, 4H, CH₂), 1.76 (m, 2H, CH₂), 1.58 (m, 4H, CH₂), 0.88 (t, *J* = 7.1 Hz, 3H, OCH₂CH₃); ¹³C{¹H} NMR (100 MHz, CDCl₃) δ 169.0 (CO), 147.2, 142.6, 141.8 and 140.5 (C), 131.6 (CH), 130.5, 128.6, 128.5 and 128.4 (Ar), 127.0 (CH), 60.8 (OCH₂CH₃), 36.7, 36.3, 32.7, 28.3 and 28.2 (CH₂), 13.8 (OCH₂CH₃); HRMS (*m/z*): calcd for C₂₀H₂₂O₂ (M)⁺, 294.3939; Found: 294.3948.

For **39h**: ¹H NMR (400 MHz, CDCl₃) δ 7.51 (s, 1H, CH), 7.3-7.2 (m, 5H, Ar), 7.01 (s, 1H, CH), 3.98 (q, *J* = 7.2 Hz, 2H, OCH₂CH₃), 2.70 (m, 4H, CH₂), 1.61 (m, 4H, CH₂), 1.29 (m, 4H, CH₂), 0.88 (t, *J* = 7.2 Hz, 3H, OCH₂CH₃); ¹³C{¹H} NMR (100 MHz, CDCl₃) δ 169.1 (CO), 145.1, 140.5, 139.6 and 138.5 (C), 132.0 (Ar), 131.5 and 130.7 (CH), 127.9, 126.9 and 126.3 (Ar), 60.7 (OCH₂CH₃), 32.3, 32.2, 32.1, 31.9, 26.0 and 25.9 (CH₂), 13.8 (OCH₂CH₃); GC-MS *m/z*: 308; Anal. Calcd for C₂₁H₂₄O₂: C, 81.78; H, 7.84. Found: C, 81.78; H, 7.68.

For **60a**: ¹H NMR (400 MHz, CDCl₃) δ 7.5-7.3 (m, 4H, Ar), 4.30 (q, *J* = 7.1 Hz, 2H, OCH₂CH₃), 3.77 (s, 2H, CH₂), 3.05 (t, *J* = 7.6 Hz, 2H, CH₂CH₂CH₃), 1.70 (m, 2H, CH₂CH₂CH₃), 1.05 (t, *J* = 7.1 Hz, 3H, OCH₂CH₃), 0.91 (t, *J* = 7.5 Hz, 3H, CH₂CH₂CH₃); ¹³C{¹H} NMR (100 MHz, CDCl₃) δ 165.9 (CO), 155.9 ((CH₂)C=C(CO)), 127.5, 126.6, 124.2 and 122.9 (Ar), 121.4 ((CH₂)C=C(CO)), 60.0 (OCH₂CH₃), 39.0, 28.7 and 22.7 (CH₂), 14.2 (OCH₂CH₃); HRMS (*m/z*): calcd for C₁₅H₁₈O₂ (M)⁺, 230.3071; Found: 230.3062.

For **60b**: ^1H NMR (400 MHz, CDCl_3) δ 7.4-7.2 (m, 4H, Ar), 4.19 (q, $J = 7.1$ Hz, 2H, OCH_2CH_3), 2.83 (dd, $J = 7.5, 7.3$ Hz, 2H, CH_2), 2.71 (dd, $J = 7.5, 7.3$ Hz, 2H, CH_2), 2.48 (t, $J = 7.4$ Hz, 2H, $\text{CH}_2\text{CH}_2\text{CH}_3$), 1.56 (m, 2H, $\text{CH}_2\text{CH}_2\text{CH}_3$) 1.05 (t, $J = 7.1$ Hz, 3H, OCH_2CH_3), 0.89 (t, $J = 7.5$ Hz, 3H, $\text{CH}_2\text{CH}_2\text{CH}_3$); $^{13}\text{C}\{^1\text{H}\}$ NMR (100 MHz, CDCl_3) δ 169.4 (CO), 145.0 ($(\text{CH}_2)\text{C}=\text{C}(\text{CO})$), 138.1, 134.8, 128.4, and 127.8 (Ar), 127.7 ($(\text{CH}_2)\text{C}=\text{C}(\text{CO})$), 125.0 (Ar), 60.5 (OCH_2CH_3), 31.3, 28.5, 25.3 and 23.2 (CH_2), 14.5 (OCH_2CH_3); GC-MS m/z : 293; Anal. Calcd for $\text{C}_{16}\text{H}_{20}\text{NO}$: C, 78.65; H, 8.25. Found: C, 78.41; H, 7.99.

For Chapter 4

General Procedure of the Catalytic Reaction. In air, the complex **80** (6 mg, 10 μmol), an alkane substrate (1.0 mmol) and $t\text{-BuOOH}$ (70 wt% in H_2O , 0.43 mL, 3.0 mmol) were dissolved in water (3 mL) in a 25 mL Schlenk tube equipped with a magnetic stirring bar. The reaction mixture was stirred at 20 $^\circ\text{C}$ for 2-24 h. The reaction tube was opened to air and the solution was extracted with CH_2Cl_2 (10 mL). The solution was filtered through a small pad of silica gel. An internal standard (C_6Me_6 , 20 mg) was added to the solution, and the product yield was determined by GC. The ketone product was readily isolated by a column chromatography on silica gel (hexane/EtOAc).

Synthesis of 80. In a 25 mL Schlenk tube equipped with a Teflon stopcock and a magnetic stirring bar, the complex **82** (100 mg, 0.19 mmol), NaBF_4 (90 mg, 0.95 mmol) and $t\text{-BuOOH}$ (5.5 M in decane, 0.42 mL, 1.9 mmol) were dissolved in CH_2Cl_2 (5 mL). The reaction mixture was stirred for 5 h at room temperature. The solvent was removed under vacuum. The residue was recrystallized in $\text{CH}_2\text{Cl}_2/n\text{-hexanes}$ to obtain the product

80 (85 mg, 73% yield). Single crystals of complex **80** suitable for X-ray crystallographic analysis were obtained from CH₂Cl₂/*n*-hexanes solution. The Evans NMR method was used to measure the magnetic moment of the complex by following the experimental procedure described in: Girolami, G. S.; Rauchfuss, T. B.; Angelici, R. J. *Synthesis and Technique in Inorganic Chemistry: A Laboratory Manual*, University Science Books: Sausalito, CA, 1999, pp. 125-126.

For **80**: Anal. Calcd for C₂₀H₂₄BCl₂F₄N₄O₂Ru: C, 39.30; H, 3.96. Found C, 38.70; H, 3.77. $\mu_{\text{eff}} = 1.55 B_M$ at 293 K.

Synthesis of 81. In a glove box, 4,4-dimethyl-2-(2-pyridyl)oxazoline (0.21 g, 1.2 mmol) and [Ru(COD)Cl₂]_x (0.16 g, 0.5 mmol) were dissolved in ClCH₂CH₂Cl (15 mL) in a 25 mL Schlenk tube equipped with a magnetic stirring bar and Teflon stopcock. The reaction tube was brought out of the box, and was stirred in an oil bath at 50 °C for 24 h. After the reaction tube was cooled to room temperature, the volatiles were removed under vacuum, and the residue was recrystallized in CH₂Cl₂/*n*-hexanes to obtain a crude product mixture. The mixture was further purified by flash column chromatography (*n*-hexanes/EtOAc = 4:1) to afford analytically pure product **81** (0.15 g, 65% yield). Single crystals of **81** suitable for X-ray crystallographic analysis were obtained from slow evaporation of CH₂Cl₂ solution.

For **81**: ¹H NMR (400 MHz, CDCl₃) δ 8.05 (ddd, *J* = 5.3, 1.0, 0.7 Hz, py-6-H), 7.86-7.96 (m, 2H, py-3 and 4-H), 7.50 (ddd, *J* = 12.6, 5.3, 2.0 Hz, py-5-H), 5.03 (t, *J* = 2.5 Hz, =CH), 4.52 (t, *J* = 2.6 Hz, =CH), 4.46 (s, 2H, OCH₂), 2.61-2.78 (m, 4H, CH₂), 2.03-2.21 (m, 4H, CH₂), 1.52 (s, 6H, CH₃); ¹³C NMR (100 MHz, CDCl₃) δ 166.6 (N=CO), 150.0,

148.0, 138.2, 128.0 and 126.2 (py), 89.5 and 89.2 (=CH), 82.5 (OCH₂), 70.3 (CCH₃), 30.5 and 29.0 (CH₂), 27.5 (CCH₃); Anal. Calcd for C₁₈H₂₄Cl₂N₂ORu: C, 47.37; H, 5.30. Found: C, 47.13; H, 5.22.

Synthesis of 82. In a glove box, [Ru(COD)Cl₂]_x (0.20 g, 0.44 mmol) and 4,4-dimethyl-2-(2-pyridyl)oxazoline (0.34 g, 1.94 mmol) were dissolved in ClCH₂CH₂Cl (15 mL) in a 25 mL Schlenk tube equipped with a Teflon stopcock and a magnetic stirring bar. The reaction mixture was stirred in an oil bath at 100 °C for 24 h. After cooling to room temperature, the solvent was removed under vacuum. The residue was recrystallized in CH₂Cl₂/*n*-hexanes to obtain a crude product mixture. The product mixture was further purified by flash chromatography (*n*-hexanes/EtOAc = 4:1) to afford analytically pure product **82** (0.30 g, 65% yield). Alternatively, complex **81** (0.20 g, 0.44 mmol) and pymox-Me₂ (0.34 g, 1.94 mmol) were dissolved in ClCH₂CH₂Cl (15 mL) in a 25 mL Schlenk tube. The reaction mixture was stirred in an oil bath at 100 °C for 24 h. After cooling to room temperature, the solvent was removed under vacuum. The residue was purified by flash column chromatography (*n*-hexanes/EtOAc = 4:1) to afford pure product **82** (0.25 g, 55% yield). Single crystals of **82** suitable for X-ray crystallographic analysis were obtained from CH₂Cl₂/*n*-hexanes solution.

For **82**: ¹H NMR (400 MHz, CDCl₃) δ 10.01 and 10.12 (s, py-6-H), 7.83-7.88 and 7.90-7.95 (m, 2H, py-3 and 4-H), 7.53-7.63 and 7.25-7.39 (m, py-5-H), 4.62 and 4.53 (s, OCH₂), 1.15 and 0.65 (s, CCH₃); ¹³C NMR (100 MHz, CDCl₃) δ 166.8 and 166.5 (N=CO), 156.2, 155.2, 151.6, 151.01, 133.1, 132.9, 132.8, 132.6, 126.1 and 124.9 (py), 83.4 and 82.7 (OCH₂), 70.6 and 70.3 (CCH₃), 28.2 and 27.1 (CCH₃); Anal. Calcd for

C₂₀H₂₄Cl₂N₄O₂Ru: C, 45.81; H, 4.61. Found C, 44.92; H, 4.54.

Catalyst Recycling Experiment. The complex **80** (6 mg, 10 μ mol) was charged with ethylbenzene (0.12 mL, 1.0 mmol), *t*-BuOOH (70 wt% in H₂O, 0.43 mL, 3.0 mmol) and H₂O (2.5 mL) in a thick-walled 25 mL Schlenk tube equipped with a magnetic stirring bar. The reaction mixture was stirred for 16 h at 20 °C. After the reaction was completed, the reaction tube was opened to air and the solution was extracted with CH₂Cl₂ (10 mL). The extracted solution was filtered through a small pad of silica gel and analyzed by GC. The second and third runs were repeated by using the same aqueous solution. The product yield as determined by GC.

Hammett Study. In five separate tubes, an equal amount of the complex **80** (6 mg, 10 μ mol), *p*-X-C₆H₄CH₂CH₃ (X = OMe, Me, H, F, Cl) (0.12 mL, 1.0 mmol) and *t*-BuOOH (70 wt% in H₂O, 0.43 mL, 3.0 mmol) were dissolved in H₂O (1.5 mL) and *n*-hexanes (1.0 mL) in a 25 mL Schlenk tube equipped with a magnetic stirring bar in air. The reaction tubes were stirred at 20 °C. A small portion of the aliquot was drawn periodically from the organic layer, and the conversion was determined by GC. The k_{obs} was estimated from a first-order plot of $-\ln([\text{ArCH}_2\text{CH}_3]_t/[\text{ArCH}_2\text{CH}_3]_0)$ vs time.

Isotope Effect Study. In two separate tubes, complex **80** (6 mg, 10 μ mol) was charged with ethylbenzene and ethylbenzene-*d*₁₀ (0.12 mL, 1.0 mmol), *t*-BuOOH (70 wt% in H₂O, 0.43 mL, 3.0 mmol), H₂O (1.5 mL) and *n*-hexanes (1.0 mL) in a 25 mL Schlenk tube equipped with a magnetic stirring bar in air. The reaction tube was stirred at 20 °C.

A small portion of the aliquot was drawn periodically from the organic layer, and the product conversion was determined by GC. The k_{obs} was obtained from a first-order plot of $-\ln([\text{ethylbenzene}]_t/[\text{ethylbenzene}]_0)$ vs time.

Cyclic Voltammetry of 80. In a volumetric flask, the sample solution was prepared by dissolving complex **80** (10 mg, 1.6 mM) and an electrolyte (0.25 M of Bu_4NPF_6) in 10 mL of CH_2Cl_2 . Electrochemical measurements were collected at a scan rate of 200 mV/s from a three three-electrode cell composed of a Ag/AgCl electrolyte, a platinum working electrode, and a glassy carbon counter electrode.

Catalytic Oxidation Reaction of Ethylbenzene with TEMPO. In air, complex **80** (6 mg, 10 μmol) was charged with ethylbenzene (0.12 mL, 1.0 mmol), *t*-BuOOH (70 wt% in H_2O , 0.43 mL, 3.0 mmol), TEMPO (16 mg, 0.1 mmol), H_2O (1.5 mL) and *n*-hexanes (1.0 mL) in a thick-walled 25 mL Schlenk tube equipped with a magnetic stirring bar. The reaction mixture was stirred for 24 h at 20 °C. After the reaction was completed, the reaction tube was opened to air. The solution was extracted with CH_2Cl_2 (10 mL) and organic solution was filtered through a small pad of silica gel. The product yield as determined by GC was 34% (without TEMPO, 40% conversion). It should be noted that *n*-hexanes was added to dissolve TEMPO, and under these biphasic conditions, the reaction rate was considerably lower than in pure water.

Table 19. Crystal Data and Structure Refinement for **30a**.

Empirical formula	$C_{38}H_{55}BCl_2F_4NO_2PRu$
Formula weight	847.58
Temperature	100(2) K
Wavelength	0.7107 Å
Crystal system	Triclinic
Space group	P-1
Unit cell dimensions	$a = 10.23664(13)$ Å $\alpha = 100.1596(12)^\circ$ $b = 12.0713(2)$ Å $\beta = 102.3207(11)^\circ$ $c = 16.7295(2)$ Å $\gamma = 103.8371(12)^\circ$
Volume	1903.84(5) Å ³
Z	2
Density (calculated)	1.479 Mg/m ³
Absorption coefficient	0.649 mm ⁻¹
F(000)	880
Crystal size	0.4281 x 0.2686 x 0.1765 mm ³
Theta range for data collection	3.38 to 37.83°
Index ranges	$-17 \leq h \leq 17$, $-20 \leq k \leq 20$, $-28 \leq l \leq 28$
Reflections collected	95037
Independent reflections	19744 [R(int) = 0.0279]
Absorption correction	Numerical
Max. and min. transmission	0.915 and 0.811
Refinement method	Full-matrix least-squares on F ²
Data / restraints / parameters	19744 / 0 / 487
Goodness-of-fit on F ²	1.004
Final R indices [I > 2σ(I)]	R ₁ = 0.0214, wR ₂ = 0.0609
R indices (all data)	R ₁ = 0.0270, wR ₂ = 0.0625
Largest diff. peak and hole	0.692 and -0.496 e.Å ⁻³

Table 20. Crystal Data and Structure Refinement for **56**.

Empirical formula	C ₄₀ H ₅₉ BCl ₂ F ₄ NO ₃ PRu	
Formula weight	891.63	
Temperature	100(2) K	
Wavelength	0.7107 Å	
Crystal system	Monoclinic	
Space group	C 2	
Unit cell dimensions	a = 25.7127(4) Å	α = 90.00°
	b = 10.6683(2) Å	β = 94.9531(14)°
	c = 15.1324(2) Å	γ = 90.00°
Volume	4135.48 Å ³	
Z	4	
Density (calculated)	1.432 Mg/m ³	
Absorption coefficient	0.603 mm ⁻¹	
F(000)	1856	
Crystal size	0.3531 x 0.2366 x 0.2077 mm ³	
Theta range for data collection	3.35 to 32.83°	
Index ranges	-38 ≤ h ≤ 38, -160 ≤ k ≤ 15, -22 ≤ l ≤ 23	
Reflections collected	34927	
Independent reflections	13807 [R(int) = 0.0323]	
Absorption correction	Numerical	
Refinement method	Full-matrix least-squares on F ²	
Data / restraints / parameters	13807 / 145 / 406	
Goodness-of-fit on F ²	1.075	
Final R indices [I > 2σ(I)]	R ₁ = 0.0474, wR ₂ = 0.1135	
R indices (all data)	R ₁ = 0.0598, wR ₂ = 0.1197	
Largest diff. peak and hole	0.955 and -0.994 e.Å ⁻³	

Table 21. Crystal Data and Structure Refinement for **80**.

Empirical formula	C ₂₁ H ₂₆ BCl ₄ F ₄ N ₄ O ₂ Ru	
Formula weight	696.14	
Temperature	100(2) K	
Wavelength	1.54178 Å	
Crystal system	Monoclinic	
Space group	P 21/c	
Unit cell dimensions	a = 8.35260(10) Å	α = 90°
	b = 28.1943(4) Å	β = 108.2210(10)°
	c = 12.6986(2) Å	γ = 90°
Volume	2840.52(7) Å ³	
Z	4	
Density (calculated)	1.628 Mg/m ³	
Absorption coefficient	8.407 mm ⁻¹	
F(000)	1396	
Crystal size	0.55 x 0.41 x 0.05 mm ³	
θ range for data collection	3.99 to 67.75°	
Index ranges	-9 ≤ h ≤ 9, 0 ≤ k ≤ 33, 0 ≤ l ≤ 15	
Reflections collected	23226	
Independent reflections	5024 [R(int) = 0.0211]	
Completeness to θ = 67.75°	97.6 %	
Absorption correction	Numerical	
Max. and min. transmission	0.6786 and 0.0905	
Refinement method	Full-matrix least-squares on F ²	
Data / restraints / parameters	5024 / 9 / 370	
Goodness-of-fit on F ²	0.969	
Final R indices [I > 2σ(I)]	R ₁ = 0.0478, wR ₂ = 0.1237	
R indices (all data)	R ₁ = 0.0489, wR ₂ = 0.1245	
Largest diff. peak and hole	1.507 and -1.065 e.Å ⁻³	

Table 22. Crystal Data and Structure Refinement for **81**.

Empirical formula	$C_{18.5}H_{25}C_{13}N_2ORu$	
Formula weight	498.83	
Temperature	100(2) K	
Wavelength	1.54178 Å	
Crystal system	Monoclinic	
Space group	P21/c	
Unit cell dimensions	$a = 16.4410(4)$ Å	$\alpha = 90^\circ$
	$b = 9.8816(3)$ Å	$\beta = 110.3760(10)^\circ$
	$c = 12.8838(3)$ Å	$\gamma = 90^\circ$
Volume	$1962.17(9)$ Å ³	
Z	4	
Density (calculated)	1.689 Mg/m ³	
Absorption coefficient	10.305 mm ⁻¹	
F(000)	1012	
Crystal size	0.50 x 0.44 x 0.32 mm ³	
θ range for data collection	5.32 to 67.53°	
Index ranges	$-19 \leq h \leq 17, 0 \leq k \leq 11, 0 \leq l \leq 15$	
Reflections collected	16178	
Independent reflections	3383 [R(int) = 0.0305]	
Completeness to $\theta = 67.53^\circ$	95.6 %	
Absorption correction	Numerical	
Max. and min. transmission	0.1371 and 0.0791	
Refinement method	Full-matrix least-squares on F ²	
Data / restraints / parameters	3383 / 0 / 332	
Goodness-of-fit on F ²	1.115	
Final R indices [$I > 2\sigma(I)$]	$R_1 = 0.0211, wR_2 = 0.0516$	
R indices (all data)	$R_1 = 0.0212, wR_2 = 0.0517$	
Extinction coefficient	0.00074(5)	
Largest diff. peak and hole	0.639 and -0.452 e.Å ⁻³	

Table 23. Crystal Data and Structure Refinement for **82**.

Empirical formula	$C_{20}H_{24}C_{12}N_4O_{2.14}Ru$	
Formula weight	526.68	
Temperature	100(2) K	
Wavelength	1.54178 Å	
Crystal system	Monoclinic	
Space group	P 21/c	
Unit cell dimensions	$a = 10.72140(10)$ Å	$\alpha = 90^\circ$
	$b = 14.1607(2)$ Å	$\beta = 97.3240(10)^\circ$
	$c = 14.6702(2)$ Å	$\gamma = 90^\circ$
Volume	2209.09(5) Å ³	
Z	4	
Density (calculated)	1.584 Mg/m ³	
Absorption coefficient	8.173 mm ⁻¹	
F(000)	1069	
Crystal size	0.29 x 0.15 x 0.10 mm ³	
θ range for data collection	4.16 to 68.00°	
Index ranges	$-12 \leq h \leq 12, 0 \leq k \leq 16, 0 \leq l \leq 17$	
Reflections collected	18294	
Independent reflections	3921 [R(int) = 0.0163]	
Completeness to $\theta = 68.00^\circ$	97.6 %	
Absorption correction	Numerical	
Max. and min. transmission	0.4954 and 0.2003	
Refinement method	Full-matrix least-squares on F ²	
Data / restraints / parameters	3921 / 0 / 272	
Goodness-of-fit on F ²	0.981	
Final R indices [I > 2 σ (I)]	$R_1 = 0.0194, wR_2 = 0.0513$	
R indices (all data)	$R_1 = 0.0197, wR_2 = 0.0515$	
Extinction coefficient	0.00020(3)	
Largest diff. peak and hole	0.405 and -0.295 e.Å ⁻³	

References

- (1) Recent reviews: (a) Ritleng, V.; Sirlin, C.; Pfeffer, M. *Chem. Rev.* **2002**, *102*, 1731. (b) Kakiuchi, F.; Murai, S. In *Activation of Unreactive Bonds and Organic Synthesis*; Murai, S. Ed.; Springer: New York, 1999. (c) Chen, X.; Engle, K. M.; Wang, D.-H.; Yu, J.-Q. *Angew. Chem., Int. Ed.* **2009**, *48*, 5094–5115. (d) Colby, D. A.; Bergman, R. G.; Ellman, J. A. *Chem. Rev.* **2010**, *110*, 624–655. (e) Lyons, T. W.; Sanford, M. S. *Chem. Rev.* **2010**, *110*, 1147–1169.
- (2) (a) Heck, R. F. In *Comprehensive Organic Synthesis*; Trost, B. M., Fleming, I., Eds.; Pergamon Press: Oxford, 1991; Vol. 4. (b) Beletskaya, I. P.; Cheprakov, A. V. *Chem. Rev.* **2000**, *100*, 3009–3066.
- (3) Murai, S.; Kakiuchi, F.; Sekine, S.; Tanaka, Y.; Kamatani, A.; Sonoda, M.; Chatani, N. *Nature* **1993**, *366*, 529.
- (4) (a) Murai, S.; Kakiuchi, F.; Sekine, S.; Tanaka, Y.; Kamatani, A.; Sonoda, M.; Chatani, N. *Pure Appl. Chem.* **1994**, *66*, 1527. (b) Trost, B. M.; Imi, K.; Davies, I. W. *J. Am. Chem. Soc.* **1995**, *117*, 5371. (c) Kakiuchi, F.; Sekine, S.; Tanaka, Y.; Kamatani, A.; Sonoda, M.; Chatani, N.; Murai, S. *Bull. Chem. Soc. Jpn.* **1995**, *68*, 62. (d) Sonoda, M.; Kakiuchi, F.; Chatani, N.; Murai, S. *J. Organomet. Chem.* **1995**, *504*, 151. (e) Kakiuchi, F.; Tanaka, Y.; Sato, T.; Chatani, N.; Murai, S. *Chem. Lett.* **1995**, 679. (f) Sonoda, M.; Kakiuchi, F.; Kamatani, A.; Chatani, N.; Murai, S. *Chem. Lett.* **1996**, 109. (g) Kakiuchi, F.; Yamauchi, M.; Chatani, N.; Murai, S. *Chem. Lett.* **1996**, 111.
- (5) (a) Guo, H.; Huang, D.; Weber, W. P. *Polym. Prep.* **1999**, *40*, 70. (b) Londergan, T. M.; Teng, C. J.; Weber, W. P. *Polym. Prep.* **1999**, *40*, 154. (c) Gupta, S.; Londergan, T. M.; Paulasaari, J. K.; Sargent, J. R.; Weber, W. P. *Polym. Mater. Sci. Eng.* **1999**, *80*, 445.
- (6) (a) Harris, P. W. R.; Woodgate, P. D. *J. Organomet. Chem.* **1996**, *506*, 339. (b) Harris, P. W. R.; Woodgate, P. D. *J. Organomet. Chem.* **1997**, *530*, 211. (c) Harris, P. W. R.; Richard, C. E. F.; Woodgate, P. D. *J. Organomet. Chem.* **1999**, *589*, 168.

- (7) (a) Lim, Y.-G.; Kim, Y. H.; Kang, J.-B. *J. Chem. Soc., Chem. Commun.* **1994**, 2267. (b) Lim, Y.-G.; Kang, J.-B.; Kim, Y. H. *J. Chem. Soc., Perkin Trans. I* **1996**, 2201. (c) Lim, Y.-G.; Kang, J.-B.; Kim, Y. H. *Chem. Commun.* **1996**, 585. (d) Lim, Y.-G.; Kang, J.-B.; Kim, Y. H. *J. Chem. Soc., Perkin Trans. I* **1998**, 699. (e) Lim, Y.-G.; Kang, J.-B.; Koo, B. T. *Tetrahedron Lett.* **1999**, 40, 7691.
- (8) Lenges, C. P.; Brookhart, M. *J. Am. Chem. Soc.* **1999**, 121, 6616.
- (9) Guari, Y.; Sabo-Etienne, S.; Chaudret, B. *J. Am. Chem. Soc.* **1998**, 120, 4228.
- (10) (a) Busch, S.; Leitner, W. *Chem. Commun.* **1999**, 2305. (b) Busch, S.; Leitner, W. *Adv. Synth. Catal.* **2001**, 343, 192.
- (11) (a) Halbritter, G.; Knoch, F.; Wolski, A.; Kisch, H. *Angew. Chem., Int. Ed. Engl.* **1994**, 33, 1603. (b) Halbritter, G.; Knoch, F.; Kisch, H. *J. Organomet. Chem.* **1995**, 492, 87. (c) Aulwurm, U. R.; Melchinger, J. U.; Kisch, H. *Organometallics* **1995**, 14, 3385. (d) Durr, U.; Henemann, F. W.; Kisch, H. *J. Organomet. Chem.* **1997**, 541, 307.
- (12) Jun, C.-H.; Hong, J.-B.; Kim, Y.-H.; Chung, K.-W. *Angew. Chem., Int. Ed.* **2000**, 39, 3440.
- (13) Tan, K. L.; Bergman, R. G.; Ellman, J. A. *J. Am. Chem. Soc.* **2001**, 123, 2685.
- (14) Chen, H.; Schlecht, S.; Semple, T. C.; Hartwig, J. F. *Science* **2000**, 287, 1995.
- (15) (a) Wasa, M.; Engle, K. M.; Yu, J.-Q. *J. Am. Chem. Soc.* **2010**, 132, 3680. (b) Yoo, E. J.; Wasa, M.; Yu, J.-Q. *J. Am. Chem. Soc.* **2010**, 132, 17378.
- (16) (a) Tan, K. L.; Bergman, R. G.; Ellman, J. A. *J. Am. Chem. Soc.* **2001**, 123, 2685. (b) Thalji, R. K.; Ahrendt, K. A.; Bergman, R. G.; Ellman, J. A. *J. Am. Chem. Soc.* **2002**, 124, 13964.
- (17) Jones, W. D.; Feher, F. J. *Organometallics* **1983**, 2, 562.
- (18) Liu, F.; Pak, E. B.; Singh, B.; Jensen, C. M.; Goldman, A. S. *J. Am. Chem. Soc.* **1999**, 121, 4086.
- (19) Renkema, K. B.; Kissin, Y. V.; Goldman, A. S. *J. Am. Chem. Soc.* **2003**, 126, 7770.
- (20) Yi, C. S.; Lee, D. W. *Organometallics* **2009**, 28, 4266.

- (21) Li, Z.; Li, C. *J. Am. Chem. Soc.* **2002**, *126*, 11810.
- (22) Davies, H.; Hansen, T.; Churchill, M. R. *J. Am. Chem. Soc.* **2000**, *122*, 3063.
- (23) Oi, S.; Ogino, Y.; Fukita, S.; Inoue, Y. *Org. Lett.* **2002**, *4*, 1783.
- (24) Martinez, R.; Simon, M.-O.; Chevalier, R.; Pautigny, C.; Genet, J.-P.; Darses, S. *J. Am. Chem. Soc.* **2009**, *131*, 7887.
- (25) Patureau, F. W.; Glorius, F. *J. Am. Chem. Soc.* **2010**, *132*, 9982.
- (26) Patureau, F. W.; Besset, T.; Glorius, F. *Angew. Chem. Int. Ed.* **2011**, *50*, 1064.
- (27) Wang, X.; Lu, Y.; Dai, H.-X.; Yu, J.-Q. *J. Am. Chem. Soc.* **2010**, *132*, 12203.
- (28) Kalyani, D.; Sanford, M. S. *Org. Lett.* **2005**, *7*, 4149.
- (29) Jia, C.; Piao, D.; Oyamada, J.; Lu, W.; Kitamura, T.; Fujiwara, Y. *Science* **2000**, *287*, 1992.
- (30) Weissman, H.; Song, X.; Milstein, D. *J. Am. Chem. Soc.* **2001**, *123*, 337.
- (31) Cho, J.-Y.; Tse, M. K.; Holmes, D.; Maleczka Jr., R. E.; Smith, M. R. *Science* **2002**, *295*, 305.
- (32) Tsukada, N.; Hartwig, J. F. *J. Am. Chem. Soc.* **2005**, *127*, 5022.
- (33) Jun, C.-H.; Moon, C. W.; Kim, Y.-M.; Lee, H.; Lee, J. H. *Tetrahedron Lett.* **2002**, *43*, 5604.
- (34) Colby, D. A.; Bergman, R. G.; Ellman, J. A. *J. Am. Chem. Soc.* **2006**, *128*, 5604.
- (35) DeBoef, B.; Pastine, S. J.; Sames, D. *J. Am. Chem. Soc.* **2004**, *126*, 6556.
- (36) Pastine, S. J.; Gribkov, D. V.; Sames, D. *J. Am. Chem. Soc.* **2006**, *128*, 14220.
- (37) Chatani, N.; Asaumi, T.; Yorimitsu, S.; Ikeda, T.; Kakiuchi, F.; Murai, S. *J. Am. Chem. Soc.* **2001**, *123*, 10935.
- (38) Yi, C. S.; Yun, S. Y. *Organometallics* **2004**, *23*, 5392.
- (39) Liu, C.; Han, X.; Wang, X.; Widenhofer, R. A. *J. Am. Chem. Soc.* **2004**, *126*, 3700.
- (40) Liu, C.; Widenhofer, R. A. *J. Am. Chem. Soc.* **2004**, *126*, 10250.
- (41) Wang, X.; Lane, B. S.; Sames, D. J. *J. Am. Chem. Soc.* **2005**, *127*, 4996.
- (42) Li, Z.; Li, C.-J. *J. Am. Chem. Soc.* **2005**, *127*, 6968.

- (43) Moore, E. J.; Pretzer, W. R.; O'Connell, T. J.; Harris, J.; LaBounty, L.; Chou, L.; Grimmer, S. S. *J. Am. Chem. Soc.* **1992**, *114*, 5888.
- (44) Murakami, M.; Hori, S. *J. Am. Chem. Soc.* **2003**, *125*, 4720.
- (45) Matsuura, Y.; Tamura, M.; Kochi, T.; Sato, M.; Chatani, N.; Kakiuchi, F. *J. Am. Chem. Soc.* **2007**, *129*, 9858.
- (46) Cho, S. H.; Hwang, S. J.; Chang, S. *J. Am. Chem. Soc.* **2008**, *130*, 9254.
- (47) Gao, K.; Yoshikai, N. *J. Am. Chem. Soc.* **2011**, *133*, 400.
- (48) Tsujita, H.; Ura, Y.; Matsuki, S.; Wada, K.; Mitsudo, T.; Kondo, T. *Angew. Chem. Int. Ed.* **2007**, *46*, 5160.
- (49) Inoue, S.; Shiota, H.; Fukumoto, Y.; Chatani, N. *J. Am. Chem. Soc.* **2009**, *131*, 6898.
- (50) Tsuchikama, K.; Kasagawa, M.; Endo, K.; Shibata, T. *Org. Lett.* **2009**, *11*, 1821.
- (51) Shibata, Y.; Otake, Y.; Hirano, M.; Tanaka, K. *Org. Lett.* **2009**, *11*, 689.
- (52) Tsai, A. S.; Brasse, M.; Bergman, R. G.; Ellman, J. A. *Org. Lett.* **2011**, *13*, 540.
- (53) Wang, F.; Song, G.; Li, X. *Org. Lett.* **2010**, *12*, 5430.
- (54) Rakshit, S.; Patureau, F. W.; Glorius, F. *J. Am. Chem. Soc.* **2010**, *132*, 9585.
- (55) Jia, C.; Kitamura, T.; Fujiwara, Y. *Acc. Chem. Res.* **2001**, *34*, 633
- (56) (a) Dick, A. R.; Hull, K. L.; Sanford, M. S. *J. Am. Chem. Soc.* **2004**, *126*, 2300. (b) Wan, X.; Ma, Z.; Li, B.; Zhang, K.; Cao, S.; Zhang, S.; Shi, Z. *J. Am. Chem. Soc.* **2006**, *128*, 7416. (c) Thu, H.-Y.; Yu, W.-Y.; Che, C.-M. *J. Am. Chem. Soc.* **2006**, *128*, 9048.
- (57) (a) Stuart, D. R.; Fagnou, K. *Science* **2007**, *316*, 1172. (b) Stuart, D. R.; Villemure, E.; Fagnou, K. *J. Am. Chem. Soc.* **2007**, *129*, 12072. (c) Campeau, L.-C.; Schipper, D. J.; Fagnou, K. *J. Am. Chem. Soc.* **2008**, *130*, 3266.
- (58)(a) Boele, D. K. M.; van Strijdonck, G. P. F.; de Vries, A. H. M.; Kamer, P. C. J.; de Vries, J. G.; van Leeuwen, P. W. N. M. *J. Am. Chem. Soc.* **2002**, *124*, 1586. (b) Beck, E. M.; Grimster, N. P.; Hatley, R.; Gaunt, M. J. *J. Am. Chem. Soc.* **2006**, *128*, 2528. (c) Matsuura, Y.; Tamura, M.; Kochi, T.; Sato, M.; Chatani, N.; Kakiuchi, F. *Am. Chem. Soc.* **2007**, *129*, 9858. (d) Cai, G.; Fu, Y.; Wan, X.; Shi, Z. *Am. Chem. Soc.* **2007**, *129*,

7666. (e) Cho, S. H.; Hwang, S. J.; Chang, S. *J. Am. Chem. Soc.* **2008**, *130*, 9254. (f) Tsuchikama, K.; Kasagawa, M.; Endo, K.; Shibata, T. *Org. Lett.* **2009**, *11*, 1821. (g) Wu, J.; Cui, X.; Chen, L.; Jiang, G.; Wu, Y. *J. Am. Chem. Soc.* **2009**, *131*, 13888. (h) Patureau, F. W.; Glorius, F. *J. Am. Chem. Soc.* **2010**, *132*, 9982.
- (59) Wang, D.-H.; Engle, K. M.; Shi, B.-F.; Yu, J.-Q. *Science* **2010**, *327*, 315.
- (60) (a) Yi, C. S.; Lee, D. W. *Organometallics* **2009**, *28*, 4266. (b) Yi, C. S.; Lee, D. W. *Organometallics* **2010**, *29*, 1883. (c) Yi, C. S.; Zeczycki, T. N.; Guzei, I. A. *Organometallics* **2006**, *25*, 1047.
- (61) (a) Yi, C. S.; Lee, D. W.; Chen, Y. *Organometallics* **1999**, *18*, 2043. (b) Yi, C. S.; He, Z.; Lee, D. W.; Rheingold, A. L.; Lam, K.-C. *Organometallics* **2000**, *19*, 2036. (c) Yi, C. S.; He, Z.; Lee, D. W. *Organometallics* **2001**, *20*, 802.
- (62) (a) Singleton, D. A.; Thomas, A. A. *J. Am. Chem. Soc.* **1995**, *117*, 9357. (b) Frantz, D. E.; Singleton, D. A.; Snyder, J. P. *J. Am. Chem. Soc.* **1997**, *119*, 3383.
- (63) Melander, L.; Saunders, W. H., Jr. *Reaction Rates of Isotopic Molecules*; Wiley: New York, 1980, pp 95-102.
- (64) (a) Jazzar, R. F. R.; Mahon, M. F.; Whittlesey, M. K. *Organometallics* **2001**, *20*, 3745. (b) Drouin, S. D.; Amoroso, D.; Yap, G. P. A.; Fogg, D. E. *Organometallics* **2002**, *21*, 1042.
- (65) (a) Ueno, S.; Mizushima, E.; Chatani, N.; Kakiuchi, F. *J. Am. Chem. Soc.* **2006**, *128*, 16516. (b) Giri, R.; Lam, J. K.; Yu, J.-Q. *J. Am. Chem. Soc.* **2010**, *132*, 686.
- (66) (a) Lu, P.; Paulasaari, J.; Jin, K.; Bau, R.; Weber, W. P. *Organometallics* **1998**, *17*, 584. (b) Lenges, C. P.; Brookhart, M. *J. Am. Chem. Soc.* **1999**, *121*, 6616.
- (67) (a) Stoutland, P. O.; Bergman, R. G. *J. Am. Chem. Soc.* **1985**, *107*, 4581. (b) Renkema, K. B.; Kissin, Y. V.; Goldman, A. S. *J. Am. Chem. Soc.* **2003**, *125*, 7770.
- (68) Recent review: (a) Flynn, A. B.; Ogilvie, W. W. *Chem. Rev.* **2007**, *107*, 4698. (b) Arai, T.; Suemitsu, Y. *Pure Appl. Chem.* **2010**, *82*, 1458.

- (69) (a) Negishi, E.; Huang, Z.; Wang, G.; Mohan, S.; Wang, C.; Hattori, H. *Acc. Chem. Res.* **2008**, *41*, 1474. (b) Itami, K.; Kamei, T.; Yoshida, J. *J. Am. Chem. Soc.* **2003**, *125*, 14670.
- (70) (a) Hojo, D.; Noguchi, K.; Tanaka, K. *Angew. Chem., Int. Ed.* **2009**, *48*, 8129. (b) Ni, Y.; Kassab, R. M.; Chevliakov, M. V.; Montgomery, J. *J. Am. Chem. Soc.* **2009**, *131*, 17714.
- (71) (a) Stüdemann, T.; Knochel, P. *Angew. Chem.* **1997**, *109*, 132. (b) Itami, K.; Kamei, T.; Yoshida, J.-I. *J. Am. Chem. Soc.* **2003**, *125*, 14670. (c) Lemay, A. B.; Vulic, K. S.; Ogilvie, W. W. *J. Org. Chem.* **2006**, *71*, 3615.
- (72) (a) Zhou, C.; Larock, R. C. *J. Org. Chem.* **2005**, *70*, 3765. (b) Zhou, C.; Larock, R. C. *J. Org. Chem.* **2006**, *71*, 3184. (c) McKinley, N. F.; O'Shea, D. F. *J. Org. Chem.* **2006**, *71*, 9552.
- (73) (a) Berlin, J. M.; Campbell, K.; Ritter, T.; Funk, T. W.; Chlenov, A.; Grubbs, R. H. *Org. Lett.* **2007**, *9*, 1339. (b) Stenne, B.; Timperio, J.; Savoie, J.; Dudding T.; Collins, S. K. *Org. Lett.* **2010**, *12*, 2032. (c) Gansäuer, A.; Pierobon, M.; Bluhm, H. *Angew. Chem. Int. Ed.* **2002**, *114*, 3341.
- (74) (a) Berlin, J. M.; Campbell, K.; Ritter, T.; Funk, T. W.; Chlenov, A.; Grubbs, R. H. *Org. Lett.* **2007**, *9*, 1339. (b) Vorfalt, T.; Leuthäüßer, S.; Plenio, H. *Angew. Chem. Int. Ed.* **2009**, *48*, 5191. (c) Stenne, B.; Timperio, J.; Savoie, J.; Dudding, T.; Collins, S. K. *Org. Lett.* **2010**, *12*, 2032. (d) Donohoe, T. J.; Race, N. J.; Bower, J. F.; Callens, C. K. *Org. Lett.* **2010**, *12*, 4094.
- (75) (a) Ho, C.-Y.; Ohmiya, H.; Jamison, T. F. *Angew. Chem. Int. Ed.* **2008**, *47*, 1893. (b) Matsubara, R.; Jamison, T. F. *J. Am. Chem. Soc.* **2010**, *132*, 6880. (c) Ogoshi, S.; Hada,

T.; Ohashi, M. *J. Am. Chem. Soc.* **2009**, *131*, 10350. (d) Li, W.; Chen, N.; Montgomery, J. *Angew. Chem. Int. Ed.* **2010**, *49*, 8712.

(76) Recent review: (a) Derien, S.; Monnier, F.; Dixneuf, P. H. In *Ruthenium Catalysts and Fine Chemistry*; Bruneau, C.; Dixneuf, P. H. Ed.; Springer: Berlin, 2004. (b) Yamamoto, Y.; Itoh, K. In *Ruthenium in Organic Synthesis*; Murahashi, S.-I. Ed.; Wiley-VCH: Weinheim, 2004. (c) Kakiuchi, F.; Murai, S. In *Activation of Unreactive Bonds and Organic Synthesis*; Murai, S. Ed.; Springer: New York, 1999. (d) Colby, D. A.; Bergman, R. G.; Ellman, J. A. *Chem. Rev.* **2010**, *110*, 624-655. (e) Beccalli, E. M.; Broggini, G.; Martinelli, M.; Sottocornola, S. *Chem. Rev.* **2007**, *107*, 5318-5365. (f) Ritleng, V.; Sirlin, C.; Pfeffer, M. *Chem. Rev.* **2002**, *102*, 1731-1770. (g) Trost, B. M.; Toste, D.; Pinkerton, A. B. *Chem. Rev.* **2001**, *101*, 2067-2098. (h) Jang, H.-Y.; Krische, M. J. *Acc. Chem. Res.* **2004**, *37*, 653-601.

(77) (a) Yi, C. S.; Lee, D. W. *Organometallics* **2009**, *28*, 4266-4268. (b) Yi, C. S.; Lee, D. W. *Organometallics* **2010**, *29*, 1883-1885. (c) Kwon, K.-H.; Lee, D. W.; Yi, C. S. *Organometallics* **2010**, *29*, 5748-5750. (d) Kwon, K.-H.; Lee, D. W.; Yi, C. S. *Angew. Chem. Int. Ed.* **2011**, *50*, 1692-1695.

(78) (a) Sheldon, R. A.; Kochi, J. K. *Metal-Catalyzed Oxidations of Organic Compounds*; Academic Press: New York, 1981; (b) Shilov, A. E. *Activation of Saturated Hydrocarbons by Transition Metal Complexes*; Reidel: Dordrecht, The Netherlands, 1984. (c) Hill, C. L.; *Activation and Functionalization of Alkanes*; Wiley: New York, 1989. (d) Shilov, A. F.; Shulpin, G. A. *Chem. Rev.* **1997**, *97*, 2879.

- (79) (a) Hill, C. L. *Activation and Functionalization of Alkanes*; Wiley: New York, 1989.
(b) Haines, A. H. *Methods for the Oxidation of Organic Compounds, Alkanes, Alkenes Alkynes and Arenes*; Academic Press: London, 1985, Chapter 2.
- (80) Murahashi, S. I.; Komiya, N.; Oda, Y.; Kuwabara, T.; Noto, T. *J. Org. Chem.* **2000**, *65*, 9186.
- (81) Blake, R. C., II; Coon, M. J. *J. Biol. Chem.* **1981**, *256*, 12127.
- (82) Khanna, R. K.; Pauling, T. M.; Vajpayee, D. *Tetrahedron Lett.* **1991**, *32*, 3759.
- (83) (a) Sakurai, H.; Hosomi, A. *J. Am. Chem. Soc.* **1967**, *89*, 458. (b) Walling, C.; McGuinness, J. A. *J. Am. Chem. Soc.* **1969**, *91*, 2053.
- (84) Russell, G. A. *Free Radicals*; Kochi, J. K., Ed.; Wiley: New York, 1973; Vol. 1, pp 275-331.
- (85) Hjelmeland, L. M.; Aronow, L.; Trudell, J. R. *Biochem. Biophys. Res. Commun.* **1977**, *76*, 541.
- (86) Kim, J.; Harrison, R. G.; Kim, C.; Que, L., Jr. *J. Am. Chem. Soc.* **1996**, *118*, 4373.
- (87) Che, C. M.; Cheng, K. W.; Chan, M. C. W.; Lau, T. C.; Mak, C. K. *J. Org. Chem.* **2000**, *65*, 7996.
- (88) Goldstein, A. S.; Beer, R. H.; Drago, R. S. *J. Am. Chem. Soc.* **1994**, *116*, 2424.
- (89) (a) Doyle, M. P.; Catino, A. J.; Forslund, R. J. *J. Am. Chem. Soc.* **2004**, *126*, 13622.
- (90) (a) Bartlett, P. D.; Gunther, P. *J. Am. Chem. Soc.* **1966**, *88*, 3288. (b) Bartlett, P. D.; Guaraldi, G. *J. Am. Chem. Soc.* **1967**, *89*, 4799.
- (91) (a) Kochi, J. K. *Tetrahedron* **1962**, *18*, 483. (b) Kochi, J. K.; Mains, H. E. *J. Org. Chem.* **1965**, *30*, 1862. (c) Minisci, F. *Acc. Chem. Res.* **1975**, *8*, 165. (d) Araneo, S.; Fontana, F.; Minisci, F.; Recupero, F.; Serri, A. *Chem. Commun.* **1995**, 1399. (e) Minisci,

F.; Fontana, F.; Araneo, S.; Recupero, F.; Banfi, S.; Quici, S. *J. Am. Chem. Soc.* **1995**, *117*, 226.

(92) White, M. C.; Chen, M. C. *Science*. **2007**, *318*, 783.

(93) Crabtree, R. H. *The Organometallic Chemistry of Transition Metals*; 3rd Ed.; Wiley International, New York, 2005.

(94) Cornil, B.; Herrmann, W. A. *Catalysis from A to Z*; Schlogl, R., Ed.; John Wiley & Sons, 2008.

(95) Li, C. J. *Acc. Chem. Res.*, 2002, *35*, 533.

(96) Herrerias, C. I.; Yao, X.; Li, Z.; Li, C. J. *Chem. Rev.* **2007**, *107*, 2546.

(97) (a) Lersch, M.; Tilset, M. *Chem. Rev.* **2005**, *105*, 2471. (b) *Activation of Small Molecules*; William B. Tolman., Eds.; Wiley-VCH: Weinheim, 2006. (c) Periana, R. A.; Taube, D. J.; Gamble, S.; Taube, H.; Satoh, T.; Fujii, H. *Science* **1998**, *280*, 560.

(98) Le Bras, J.; Muzart, J. *Tetrahedron Lett.* **2002**, *43*, 431.

(99) Sun, W.; Wang, H.; Xia, C.; Li, J.; Zhao, P. *Angew. Chem. Int. Ed.* **2003**, *42*, 1042.

(100) Wei, C.; Li, C.-J. *J. Am. Chem. Soc.* **2002**, *124*, 5638.

(101) Hirai, Y.; Kojima, T.; Mizutani, Y.; Shiota, Y.; Yoshizawa, K.; Fukuzumi, S. *Angew. Chem. Int. Ed.* **2008**, *47*, 1.

(102) Doyle, M. P.; Choi, H. *Org. Lett.* **2007**, *9*, 5349.

(103) Mchaughlin, E. C.; Doyle, M. P. *J. Org. Chem.* **2008**, *73*, 4317.

(104) Che, C. M.; Jiang, G.; Chen, J.; Thu, H. Y.; Huang, J. S.; Zhu, N. *Angew. Chem. Int. Ed.* **2008**, *47*, 1.

(105) Cornil, B.; Herrmann, W. A. *Catalysis from A to Z*; Schlogl, R., Ed.; John Wiley & Sons, 2008.

- (106) Brunner, H.; Obermann, U.; Wimmer, P. *J. Organomet. Chem.* **1986**, *316*, C1.
- (107) McManus, H.; Guiry, P. J. *Chem. Rev.* **2004**, *104*, 4151.
- (108) For examples of Ru(III)-porphyrin complexes in alkane oxidation reactions, see:
Ohtake, H.; Higuchi, T.; and Hirobe, M. *J. Am. Chem. Soc.* **1992**, *114*, 10660-10662. (b)
Groves, J. T.; Bonchio, M.; Carofiglio, T.; Shalyaev, K. *J. Am. Chem. Soc.* **1996**, *118*,
8961-8962.
- (109) Kher, S. M.; Kulkarni, G. H. *Indian J. Chem. Section B* **1989**, *28B*, 675.
- (110) Oku, A.; Abe, M.; Iwamoto, M. *J. Org. Chem.* **1994**, *59*, 7445.
- (111) Van, D. W.; Anton J. A.; Cerfontain, H. *Tetrahedron* **1981**, *37*, 2121.

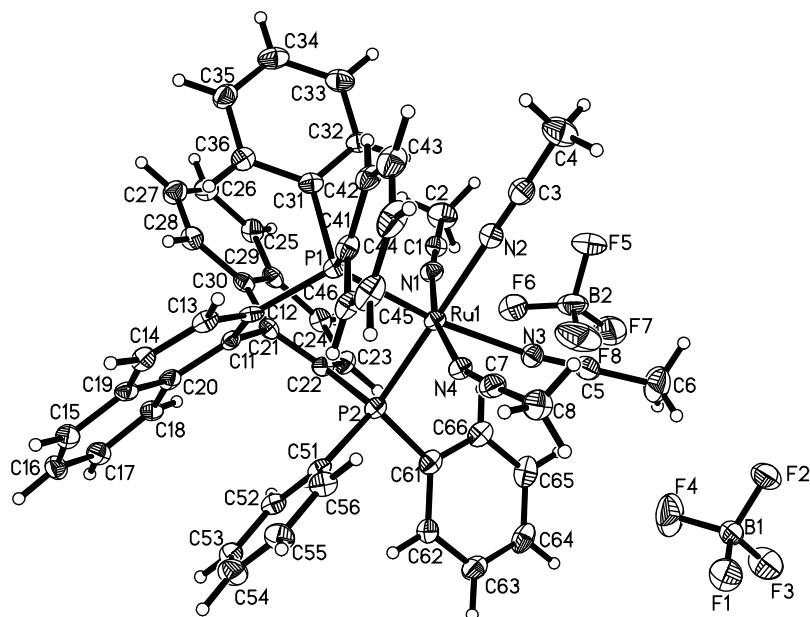


Figure A3. Molecular Structure of **92**.

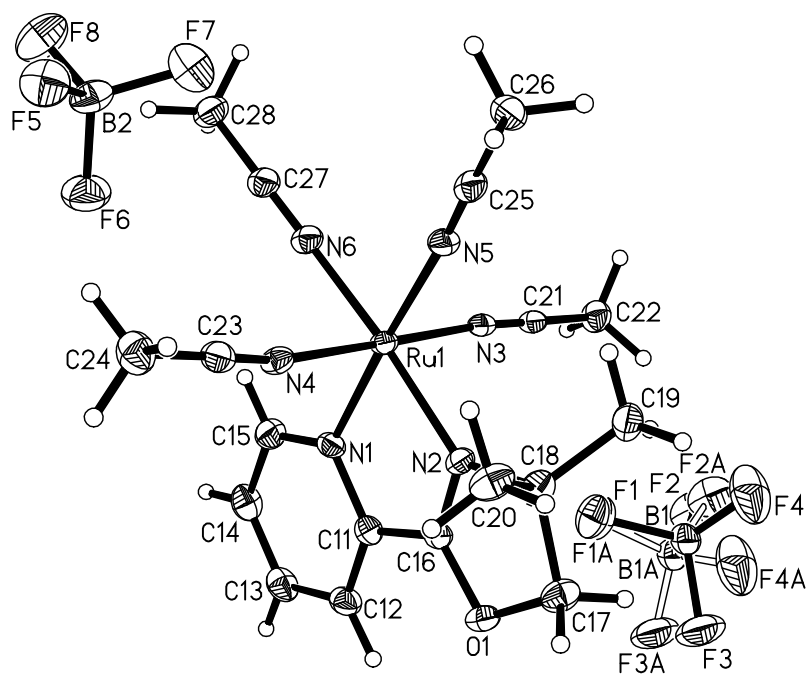


Figure A4. Molecular Structure of **93**.

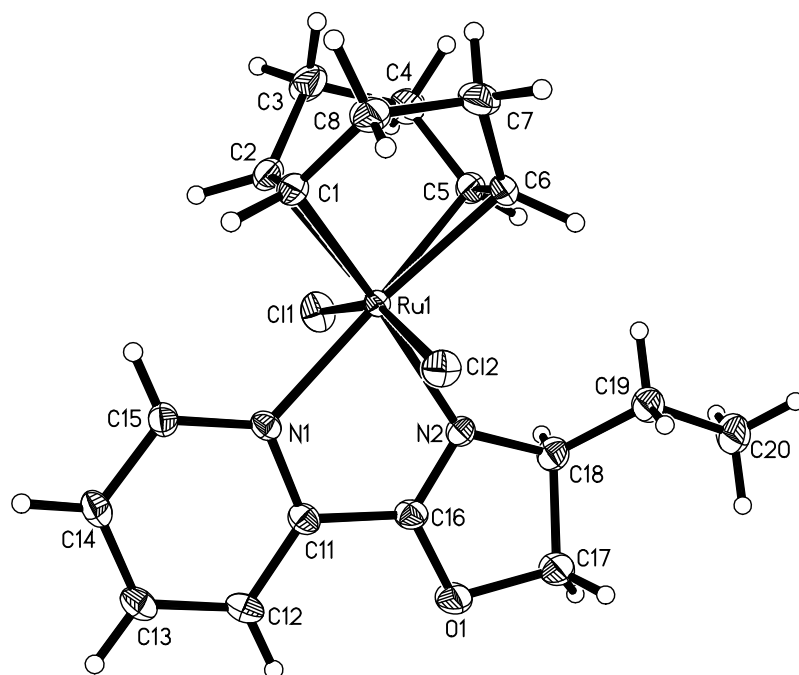


Figure A7. Molecular Structure of **96**.

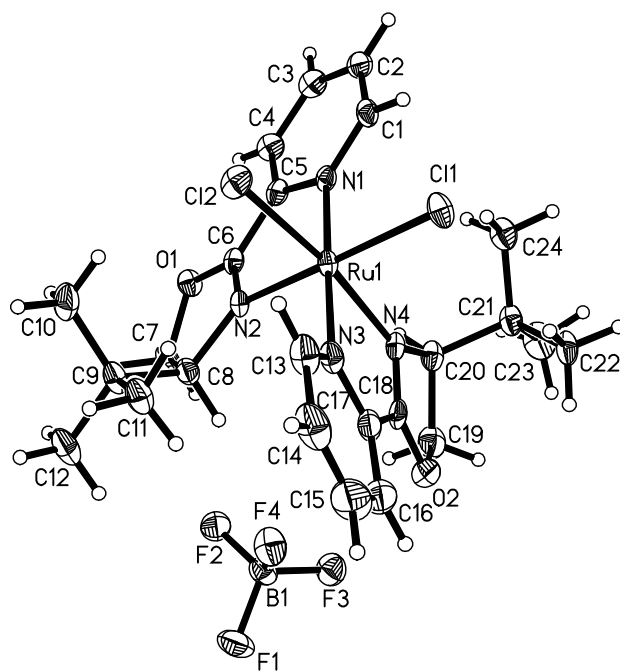


Figure A8. Molecular Structure of **97**.

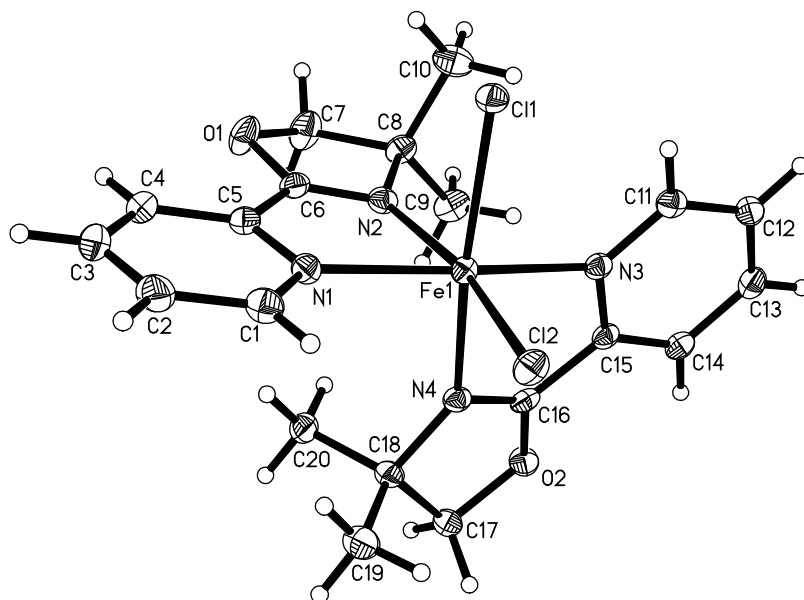


Figure A9. Molecular Structure of **98**.

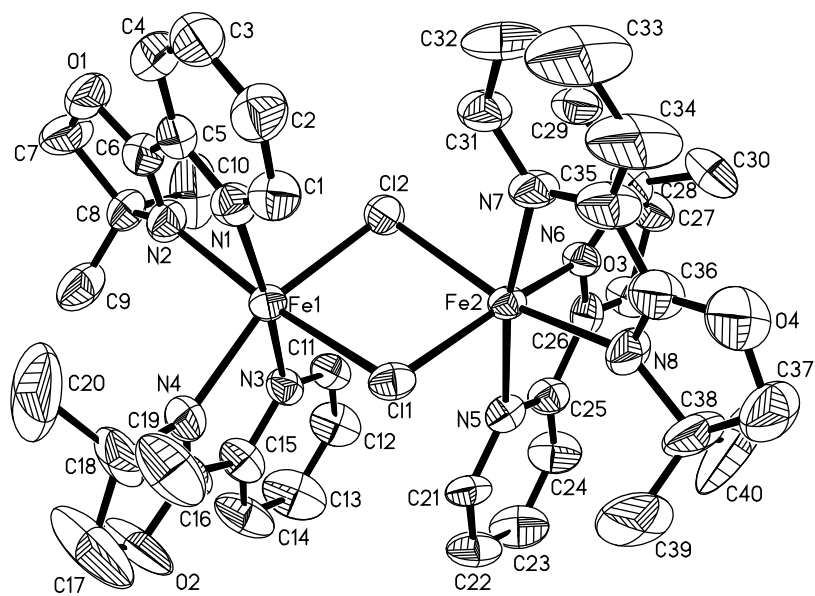


Figure A10. Molecular Structure of **99**.

Appendix B

Table B1. Crystal Data and Structure Refinement for **90**.

Identification code	yiha	
Empirical formula	C ₅₆ H ₇₉ F ₆ NO ₃ P ₂ Ru	
Formula weight	1091.21	
Temperature	100(2) K	
Wavelength	1.54178 Å	
Crystal system	Triclinic	
Space group	P -1	
Unit cell dimensions	a = 10.9483(2) Å	α = 84.2760(10) °
	b = 11.7453(2) Å	β = 75.6230(10) °
	c = 21.8972(4) Å	γ = 81.6590(10) °
Volume	2692.78(8) Å ³	
Z	2	
Density (calculated)	1.346 Mg/m ³	
Absorption coefficient	3.448 mm ⁻¹	
F(000)	1148	
Crystal size	0.30 x 0.19 x 0.12 mm ³	
Theta range for data collection	2.09 to 67.19°.	
Index ranges	-12 ≤ h ≤ 13, -13 ≤ k ≤ 13, 0 ≤ l ≤ 25	
Reflections collected	22577	
Independent reflections	8864 [R(int) = 0.0172]	
Completeness to theta = 67.19°	92.0 %	
Absorption correction	Numerical	
Max. and min. transmission	0.6824 and 0.4244	
Refinement method	Full-matrix least-squares on F ²	
Data / restraints / parameters	8864 / 0 / 630	
Goodness-of-fit on F ²	1.148	
Final R indices [I > 2σ(I)]	R ₁ = 0.0305, wR ₂ = 0.0735	
R indices (all data)	R ₁ = 0.0310, wR ₂ = 0.0738	
Largest diff. peak and hole	0.866 and -0.356 e.Å ⁻³	

Table B2. Crystal Data and Structure Refinement for **91**.

Identification code	yika	
Empirical formula	$C_{98}H_{82}BCl_3F_4N_2O_3P_4Ru_2$	
Formula weight	1853.72	
Temperature	100(2) K	
Wavelength	1.54178 Å	
Crystal system	Triclinic	
Space group	P -1	
Unit cell dimensions	$a = 15.1928(3) \text{ \AA}$ $b = 16.5925(4) \text{ \AA}$ $c = 20.8247(4) \text{ \AA}$	$\alpha = 67.2570(10)^\circ$ $\beta = 87.3490(10)^\circ$ $\gamma = 63.8770(10)^\circ$
Volume	$4297.92(14) \text{ \AA}^3$	
Z	2	
Density (calculated)	1.432 Mg/m^3	
Absorption coefficient	4.902 mm^{-1}	
F(000)	1895	
Crystal size	$0.25 \times 0.22 \times 0.17 \text{ mm}^3$	
Theta range for data collection	3.13 to 67.01° .	
Index ranges	$-17 \leq h \leq 17, 0 \leq k \leq 19, 0 \leq l \leq 24$	
Reflections collected	35625	
Independent reflections	14081 [R(int) = 0.0253]	
Completeness to $\theta = 67.01^\circ$	97.8 %	
Absorption correction	Numerical	
Max. and min. transmission	0.4895 and 0.3737	
Refinement method	Full-matrix least-squares on F^2	
Data / restraints / parameters	14081 / 10 / 1100	
Goodness-of-fit on F^2	0.995	
Final R indices [I > 2 σ (I)]	$R_1 = 0.0384, wR_2 = 0.1001$	
R indices (all data)	$R_1 = 0.0433, wR_2 = 0.1027$	
Largest diff. peak and hole	0.532 and $-0.589 \text{ e.\AA}^{-3}$	

Table B3. Crystal Data and Structure Refinement for **92**.

Identification code	yika	
Empirical formula	$C_{52}H_{44}B_2F_8N_4P_2Ru$	
Formula weight	1061.54	
Temperature	100(2) K	
Wavelength	1.54178 Å	
Crystal system	Monoclinic	
Space group	P 21/n	
Unit cell dimensions	a = 15.4945(4) Å	$\alpha = 90^\circ$
	b = 14.6409(4) Å	$\beta = 108.2400(10)^\circ$
	c = 21.9804(5) Å	$\gamma = 90^\circ$
Volume	4735.8(2) Å ³	
Z	4	
Density (calculated)	1.489 Mg/m ³	
Absorption coefficient	3.946 mm ⁻¹	
F(000)	2160	
Crystal size	0.15 x 0.11 x 0.05 mm ³	
Theta range for data collection	3.09 to 67.26°.	
Index ranges	$-18 \leq h \leq 17, 0 \leq k \leq 17, 0 \leq l \leq 26$	
Reflections collected	39472	
Independent reflections	8231 [R(int) = 0.0663]	
Completeness to theta = 67.26°	96.9 %	
Absorption correction	Numerical	
Max. and min. transmission	0.8271 and 0.5890	
Refinement method	Full-matrix least-squares on F ²	
Data / restraints / parameters	8231 / 0 / 626	
Goodness-of-fit on F ²	1.045	
Final R indices [I > 2sigma(I)]	R ₁ = 0.0417, wR ₂ = 0.0926	
R indices (all data)	R ₁ = 0.0583, wR ₂ = 0.0984	
Largest diff. peak and hole	0.458 and -0.557 e.Å ⁻³	

Table B4. Crystal Data and Structure Refinement for **93**.

Identification code	yima	
Empirical formula	$C_{18}H_{24}B_2F_8N_6ORu$	
Formula weight	615.12	
Temperature	100(2) K	
Wavelength	1.54178 Å	
Crystal system	Monoclinic	
Space group	P 21/n	
Unit cell dimensions	$a = 7.5577(2)$ Å	$\alpha = 90^\circ$
	$b = 9.8463(2)$ Å	$\beta = 90.0130(10)^\circ$
	$c = 34.0339(9)$ Å	$\gamma = 90^\circ$
Volume	$2532.65(11)$ Å ³	
Z	4	
Density (calculated)	1.613 Mg/m ³	
Absorption coefficient	5.772 mm ⁻¹	
F(000)	1232	
Crystal size	$0.59 \times 0.14 \times 0.12$ mm ³	
Theta range for data collection	3.90 to 67.18° .	
Index ranges	$-8 \leq h \leq 8, 0 \leq k \leq 11, 0 \leq l \leq 39$	
Reflections collected	21068	
Independent reflections	4394 [R(int) = 0.0299]	
Completeness to theta = 67.18°	97.1 %	
Absorption correction	Numerical	
Max. and min. transmission	0.5443 and 0.1319	
Refinement method	Full-matrix least-squares on F ²	
Data / restraints / parameters	4394 / 10 / 346	
Goodness-of-fit on F ²	1.072	
Final R indices [I > 2sigma(I)]	$R_1 = 0.0201, wR_2 = 0.0521$	
R indices (all data)	$R_1 = 0.0201, wR_2 = 0.0521$	
Largest diff. peak and hole	0.438 and -0.350 e.Å ⁻³	

Table B5. Crystal Data and Structure Refinement for **94**.

Identification code	yin5	
Empirical formula	C ₄₅ H ₆₀ Cl ₄ N ₄ O ₂ Ru ₂	
Formula weight	1032.91	
Temperature	100(2) K	
Wavelength	1.54178 Å	
Crystal system	Monoclinic	
Space group	C 2	
Unit cell dimensions	a = 30.0297(13) Å	α = 90°
	b = 9.1898(4) Å	β = 95.619(2)°
	c = 15.8658(7) Å	γ = 90°
Volume	4357.4(3) Å ³	
Z	4	
Density (calculated)	1.575 Mg/m ³	
Absorption coefficient	8.202 mm ⁻¹	
F(000)	2120	
Crystal size	0.40 x 0.35 x 0.12 mm ³	
Theta range for data collection	2.80 to 67.90°.	
Index ranges	-35 ≤ h ≤ 35, -10 ≤ k ≤ 10, -18 ≤ l ≤ 18	
Reflections collected	17156	
Independent reflections	7134 [R(int) = 0.0674]	
Completeness to theta = 67.90°	96.1 %	
Absorption correction	Semi-empirical from equivalents	
Max. and min. transmission	0.4394 and 0.1379	
Refinement method	Full-matrix least-squares on F ²	
Data / restraints / parameters	7134 / 1 / 516	
Goodness-of-fit on F ²	1.037	
Final R indices [I > 2σ(I)]	R ₁ = 0.0492, wR ₂ = 0.1305	
R indices (all data)	R ₁ = 0.0493, wR ₂ = 0.1308	
Absolute structure parameter	0.017(11)	
Largest diff. peak and hole	1.565 and -0.830 e.Å ⁻³	

Table B6. Crystal Data and Structure Refinement for **95**.

Identification code	yioa	
Empirical formula	C ₂₂ H ₂₄ Cl ₂ N ₂ ORu	
Formula weight	504.40	
Temperature	100(2) K	
Wavelength	0.71073 Å	
Crystal system	Monoclinic	
Space group	P 21	
Unit cell dimensions	a = 7.0471(6) Å	α = 90°
	b = 16.9054(15) Å	β = 99.8740(10)°
	c = 8.4172(8) Å	γ = 90°
Volume	987.92(15) Å ³	
Z	2	
Density (calculated)	1.696 Mg/m ³	
Absorption coefficient	1.080 mm ⁻¹	
F(000)	512	
Crystal size	0.18 x 0.14 x 0.10 mm ³	
Theta range for data collection	2.41 to 32.12°.	
Index ranges	-10 ≤ h ≤ 10, -25 ≤ k ≤ 25, 0 ≤ l ≤ 12	
Reflections collected	16325	
Independent reflections	6407 [R(int) = 0.0182]	
Completeness to theta = 32.12°	95.1 %	
Absorption correction	Numerical	
Max. and min. transmission	0.8997 and 0.8293	
Refinement method	Full-matrix least-squares on F ²	
Data / restraints / parameters	6407 / 1 / 349	
Goodness-of-fit on F ²	1.032	
Final R indices [I > 2σ(I)]	R ₁ = 0.0179, wR ₂ = 0.0446	
R indices (all data)	R ₁ = 0.0183, wR ₂ = 0.0448	
Absolute structure parameter	-0.015(14)	
Largest diff. peak and hole	1.004 and -0.294 e.Å ⁻³	

Table B7. Crystal Data and Structure Refinement for **96**.

Identification code	yipa	
Empirical formula	C ₁₈ H ₂₄ Cl ₂ N ₂ ORu	
Formula weight	456.36	
Temperature	100(2) K	
Wavelength	0.71073 Å	
Crystal system	Monoclinic	
Space group	C 2	
Unit cell dimensions	a = 30.3970(13) Å	α = 90°
	b = 8.7145(4) Å	β = 96.9560(10)°
	c = 15.8881(7) Å	γ = 90°
Volume	4177.7(3) Å ³	
Z	8	
Density (calculated)	1.451 Mg/m ³	
Absorption coefficient	1.013 mm ⁻¹	
F(000)	1856	
Crystal size	0.44 x 0.38 x 0.28 mm ³	
Theta range for data collection	1.29 to 32.05°.	
Index ranges	-45 ≤ h ≤ 43, -12 ≤ k ≤ 12, 0 ≤ l ≤ 23	
Reflections collected	34398	
Independent reflections	13508 [R(int) = 0.0161]	
Completeness to theta = 32.05°	95.1 %	
Absorption correction	Numerical	
Max. and min. transmission	0.7646 and 0.6642	
Refinement method	Full-matrix least-squares on F ²	
Data / restraints / parameters	13508 / 1 / 497	
Goodness-of-fit on F ²	1.007	
Final R indices [I > 2σ(I)]	R ₁ = 0.0198, wR ₂ = 0.0520	
R indices (all data)	R ₁ = 0.0208, wR ₂ = 0.0527	
Absolute structure parameter	-0.028(14)	
Largest diff. peak and hole	0.920 and -0.372 e.Å ⁻³	

Table B8. Crystal Data and Structure Refinement for **97**.

Identification code	yita	
Empirical formula	$C_{26}H_{34}BCl_8F_4N_4O_{2.37}Ru$	
Formula weight	911.89	
Temperature	100(2) K	
Wavelength	1.54178 Å	
Crystal system	Orthorhombic	
Space group	P 21 21 21	
Unit cell dimensions	$a = 11.19480(10)$ Å	$\alpha = 90^\circ$
	$b = 13.9654(2)$ Å	$\beta = 90^\circ$
	$c = 23.7007(3)$ Å	$\gamma = 90^\circ$
Volume	$3705.36(8)$ Å ³	
Z	4	
Density (calculated)	1.635 Mg/m ³	
Absorption coefficient	9.200 mm ⁻¹	
F(000)	1832	
Crystal size	0.36 x 0.20 x 0.10 mm ³	
Theta range for data collection	3.67 to 68.08°.	
Index ranges	$-13 \leq h \leq 13, 0 \leq k \leq 16, 0 \leq l \leq 28$	
Reflections collected	31221	
Independent reflections	6686 [R(int) = 0.0294]	
Completeness to theta = 68.08°	99.1 %	
Absorption correction	Numerical	
Max. and min. transmission	0.4598 and 0.1364	
Refinement method	Full-matrix least-squares on F ²	
Data / restraints / parameters	6686 / 0 / 432	
Goodness-of-fit on F ²	1.002	
Final R indices [I > 2σ(I)]	R ₁ = 0.0271, wR ₂ = 0.0663	
R indices (all data)	R ₁ = 0.0279, wR ₂ = 0.0667	
Absolute structure parameter	-0.019(7)	
Extinction coefficient	0.00015(3)	
Largest diff. peak and hole	1.269 and -0.799 e.Å ⁻³	

Table B9. Crystal Data and Structure Refinement for **98**.

Identification code	yiwa	
Empirical formula	C ₂₂ H ₂₆ Cl ₈ Fe N ₄ O ₂	
Formula weight	717.92	
Temperature	100(2) K	
Wavelength	1.54178 Å	
Crystal system	Monoclinic	
Space group	P 21/c	
Unit cell dimensions	a = 15.6717(2) Å	α = 90°
	b = 10.50400(10) Å	β = 107.3650(10)°
	c = 19.0499(2) Å	γ = 90°
Volume	2992.98(6) Å ³	
Z	4	
Density (calculated)	1.593 Mg/m ³	
Absorption coefficient	10.854 mm ⁻¹	
F(000)	1456	
Crystal size	0.33 x 0.27 x 0.22 mm ³	
Theta range for data collection	4.86 to 67.95°.	
Index ranges	-18 ≤ h ≤ 16, 0 ≤ k ≤ 12, 0 ≤ l ≤ 22	
Reflections collected	25014	
Independent reflections	5242 [R(int) = 0.0319]	
Completeness to theta = 67.95°	96.3 %	
Absorption correction	Numerical	
Max. and min. transmission	0.1987 and 0.1241	
Refinement method	Full-matrix least-squares on F ²	
Data / restraints / parameters	5242 / 0 / 339	
Goodness-of-fit on F ²	1.014	
Final R indices [I > 2σ(I)]	R ₁ = 0.0271, wR ₂ = 0.0659	
R indices (all data)	R ₁ = 0.0314, wR ₂ = 0.0675	
Extinction coefficient	0.00011(3)	
Largest diff. peak and hole	0.259 and -0.207 e.Å ⁻³	

Table B10. Crystal Data and Structure Refinement for **99**.

Identification code	yilca	
Empirical formula	$C_{43}H_{54}B_2Cl_8F_8Fe_2N_8O_4$	
Formula weight	1315.86	
Temperature	100(2) K	
Wavelength	1.54178 Å	
Crystal system	Monoclinic	
Space group	P 21	
Unit cell dimensions	$a = 12.3494(4)$ Å	$\alpha = 90^\circ$
	$b = 18.2325(6)$ Å	$\beta = 92.442(2)^\circ$
	$c = 12.6916(4)$ Å	$\gamma = 90^\circ$
Volume	$2855.05(16)$ Å ³	
Z	2	
Density (calculated)	1.531 Mg/m ³	
Absorption coefficient	8.160 mm ⁻¹	
F(000)	1340	
Crystal size	0.57 x 0.18 x 0.15 mm ³	
Theta range for data collection	3.49 to 67.90°.	
Index ranges	$-14 \leq h \leq 14, -21 \leq k \leq 21, 0 \leq l \leq 15$	
Reflections collected	23677	
Independent reflections	9781 [R(int) = 0.0396]	
Completeness to theta = 67.90°	97.9 %	
Absorption correction	Numerical	
Max. and min. transmission	0.3801 and 0.0898	
Refinement method	Full-matrix least-squares on F ²	
Data / restraints / parameters	9781 / 46 / 735	
Goodness-of-fit on F ²	1.028	
Final R indices [I > 2sigma(I)]	R ₁ = 0.0622, wR ₂ = 0.1521	
R indices (all data)	R ₁ = 0.0811, wR ₂ = 0.1652	
Absolute structure parameter	0.001(6)	
Largest diff. peak and hole	0.886 and -0.452 e.Å ⁻³	